



UNIVERSITY OF

LIVERPOOL

Functionalised Dipeptides As Hydrogelators For Energy Transfer And As Drug Delivery Vehicles

Thesis submitted in accordance with the requirements of the
University of Liverpool for the degree of **Doctor of Philosophy**

By **Salmah Mohamed Awhida**

Under the supervision of **Dr. Dave Adams**

January 2015

Declaration

I declare that this is my own work and has not been submitted in any form for another degree or qualification of the University of Liverpool or any other university or any other institute of learning. Information derived from the published work of others has been acknowledged in the text and list of references is given.

Salmah Awhida

Acknowledgements

Put God in the centre and everything will come together

To Him I give thanks for making all things possible!

I would like to express my special appreciation and thanks to my supervisor Dr. Dave Adams, you have been a tremendous mentor for me. I would like to thank you for encouraging my research and for allowing me to grow as a research scientist. I also want to thank you for letting my defence be an enjoyable moment, and for your brilliant comments and suggestions, thanks to you. Without your continuous encouragement for improving my thesis, I can hardly finish it. The professional training and the style I learned from you will benefit me in my future career. I would especially like to thank **Dan Holden** for measuring the size of some of molecules. As well I would like to thank **Andre Cardoso** for measuring the confocal microscopy for some of my samples. I also thank the great people in my group past and present, especially people in my office, namely **Jaclyn Raeburn, Chen Lin, Emilly Darper** and **Thanchanok Ratvijitvech** for their time, help, advice and inspiring discussions. All of you have been there to support me when I recruited patients and collected data for my PhD thesis.

A special thanks to my family. Your love is the greatest gift of all, my husband, **Khairy Benesa**. He came to UK to stay with me and quit his job in Libya. His arrival eased my upset and worries. He has supported me in multiple capacities over the last four years and he encouraged me to pursue and finish my PhD and was always my support in the moments when there was no one to answer my queries. For such a sacrifice, I know I cannot say thank you enough. My sweet kids **Malek** and **Merna**, their smile removed all my tiredness from the whole day work in the lab.

Special thanks to my father who lives in different world. He was always encouraging me to study and complete my PhD. I wished him to be alive to see me in this stage. God made him in paradise. A lot of thanks to my mother who is in Libya, always encourage me and pray for me when we talked by phone. Thanks to my siblings, my brothers and sisters, and all the family for their love and support. Words cannot express how grateful I am to my mother-in law, brothers-in-law, and sisters-in-law for their prayer for me and supporting me all the time. I would also like to thank all of my friends who supported me to strive towards my goal during my time in Liverpool.

Finally, I would like to thank my Libyan Embassy for funding.

Thank you all.

Abstract

This thesis will cover aspects of functionalised dipeptide hydrogels and their application in energy transfer and as vehicles for drug delivery. In the first section, a large number of dipeptides conjugated to different aromatic groups were synthesised. We synthesised 35 dipeptides conjugated to different aromatic groups (naphthalene, anthracene, phenanthrol, anthraquinone, carbazole and pyrene). We synthesised a large number of dipeptides with different hydrophobicity and different aromatic groups in order to study their ability to form gels and study the mechanical properties of the gels.

The second part of this thesis will investigate the formation of hydrogels based on dipeptides with different aromatic groups. The focus in this section was on the gelation as well as the effect of changing the solvent and changing the amino acids used. This section then explores the properties of the resulting hydrogels. A number of different dipeptides containing different amino acids were tested, some of which formed gels and others. The dipeptides also had different pK_a values. This factor was shown to be important in driving the preferential selection of a certain amino acids.

The thesis then describes energy transfer which can occur between two dipeptides (pyrene and anthracene dipeptides), or between a dipeptide and a dansyl derivative (phenanthrol and dansyl, or carbazole and dansyl). These results showed that energy transfers can occur in these specific hydrogels. In all other cases, no evidence for energy transfer was found. This may imply that the packing of the fibres is important for energy transfer and this should be the focus of future work.

The final section of this thesis describes the controlled release of model dyes from these gels. We studied controlled release from FmocFF hydrogels and from one other functionalised dipeptide hydrogel at different gelator concentrations and at different pH. The release of the dye from the hydrogel can be controlled by different factors, including the pH, peptide concentration, the microstructure and the mesh size. Furthermore, choosing the right method to prepare hydrogel allows us to control the microstructure for hydrogel to be injectable. Therefore, by controlling these entire factors we can use these kinds of hydrogels for drug delivery applications.

Table of Contents

Declaration	0
Acknowledgements	2
Abstract	3
CHAPTER 1	7
Introduction.....	7
1- Introduction:	8
1.1- Gel:	8
1.2- Low molecular weight hydrogels (LMWG):	11
1.3- Hydrogelation approaches:	12
1.4- Interaction resulting in self-assembly:	16
1.5- The hydrogelation mechanism:	17
1.6- Dipeptide hydrogels:	17
1.6.1- <i>Dipeptide Hydrogels conjugated to aromatic groups:</i>	19
1.6.1.1- Fmoc-dipeptide hydrogels:	20
1.6.1.2- Pyrene dipeptide hydrogels:	21
1.6.1.3- Anthraquinone dipeptide hydrogels:	22
1.6.1.4- Naphthalene dipeptide hydrogels:	23
1.7- Applications of dipeptide hydrogels:	26
1.7.1- <i>Cell culture:</i>	26
1.7.2- <i>Fluorescence and energy transfer:</i>	27
1.7.3- <i>Controlled release:</i>	27
1.8- Aim of the project:	29
1.9- References:	30
CHAPTER 2	34
Dipeptide synthesis	34
2- Dipeptide synthesis:	35
2.1- Introduction:	35
2.2- <i>Dipeptide synthesis:</i>	36
2.2.1- Naphthalene dipeptides:	36
2.2.2- Phenanthrol dipeptides:	64
2.2.3- Anthraquinone dipeptide:	72
2.2.4- Carbazole dipeptides:	76
2.2.5- Anthracene dipeptides:	85

2.2.6-	Pyrene dipeptides:	94
2.3-	Result and Discussion:.....	98
2.3.1-	<i>Dipeptides synthesis</i> :.....	98
2.4-	Conclusion:	113
2.5-	References:	115
CHAPTER 3.....		116
Hydrogel Formation And Their Properties		116
3-	Hydrogel formation and their properties	117
3.1-	Introduction:.....	117
3.2-	Experimental Section:	118
3.2.1-	<i>Gel formation (Hydrogels based on dipeptide derivatives)</i> :.....	118
3.2.2-	<i>pH and pK_a measurements</i> :.....	119
3.2.3-	<i>Rheology studies</i> :	119
3.2.4-	<i>Fourier-transform Infra-Red Spectroscopy (FT-IR)</i> :	120
3.2.5-	<i>Scanning electron microscopy (SEM)</i> :.....	120
3.3-	Result and discussion:	121
3.3.1-	<i>Hydrogel and Rheology</i> :.....	121
3.3.1.1-	Hydrogelation of naphthalene dipeptides:.....	121
3.3.1.2-	Hydrogelation of phenanthrol dipeptides:	129
3.3.1.3-	Hydrogelation of anthraquinone dipeptides:	131
3.3.1.4-	Hydrogelation of carbazole dipeptides:.....	132
3.3.1.5-	Hydrogelation of anthracene dipeptides:.....	134
3.3.1.6-	Hydrogelation of pyrene dipeptides:	137
3.3.2-	<i>pH and pK_a measurements</i> :.....	141
3.3.3-	<i>FT-IR of Hydrogels</i> :	148
3.4-	Conclusion:	150
3.5-	References:	152
CHAPTER 4.....		154
Fluorescence And Energy Transfer		154
4-	Fluorescence and energy transfer:	155
4.1-	Introduction:.....	155
4.1.1-	Mechanism of energy transfer:.....	157
4.1.1.1-	<i>Förster energy transfer</i> :	157
4.1.1.2-	<i>Dexter energy transfer</i> :	158

4.2-	Experimental section:	159
4.2.1-	<i>Fluorescence studies:</i>	159
4.2.2-	<i>Energy transfer in hydrogels and organogels:</i>	160
4.2.2.1-	Mix two dipeptides:	160
4.2.2.2-	Mix dipeptide and dansyl:	161
4.3-	Results and discussion:	162
4.3.1-	<i>Fluorescence study:</i>	162
4.3.2-	<i>Energy transfer in hydrogels and organogels:</i>	174
4.4-	Conclusion:	186
4.5-	References:	188
CHAPTER 5		190
5-	The controlled release:	191
5.1-	Introduction:	191
5.2-	Experimental section:	193
5.2.1-	<i>Hydrogel loaded dyes preparation:</i>	195
5.2.1.1-	Release from FmocFF gels:	195
5.2.1.2-	Release from gels formed from 42:	195
5.2.2-	<i>Release study:</i>	196
5.2.2.1-	FmocFF and compound 42:	196
5.3-	Result and discussion:	196
5.3.1-	<i>Calibration curves:</i>	196
5.3.2-	<i>FmocFF loaded dye hydrogel and release study:</i>	199
5.3.2.1-	Release study at different pHs and dyes at the same concentration of the peptide (5 mg/mL):	200
5.3.2.2-	Release study at different concentration of the peptide and dyes at the same pH:	203
5.3.2.3-	Compare the release study of different dyes at the same pH (pH5) and the same concentration (5 mg/mL):	206
5.3.2.4-	Diffusion coefficient:	209
5.3.3-	<i>Compound 42 release study:</i>	213
5.4-	Conclusion:	219
5.5-	References:	220
CHAPTER 6		222
Conclusion		222
5.1-	Conclusion:	223

CHAPTER 1

Introduction

1- Introduction:

1.1- Gel:

A gel is a material that is easier to recognise than to define¹. Lloyds explained a gel as a material that consists of two components, liquid and solid; and it has more solid-like than liquid-like properties². Others defined a gel as a material of solid- and liquid-like states that result from the transition of liquid state to solid state by some conditions³ (Fig. 1.1). Most researchers describe the gels as materials that contain two components, a solid and a liquid component. Generally, we can define a gel as a substance that is formed from materials that provide a three dimensional network. Gels are important because they have been used for many applications, including in cosmetics and personal care (contact lenses, toothpaste), food stuffs (jelly and puddings) and medical applications such as drug delivery⁴ and tissue engineering^{1, 5} and cell culturing^{6, 7}. Moreover, they have also been used in plant growth⁸ and in chemical sensing agents^{9, 10}.

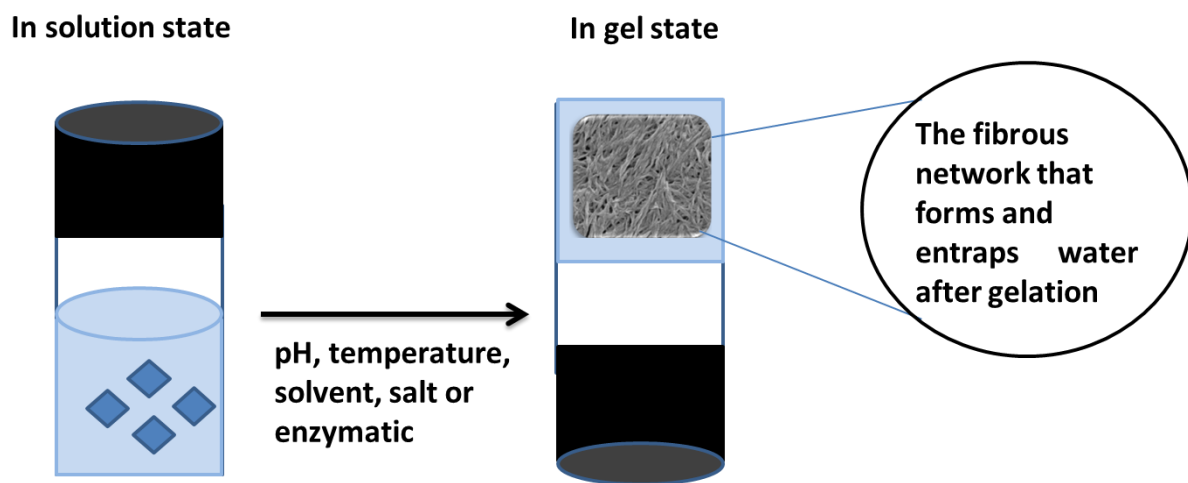


Figure 1.1: The transition of material from liquid state to gel state by some conditions.

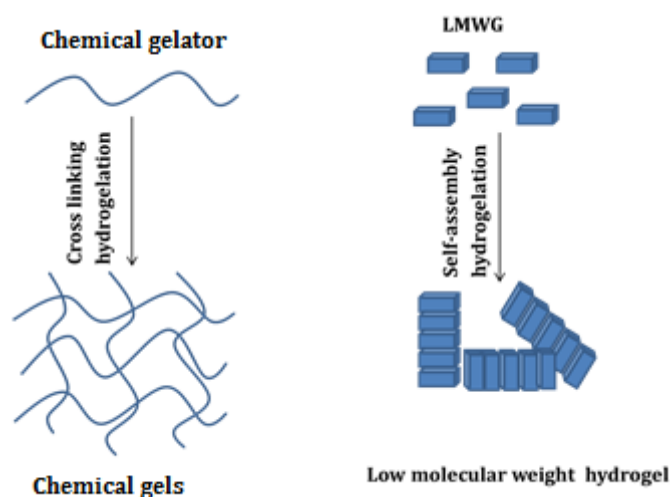
Gels can be organogels, where the liquid component is an organic solvent or hydrogels, where the liquid component is water (the focus of this thesis). Hydrogels can be classified commonly into chemical gels and physical gels and can be used in a wide range of applications, due to their compatibility with water.

Chemical gels are gels that are formed by covalent bonds between compounds leading to the formation of irreversible networks such as polymer gel^{3, 11} (synthetic polymers

such as cross-linked poly(ethylene oxide) (PEO), poly(sodium acrylate) (PSA), and polypeptides¹² or naturally polymers such as alginate, pectin, collagen¹³ and gelatine^{14,12}). For example, dextran consists of α -1,6-linked-D-glucopyranoses with some degree of 1,3-branching can form hydrogels when cross-linked^{13, 15} and it also used for protein delivery¹³. Also, gelatine gels have been used as a protein delivering in biomedical applications¹³. Collagen is a protein that can be found in body tissues¹⁶. Polymer hydrogels can have limited uses in biomedical applications. This is because of the presence of radicals and initiators that are present from the polymerisation process used to form the gels. These can damage biological materials¹⁷.

In contrast, physical gels are gels that form by non-covalent interactions leading to the formation of reversible networks such as gels that formed from low molecular weight gelators (LMWG) (small molecules) (discussed in more details below and are the focus of this Thesis).

The difference between the LMWG hydrogels and chemical gels is that the interactions between gelator molecules of the LMWG consist of non-covalent interactions leading to self-assembly, instead of chemical (covalently-bonded) crosslinks (Scheme 1.1).



Scheme 1.1: Schematic showing the differences between a chemical gels (left) and a molecular hydrogelator (right).

LMWGs are important because a LMWG hydrogel can be used as a temporary scaffold in biological applications rather than using a polymer hydrogel scaffold. These LMWG

scaffolds could easily be released and removed when no longer needed. The difference between the bonds in LMWG and the chemical gel is the effect on the reversibility of the gel. For instance, LMWG hydrogel can melt and reform on heating and cooling. Also LMWG hydrogel has a wide range of different mechanical properties, where this is an important characteristic. For example, the LMWGs have a tendency to break at low strain¹⁸. Moreover, the transition of gel-sol of LMWG can be form easier than that in the polymers hydrogel¹⁹. Examples of the use of LMWG for biomedical applications are hydrogels formed from FmocFF (F= phenylalanine), which have been used as a temporary scaffold for cell culturing (Fig. 1.2)⁷ or controlled drug release⁴. Gazit *et al.* have previously demonstrated the self-assembly of diphenylalanine alone²⁰. Furthermore, they had reported that aromatic moieties are important in the self-assembly of these fibrils *via* aromatic stacking interactions²⁰. Uljin's group have reported that the when the amino acid in the molecule is changed, the compatibility of gel mixtures of Fmoc-dipeptide and Fmoc-peptide will be different²¹.

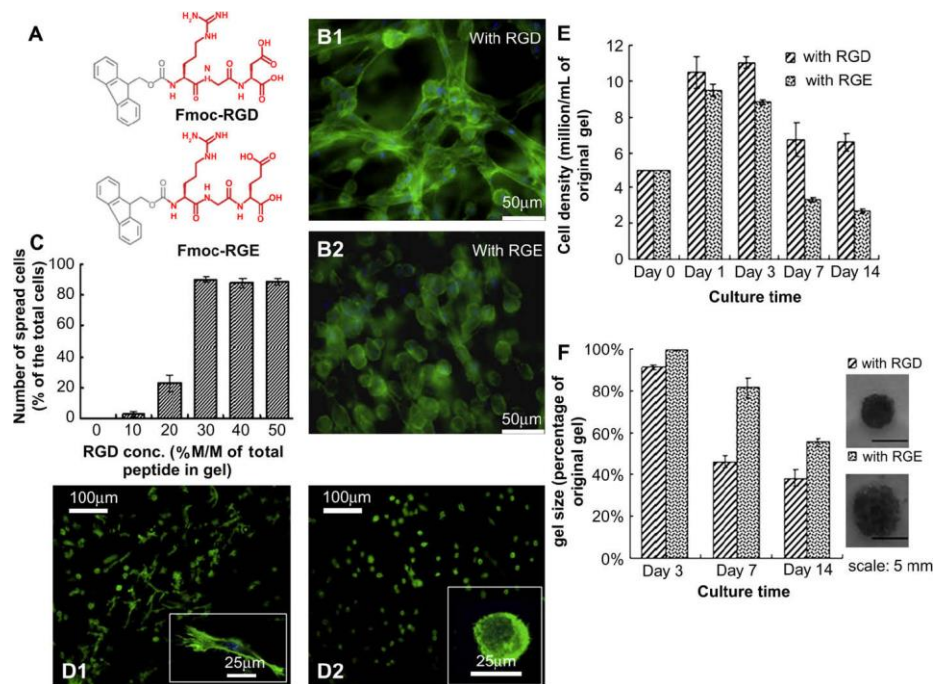


Figure 1.2: The Fmoc-FF/RGD hydrogel promotes cell adhesion with subsequent cell spreading and proliferation. (A) The chemical structures of the two Fmoc peptide derivatives. (B) Cell adhesion and morphology in the Fmoc-FF/RGD and Fmoc FF/RGE hydrogels (C) The influence of cell spreading by Fmoc-RGD concentration also influenced cell spreading (D) Integrin blocking experiments showed direct interaction of the cells with RGD after 20 h: Cells with unblocked $\alpha 5 \beta 1$ integrins were able to spread and directly attach to the RGD sites on the nanofibres (D1); Cells with blocked $\alpha 5 \beta 1$ integrins were unable to attach to the RGD sites and remained rounded (D2). (E) Cell increase in the Fmoc-FF/RGD and Fmoc-FF/RGE hydrogels (F) Contraction of the cell-gel constructs⁷.

1.2- Low molecular weight hydrogels (LMWG):

Low molecular weight hydrogels (LMWG) or supramolecular hydrogels are hydrogels that are formed by the self-assembly of small molecules in water. These molecules are aggregated to form fibres that lead to form hydrogels²². These LMWG contain a network of nanofibres and water. Although the design of LMWG is not fully understood²³, they have been widely used over the last few years. The final hydrogel properties can be tuned by changing the molecular structure or the method of the self-assembly²⁴.

To determine the properties and the structure of the hydrogel, different techniques can be used such as spectroscopy (NMR, IR, UV-vis, and fluorescence), microscopy (scanning electron microscopy (SEM), transmission electron microscopy (TEM)), diffraction (X-ray scattering (SAXS), small angle neutron scattering (SANS) and rheology²². SAXS and SANS can provide information about the superstructures formed by fibres. The crystal structure may provide insights of the stability of the interactions as the gel can form fibres and also it can show different molecular packing from the structure of the gel/fibre phase²⁵. Rheology studies the strength of the gel, where it can measure and link the properties of deformation of the solid state and flow of the liquid state. IR can give information about the functional groups that lead to form H-bonding interactions. These interactions might lead to the formation of different structures arrangements such as parallel β -sheets or anti-parallel β -sheets (Fig. 1.3). Fluorescence spectroscopy can detect different aromatic groups in solution and gel state and this is useful for studying energy transfer. SEM and TEM can be used to study the formation of the fibres after the hydrogel has formed.

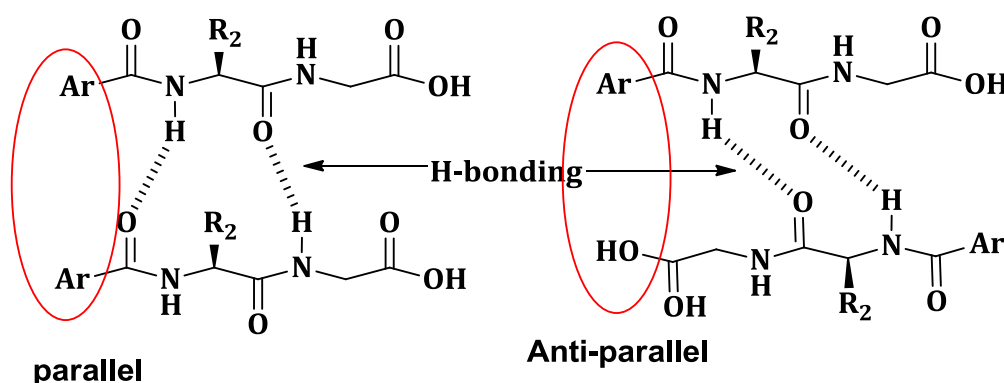


Figure 1.3: H-bonding interactions between the functional groups in dipeptides that may lead to form parallel arrangement (left) or anti-parallel arrangement (right).

LMWG can be prepared from different molecules such as cholesterol, sugars, amino acids, gemini surfactants and others. The molecular structure of LMWG has been studied before^{24, 26-37}. The strength of the hydrogel can be affected by several conditions. For example, a number of reviews have illustrated that the addition of other compounds such as polymers to the gel can increase the strength of the gel³⁸. For example, addition of poly(acrylic acid) into a gel led to increase the strength of the gel³⁸. Furthermore, Adhikari *et al.* showed that the strength of the gel increased after addition of a graphene to the gel³⁹.

Dipeptide hydrogels are now commonly demonstrated and used as a LMWG due to their low cost and a large number of dipeptides that form hydrogels successfully^{24, 26, 34, 40, 41}. These LMWG based on dipeptides contain two amino acids coupled together and attached to alkyl tail (dipeptide amphiphile) or to aromatic ring (functionalised dipeptides)⁴². In general, the structure of LMWG such as dipeptides conjugated to aromatic groups can be divided into two regions: a hydrophilic region which is compatible with water via H-bonding and a hydrophobic region which make π - π interactions leading to the self-assembly of the LMWG and forming fibres that lead to the formation of the matrix of the hydrogel^{24, 34, 43,24, 31, 34}. LMWG can be affected by small change in the structure leading to gel or non-gel results; and the design rules of the LMWG are still not clear^{24, 26, 29, 31, 34}. Also, changing the method of preparing the dipeptide hydrogel can result in a significant change to the final mechanical properties of the hydrogel^{23, 24, 44}. These LMWG hydrogels can be prepared using different approaches under the physical conditions and they have been used for different applications. Currently the packing of the molecules in the fibres forming the matrix is not clearly understood²⁴⁻²⁶.

1.3- Hydrogelation approaches:

Hydrogelation of LMWG can be achieved by using different approaches. The general method to prepare dipeptide hydrogels is by dissolving the hydrogelators into an aqueous solution and then change the temperature⁴⁵, pH⁴⁶, add a salt, or use an enzyme to start the self-assembly, leading to the formation of fibres that entrap in water resulting in hydrogelation (Fig. 1.4). According to other research, changing the method can affect the mechanical properties of the hydrogel formed²⁴. Raeburn *et al.* reported

that FmocFF can form hydrogel with different mechanical properties using different methods including pH switch and solvent method. They showed that the differences in the mechanical properties of the gel depend on the pH of the medium and the fraction of the DMSO. The gel formed in both methods has different rheological properties. Therefore, it can be clearly seen that the mechanical properties of the hydrogel can be affected by modifying the way of its preparation²⁴.

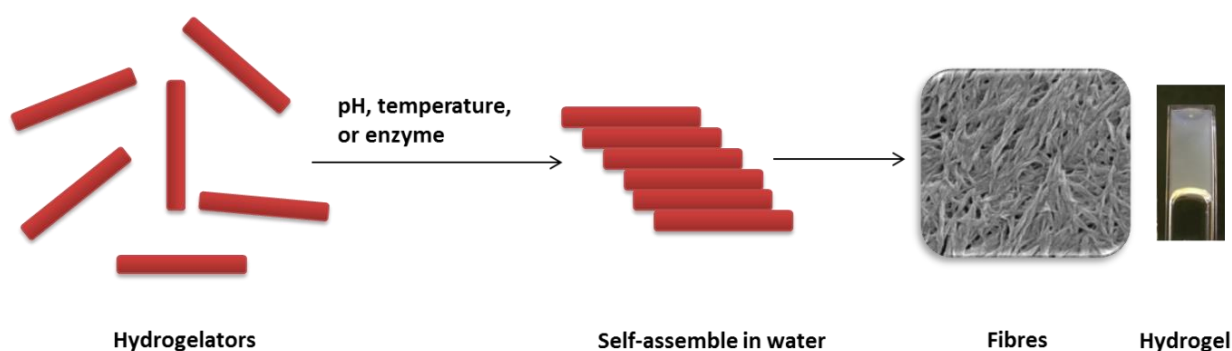


Figure 1.4: Self-assembly of hydrogelators to form hydrogel.

Physical hydrogels can be formed as follow:

1- Changing the pH:

This is the most popular method to prepare hydrogels from functionalised dipeptides, because many LMWG are pH sensitive, therefore a pH method is simple to utilise. In this method, the peptide is dissolved at high pH, deprotonating the carboxylic acid (in case of a dipeptide); where the *N*-terminus protected. When the pH is lowered below the apparent pK_a , the carboxylic acid is re-protonated allowing self-assembly starting by making non-covalent interactions such as H-bonding, π - π stacking and hydrophobic interactions^{26, 30, 33, 34, 41, 47}. Lowering the pH can be achieved by adding HCl or by using glucono- δ -lactone (GdL)^{24-26, 31}. For example, Yang *et al.* synthesised naphthalene dipeptide derivatives, then prepared a hydrogel by dissolving the gelators at high pH. A small volume of 1 M HCl was added to the solution to allow the formation of the hydrogels after the final pH of the gels reached 2⁴⁸. Ulijn *et al.* prepared FmocFF hydrogels using HCl, sometimes using heating and cooling along with the addition of

acid⁴⁵. Here, heterogeneity of the final gel resulted⁴⁶. Adams *et al.* recently reported an alternative method by utilising GdL to lower a pH in the hydrogelation process³³. GdL hydrolyses slowly in water to give gluconic acid^{33, 49} (Fig. 1.5) and this hydrolysis of GdL leads to decrease in pH. As a result, a more homogeneous hydrogel was formed. Many researchers have prepared hydrogels using this method^{33, 41, 50}.

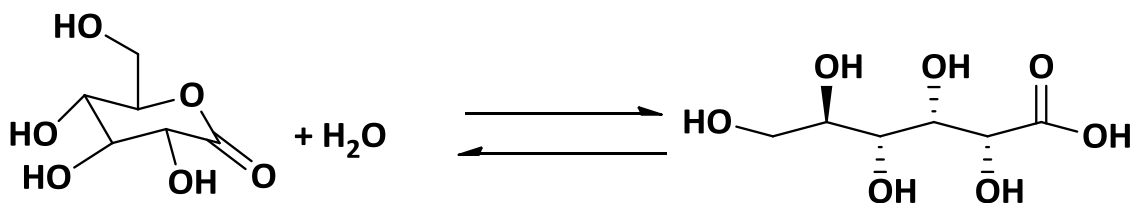


Figure 1.5: The hydrolysis of glucono- δ -lactone (GdL) to gluconic acid.

2- Enzyme method:

In this method, instead of breaking a peptide bond between amino acids, an enzyme can be used to form a peptide bond. The newly formed peptide self-assembles, trapping the solvent and hence producing hydrogels. Wang *et al.* demonstrated that hydrogel can be formed using phosphatase instead of protease at low concentration of hydrogelator⁵¹. Xu's group^{35, 52} and Uljin's group⁵³ have illustrated assembly methods using enzymes. They have used tyrosine-phosphate linked to an Fmoc group in a buffer solution. Xinming *et al.* have also used tyrosine-phosphate to prepare hydrogel based naphthalene-conjugated peptide. The dephosphorylation reaction that followed resulted in the formation of the gel⁵⁴. Furthermore, Fmoc dipeptide hydrogels have been prepared using an enzymatic trigger⁵⁵. This involves the methyl ester hydrolysis from the C-terminus of an Fmoc-conjugated dipeptide, to produce a hydrogel. The use of a two-enzyme system to trigger both the gelation and gel-sol transition has also been demonstrated⁵⁵.

3- Solvent method:

In this method, the LMWG is dissolved in an appropriate solvent and then deionised water added to trigger the formation of the hydrogel. To form a hydrogel using this method, a balance between the hydrophobic and the hydrophilic region in the peptide is

needed. Here, the most popular solvent used is perhaps dimethylsulfoxide (DMSO). The differences between this method and the pH method are the speed of hydrogelation process and the mechanical properties of the hydrogel formed^{24,26, 45}. Here, the hydrogel can form quickly in few minutes, while in the pH method using the GdL the formation of the hydrogel is slow as the change of the pH is also slow³⁴. The popularity of using this method has been increased recently because it is easy to prepare the hydrogel^{26, 40}. Also, hydrogels prepared in this way have been shown to be stable over a wide pH range and formed homogeneous gels⁴. It has been reported that the formation of the hydrogel can be affected by the solvent used⁵⁶.

4- Temperature method:

Here, the hydrogel can form by changing the temperature³⁴. At high temperature, the dipeptides can be soluble in water. Decreasing the solubility by then cooling allows the self-assembly to occur, leading to the formation of the hydrogel. Vegners *et al.*⁵⁷ prepared hydrogels based on Fmoc-dipeptide using the temperature method. Tang *et al.* demonstrated the formation of the hydrogel by changing the temperature (heat/cool). They added NaOH to the solution of peptide (FmocFF) in water to obtain a clear solution. Then they added diluted HCl to acidify the sample and lower the pH. The sample was heated to 80°C and left to cool overnight and a hydrogel was formed⁴⁵. Also, another example of a hydrogel formed by temperature trigger was reported by Debnath *et al.* They prepared Fmoc-dipeptide hydrogels by lowering the temperature of different solutions that contain the hydrogelator with a cationic C-terminus⁵⁸. Many researchers have used a temperature trigger to form LMWG, where heat-cool cycle of a gel being a common way of demonstrating the healable properties of a gel⁴⁰.

5- Adding salt:

In this method, the ability to form hydrogels associates with the hydrophobicity of the dipeptides, which determines whether worm-like micelles are formed at high pH⁵⁹. It has been reported that the hydrogel can be formed at high pH by adding a salt, such as calcium chloride to the stock solution of dipeptide. Also, the hydrogel can be formed by adding other salts, including trivalent or polyvalent salts⁵⁹. Furthermore, it has been reported that there is correlation between adding the salt to form gel and the hydrophobicity. Here, the dipeptide forms a hydrogel above the pK_a when the salt was

added³⁰. Roy *et al.* have also used enzyme trigger to form Fmoc-dipeptide hydrogel with addition of salts⁶⁰. They have reported that the mechanical strength of the gel was increased after adding the salt. Other research demonstrated that when divalent cations were added, the charge on the C-terminus may be screened leading to non-covalent crosslinking between the salt cation and gelator anion, and the formation of the hydrogel above of the pK_a of the gelator^{59, 61}.

Many hydrogels have been prepared using different methods. It can be seen that changing the approaches of preparing hydrogel can lead to a specific LMWG being a non-gel or a gel former²⁴. Why gels or non-gels form by changing the method is still not fully understood.

1.4- Interaction resulting in self-assembly:

Hydrogels can be formed by the self-assembly of dipeptides in water. The self-assembly is driven by non-covalent interactions such as H-bonding, and hydrophobic interactions. H-bonding interactions can be formed between amino acids, and aromatic groups can interact together via π - π stacking interactions. These interactions lead to the formation of one-dimensional structures that grow and entangle to form fibres, which entraps the water to form a hydrogel. These type of interactions are weak individually, but they can together lead to self-assemble and form a stable hydrogel^{4, 7, 26, 27, 30, 33, 34, 41, 44, 47}. It has been reported that a change of the order may lead to significant change to the hydrogelation process^{30, 31, 41}. For instance, if we compare between dipeptides that have similar amino acids and different substitution positions of a bromine atom, we note that they have different gelation results²⁷.

The relationship between sequence and structure has been further looked at by Adams *et al.* who reported that NapGA (G= Glycine, A= Alanine) formed a hydrogel but NapAG formed a crystal²⁷. Also, Ulijn *et al.* reported that FmocFG forms gel, but FmocGF does not⁶². Therefore, it can be clearly seen that slight change in the peptide structure can affect and change the formation of the hydrogel.

1.5- The hydrogelation mechanism:

It has been noted that when using pH method, the solution generally starts clear and remains clear during the hydrogelation process^{26, 31, 33}. In some cases, a clear solution starts to become turbid after gelation, and in this case the turbidity may be caused by the large scattering light from the fibrous structures^{24, 29, 33}. On the other hand, using the solvent method, the samples usually start as turbid solutions and clarification occurs during the hydrogelation process²⁴. From previous research, it can be clearly seen that changing the way of preparing hydrogels can lead to dramatic change of the mechanism and the mechanical properties of the hydrogel^{31, 41}. Also, small changes in the molecular structure can affect the formation of the hydrogel^{24, 26, 31, 41}. Furthermore, it has been reported that there is no correlation between the molecular structure and the formation of the hydrogel³¹. In general, it remains unclear what kind of molecules will form gel and what factors that may lead to form hydrogel^{23, 31}. Moreover, it is been reported that there is correlation between the pK_a and the pH at which the hydrogel formed^{41, 45}.

1.6- Dipeptide hydrogels:

A general design of the dipeptides includes R group which is could be aromatic or alkyl group that attached to two coupled amino acid (dipeptide) by linker such as OCH_2 or CH_2 (Fig. 1.6). Naturally, there are 20 amino acids (Fig. 1.7). Amino acids have the same basic structure: a carboxylic acid end group (C-terminus); a primary amine end group (N-terminus) and an R-group on the central carbon connecting the termini. They are all chiral, except glycine, and exist in Nature as the L-form. Depending on the group of the amino acid, they can be classified as hydrophobic, hydrophilic, charged or "other"⁶³.

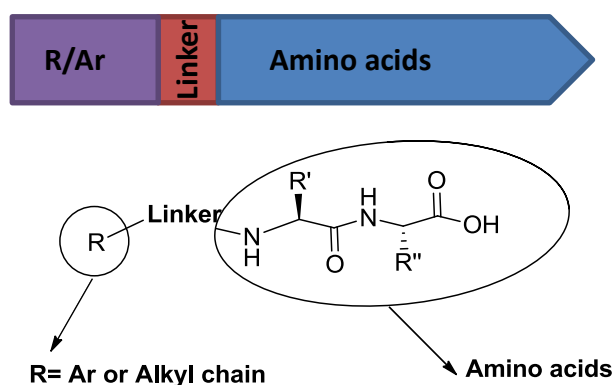


Figure 1.6: the general design of the dipeptide.

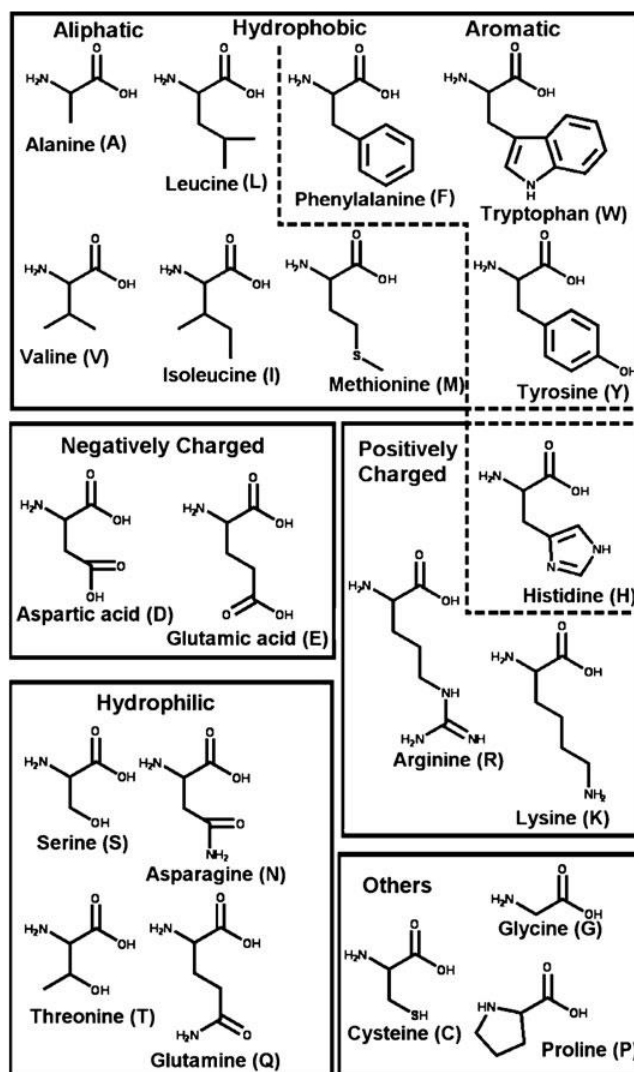


Figure 1.7: Amino acid structures are shown with their common name and the one letter abbreviations that are commonly used in peptide sequences⁶³.

Currently, dipeptides with suitable functional groups have wide interest for use as a hydrogelators^{24, 26, 32, 40, 41, 45, 47, 64-66}. For example, dipeptides conjugated to aromatic group such as naphthalene or fluorenylmethoxycarbonyl (Fmoc) were used to form hydrogels³¹. They have been utilised in many applications such as drug delivery^{67, 68}, tissue engineering⁶⁷⁻⁶⁹, cell culturing⁷⁰ and energy transfer⁷¹. More specifically, dipeptides conjugated to aromatic groups such as naphthalene^{34, 41, 48}, Fmoc^{34, 72}, and pyrene⁷³ (Fig. 1.8) have been widely used for different applications such as cell culturing, energy transfer, conductivity, and drug delivery^{14, 34, 44}. As described above, they can self-assemble in water forming fibres by non-covalent interactions such as H-bonding, and π - π stacking^{1, 24, 31} to form the matrix of the hydrogel. After self-assembly

occurs, one dimensional fibril structures are formed which leads to a network which entraps the water to form hydrogel^{24, 26, 46}. The water is the primary component of the hydrogel⁴⁸. The advantage of forming hydrogel by non-covalent interactions is that the hydrogel tend to have rapid response to the chemical and physical stimuli such as pH and temperature.

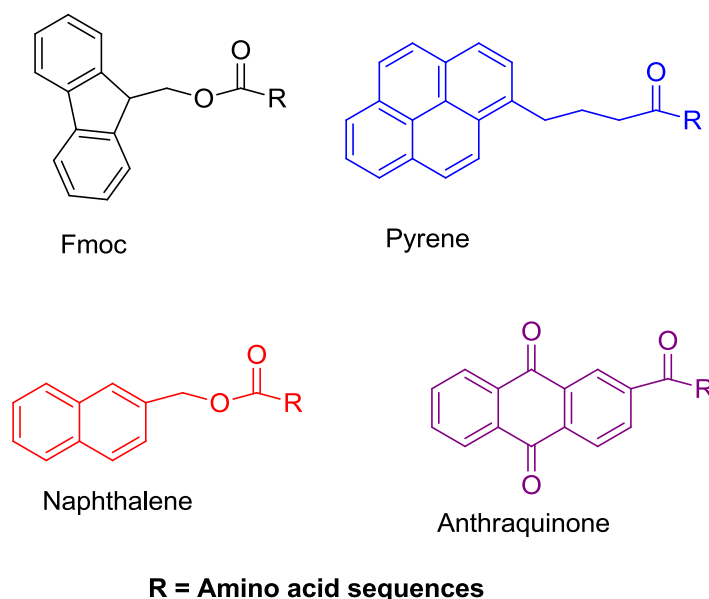


Figure 1.8: Chemical structure of functionalised dipeptides; Fmoc^{34, 72}, pyrene⁷³, naphthalene^{41, 34, 48} and anthraquinone⁷⁴.

1.6.1- Dipeptide Hydrogels conjugated to aromatic groups:

There are many peptide conjugates that have been used widely as an efficient hydrogelators, such as dipeptides conjugated to aromatic groups and dipeptide amphiphiles^{24, 26, 27, 30, 31, 37, 48}. Here, the project focuses on dipeptides conjugated to aromatic groups.

Functionalised dipeptides have been shown to be good hydrogelators³¹, including Fmoc, naphthalene, pyrene and anthraquinone dipeptides. They have been used in a wide range of applications such as energy transfer and drug delivery. They used for biomedical applications because of their biocompatibility as they contain above 97% water. One of the main advantages of using the aromatic rings is that they provide π - π stacking interaction leading to one dimensional assembly result in fibre formation³¹.

1.6.1.1- Fmoc-dipeptide hydrogels:

The Fmoc group is a common protecting group that can also be used to form efficient hydrogelators^{26, 31}. Peptides conjugated to Fmoc group has synthesised elsewhere^{26, 31-34, 57, 72, 75}, such as FmocFG³² (F = phenylalanine, G = Glycine), FmocVD⁷⁶ (V = valine, D = aspartic acid) and FmocFF²⁶. For example, FmocLD (L = leucine), FmocAD (A= alanine), and FmocID (I = isoleucine) hydrogels were prepared by cooling solutions at a concentration of 0.5 wt%⁵⁷. Zhang *et al.* have prepared hydrogels based Fmoc-dipeptides by pH control (at low pH), such as FmocAA, FmocGG, FmocGS (S = serine) and FmocGT (T = threonine)⁷². The most common Fmoc-dipeptide hydrogel is FmocFF, because it is a good hydrogel for biomedical applications^{4, 62}. Gels have been prepared from FmocFF using different methods. One of the approaches is the solvent method (see section 1.3)^{24, 30, 31, 34}. The hydrogel can be prepared by dissolving the dipeptide in DMSO and then adding deionised water or buffer at a concentration of 5 mg/mL. FmocFF forms a transparent hydrogel using this method (Fig. 1.9)⁴⁶. Alternatively, Ulijn *et al.* prepared FmocFF hydrogel using HCl⁶². They dissolved the dipeptide in a buffer at pH 8 and then concentrated HCl was added to control the pH. Another method has been utilised to prepare FmocFF hydrogels, the GdL method³³. This method depends of the hydrolysis of GdL to gluconic acid to lower the pH. The mechanical properties of Fmoc-dipeptide hydrogel were studied. In DMSO method, the rheology results of FmocFF showed that the storage modulus (G') was higher than the loss modulus (G''), with a G' of 10^4 Pa, while in HCl method G' varied, from 1,900 Pa⁷, 10^4 Pa⁴⁶, and 21,000 Pa^{21,32}. Recently, other research demonstrated that Fmoc-dipeptide hydrogels can be formed using enzymes⁷⁷.

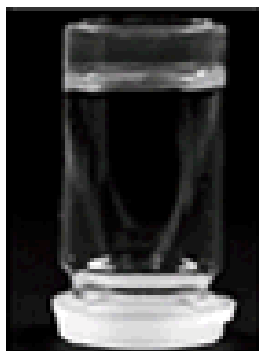


Figure 1.9: The image of FmocFF hydrogel that we have prepared using the DMSO: Water method⁴⁶

The IR spectra of Fmoc-dipeptides hydrogels were also studied. For example, in the solvent method, the IR of FmocFF showed peaks at 1607, 1658 and 1691 cm^{-1} , which refer to the presence of β -sheets and β -turns⁴. Furthermore, IR showed peaks at 1653 cm^{-1} and 1690 cm^{-1} with subsequent results referring to β -sheets conformation. On the other hand, using the HCl method, IR spectroscopy of Fmoc-dipeptides showed a strong peak at 1630 cm^{-1} assigned to anti-parallel β -sheets³¹.

Moreover, pK_a measurements were carried out for Fmoc-dipeptides using HCl titration. For example, pK_a titration with HCl showed that FmocFF hydrogel has two apparent pK_a values, pK_a 1 of 9.9 and pK_a 2 of 5.8. This means that the self-assembly process results in two different structural transitions. The report showed that the difference of the pH values in the titration results in different IR spectra. As a result, it can be clearly seen that the formation of the hydrogel can be affected by the kinetic process^{31, 33}. Adams *et al.* reported a new method to prepare hydrogel based on Fmoc-dipeptides. They have used the GdL method (see section 1.3) and they found that this method allows studying the hydrogelation process to give more understanding of the mechanism of hydrogelation³⁴. Moreover, they studied the correlation between the molecular structure, gel properties and the behaviour of the gelation of Fmoc-dipeptides. They synthesised Fmoc-dipeptides to study their ability to form gel. They described that supporting hydrogel was formed at intermediate hydrophobicity ($2.8 < \log P < 5.5$) at pH 4³². In 2012, Raeburn *et al.* demonstrated the understanding of the mechanical properties of FmocFF hydrogel using different methods, pH method and DMSO method. They showed that the method of the formation of the gel affected the final pH of the gel and can control the rheological properties of the gel. They also reported that when using solvent method, the hydrogel of FmocFF formed at pH 4 which is not suitable for some biological applications²⁶.

1.6.1.2- Pyrene dipeptide hydrogels:

Peptide amphiphiles conjugated to pyrene have been synthesised using different methods⁷⁸. Dipeptides based on pyrene have also been demonstrated to form gels by Zhang *et al.*⁷³. They illustrated an increase of the mechanical properties of hydrogels that formed via self-assembly in water by using method based on molecular recognition. A weak hydrogel was formed using pyrene-D-Ala-D-Ala (Fig. 1.10) with a storage modulus (G') of 120 Pa. The strength of pyrene hydrogel was increased when it bound to

vancomycin to result in more strong hydrogel with G' of 160000 Pa. Furthermore, when L-Ala-L-Ala was used, it formed hydrogel with ten times lower in G' over the gelator alone (Fig. 1.10).

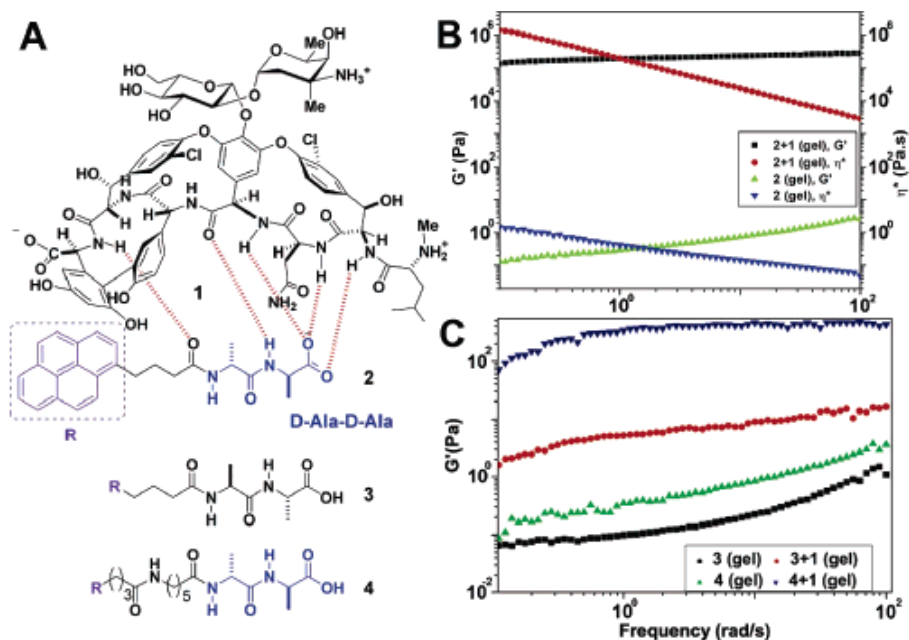


Figure 1.10: (A) Molecular structures of vancomycin (1), and the ligands derivatives of (2-4). (B) Linear viscoelastic frequency sweep responses of the hydrogels of 2 and 2+1 at strain of 1% and 0.1%, respectively. (C) Linear viscoelastic frequency sweep responses of the hydrogels of 3, 4, 3+1, and 4+1 at 1% strain. The concentrations of 1, 2, 3, and 4 are all 30 mM⁷³.

1.6.1.3- Anthraquinone dipeptide hydrogels:

Peptides conjugated to an anthraquinone aromatic group have been prepared⁷⁴. Five anthraquinone peptides were synthesised previously (Fig. 1.11)⁷⁴. Hydrogels were prepared using two different methods, the solvent method and HCl method. They have used anthraquinone moiety because it is well-known as an electroactive material. They prepared hydrogels by self-assembly to utilise in conformal display. Anthraquinone-dipeptides formed a successful hydrogel and were capable of redox reactions. This redox creates changes on the anthraquinone lead to collapse of the supramolecular hydrogel network.

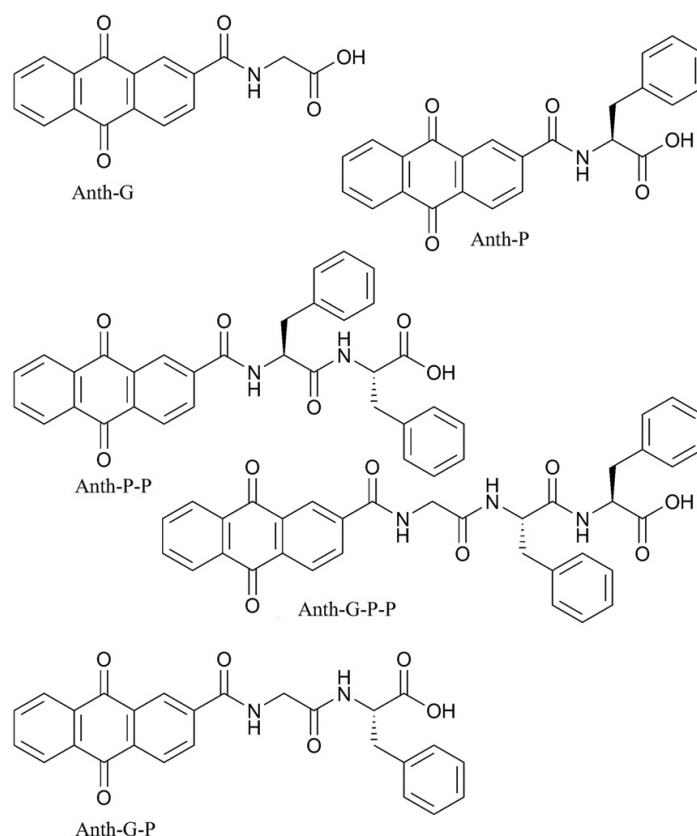


Figure 1.11: Five anthraquinone derivatives are shown above. An L-phenylalanine is represented by a 'P,' a glycine is shown by a 'G' and these units are added to the anthraquinone group, 'Anth'⁷⁴.

1.6.1.4- Naphthalene dipeptide hydrogels:

Dipeptide hydrogels based on naphthalene have received great attention. Xu *et al.* have formed naphthalene dipeptide hydrogels at concentration of 1 mg/mL and pH 4. They also, prepared hydrogels based on LMWG using the temperature method (i.e. a heat-cool cycle). They also reported that naphthalene linked with OCH₂ to the amino acid sequence formed gels, while that linked with CH₂ did not form gels⁴⁸. This shows that the linker can affect the formation of the hydrogel⁴⁸. They also demonstrated the hydrogelation of naphthalene dipeptides and they showed that two hydrogelators formed helical nanofibres. Furthermore, they described that cell cytotoxicity assay indicates that naphthalene hydrogelators are biocompatible because their structure almost water. This gives reason for using naphthalene group commonly in medical applications⁴⁸. In the other research, they demonstrated the use of 1-naphthalene diphenylalanine (naphthalene-FF) for the disruption of the dynamics of microtubules⁷⁹. They incubated cells with naphthalene-FF at different concentrations. They found that naphthalene-dipeptides self-assemble to form nanofibres above 320-340 μM. These

nanofibres disrupt the dynamics of the microtubules and thus cause apoptosis of glioblastoma cells⁷⁹. Furthermore, they synthesised and characterised hydrogelators based on the naphthalene motif that were conjugated to β -amino acids⁷⁹. They synthesised the dipeptides with different amino acids and different linkers between the aromatic group and the amino acid sequences, ($-\text{OCH}_2$, $-\text{CH}_2$). They reported that the change of the structure can lead to a dramatic change of the mechanical properties of the hydrogel³⁶. Moreover, they demonstrated the rheological properties and the molecular structure of hydrogel based on naphthalene motif. They evaluated the effect of phenylalanine on the mechanical properties of naphthalene hydrogels. There was a correlation between the molecular structure and the rheology of the naphthalene hydrogel³⁷. In 2014, Xu's group studied the synthesis and the properties of hydrogel based naphthalene attached to taurine⁸⁰. They showed that nanostructure resulted from the self-assembly of naphthalene attached to taurine. The hydrogelation process showed that the hydrogel with taurine formed at high concentration (2 wt%) in PBS buffer, while without taurine the hydrogel formed at low concentration (0.4 wt%). This result indicated that the hydrogel can be formed at high concentration when it attached to taurine and this may due to the presence of sulfonic group that increase the hydrophilicity of the hydrogel.

Chen *et al.* demonstrated that naphthalene dipeptides containing substituents such as bromine can form hydrogels using GdL method³⁰. They have shown that after adding the GdL the carboxylic acid (C-terminus) was protonated to start self-assembly leading to the formation of the π - π stacking and β -sheets. They have provided details of self-assembly process lead to hydrogelation and they reported that the process of self-assembly can affect the formation of the hydrogel^{30, 41, 81}. They also studied the formation of hydrogel based on naphthalene dipeptide at high pH by addition of Ca^{2+} to the solution⁵⁹. Furthermore, they showed that there is correlation between the hydrogel formation and the hydrophobicity. They also reported that there is no correlation between the rheological properties and the viscosity of the solution. Chen *et al.* also applied naphthalene dipeptides for energy transfer. They reported that energy transfer occurred between naphthalene diphenylalanine and a dansyl derivative leading to emission at 485 nm. In addition there was emission at 355 nm from naphthalene diphenylalanine alone (Fig. 1.12). Also, a transparent self-supporting hydrogel at a

concentration of 2.2 mM and at pH of 4 was formed from naphthalene diphenylalanine⁷¹. Houton *et al.* synthesised and extended library of naphthalene dipeptides and studied their properties. They have prepared the hydrogels using the GdL method at concentration of 5mg/mL of the peptide. Some of these dipeptides crystallised from water. They studied the crystal structure of naphthalene dipeptides and they reported a comparison between gel/fibre phase and the crystal phase²⁵. They have illustrated that minor change in the structure of the peptide lead to significant modification in the formation of the hydrogel and their properties. Wallace *et al.* have studied the mesh size of naphthalene diphenylalanine hydrogel using pulsed field gradient NMR (PFG-NMR). They prepared the hydrogel using the salt-triggered method by adding Ca⁺² to the solution of the dipeptide. They found that worm-like micelles were formed at pH 12 in the solution of the dipeptide at 0.55 wt%. The addition of Ca²⁺ led to cross-linking of these micelles. They reported that studying the mesh size of the hydrogel can be useful because this can help for specific applications such as drug delivery⁸². Moreover, naphthalene dipeptides as LMWG have studied in the presence of dextran. The results showed that the addition of dextran affected the mechanical properties of the hydrogel. It has also been demonstrated that adding polymer to naphthalene dipeptides to form gel affected their mechanical properties³⁸.

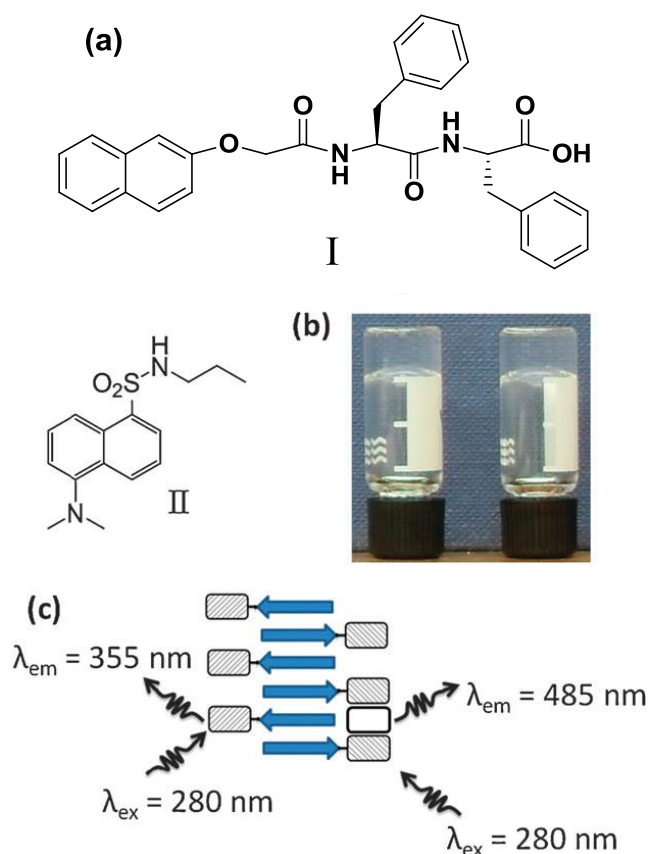


Figure 1.12: (a) Structure of naphthalene-diphenylalanine (I) and dansyl derivative (II). (b) I forms a transparent self-supporting hydrogel at a concentration of 2.2 mM and a pH of 4 (left). A transparent self-supporting gel was also formed in the presence of II (0.084 mM). (c) Energy transfer occurs between I and II (white rectangle) hosted within the fibres that form via hydrogen-bonding between dipeptides leading to emission at 485 nm in addition to emission at 355 nm from I alone⁷¹.

1.7- Applications of dipeptide hydrogels:

Hydrogel based functionalised dipeptides have been used widely in different applications such as cell culture, energy transfer and drug delivery³⁴.

1.7.1- Cell culture:

Hydrogels based on Fmoc-dipeptide such as FmocFF have been utilised for cell culturing^{4, 83}. The solvent method and pH method were used to prepare the gel. Also, FmocFF gels have been used for biological applications, as a temporary scaffold for cell culturing⁷. Ulijn's group^{7, 21, 83} have also reported cell growth within hydrogels prepared from FmocFF as well as those prepared from mixtures of FmocFF and Fmoc-amino acids.

1.7.2- Fluorescence and energy transfer:

Energy transfer is a system that includes molecules formed fibres contains donor and acceptor; the donor can be used to transfer energy to the acceptor⁸⁴. Hence, transfer energy between different aromatic groups (from donor to acceptor) has been used in many applications including molecular electronics^{71, 85, 86} and light-harvesting^{85, 87, 88}. Materials such organogels (gels which contain organic solvent) were used as a chromophore for energy transfer⁸⁹. MacPhee *et al.* reported that energy transfer occurred between donor and acceptor based peptides⁹⁰. Furthermore, Chen *et al.* demonstrated that efficient energy transfer occurred between naphthalene dipeptides and dansyl derivatives and between naphthalene and anthracene dipeptides (Fig. 1.12)⁷¹. Others reported that light-harvesting hydrogels have prepared using cationic glutamate derivatives with anionic naphthalene and anthracene-based fluorophores¹⁰⁵. In addition, it has been found there can be energy transfer between a naphthalene-based hydrogelator and a dansyl^{71, 91}. Supratim *et al.* demonstrated energy transfer between pyrene (donor) and porphyrin (acceptor) derivatives⁶⁸. Furthermore, efficient transfer of excitation energy during nano-structures has been evidenced in an anthracene light-harvesting matrix doped with less than 1 mol% of a tetracene energy trap by Alexandre *et al.*⁹². They have shown that anthracenes, tetracenes and pentacenes self-assemble into stable nano-structures due to a 2,3-bis-*n*-alkoxy substitution. The fibres forming these 3-D supramolecular networks could be aligned with intense magnetic fields or mechanically, creating these materials of interest for different applications⁹². Moreover, pyrene conjugated to oligopeptides has reported to form a fluorescent hydrogels⁹³.

1.7.3- Controlled release:

LMWG hydrogels have been prepared using different methods^{26, 29-32, 34, 36, 46, 51, 64, 69, 94}. These hydrogels have been used in some biomedical applications such as cell culturing^{83, 95} and drug delivery^{96-98, 4, 99}. Drug delivery in hydrogels has had great attention since the 1960s¹⁰⁰. The concentration of the drug in a drug delivery system increases to reach the maximum peak and then it falls off so that another dose needs to maintain the effective of the drug. The toxicity from the drug may cause, if the concentration of the drug increases above the maximum range. Also, if the concentration of the drug falls below the minimum level, the drug will be ineffective¹⁰¹.

Therefore, to control and maintain the effective level of drugs, we have to study new controlled release systems.

LMWG hydrogels based on peptides have been used for controlled release^{99, 102, 103} such as hydrogels based on FmocF, FmocY⁹⁶ and FmocFF^{33, 46, 83}. Moreover, a hybrid hydrogel based on FmocFF and konjac glucomannan (KGM) has been demonstrated for the controlled release¹⁰⁴. The hydrogel was prepared by the self-assembly of FmocFF in a solution of KGM. This study provides a new self-assembly of peptide-polysaccharide hybrid hydrogels and also provides a new sustained-release drug carrier. Docetaxel was used as a model of hydrophobic drugs and incorporated into hydrogel to study the release properties of the hydrogel. The results showed that the release rate increased with hydrogel prepared in KGM more than that without the KGM. Also the mechanical properties showed that the hybrid hydrogel (FmocFF conjugate to KGM) had a higher storage modulus (G') than the FmocFF hydrogel. This means that KGM increased the mechanical properties of the hydrogel. The controlled release of a model dye from the hydrogel to a solution placed on the top of the hydrogel was studied^{4, 105}.

1.8- Aim of the project:

Dipeptides hydrogels have great attention in many applications. Previously, hydrogels based on functionalised dipeptides have been used in energy transfer, cell culture and controlled release. In this thesis, we aim to:

- 1- Synthesise a large number of dipeptides conjugated to different aromatic moieties such as naphthalene, anthracene, pyrene, phenanthrol, anthraquinone and carbazole in order to study their ability to form hydrogels because it is still unclear why some dipeptides formed gel and others not when small change in the structure applied.
- 2- Study the mechanical properties, as well as carrying out pK_a and pH measurements of the hydrogel that formed using formed different methods, the solvent method (DMSO: Water) or the GdL method³³
- 3- Study the fluorescence and energy transfer between different aromatic groups.
- 4- Demonstrate the controlled release of dyes from different gels at different concentrations and different pHs using the DMSO: water method.

1.9- References:

1. R. G. Weiss and P. Terech, *Molecular Gels [electronic book] : Materials with Self-Assembled Fibrillar Networks / edited by Richard G. Weiss and Pierre Terech*, Dordrecht : Springer, , 2006.
2. D. Jordan Lloyd, *Chemical Catalog Company, New York* 1926, **1**, 767-782.
3. D. Collin, R. Covis, F. Allix, B. Jamart-Gregoire and P. Martinoty, *Soft Matter*, 2013, **9**, 2947-2958.
4. A. Mahler, M. Reches, M. Rechter, S. Cohen and E. Gazit, *Advanced Materials*, 2006, **18**, 1365-1370.
5. D. G. Wallace and J. Rosenblatt, *Advanced Drug Delivery Reviews*, 2003, **55**, 1631-1649.
6. E. S. Place, J. H. George, C. K. Williams and M. M. Stevens, *Chemical Society Reviews*, 2009, **38**, 1139-1151.
7. M. Zhou, A. M. Smith, A. K. Das, N. W. Hodson, R. F. Collins, R. V. Ulijn and J. E. Gough, *Biomaterials*, 2009, **30**, 2523-2530.
8. E. Karadağ, D. Saraydin, Y. Çaldıran and O. Güven, *Polymers for Advanced Technologies*, 2000, **11**, 59-68.
9. K. Y. Lee, D. J. Mooney. , *Chemical reviews*, 2001, **101**, 1869-1879.
10. S. Yamaguchi, I. Yoshimura, T. Kohira, S.-I. Tamaru and I. Hamachi, *Journal of the American Chemical Society*, 2005, **127**, 11835-11841.
11. F. Kremer, W. Leipzig, A. Richtering., *Progress in Colloid and Polymer Science*, 2009, **136**, 1-47.
12. J. P. Congqi Y. and Darrin, 2010, **39**, 3528-3540.
13. T. Vermonden, R. Censi and W. E. Hennink, *Chemical Reviews*, 2012, **112**, 2853-2888.
14. C. Yan and D. J. Pochan, *Chemical Society Reviews*, 2010, **39**, 3528-3540.
15. W. N. E. van Dijk-Wolthuis, O. Franssen, H. Talsma, M. J. van Steenbergen, J. J. Kettenes-van den Bosch and W. E. Hennink, *Macromolecules*, 1995, **28**, 6317-6322.
16. H. F. A. B. Lodish, S Lawrence Zipursky, Paul Matsudaira, David Baltimore, and James Darnell., *Molecular cell biology [electronic book] / Harvey Lodish ... [et al.]*, New York : W.H. Freeman, c2000. 4th ed., 2000.
17. J. L. I. a. J. A. Burdick, *Tissue Engineering.* , 2007, **13**, 2369-2385.
18. F. M. Menger and K. L. Caran, *Journal of the American Chemical Society*, 2000, **122**, 11679-11691.
19. V. Javvaji, A. G. Baradwaj, G. F. Payne and S. R. Raghavan, *Langmuir*, 2011, **27**, 12591-12596.
20. M. Reches and E. Gazit, *Science*, 2003, **300**, 625-627.
21. V. Jayawarna, S. M. Richardson, A. R. Hirst, N. W. Hodson, A. Saiani, J. E. Gough and R. V. Ulijn, *Acta Biomaterialia*, 2009, **5**, 934-943.
22. G. C. Maity, *Journal of physical sciences*, 2008, **12**, 173-186.
23. J. H. van Esch, *Langmuir*, 2009, **25**, 8392-8394.
24. J. Raeburn, A. Zamith Cardoso and D. J. Adams, *Chemical Society Reviews*, 2013, **42**, 5143-5156.
25. K. A. Houton, K. L. Morris, L. Chen, M. Schmidtman, J. T. A. Jones, L. C. Serpell, G. O. Lloyd and D. J. Adams, *Langmuir*, 2012, **28**, 9797-9806.
26. J. Raeburn, G. Pont, L. Chen, Y. Cesbron, R. Levy and D. J. Adams, *Soft Matter*, 2012, **8**, 1168-1174.
27. E. K. Johnson, D. J. Adams and P. J. Cameron, *Journal of Materials Chemistry*, 2011, **21**, 2024-2027.
28. L. Chen, S. Revel, K. Morris, D. G. Spiller, L. C. Serpell and D. J. Adams, *Chemical Communications*, 2010, **46**, 6738-6740.
29. L. Chen, S. Revel, K. Morris, L. C. Serpell and D. J. Adams, *Langmuir*, 2010, **26**, 13466-13471.

30. L. Chen, K. Morris, A. Laybourn, D. Elias, M. R. Hicks, A. Rodger, L. Serpell and D. J. Adams, *Langmuir*, 2009, **26**, 5232-5242.
31. D. J. Adams and P. D. Topham, *Soft Matter*, 2010, **6**, 3707-3721.
32. D. J. Adams, L. M. Mullen, M. Berta, L. Chen and W. J. Frith, *Soft Matter*, 2010, **6**, 1971-1980.
33. D. J. Adams, M. F. Butler, W. J. Frith, M. Kirkland, L. Mullen and P. Sanderson, *Soft Matter*, 2009, **5**, 1856-1862.
34. D. J. Adams, *Macromolecular Bioscience*, 2011, **11**, 160-173.
35. Z. Yang, G. Liang and B. Xu, *Accounts of Chemical Research*, 2008, **41**, 315-326.
36. Z. Yang, G. Liang and B. Xu, *Chemical Communications*, 2006, 738-740.
37. J. Shi, Y. Pan, Y. Gao and B. Xu, *MRS Online Proceedings Library*, 2012, **1418**, mrsf11-1418-1l1406-1403 doi:1410.1557/opl.2012.1331.
38. G. Pont, L. Chen, D. G. Spiller and D. J. Adams, *Soft Matter*, 2012, **8**, 7797-7802.
39. B. Adhikari and A. Banerjee, *Soft Matter*, 2011, **7**, 9259-9266.
40. L. Chen, J. Raeburn, S. Sutton, D. G. Spiller, J. Williams, J. S. Sharp, P. C. Griffiths, R. K. Heenan, S. M. King, A. Paul, S. Furzeland, D. Atkins and D. J. Adams, *Soft Matter*, 2011, **7**, 9721-9727.
41. L. Chen, S. Revel, K. Morris, L. C. Serpell and D. J. Adams, *Langmuir*, 2010, **26**, 13466-13471.
42. F. Zhao, Y. Gao, J. Shi, H. M. Browdy and B. Xu, *Langmuir*, 2010, **27**, 1510-1512.
43. C. Colquhoun, E. R. Draper, E. G. B. Eden, B. N. Cattoz, K. L. Morris, L. Chen, T. O. McDonald, A. E. Terry, P. C. Griffiths, L. C. Serpell and D. J. Adams, *Nanoscale*, 2014, **6**, 13719-13725.
44. M. de Loos, B. L. Feringa and J. H. van Esch, *European Journal of Organic Chemistry*, 2005, **2005**, 3615-3631.
45. C. Tang, A. M. Smith, R. F. Collins, R. V. Ulijn and A. Saiani, *Langmuir*, 2009, **25**, 9447-9453.
46. A. M. Smith, R. J. Williams, C. Tang, P. Coppo, R. F. Collins, M. L. Turner, A. Saiani and R. V. Ulijn, *Advanced Materials*, 2008, **20**, 37-41.
47. K. L. Morris, L. Chen, J. Raeburn, O. R. Sellick, P. Cotanda, A. Paul, P. C. Griffiths, S. M. King, R. K. O'Reilly, L. C. Serpell and D. J. Adams, *Nature Communications* 2013, **4**, 1480.
48. Z. Yang, G. Liang, M. Ma, Y. Gao and B. Xu, *Journal of Materials Chemistry*, 2007, **17**, 850-854.
49. Y. Pocker and E. Green, *Journal of the American Chemical Society*, 1973, **95**, 113-119.
50. A. Aufderhorst-Roberts, W. J. Frith and A. M. Donald, *Soft Matter*, 2012, **8**, 5940-5946.
51. H. Wang, C. Ren, Z. Song, L. Wang, X. Chen and Z. Yang, *Nanotechnology*, 2010, **21**, 1-5.
52. Z. Yang, H. Gu, D. Fu, P. Gao, J. K. Lam and B. Xu, *Advanced Materials*, 2004, **16**, 1440-1444.
53. S. Toledano, R. J. Williams, V. Jayawarna and R. V. Ulijn, *Journal of the American Chemical Society*, 2006, **128**, 1070-1071.
54. X. Li, Y. Gao, Y. Kuang and B. Xu, *Chemical Communications*, 2010, **46**, 5364-5366.
55. A. K. Das, R. Collins and R. V. Ulijn, *Small*, 2008, **4**, 279-287.
56. D. Dasgupta, S. Srinivasan, C. Rochas, A. Ajayaghosh and J. M. Guenet, *Langmuir*, 2009, **25**, 8593-8598.
57. R. Vegners, I. Shestakova, I. Kalvinsh, R. M. Ezzell and P. A. Janmey, *Journal of Peptide Science*, 1995, **1**, 371-378.
58. S. Debnath, A. Shome, D. Das and P. K. Das, *The Journal of Physical Chemistry B*, 2010, **114**, 4407-4415.
59. L. Chen, T. O. McDonald and D. J. Adams, *RSC Advances*, 2013, **3**, 8714-8720.
60. S. Roy, N. Javid, J. Sefcik, P. J. Halling and R. V. Ulijn, *Langmuir*, 2012, **28**, 16664-16670.
61. L. Chen, G. Pont, K. Morris, G. Lotze, A. Squires, L. C. Serpell and D. J. Adams, *Chemical Communications*, 2011, **47**, 12071-12073.
62. V. Jayawarna, M. Ali, T. A. Jowitt, A. F. Miller, A. Saiani, J. E. Gough and R. V. Ulijn, *Advanced Materials*, 2006, **18**, 611-614.

63. R. V. Ulijn and A. M. Smith, *Chemical Society Reviews*, 2008, **37**, 664-675.
64. J. Raeburn, T. O. McDonald and D. J. Adams, *Chemical Communications*, 2012, **48**, 9355-9357.
65. E. K. Johnson, D. J. Adams and P. J. Cameron, *Journal of the American Chemical Society*, 2010, **132**, 5130-5136.
66. A. R. Hirst, I. A. Coates, T. R. Boucheteau, J. F. Miravet, B. Escuder, V. Castelletto, I. W. Hamley and D. K. Smith, *Journal of the American Chemical Society*, 2008, **130**, 9113-9121.
67. W. T. Truong, Y. Su, J. T. Meijer, P. Thordarson and F. Braet, *Chemistry – An Asian Journal*, 2011, **6**, 30-42.
68. S. Banerjee, R. K. Das and U. Maitra, *Journal of Materials Chemistry*, 2009, **19**, 6649-6687.
69. Y. Wang, Z. Zhang, L. Xu, X. Li and H. Chen, *Colloids and Surfaces B: Biointerfaces*, 2013, **104**, 163-168.
70. G. Cheng, V. Castelletto, R. R. Jones, C. J. Connon and I. W. Hamley, *Soft Matter*, 2011, **7**, 1326-1333.
71. L. Chen, S. Revel, K. Morris and D. J. Adams, *Chemical Communications*, 2010, **46**, 4267-4269.
72. Y. Zhang, H. Gu, Z. Yang and B. Xu, *Journal of the American Chemical Society*, 2003, **125**, 13680-13681.
73. Y. Zhang, Z. Yang, F. Yuan, H. Gu, P. Gao and B. Xu, *Journal of the American Chemical Society*, 2004, **126**, 15028-15029.
74. K. H. Scott L Jones, Pall Thordarson and Francois Ladouceur, *Journal of Physics: Condensed Matter*, 2010, **22**, 1-7.
75. D. J. Adams and I. Young, *Journal of Polymer Science Part A: Polymer Chemistry*, 2008, **46**, 6082-6090.
76. B. Adhikari and A. Banerjee, *Chemistry – A European Journal*, 2010, **16**, 13698-13705.
77. R. J. Williams, A. M. Smith, R. Collins, N. Hodson, A. K. Das and R. V. Ulijn, *Nat Nano*, 2009, **4**, 19-24.
78. M. O. Guler, R. C. Claussen and S. I. Stupp, *Journal of Materials Chemistry*, 2005, **15**, 4507-4512.
79. Y. Kuang and B. Xu, *Angewandte Chemie International Edition*, 2013, **52**, 6944-6948.
80. Y. Kuang, Y. Gao, J. Shi, J. Li and B. Xu, *Chemical Communications*, 2014, **50**, 2772-2774.
81. A. Z. Cardoso, A. E. Alvarez Alvarez, B. N. Cattoz, P. C. Griffiths, S. M. King, W. J. Frith and D. J. Adams, *Faraday Discussions*, 2013, **166**, 101-116.
82. M. Wallace, D. J. Adams and J. A. Iggo, *Soft Matter*, 2013, **9**, 5483-5491.
83. M. A. V. Jayawarna, T. A. Jowitt, A. E. Miller, A. Saiani, J. E. Gough and R. V. Ulijn *Advance Mater*, 2006, **18**, 611-614.
84. D. Rizkov, J. Gun, O. Lev, R. Sicsic and A. Melman, *Langmuir*, 2005, **21**, 12130-12138.
85. A. Ajayaghosh, V. K. Praveen and C. Vijayakumar, *Chemical Society Reviews*, 2008, **37**, 109-122.
86. L. Zang, Y. Che and J. S. Moore, *Accounts of Chemical Research*, 2008, **41**, 1596-1608.
87. K. V. Rao, K. K. R. Datta, M. Eswaramoorthy and S. J. George, *Angewandte Chemie International Edition*, 2011, **50**, 1179-1184.
88. K. V. Rao, K. K. R. Datta, M. Eswaramoorthy and S. J. George, *Chemistry – A European Journal*, 2012, **18**, 2184-2194.
89. V. D. Rao, K. Eswaramoorthy, M. and George, S. , *Angew. Chem. Int. Ed.*, 2010, **49**, 1-7.
90. K. J. Channon, G. L. Devlin and C. E. MacPhee, *Journal of the American Chemical Society*, 2009, **131**, 12520-12521.
91. M. Montalti, L. S. Dolci, L. Prodi, N. Zaccheroni, M. C. A. Stuart, K. J. C. van Bommel and A. Friggeri, *Langmuir*, 2006, **22**, 2299-2303.
92. A. L. Olive, A. Guerzo, C. Belin, J. Reichwagen, H. Hopf and J.-P. Desvergne, *Research on Chemical Intermediate*, 2008, **34**, 137-145.
93. B. Adhikari, J. Nanda and A. Banerjee, *Chemistry – A European Journal*, 2011, **17**, 11488-11496.
94. C. Tang, R. Ulijn and A. Saiani, *The European Physical Journal* 2013, **36**, 1-11.

95. S. R. Thomas Liebmann, Victor Akpe and Hjalmar Brismar, *BMC Biotechnol.*, 2007, **7**, 1-11.
96. S. Sutton, N. L. Campbell, A. I. Cooper, M. Kirkland, W. J. Frith and D. J. Adams, *Langmuir*, 2009, **25**, 10285-10291.
97. C. K. He, Sung Wan; Lee, Doo Sung, *J. Controlled Release*, 2008, **127**, 189-207.
98. T. R. K. Hoare, Daniel S., *Polymer*, 2008, **49**, 1993-2007.
99. J. J. Panda, A. Mishra, A. Basu and V. S. Chauhan, *Biomacromolecules*, 2008, **9**, 2244-2250.
100. S. Koutsopoulos and S. Zhang, *Journal of Controlled Release*, 2012, **160**, 451-458.
101. F. Bierbrauer, *Hydrogel Drug Delivery: Diffusion Models*, 2012.
102. Y. Nagai, L. D. Unsworth, S. Koutsopoulos and S. Zhang, *Journal of Controlled Release*, 2006, **115**, 18-25.
103. P. L. P. Ritger, Nikolaos A., *Journal of Controlled Release*, 1987, **5**, 23-36.
104. R. Huang, W. Qi, L. Feng, R. Su and Z. He, *Soft Matter*, 2011, **7**, 6222-6230.
105. G. Liang, Z. Yang, R. Zhang, L. Li, Y. Fan, Y. Kuang, Y. Gao, T. Wang, W. W. Lu and B. Xu, *Langmuir*, 2009, **25**, 8419-8422.

CHAPTER 2

Dipeptide synthesis

2- Dipeptide synthesis:

2.1- Introduction:

Peptides can be synthesised by coupling the carboxylic acid (or C-terminus) of one amino acid to the amino group (or N-terminus) of another¹⁻⁴. Functionalised dipeptides can be prepared by solution-phase^{2, 3, 5-8} and solid-phase^{3, 5, 9, 10} amino acid coupling techniques. In solid phase peptide synthesis (SPPS), the C-terminus of the first amino acid is coupled with a solid support and N-terminus remains free to react with C-terminus of the second amino acid. This method is useful to synthesise peptides with medium sequence (up to 50 residues)^{3, 5, 10}. The protecting group is then removed and the peptide sequence obtained. In the solution phase method, a chemical protecting group is used to protect C-terminus of the first amino acid which is then dissolved in an appropriate organic solvent to continue with the synthesis steps to produce the peptide sequence. This method is normally used to synthesise short peptide sequences (up to 10 residues)^{3, 5}. Different reagents including *N,N*-dicyclohexylcarbodiimide (DCC)^{5, 11} and isobutylchloroformate (IBCF)^{12, 13} have been used to couple the amino acids and form the peptide. The DCC coupling method uses hydroxylbenzotriazole (HOBT) catalyst and *N*-methylmorpholine (NMM), whereas IBCF can be used directly as the coupling agent^{13, 14}. The 9-fluorenyl methyloxycarbony group (Fmoc group) has had great attention as a protecting group in the peptide synthesis field^{4, 15}. Fmoc peptide derivatives have been synthesised using different methods¹⁵. For example, FmocLG (L = Leucine, G = Glycine) was synthesised using IBCF method in the solution phase strategy, followed by the deprotection of the *t*-butyl group by dissolving the Fmoc-dipeptide in chloroform in the presence of trifluoroacetic acid (TFA)^{12, 16}. Other dipeptides conjugated to Fmoc have been synthesised elsewhere^{3, 4, 7, 11, 12, 16-18}, such as FmocFG¹⁶ (F = Phenylalanine), FmocVD⁸ (V = Valine, D = Aspartic acid) and FmocFF¹⁷. Furthermore naphthalene dipeptides have been synthesised previously¹⁹⁻²¹. In this project, we have used the IBCF method to synthesise functionalised dipeptide derivatives with different aromatic protecting groups such as naphthalene, anthracene, pyrene, phenanthrol, anthraquinone and carbazole in order to study their ability to form gel and their properties.

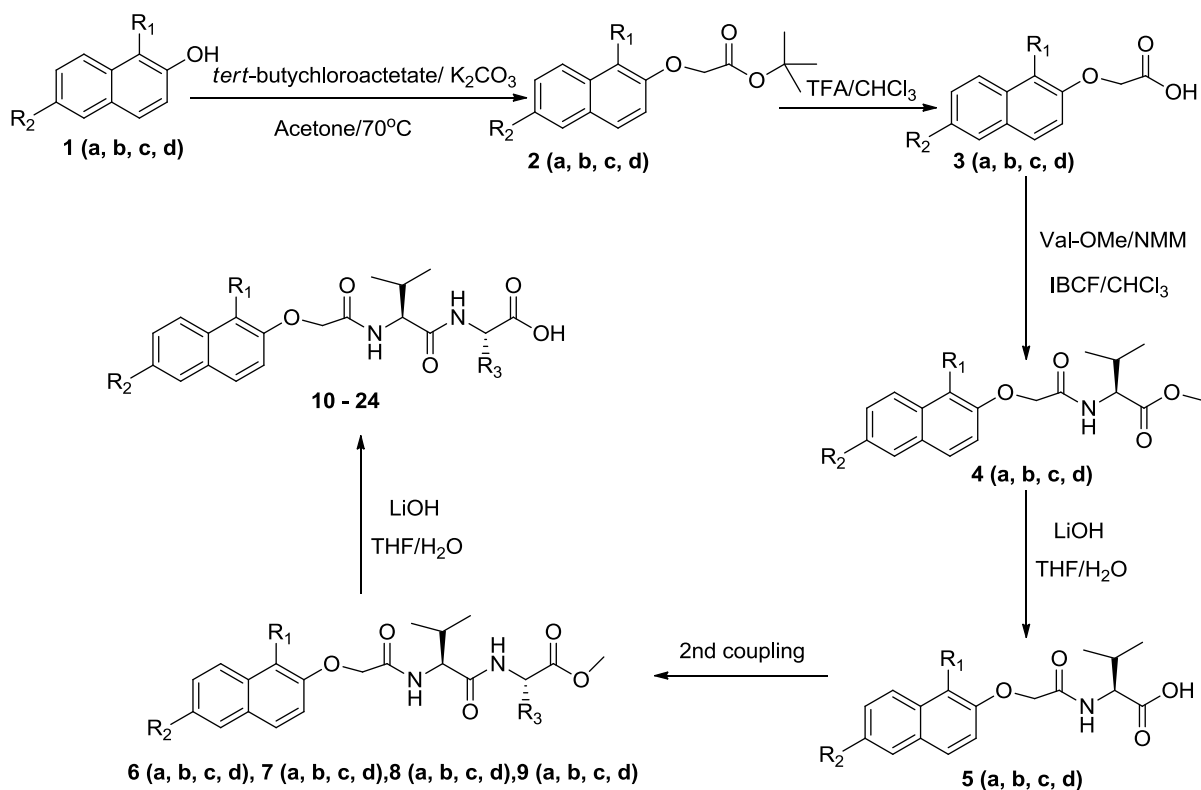
2.2- Dipeptide synthesis:

2.2.1- Naphthalene dipeptides:

As stated, naphthalene dipeptides have been synthesised previously using IBCF and DCC methods^{5, 11-13}. In this project, a large number of naphthalene dipeptides were synthesised. We have used valine methyl ester hydrochloride in the first coupling of naphthalene dipeptide synthesis because it is a hydrophobic amino acid expected to help form good hydrogels as demonstrated in previous research¹⁹. In the second coupling step, three different amino acids, valine methyl ester, alanine methyl ester, glycine methyl ester and phenylalanine ethyl ester hydrochloride were used, because they have different hydrophobicity, which is expected to be an important factor for hydrogelators according to previous literature^{14, 19-22}. These amino acids were used to synthesise naphthalene dipeptides with different orders of the amino acids and different positions of substitution because small changes in the molecular structure can change the mechanical properties of the hydrogel¹⁴. We aimed to prepare a library of gels in order to study some applications such as energy transfer and drug delivery.

From naphthol:

According to Chen's research, naphthalene was coupled to the amino acids using different linkers, $-\text{CH}_2$ and $-\text{OCH}_2$, because this can affect the formation of the hydrogel¹⁴. Here, we have linked the naphthalene to amino acids by $-\text{OCH}_2$ as shown in the Scheme 2.1.



Scheme 2.1: The general reaction of naphthalene dipeptide synthesis based on naphthol ring using IBCF method.

Compound					Functional group	
1	2	3	4	5	R ₁	R ₂
a	a	a	a	a	H	H
b	b	b	b	b	H	Br
c	c	c	c	c	Br	Br
d	d	d	d	d	Br	H

Table 2.1: R₁ and R₂ groups of the general structure of compounds 1 - 5 in the Scheme 2.1.

Compound	R ₁	R ₂	R ₃			
			a	b	c	d
6	H	H	CH(CH ₃) ₂	CH ₃	H	CH ₂ Ph
7	H	Br	CH(CH ₃) ₂	CH ₃	H	CH ₂ Ph
8	Br	Br	CH(CH ₃) ₂	CH ₃	H	CH ₂ Ph
9	Br	H	CH(CH ₃) ₂	CH ₃	H	CH ₂ Ph

Table 2.2: R₁, R₂ and R₃ groups of the general structure of compounds 6 - 9 in the Scheme 2.1.

Dipeptides	R₁	R₂	R₃	Abbreviation
10	H	H	CH(CH ₃) ₂	2nap-VVOH
11	H	H	CH ₃	2nap-VAOH
12	H	H	H	2nap-VGH
13	H	H	CH ₂ Ph	2nap-VFOH
14	H	Br	CH(CH ₃) ₂	6Brnap-VVOH
15	H	Br	CH ₃	6Brnap-VAOH
16	H	Br	H	6Brnap-VGOH
17	H	Br	CH ₂ Ph	6Brnap-VFOH
18	Br	Br	CH(CH ₃) ₂	1,6diBrnap-VVOH
19	Br	Br	CH ₃	1,6diBrnap-VAOH
20	Br	Br	H	1,6diBrnap-VGOH
21	Br	Br	CH ₂ Ph	1,6diBrnap-VFOH
22	Br	H	CH(CH ₃) ₂	1Brnap-VVOH
23	Br	H	CH ₃	1Brnap-VAOH
24	Br	H	H	1Brnap-VGOH
25	Br	H	CH ₂ Ph	1Brnap-VFOH

Table 2.3: R₁, R₂ and R₃ groups of the general structure of compounds 10 – 25 in the Scheme 2.1 and their abbreviation.

Experimental section:

Materials: All chemicals were purchased from Sigma-Aldrich and used as received without purification.

NMR: ^1H NMR spectra were recorded at 400.13 MHz using a Bruker Avance 400 NMR spectrometer. ^{13}C NMR spectra were recorded at 400.1 MHz.

Mass spectroscopy: Mass spectroscopies were recorded by the University of Liverpool mass spectroscopy service using Micromass LCT Mass Spectrometer and Trio-1000 Mass Spectrometer.

Synthesis

A general method to prepare dipeptides used by Chen *et al.*⁸ was followed.

To a stirred solution of 2-naphthol, 1-bromo-2-naphthol, 6-bromo-2-naphthol or 1,6-dibromo-2-naphthol (10.0 g) and K_2CO_3 (3 eq.) in acetone (200 mL) was added *tert*-butyl chloroacetate (1.1 eq.) and the solution was heated to reflux at 70 °C overnight. Chloroform (200 mL) was added to the resulting suspension in a separating funnel and water (100 mL) added. Then, the organic phase was washed with water (4 x 200 mL). The solution was dried with magnesium sulphate and the solvent was removed *in vacuo* to give compounds **2 (a – d)** as shown in the Scheme 2.1 that have different R groups as shown in the Table 2.1. The yield was between 73 – 87% and the impurity (*tert*-butyl chloroacetate) was calculated by NMR spectroscopy to be between 7 – 13%. The resulting product was then purified using flash column chromatography (10% ethyl acetate in hexane). The yield was typically 60 – 70% and the final product was between 94 - 99% pure.

^1H , ^{13}C NMR and mass spectroscopy of the resulting products:

Tert-Butyl-2-(naphthalen-2-yloxy) acetate (2a):

^1H NMR (CDCl_3): 7.75 (d, ArH, 1H, $^3\text{J}_{\text{HH}} = 8.1\text{Hz}$), 7.73(d, ArH, 1H, $^3\text{J}_{\text{HH}} = 8.9\text{Hz}$), 7.67 (d, ArH, 1H, $^3\text{J}_{\text{HH}} = 8.2\text{Hz}$), 7.40 (t, ArH, 1H, $^3\text{J}_{\text{HH}} = 6.9\text{Hz}$), 7.31(t, ArH, 1H, 6.8Hz), 7.22 (dd, ArH, 1H, $^3\text{J}_{\text{HH}} = 8.9$), 7.04 (d, ArH, 1H, $^3\text{J}_{\text{HH}} = 2.6\text{Hz}$), 4.60 (s, $\text{OCH}_2\text{C}=\text{O}$, 2H), 1.48 (s, $\text{C}(\text{CH}_3)_3$, 9H) ppm. ^{13}C NMR (CDCl_3): 168.0, 155.8, 134.3, 129.6, 129.3, 127.7, 126.8,

126.4, 124.0, 118.6, 109.4, 107.1, 82.4, 65.8, 28.0 ppm. MS: ES⁺: [M+Na]⁺. Accurate mass calculated: 281.1155 Found 281.1154.

Tert-Butyl-2-(6-bromonaphthalen-2-yloxy) acetate (2b):

¹H NMR (CDCl₃): 7.91 (s, ArH, 1H), 7.67(d, ArH, 1H, ³J_{HH} = 9.1Hz), 7.57 (d, ArH, 1H, ³J_{HH} = 8.8Hz), 7.50 (d, ArH, 1H, ³J_{HH} = 2.0Hz), 7.24(d, ArH, 1H, ³J_{HH} = 2.6Hz), 7.02 (s, ArH, 1H, ³J_{HH} = 2.6Hz), 4.61 (s, OCH₂C=O, 2H), 1.49 (s, OC(CH₃)₃, 9H) ppm. ¹³C NMR (CDCl₃): 167.7, 156.1, 132.7, 130.3, 129.7 (d, j = 7.2 Hz), 128.7, 128.4, 119.6, 117.4, 107.0, 82.5, 65.7, 28.06, 27.9 ppm. MS: ES⁺ ([M+Na]⁺). Accurate mass calculated: 359.0259. Found 359.0262.

Tert-Butyl-2-(1,6-dibromonaphthalen-2-yloxy)acetate (2c):

¹H NMR (CDCl₃): 8.08(d, ArH, 1H, ³J_{HH} = 9.5Hz), 7.90(d, ArH, 1H, ³J_{HH} = 2.0Hz), 7.65 (d, ArH, 1H, ³J_{HH} = 8.1Hz), 7.60 (d, ArH, 1H, ³J_{HH} = 5.4Hz), 7.12(d, ArH, 1H, ³J_{HH} = 8.8Hz), 4.71 (s, OCH₂C=O, 2H), 1.47 (s, OC (CH₃)₃, 9H)ppm. ¹³C NMR (CDCl₃): 203.5, 167.4, 152.7, 131.8, 131.09, 131.06, 129.8, 128.3, 127.8, 118.7, 115.6, 109.9, 82.7, 67.2, 30.7, 28.05 ppm. MS: ES⁺: [M+Na]⁺. Accurate mass calculated: 436.9364. Found 436.9370.

Tert-Butyl-2-(1-bromonaphthalen-2-yloxy) acetate (2d):

¹H NMR (CDCl₃): 8.10 (d, ArH, 1H, ³J_{HH} = 11.7Hz), 7.71(d, ArH, 1H, ³J_{HH} = 9.3Hz), 7.52 (t, ArH, 1H, ³J_{HH} = 8.1Hz), 7.35 (t, ArH, 1H, ³J_{HH} = 8.1Hz), 7.12(d, ArH, 1H, ³J_{HH} = 9.3Hz), 4.68 (s, OCH₂C=O, 2H), 1.45 (s, OC(CH₃)₃, 9H) ppm. ¹³C NMR (CDCl₃): 167.6, 152.5, 133.1, 130.2, 128.8, 128.0, 127.8, 126.4, 124.7, 114.8, 109.8, 82.5, 67.3, 41.9, 28.0, 27.7 ppm. MS: ES⁺: [M+Na]⁺. Accurate mass calculated: 359.0267 Found 359.0259.

Removal of the *tert*-butyl protection group:

The *tert*-butyl naphthalene acetate derivatives were dissolved in chloroform (30 mL), and trifluoroacetic acid (10 mL) was added. The solution was stirred overnight. Hexane was added to the solution, and then the resulting precipitate was collected by filtration to give compounds **3 (a – d)** as shown in the Scheme 2.1, with different R groups as shown in the Table 2.1. The yield was between 87 – 90%. The resulting products of all derivatives were pure and used directly in the next step of the reaction.

2-Naphthalen-2-yloxy acetic acid (3a):

¹H NMR (d₆-DMSO): 7.84 (d, ArH, 1H, ³J_{HH} = 8.2Hz), 7.79(d, ArH, 1H, ³J_{HH} = 8.2Hz), 7.46 (t, ArH, 1H, ³J_{HH} = 6.9Hz), 7.35 (t, ArH, 1H, ³J_{HH} = 6.9), 7.27(s, ArH, 1H,), 7.20 (dd, ArH, 1H, ³J_{HH} = 8.9), 7.19 (d, ArH, 1H,), 4.78 (s, OCH₂C=O, 2H), 13.7 (s, OH) ppm. ¹³C NMR (d₆-DMSO): 170.4, 155.9, 134.4, 129.7, 129.04, 127.86, 127.09, 126.82, 124.15, 118.80, 107.35, 64.89 ppm. MS: CI: Low resolution [NH₄⁺] found 202.2.

2-(6-Bromonaphthalen-2-yloxy) acetic acid (3b):

¹H NMR (d₆-DMSO): 8.12 (s, ArH, 1H,), 7.84(d, ArH, 1H, ³J_{HH} = 9.1Hz), 7.77 (d, ArH, 1H, ³J_{HH} = 8.8Hz), 7.56 (d, ArH, 1H, ³J_{HH} = 2.2Hz), 7.31(d, ArH, 1H, ³J_{HH} = 2.6Hz), 7.26 (d, ArH, 1H, ³J_{HH} = 2.6Hz), 4.81 (s, OCH₂C=O, 2H), 13.7 (s, OH) ppm. ¹³C NMR (d₆-DMSO): 169.8, 156.0, 132.6, 129.8, 129.3, 129.2, 128.9, 128.6, 119.5, 116.4, 107.1, 64.5 ppm. MS: ES⁻: [M - H]⁻. Accurate mass calculated: 302.9633. Found 302.9619

2-(1,6-Dibromonaphthalen-2-yloxy) acetic acid (3c):

¹H NMR (d₆-DMSO): 8.22 (d, ArH, 1H, ³J_{HH} = 2.0Hz), 8.02(d, ArH, 1H, ³J_{HH} = 9.1Hz), 7.95 (d, ArH, 1H, ³J_{HH} = 9.0Hz), 7.73 (d, ArH, 1H, ³J_{HH} = 9.0Hz), 7.45(d, ArH, 1H, ³J_{HH} = 9.1Hz), 4.98 (s, OCH₂C=O, 2H), 13.18 (s, OH) ppm. ¹³C NMR (d₆-DMSO): 169.8, 152.8, 144.1, 131.08, 129.9, 128.2, 127.6, 117.4, 115.8, 107.1, 65.5, 30.2 ppm. MS: ES⁻: [M - H]⁻. Accurate mass calculated: 380.8738. Found 380.8739.

2-(1-Bromonaphthalen-2-yloxy) acetic acid (3d):

¹H NMR (d₆-DMSO):8.10 (s, ArH, 1H,), 7.96(d, ArH, 1H, ³J_{HH} = 9.0Hz), 7.93(d, ArH, 1H, ³J_{HH} = 9.1Hz), 7.63 (d, ArH, 1H, ³J_{HH} = 8.2Hz), 7.46(d, ArH, 1H, ³J_{HH} = 9.1Hz), 7.40 (d, ArH, 1H,), 4.97(s, OCH₂C=O, 2H), 13.7 (s, OH) ppm. ¹³C NMR (d₆-DMSO): 170.3, 152.7, 132.6, 129.8, 129.4, 128.6, 128.5, 125.6, 124.8, 115.0, 107.6, 65.9 ppm. MS: ES⁻: [M - H]⁻. Accurate mass calculated: 278.9657. Found 278.9662.

Standard coupling methodology:

N-Methylmorpholine (2 eq.) and IBCF (1.1 eq.) was added to compound **3 (a, b, c or d)** (5.0 g) in chloroform (70 mL) at 0 °C. A solution of valine methyl ester (1.5 eq.) and NMM (2 eq.) in chloroform was added. The solution was stirred at room temperature overnight. The solution was washed with distilled water (100 mL), hydrochloric acid (2

x 100 mL, 0.1 M), aqueous potassium carbonate (100 mL, 0.1 M), and distilled water (4 x 100 mL) and dried with magnesium sulfate. The solvent was removed *in vacuo* to give compounds **4(a - d)** as shown in Scheme 2.1 that have different R groups as shown in the Table 2.1. The yield was between 77 - 85%. The impurity (an excess of valine methyl ester) was calculated by NMR spectroscopy to be between 15 - 29% for all derivatives except compounds **4a** and **4b**, which were pure and used as a crude product in the next step of the reaction. The resulting product was then purified by washing with methanol. The yield decreased typically between 55 - 65% and the purity was calculated by NMR spectroscopy between 87 - 98%.

(S)-Methyl-2-(2-(naphthalen-2-yloxy) acetamido) butanoate (4a):

¹H NMR (CDCl₃): 7.73 (d, ArH, 1H, ³J_{HH} = 8.6Hz), 7.68 (d, ArH, 1H, ³J_{HH} = 8.1Hz), 7.41 (t, ArH, 1H, ³J_{HH} = 7.0Hz), 7.33 (t, ArH, 1H, ³J_{HH} = 8.3Hz), 7.26(s, ArH, 1H,), 7.18 (d, ArH, 1H, ³J_{HH} = 10.4Hz), 7.13 (d, ArH, 1H, ³J_{HH} = 11.0Hz), 4.65(d, NHCHCH(CH₃)₂, 1H, ³J_{HH} = 4.8Hz), 4.16 (d, OCH₂C=O, 2H, ³J_{HH} = 4.1Hz), 3.67 (s, OCH₃, 3H), 2.18 (m, (CH₃)₂CH, 1H), 0.92(d,(CH₃)₂CH, 3H, ³J_{HH} = 7.4Hz), 0.89 (d,(CH₃)₂CH, 3H, ³J_{HH} = 6.8Hz) ppm.¹³C NMR (CDCl₃): 171.9, 168.09, 155.03, 134.27, 129.8, 129.5, 127.6, 126.9, 126.7, 124.3, 118.1, 107.7, 67.3, 56.7, 52.1, 31.2, 18.9, 17.7 ppm. MS: ES⁺: [M+Na]⁺. Accurate mass calculated: 338.1368 Found 338.1384.

(S)-Methyl-2-(2-((6bromonaphthalen-2-yl)oxy)acetamido)-3-methylbutanoate (4b):

¹H NMR (CDCl₃): 7.91 (s, ArH, 1H,), 7.68 (d, ArH, 1H, ³J_{HH} = 8.9Hz), 7.59 (d, ArH, 1H, ³J_{HH} = 9.0Hz), 7.50 (d, ArH, 1H, ³J_{HH} = 9.4Hz), 7.23(d, ArH, 1H, ³J_{HH} = 10.1Hz), 7.12 (d, ArH, 1H, ³J_{HH} = 2.4Hz), 6.5(d, NH, 1H, ³J_{HH} = 10.1Hz), 4.68 (s, OCH₂C=O, 2H), 4.60 (m, NHCHCH(CH₃)₂, 1H), 3.72 (s, OCH₃, 3H), 2.23 (m, (CH₃)₂CH, 1H) 0.93 d,(CH₃)₂CH, 3H, ³J_{HH} = 8.7Hz), 0.88 (d,(CH₃)₂CH, 3H, ³J_{HH} = 7.7Hz) ppm.¹³C NMR (CDCl₃): 171.9, 167.8, 155.2, 132.7, 130.5, 130.0, 129.7, 129.0, 128.6, 119.2, 117.9, 107.7, 67.3, 56.6, 52.2, 31.3, 18.9, 17.7 ppm. MS: ES⁺: [M+Na]⁺. Accurate mass calculated: 416.0473 Found 416.0473.

(S)-Methyl-2-(2-((1,6-dibromonaphthalen-2-yl)oxy)acetamido)-3-methylbutanoate (4c):

¹H NMR (CDCl₃):8.08 (d, ArH, 1H, , ³J_{HH} = 9.0Hz), 7.96 (d, ArH, 1H, , ³J_{HH} = 2.1Hz), 7.74 (d, ArH, 1H, , ³J_{HH} = 9.5Hz), 7.55 (d, NH, 1H, , ³J_{HH} = 6.1Hz), 7.64(d, ArH, 1H, , ³J_{HH} = 7.4Hz),

7.20 (d, ArH, 1H, , $^3J_{\text{HH}} = 9.0\text{Hz}$), 4.70 (s, $\text{OCH}_2\text{C}=\text{O}$, 2H), 4.66 (dd, $\text{NHCHCH}(\text{CH}_3)_2$, 1H, $^3J_{\text{HH}} = 5.4, 4.7\text{Hz}$), 3.77 (s, OCH_3 , 3H), 2.29 (m, $(\text{CH}_3)_2\text{CH}$, 1H), 1.00 (d, $(\text{CH}_3)_2\text{CH}$, 3H, $^3J_{\text{HH}} = 8.2\text{Hz}$), 0.99 (d, $(\text{CH}_3)_2\text{CH}$, 3H, $^3J_{\text{HH}} = 7.1\text{Hz}$)ppm. ^{13}C NMR (CDCl_3): 171.7, 167.3, 155.0, 131.5, 131.4, 131.2, 130.0, 128.5, 128.1, 119.0, 115.3, 82.5, 68.5, 56.8, 52.2, 31.2, 19.0, 17.6 ppm. (CDCl_3): MS: ES⁺: $[\text{M}+\text{Na}]^+$. Accurate mass calculated: 493.9579 Found 493.9593.

(S)-Methyl-2-(2-((1-bromonaphthalen-2-yl)oxy)acetamido)-3-methylbutanoate (4d):

^1H NMR (CDCl_3): 8.22 (d, ArH, 1H, $^3J_{\text{HH}} = 8.9$), 7.85 (d, ArH, 1H, $^3J_{\text{HH}} = 8.9$), 7.81 (d, ArH, 1H, $^3J_{\text{HH}} = 8.3$), 7.61 (t, ArH, 1H, $^3J_{\text{HH}} = 6.4$), 7.45(t, ArH, 1H, $^3J_{\text{HH}} = 7.2$), 7.20 (d, ArH, 1H, $^3J_{\text{HH}} = 8.9$), 4.71 (s, $\text{OCH}_2\text{C}=\text{O}$, 2H), 4.67 (dd, $\text{NHCHCH}(\text{CH}_3)_2$, 1H, $^3J_{\text{HH}} = 5.9, 4.1$), 3.76 (s, OCH_3 , 3H), 2.29 (m, $(\text{CH}_3)_2\text{CH}$, 1H), 1.01 (d, $(\text{CH}_3)_2\text{CH}$, 3H, $^3J_{\text{HH}} = 6.7\text{Hz}$), 0.99 (d, $(\text{CH}_3)_2\text{CH}$, 3H, $^3J_{\text{HH}} = 7.3$) ppm. ^{13}C NMR (CDCl_3): 171.7, 167.5, 151.4, 132.9, 130.4, 129.4, 128.2, 128.1, 126.2, 125.0, 114.3, 109.6, 68.6, 56.8, 52.2, 31.2, 19.0, 17.7 ppm. MS: ES⁺: $[\text{M}+\text{Na}]^+$. Accurate mass calculated: 416.0473 Found 416.0486.

Deprotection of the C-terminus:

A solution of THF: water (30 mL: 5 mL) was added to compounds **4 (a – d)**. Lithium hydroxide (0.5 g) was added. The solution was stirred overnight. After this time, distilled water (100 mL) was added, and then hydrochloric acid (1.0 M) was added dropwise until the pH was lowered to pH 3. The resulting precipitate was collected by filtration and washed with water to give compounds **5 (a – d)** as shown in Scheme 2.1. The yield was between 61 – 91%. The impurity (excess of valine methyl ester) was calculated by NMR spectroscopy between 3 – 14% for all derivatives except compound **5d**, which was pure and used as crude in the next step of the reaction. Compounds **5a** and **b** were then crystallised using ethanol and toluene respectively and compound **5c** was purified by washing with methanol. The yield after purification was typically between 40 – 60 % and the resulting products were between 98 – 99% pure.

(S)-3-Methyl-2-(2-(naphthalen-2-yloxy)acetamido)butanoic acid (5a):

^1H NMR (d_6 -DMSO): 8.20 (d, ArH, 1H, $^3J_{\text{HH}} = 8.1\text{Hz}$), 7.84 (d, ArH, 1H, , $^3J_{\text{HH}} = 9.0\text{Hz}$), 7.74 (d, ArH, 1H, $^3J_{\text{HH}} = 8.1\text{Hz}$), 7.46 (t, ArH, 1H, $^3J_{\text{HH}} = 7.9\text{Hz}$), 7.36(t, ArH, 1H, $^3J_{\text{HH}} = 8.0\text{Hz}$),

7.27 (t, ArH, 1H, $^3J_{\text{HH}} = 6.2\text{Hz}$), 7.16(d, ArH, 1H, $^3J_{\text{HH}} = 7.7\text{Hz}$), 6.5(d, NH, 1H, $^3J_{\text{HH}} = 7.1\text{Hz}$), 4.73 (d, OCH₂C=O, 2H), 4.25 (dd, NHCHCH(CH₃)₂, 1H, $^3J_{\text{HH}} = 8.0, 3.0\text{Hz}$), 2.13 (m, (CH₃)₂CH, 1H), 1.00 (d, (CH₃)₂CH, 3H, $^3J_{\text{HH}} = 6.9$), 0.89 (d, (CH₃)₂CH, 3H, $^3J_{\text{HH}} = 6.5\text{Hz}$) ppm. ¹³C NMR (d₆-DMSO): 172.7, 167.72, 155.6, 134.0, 129.3, 128.16, 127.4, 126.6, 125.2, 123.7, 118.5, 107.1, 66.5, 56.8, 29.8, 19.1, 17.86 ppm. MS: ES⁻: [M - H]⁻. Accurate mass calculated: 324.1212 Found 324.1222.

(S)-2-(2-((6-Bromonaphthalen-2-yl)oxy)acetamido)-3-methylbutanoic acid (5b):

¹H NMR (d₆-DMSO): 8.43 (d, ArH, 1H, $^3J_{\text{HH}} = 8.4\text{Hz}$), 8.12 (d, ArH, 1H, $^3J_{\text{HH}} = 7.4\text{Hz}$), 7.85 (d, ArH, 1H, $^3J_{\text{HH}} = 8.7\text{Hz}$), 7.71 (d, ArH, 1H, $^3J_{\text{HH}} = 8.7\text{Hz}$), 7.57(t, ArH, 1H, $^3J_{\text{HH}} = 6.2\text{Hz}$), 7.30 (t, ArH, 1H, $^3J_{\text{HH}} = 7.1\text{Hz}$), 4.73 (s, OCH₂C=O, 2H), 4.24 (dd, NHCHCH(CH₃)₂, 1H, $^3J_{\text{HH}} = 4.3, 2.6\text{Hz}$), 2.12 (m, (CH₃)₂CH, 1H), 0.88 (d, (CH₃)₂CH, 6H, $^3J_{\text{HH}} = 6.7\text{Hz}$) ppm. ¹³C NMR (d₆-DMSO): 173.1, 169.9, 156.4, 132.9, 130.2, 129.7, 129.2, 129.0, 120.1, 119.9, 116.8, 107.6, 66.9, 57.2, 30.2, 19.5, 18.3 ppm. MS: ES⁻: [M - H]⁻. Accurate mass calculated: 402.0317 Found 402.0322.

(S)-2-(2-((1,6-Dibromonaphthalen-2-yl)oxy)acetamido)-3-methylbutanoic acid (5c):

¹H NMR (d₆-DMSO): 8.24 (d, ArH, 1H, $^3J_{\text{HH}} = 2.03\text{Hz}$), 8.05 (d, NH, 1H, $^3J_{\text{HH}} = 5.4\text{Hz}$), 8.02 (d, ArH, 1H, $^3J_{\text{HH}} = 5.9\text{Hz}$), 7.97 (d, NH, 1H, $^3J_{\text{HH}} = 9.0\text{Hz}$), 7.75(d, ArH, 1H, $^3J_{\text{HH}} = 7.0\text{Hz}$), 7.47 (d, ArH, 1H, $^3J_{\text{HH}} = 9.1\text{Hz}$), 4.90 (d, OCH₂C=O, 2H, $^3J_{\text{HH}} = 6.1\text{Hz}$), 4.26 (dd, NHCHCH(CH₃)₂, 1H, $^3J_{\text{HH}} = 5.1, 3.1\text{Hz}$), 2.14 (m, (CH₃)₂CH, 1H), 0.91 (d, (CH₃)₂CH, 6H, $^3J_{\text{HH}} = 6.8\text{Hz}$) ppm. ¹³C NMR (d₆-DMSO): 172.9, 167.6, 153.0, 131.4, 131.2, 130.9, 130.4, 128.8, 127.9, 118.0, 116.6, 107.7, 68.0, 57.0, 30.4, 19.4, 18.0 ppm. MS: ES⁻: [M - H]⁻. Accurate mass calculated: 479.9422 Found 479.9431.

(S)-2-(2-((1-Bromonaphthalen-2-yl)oxy)acetamido)-3-methylbutanoic acid (5d):

¹H NMR (d₆-DMSO): 8.10 (d, ArH, 1H, $^3J_{\text{HH}} = 8.5\text{Hz}$), 8.20 (d, NH, 1H, $^3J_{\text{HH}} = 8.6\text{Hz}$), 7.98 (d, ArH, 1H, $^3J_{\text{HH}} = 9.0\text{Hz}$), 7.94 (d, ArH, 1H, $^3J_{\text{HH}} = 10.1\text{Hz}$), 7.65(t, ArH, 1H, $^3J_{\text{HH}} = 8.5\text{Hz}$), 7.48 (t, ArH, 1H, $^3J_{\text{HH}} = 7.7\text{Hz}$), 7.44(d, ArH, H, $^3J_{\text{HH}} = 9.0\text{Hz}$), 4.89 (d, OCH₂C=O, 2H, $^3J_{\text{HH}} = 5.6\text{Hz}$), 4.29 (dd, NHCHCH(CH₃)₂, 1H, $^3J_{\text{HH}} = 5.1, 3.6\text{Hz}$), 2.15 (m, (CH₃)₂CH, 1H), 0.91 (d, (CH₃)₂CH, 6H, $^3J_{\text{HH}} = 6.8\text{Hz}$) ppm. ¹³C NMR (d₆-DMSO): 172.9, 167.7, 152.5, 132.5, 130.0,

129.7, 129.6, 128.7, 125.6, 125.0, 115.5, 107.8, 68.1, 57.0, 30.4, 19.4, 18.0 ppm. MS: ES⁻: [M - H]⁻. Accurate mass calculated: 402.0317 Found 402.0331.

Standard coupling methodology:

N-Methylmorpholine (1.5 eq.) and IBCF (1.1 eq.) were added to compound **5(a - d)** (1.0 g) in chloroform (70mL) at 0 °C. A solution of L-phenylalanine ethyl ester hydrochloride, L-valine ethyl ester hydrochloride, L-alanine ethyl ester hydrochloride or glycine ethyl ester hydrochloride (1 eq.) and NMM (1.5 eq.) in chloroform was added. The solution was stirred at room temperature overnight. The solution was washed with distilled water (100 mL), hydrochloric acid (2 x 100 mL, 0.1 M), aqueous potassium carbonate (100 mL, 0.1 M), and distilled water again (4 x 100 mL) and dried with magnesium sulfate. The solvent was removed *in vacuo* to give compounds **6 - 9(a - d)** as shown in the Scheme 2.1. The yield was between 33 - 76%. The impurity (an excess of valine methyl ester) was calculated by NMR spectroscopy between 13 - 25% for all derivatives except compounds **6 (a - d)** and **7 (a - d)**, which were pure and used as crude in the next step of the reaction. Compounds **8(a - d)** and **9(a - d)** were purified by washing with methanol. The yield after purification was between 40 - 55% and compounds were 90 - 99% pure.

***(S)*-Methyl-3-methyl-2-((*S*)-3-methyl-2-(2-(naphthalen-2-yloxy)acetamido)butanamido)butanoate (6a):**

¹H NMR (CDCl₃): 7.77 (d, ArH, 1H, ³J_{HH} = 8.9Hz), 7.72 (d, ArH, 1H, ³J_{HH} = 8.1Hz), 7.44 (t, ArH, 1H, ³J_{HH} = 7.1Hz), 7.36 (t, ArH, 1H, ³J_{HH} = 7.7Hz), 7.26 (d, ArH, 1H, ³J_{HH} = 8.6Hz), 7.22 (d, ArH, 1H, ³J_{HH} = 6.7Hz), 7.16 (d, ArH, 1H, ³J_{HH} = 8.9Hz), 4.66 (d, OCH₂C=O, 2H, ³J_{HH} = 8.0Hz), 4.51 (q, OCH₂CH₃, 2H, ³J_{HH} = 7.2Hz), 4.21 (m, NHCHCH(CH₃)₂, 1H, ³J_{HH} = 7.4Hz), 4.19 (dd, NHCHCH(CH₃)₂, 1H, ³J_{HH} = 7.4, 3.2Hz), 2.16 (m, (CH₃)₂CH, 1H), 2.14 (m, (CH₃)₂CH, 1H), 1.28 (t, OCH₂CH₃, 3H, ³J_{HH} = 7.1Hz), 0.97 (d, (CH₃)₂CH, 6H, ³J_{HH} = 6.7Hz), 0.98 (d, (CH₃)₂CH, 3H, ³J_{HH} = 7.1), 0.91 (d, (CH₃)₂CH, 3H, ³J_{HH} = 6.9Hz) ppm. ¹³C NMR (CDCl₃): 171.9, 171.0, 168.62, 155.39, 134.64, 130.3, 129.9, 128.0, 127.3, 127.0, 124.7, 118.6, 107.9, 67.6, 61.7, 58.5, 57.6, 31.6, 31.4, 19.5, 19.3, 18.5, 18.0, 14.6 ppm. MS: ES⁺: [M+Na]⁺. Accurate mass calculated: 451.2209 Found 451.2191.

(S)-Methyl-2-((S)-3-methyl-2-(2-(naphthalen2yloxy)acetamido)butanamido)propanoate (6b):

¹H NMR (CDCl₃): 7.78 (d, ArH, 1H, ³J_{HH} = 9.1Hz), 7.73 (d, ArH, 1H, ³J_{HH} = 8.1Hz), 7.46 (t, ArH, 1H, ³J_{HH} = 7.0Hz), 7.37 (t, ArH, 1H, ³J_{HH} = 7.5Hz), 7.26 (s, ArH, 1H,), 7.22 (d, ArH, 1H, ³J_{HH} = 9.0Hz), 7.17 (d, NH, 1H, ³J_{HH} = 7.4Hz), 7.10(d, ArH,1H, ³J_{HH} = 11.6Hz), 6.5(d, NH, 1H, ³J_{HH} = 7.0Hz), 4.54 (dd, NHCHCH(CH₃)₂, 1H³J_{HH} = 6.8, 2.8Hz), 4.66 (d, OCH₂C=O, 2H, ³J_{HH} = 3.7Hz), 4.36 (t, NHCH(CH₃), 1H, ³J_{HH} = 7.1Hz), 4.20 (q, OCH₂CH₃, 2H, ³J_{HH} = 7.0Hz), 2.15 (m, (CH₃)₂CH, 1H), 1.28 (t, OCH₂CH₃, 3H, ³J_{HH} = 7.1Hz), 1.38 (s, CH₃, 3H), 0.95 (d, (CH₃)₂CH, 3H, ³J_{HH} = 7.4Hz), 0.93 (d, (CH₃)₂CH, 3H, ³J_{HH} = 6.4Hz) ppm. ¹³C NMR (CDCl₃): 172.96, 170.4, 168.5, 155.3, 134.6, 130.3, 129.93, 128.1, 127.3, 127.1, 124.7, 118.6, 107.9, 67.6, 62.0, 58.4, 48.5, 31.7, 19.5, 18.6, 18.4, 14.5 ppm. MS: ES⁺: [M+Na]⁺. Accurate mass calculated: 423.1896. Found 423.1892.

(S)-Ethyl-2-(3-methyl-2-(2-(naphthalen-2-yloxy)acetamido)butanamido)acetate (6c):

¹H NMR (CDCl₃): 7.79 (d, ArH, 1H, ³J_{HH} = 3.9Hz), 7.78 (d, ArH, 1H, ³J_{HH} = 3.1Hz), 7.73 (d, ArH, 1H, ³J_{HH} = 8.1Hz), 7.46 (t, ArH, 1H, ³J_{HH} = 8.5Hz), 7.37 (t, ArH, 1H, ³J_{HH} = 8.0Hz), 7.22 (d, ArH, 1H, ³J_{HH} = 8.9Hz), 7.16 (d, ArH, 1H, ³J_{HH} = 2.4Hz), 4.40 (dd, NHCHCH(CH₃)₂, 1H, ³J_{HH} = 6.6, 2.7Hz), 4.67 (d, OCH₂C=O, 2H, ³J_{HH} = 2.7Hz), 4.02 (q, OCH₂CH₃, 2H, ³J_{HH} = 7.1Hz), 3.97(d, NHCH₂C=O, 2H, ³J_{HH} = 5.5Hz), 2.20 (m, (CH₃)₂CH, 1H), 1.27 (t, OCH₂CH₃, 3H, ³J_{HH} = 7.1Hz), 0.97 (d, (CH₃)₂CH, 3H, ³J_{HH} = 7.7Hz), 0.93 (d, (CH₃)₂CH, 3H, ³J_{HH} = 7.4Hz) ppm. ¹³C NMR (CDCl₃): 171.12, 169.8, 168.8, 155.4, 134.6, 130.4, 129.9, 128.1, 127.4, 127.2, 124.8, 118.6, 107.9, 67.7, 62.0, 58.4, 41.7, 31.3, 19.6, 18.4, 14.5 ppm. MS: ES⁺: [M+Na]⁺. Accurate mass calculate: 409.1739 Found 409.1743.

(S)-Ethyl-2-((S)-3-methyl-2-(2-(naphthalen-2-yloxy)acetamido)butanamido)-3-phenyl propanoate (6d):

¹H NMR (CDCl₃): 7.80 (d, ArH, 1H, ³J_{HH} = 5.1Hz), 7.79 (d, ArH, 1H, ³J_{HH} = 4.1Hz), 7.73 (d, NH, 1H, ³J_{HH} = 8.1Hz), 7.46 (t, ArH, 1H, ³J_{HH} = 8.1Hz), 7.37 (t, ArH, 1H, ³J_{HH} = 7.4Hz), 7.21 (d, NH, 1H, , ³J_{HH} = 8.1Hz), 7.14 (s, ArH, 1H,), 7.0 (d, ArH, 1H, ³J_{HH} = 8.4Hz), 6.28 (d, NH, 1H, ³J_{HH} = 8.0Hz), 4.84(dd, NHCH(CH₂Ph, 1H, ³J_{HH} = 5.5, 3.3Hz), 1H), 4.61(d, OCH₂C=O, 2H, ³J_{HH} = 11.8Hz), 4.33 (dd, NHCHCH(CH₃)₂, 1H, ³J_{HH} = 6.6, 3.1Hz), 4.17 (q, OCH₂CH₃, 2H, ³J_{HH} = 7.1Hz), 3.07 (dd, NHCH₂Ph, 2H, ³J_{HH} = 6.4, 5.4Hz), 2.12 (m, (CH₃)₂CH, 1H), 1.24 (t,

OCH₂CH₃, 3H, ³J_{HH} = 7.1Hz), 0.92 (d, (CH₃)₂CH, 6H, ³J_{HH} = 7.7Hz), 0.88 (d, (CH₃)₂CH, 6H, ³J_{HH} = 6.4Hz) ppm. ¹³C NMR (CDCl₃): 171.1, 170.1, 168.1, 154.9, 129.9, 129.5, 129.2, 128.5, 127.7, 127.1, 126.9, 126.7, 124.3, 118.2, 107.6, 67.2, 61.6, 57.9, 53.1, 37.8, 31.0, 19.1, 17.9, 14.1 ppm. MS: ES⁺: [M+Na]⁺. Accurate mass calculated: 499.2209 Found 499.2216.

(S)-Methyl-2-((S)-2-(2-((6-bromonaphthalen-2-yl)oxy)acetamido)-3-methylbutanamido)butanoate (7a):

¹H NMR (CDCl₃): 7.93 (s, ArH, 1H,), 7.69 (d, ArH, 1H, ³J_{HH} = 8.9Hz), 7.60 (d, ArH, 1H, ³J_{HH} = 8.7Hz), 7.52 (d, ArH, 1H, ³J_{HH} = 8.0Hz), 7.24 (d, ArH, 1H, ³J_{HH} = 9.5Hz), 7.20(d, NH, 1H, ³J_{HH} = 8.4Hz), 7.12 (s, ArH, 1H,), 6.8(d, NH, 1H, ³J_{HH} = 9.9Hz), 4.64 (d, OCH₂C=O, 2H, ³J_{HH} = 6.4Hz), 4.50(q, OCH₂CH₃, 2H, ³J_{HH} = 8.5Hz), 4.39 (d, NHCHCH(CH₃)₂, 1H, ³J_{HH} = 7.4Hz), 4.20 (d, NHCHCH(CH₃)₂, 1H, ³J_{HH} = 8.3Hz), 2.15 (m, (CH₃)₂CH, 1H), 1.28 (t, OCH₂CH₃, 3H, ³J_{HH} = 7.1Hz), 0.96 (d, (CH₃)₂CH, 6H, ³J_{HH} = 6.7Hz), 0.92 (d, (CH₃)₂CH, 3H, ³J_{HH} = 6.4Hz), 0.88 (d, (CH₃)₂CH, 3H, ³J_{HH} = 6.9Hz) ppm. ¹³C NMR (CDCl₃): 171.9, 170.9, 168.3, 155.6, 133.1, 130.9, 130.4, 130.1, 129.4, 129.0, 119.7, 118.3, 107.9, 67.6, 61.7, 58.5, 57.6, 31.6, 31.3, 19.5, 19.3, 18.5, 18.0, 14.6 ppm. MS: ES⁺: [M+Na]⁺. Accurate mass calculated: 529.1314. Found 529.1311.

(S)-Methyl-2-((S)-2-(2-((6-bromonaphthalen-2-yl)oxy)acetamido)-3-methylbutanamido) propanoate (7b):

¹H NMR (CDCl₃): 7.94 (s, ArH, 1H,), 7.70 (d, ArH, 1H, ³J_{HH} = 9.0Hz), 7.61 (d, ArH, 1H, ³J_{HH} = 8.7Hz), 7.52 (d, ArH, 1H, ³J_{HH} = 6.7Hz), 7.23 (d, ArH, 1H, ³J_{HH} = 8.2Hz), 7.17 (d, NH, 1H, ³J_{HH} = 8.5), 7.11 (d, ArH, 1H, ³J_{HH} = 2.4Hz), 6.47 (d, NH, 1H, ³J_{HH} = 6.5), 4.61 (d, OCH₂C=O, 2H, ³J_{HH} = 3.7Hz), 4.54 (t, NHCH(CH₃), 1H, ³J_{HH} = 7.2Hz), 4.35 (dd, NHCHCH(CH₃)₂, 1H, ³J_{HH} = 7.0, 2.6Hz), 4.20 (q, OCH₂CH₃, 2H, ³J_{HH} = 8.0, 7.6Hz), 2.14 (m, (CH₃)₂CH, 1H), 1.39 (d, NHCH, CH₃, 3H, ³J_{HH} = 7.1Hz), 1.28 (t, OCH₂CH₃, 3H, ³J_{HH} = 7.1Hz), 0.97 (d, (CH₃)₂CH, 3H, ³J_{HH} = 7.1Hz), 0.92 (d, (CH₃)₂CH, 3H, ³J_{HH} = 6.6Hz) ppm. ¹³C NMR (CDCl₃): 172.9, 170.3, 168.2, 155.6, 133.1, 130.9, 130.4, 130.1, 129.4, 128.9, 119.7, 118.3, 107.9, 67.6, 62.0, 58.3, 48.6, 31.5, 19.4, 18.6, 18.4, 14.5 ppm. MS: ES⁺: [M+Na]⁺. Accurate mass calculated: 501.1001 found 501.1004.

(S)-Ethyl-2-(2-(2-((6-bromonaphthalen-2-yl)oxy)acetamido)-3-methylbutanamido)acetate (7c):

^1H NMR (CDCl_3): 7.93 (s, ArH, 1H), 7.70 (d, ArH, 1H, $^3J_{\text{HH}} = 9.0$), 7.60 (d, ArH, 1H, $^3J_{\text{HH}} = 8.7$), 7.52 (d, ArH, 1H, $^3J_{\text{HH}} = 8.7$), 7.24 (d, ArH, 1H, $^3J_{\text{HH}} = 9$), 7.14 (d, NH, 1H, $^3J_{\text{HH}} = 8.7$), 7.11 (d, ArH, 1H, $^3J_{\text{HH}} = 2.46$), 6.47 (d, NH, 1H, $^3J_{\text{HH}} = 7.15$), 4.65 (d, $\text{OCH}_2\text{C}=\text{O}$, 2H $^3J_{\text{HH}} = 3.24$), 4.41 (d, $\text{NHCHCH}(\text{CH}_3)_2$, 1H, $^3J_{\text{HH}} = 6.7$), 4.20 (q, OCH_2CH_3 , 2H $^3J_{\text{HH}} = 7.14$), 4.04 (d, $\text{NHCH}_2\text{C}=\text{O}$, 2H $^3J_{\text{HH}} = 5.5$), 2.18 (m, $(\text{CH}_3)_2\text{CH}$, 1H), 1.28 (t, OCH_2CH_3 , 3H, $^3J_{\text{HH}} = 7.3$), 0.94 (d, $(\text{CH}_3)_2\text{CH}$, 3H, $^3J_{\text{HH}} = 6.7\text{Hz}$), 0.92 (d, $(\text{CH}_3)_2\text{CH}$, 3H, $^3J_{\text{HH}} = 7.4\text{Hz}$) ppm. ^{13}C NMR (CDCl_3): 171.1, 169.8, 168.4, 155.6, 133.1, 130.9, 130.4, 130.1, 129.4, 128.9, 119.7, 118.3, 107.9, 67.6, 62.0, 58.4, 41.7, 31.4, 19.5, 18.4, 14.5 ppm. MS: ES^+ : $[\text{M}+\text{Na}]^+$. Accurate mass calculated: 487.0845 Found 487.0822.

(S)-Ethyl-2-((S)-2-(2-((6-bromonaphthalen-2-yl)oxy)acetamido)-3-methylbutanamido)-3-phenylpropanoate (7d):

^1H NMR (CDCl_3): 7.94 (s, ArH, 1H), 7.71 (d, ArH, 1H, $^3J_{\text{HH}} = 9.0\text{Hz}$), 7.61 (d, ArH, 1H, $^3J_{\text{HH}} = 8.0\text{Hz}$), 7.52 (d, ArH, 1H, $^3J_{\text{HH}} = 7.3\text{Hz}$), 7.26 (s, ArH, 1H), 7.20 (d, NH, 1H, $^3J_{\text{HH}} = 7.1\text{Hz}$), 7.08 (t, ArH, 1H, $^3J_{\text{HH}} = 7.0\text{Hz}$), 6.20 (d, NH, 1H, $^3J_{\text{HH}} = 7.5\text{Hz}$), 4.84 (d, $\text{NHCH}(\text{CH}_2\text{Ph})$, 1H, $^3J_{\text{HH}} = 7.5\text{Hz}$), 4.61 (d, $\text{OCH}_2\text{C}=\text{O}$, 2H, $^3J_{\text{HH}} = 10.1\text{Hz}$), 4.30 (t, $\text{NHCHCH}(\text{CH}_3)_2$, 1H, $^3J_{\text{HH}} = 6.7\text{Hz}$), 4.17 (q, OCH_2CH_3 , 2H, $^3J_{\text{HH}} = 7.1\text{Hz}$), 3.07 (dd, NHCH_2Ph , 2H, $^3J_{\text{HH}} = 5.9, 4.2\text{Hz}$), 2.11 (m, $(\text{CH}_3)_2\text{CH}$, 1H), 1.24 (t, OCH_2CH_3 , 3H, $^3J_{\text{HH}} = 7.1\text{Hz}$), 0.91 (d, $(\text{CH}_3)_2\text{CH}$, 3H, $^3J_{\text{HH}} = 6.6\text{Hz}$), 0.86 (d, $(\text{CH}_3)_2\text{CH}$, 3H, $^3J_{\text{HH}} = 6.9\text{Hz}$) ppm. ^{13}C NMR (CDCl_3): 207.4, 171.4, 170.4, 168.2, 155.6, 135.9, 133.1, 130.9, 130.4, 130.1, 129.6, 129.4, 129.0, 127.6, 119.7, 118.3, 107.9, 67.5, 62.0, 58.3, 53.5, 38.2, 31.4, 19.4, 18.3, 14.5 ppm. MS: ES^+ : $[\text{M}+\text{Na}]^+$. Accurate mass calculated: 577.1314. Found 577.1318.

(S)-Methyl-2-((S)-2-(2-((1,6-dibromonaphthalen-2-yl)oxy)acetamido)-3-methylbutanamido)-3-methylbutanoate (8a):

^1H NMR (CDCl_3): 8.08 (d, ArH, 1H, $^3J_{\text{HH}} = 9.1\text{Hz}$), 7.96 (d, ArH, 1H, $^3J_{\text{HH}} = 1.9\text{Hz}$), 7.73 (d, ArH, 1H, $^3J_{\text{HH}} = 9.0\text{Hz}$), 7.64 (d, ArH, 1H, $^3J_{\text{HH}} = 6.3\text{Hz}$), 7.54 (d, NH, 1H, $^3J_{\text{HH}} = 8.1\text{Hz}$), 7.20 (d, ArH, 1H, $^3J_{\text{HH}} = 9.8\text{Hz}$), 6.43 (d, NH, 1H, $^3J_{\text{HH}} = 8.1\text{Hz}$), 4.70 (s, $\text{OCH}_2\text{C}=\text{O}$, 2H), 4.56 (dd, $\text{NHCHCH}(\text{CH}_3)_2$, 1H, $^3J_{\text{HH}} = 5.4, 3.7\text{Hz}$), 4.45 (dd, $\text{NHCHCH}(\text{CH}_3)_2$, 1H, $^3J_{\text{HH}} = 6.4, 3.2\text{Hz}$), 3.74 (s, OCH_3 , 2H), 2.26 (m, $(\text{CH}_3)_2\text{CH}$, 1H), 2.18 (m, $(\text{CH}_3)_2\text{CH}$, 1H), 1.03 (d, $(\text{CH}_3)_2\text{CH}$, 3H, $^3J_{\text{HH}} = 4.3\text{Hz}$), 1.02 (d, $(\text{CH}_3)_2\text{CH}$, 3H, $^3J_{\text{HH}} = 2.7\text{Hz}$), 0.92 (d, $(\text{CH}_3)_2\text{CH}$, 6H, $^3J_{\text{HH}} =$

7.1Hz) ppm. ^{13}C NMR (CDCl_3): 172.1, 170.4, 167.5, 151.6, 131.5, 131.4, 131.2, 130.0, 128.4, 128.1, 119.1, 115.4, 109.9, 68.6, 58.2, 57.1, 52.2, 31.1, 31.0, 19.2, 18.9, 17.9, 17.7 ppm. MS: ES^+ : $[\text{M}+\text{Na}]^+$. Accurate mass calculated: 593.0263 Found 593.0267.

(S)-Methyl-2-((S)-2-(2-((1,6-dibromonaphthalen-2-yl)oxy)acetamido)-3-methylbutanamido)propanoate (8b):

^1H NMR (CDCl_3): 8.09 (d, ArH, 1H, $^3J_{\text{HH}} = 9.0\text{Hz}$), 7.96 (d, ArH, 1H, $^3J_{\text{HH}} = 2.1\text{Hz}$), 7.73 (d, ArH, 1H, $^3J_{\text{HH}} = 8.7\text{Hz}$), 7.65 (d, ArH, 1H, $^3J_{\text{HH}} = 8.1\text{Hz}$), 7.61 (d, NH, 1H, $^3J_{\text{HH}} = 8.1\text{Hz}$), 7.20 (d, ArH, 1H, $^3J_{\text{HH}} = 9.0\text{Hz}$), 6.43 (d, NH, 1H, $^3J_{\text{HH}} = 9.9\text{Hz}$), 4.61 (dd, $\text{NHCHCH}(\text{CH}_3)_2$, 1H, $^3J_{\text{HH}} = 9.0$, 4.3Hz), 4.70 (s, $\text{OCH}_2\text{C}=\text{O}$, 2H), 4.40 (dd, $\text{NHCH}(\text{CH}_3)$, 1H, $^3J_{\text{HH}} = 6.4$, 2.7Hz), 3.75 (s, OCH_3 , 2H), 2.25 (m, $(\text{CH}_3)_2\text{CH}$, 1H), 1.41 (d, CH_3 , 3H, $^3J_{\text{HH}} = 7.1\text{Hz}$), 1.03 (d, $(\text{CH}_3)_2\text{CH}$, 3H, $^3J_{\text{HH}} = 6.3\text{Hz}$), 1.02 (d, $(\text{CH}_3)_2\text{CH}$, 3H, $^3J_{\text{HH}} = 3.7\text{Hz}$) ppm. ^{13}C NMR (CDCl_3): 170.3, 167.9, 155.6, 132.0, 131.8, 131.6, 130.4, 128.8, 128.6, 119.5, 115.8, 69.0, 58.4, 52.9, 48.4, 31.6, 19.5, 19.4, 18.7, 18.3 ppm. MS: ES^+ : $[\text{M}+\text{Na}]^+$. Accurate mass calculated: 564.9950 Found 564.9966.

(S)-Ethyl-2-(2-(2-((1,6-dibromonaphthalen-2-yl)oxy)acetamido)-3-methylbutanamido)acetate (8c):

^1H NMR (CDCl_3): 8.09 (d, ArH, 1H, $^3J_{\text{HH}} = 9.0\text{Hz}$), 7.96 (d, ArH, 1H, $^3J_{\text{HH}} = 1.5\text{Hz}$), 7.74 (d, ArH, 1H, $^3J_{\text{HH}} = 8.9\text{Hz}$), 7.65 (d, ArH, 1H, $^3J_{\text{HH}} = 9.0\text{Hz}$), 7.58 (d, NH, 1H, $^3J_{\text{HH}} = 7.1\text{Hz}$), 7.20 (d, ArH, 1H, $^3J_{\text{HH}} = 9.0\text{Hz}$), 6.46 (d, NH, 1H, $^3J_{\text{HH}} = 4.5\text{Hz}$), 4.70 (dd, $\text{NHCHCH}(\text{CH}_3)_2$, 1H, $^3J_{\text{HH}} = 6.4$, 3.7Hz), 4.43 (s, $\text{OCH}_2\text{C}=\text{O}$, 2H), 4.05 (d, $\text{NHCH}_2\text{C}=\text{O}$, 2H, $^3J_{\text{HH}} = 5.4\text{Hz}$), 4.21 (q, OCH_2CH_3 , 2H, $^3J_{\text{HH}} = 6.4\text{Hz}$), 2.29 (m, $(\text{CH}_3)_2\text{CH}$, 1H), 1.28 (t, OCH_2CH_3 , 3H, $^3J_{\text{HH}} = 7.1\text{Hz}$), 1.04 (d, $(\text{CH}_3)_2\text{CH}$, 3H, $^3J_{\text{HH}} = 7.3\text{Hz}$), 1.03 (d, $(\text{CH}_3)_2\text{CH}$, 3H, $^3J_{\text{HH}} = 6.7\text{Hz}$) ppm. ^{13}C NMR (CDCl_3): 171.0, 169.9, 168.0, 152.0, 131.9, 131.8, 131.6, 130.4, 128.8, 128.6, 119.5, 115.7, 110.2, 69.0, 62.0, 58.5, 41.7, 31.2, 19.6, 18.2, 14.5 ppm. MS: ES^+ : $[\text{M}+\text{Na}]^+$. Accurate mass calculated: 564.9950 Found 564.9941.

(S)-Ethyl-2-((S)-2-(2-((1,6-dibromonaphthalen-2-yl)oxy)acetamido)-3-methylbutanamido)-3-phenylpropanoate (8d):

^1H NMR (CDCl_3): 8.11 (d, ArH, 1H, $^3J_{\text{HH}} = 10.0\text{Hz}$), 7.98 (d, ArH, 1H, $^3J_{\text{HH}} = 1.9\text{Hz}$), 7.75 (d, ArH, 1H, $^3J_{\text{HH}} = 8.1\text{Hz}$), 7.66 (d, ArH, 1H, $^3J_{\text{HH}} = 7.4\text{Hz}$), 7.51 (d, NH, 1H, $^3J_{\text{HH}} = 9.5\text{Hz}$), 7.11 (d, ArH, 1H, $^3J_{\text{HH}} = 6.8\text{Hz}$), 6.26 (d, NH, 1H, $^3J_{\text{HH}} = 8.8\text{Hz}$), 4.89 (dd, $\text{NHCH}(\text{CH}_2\text{Ph})$, 1H, $^3J_{\text{HH}}$

= 4.7, 2.6Hz), 4.66 (d, OCH₂C=O, 2H, ³J_{HH} = 5.8Hz), 4.35 (dd, NHCHCH(CH₃)₂, 1H, ³J_{HH} = 6.4, 2.6Hz), 4.17 (q, OCH₂CH₃, 2H, ³J_{HH} = 7.3Hz), 3.12 (t, NHCH₂Ph, 2H, ³J_{HH} = 6.7Hz), 2.23 (m, (CH₃)₂CH, 1H), 1.24 (t, OCH₂CH₃, 3H, ³J_{HH} = 7.4Hz), 0.98 (d, (CH₃)₂CH, 3H, ³J_{HH} = 6.7Hz), 0.96 (d, (CH₃)₂CH, 3H, ³J_{HH} = 7.3Hz) ppm. ¹³C NMR (CDCl₃): 171.1, 169.9, 167.4, 151.6, 135.6, 131.6, 131.4, 131.2, 130.0, 129.3, 128.6, 128.5, 128.4, 128.2, 127.1, 119.1, 115.3, 109.9, 68.5, 61.6, 58.0, 53.0, 52.8, 37.8, 30.8, 19.2, 17.8, 14.0 ppm. MS: ES⁺: [M+Na]⁺. Accurate mass calculated: 655.0419 Found 655.0420.

***(S)*-Methyl-2-((*S*)-2-(2-((1-bromonaphthalen-2-yl)oxy)acetamido)-3-methylbutanamido)propanoate (9a):**

¹H NMR (CDCl₃): 8.22 (d, ArH, 1H, ³J_{HH} = 8.7Hz), 7.85 (d, ArH, 1H, ³J_{HH} = 9.0Hz), 7.80 (d, ArH, 1H, ³J_{HH} = 8.7Hz), 7.64 (d, NH, 1H, ³J_{HH} = 7.0Hz), 7.59 (t, ArH, 1H, ³J_{HH} = 6.1Hz), 7.45 (t, ArH, 1H, ³J_{HH} = 7.0Hz), 7.19 (d, ArH, 1H, ³J_{HH} = 8.9Hz), 6.44 (d, NH, 1H, ³J_{HH} = 7.9Hz), 4.72 (s, OCH₂C=O, 2H), 4.57 (dd, NHCHCH(CH₃)₂, 1H, ³J_{HH} = 5.3, 3.7Hz), 4.43 (dd, NHCHCH(CH₃)₂, 1H, ³J_{HH} = 6.4, 3.2Hz), 3.74 (s, OCH₂CH₃, 2H), 2.28 (m, (CH₃)₂CH, 1H), 2.18 (m, (CH₃)₂CH, 1H), 1.02 (d, (CH₃)₂CH, 6H, ³J_{HH} = 5.5Hz), 0.94 (d, (CH₃)₂CH, 3H, ³J_{HH} = 7.4Hz), 0.90 (d, (CH₃)₂CH, 3H, ³J_{HH} = 6.9Hz) ppm. ¹³C NMR (CDCl₃): 172.9, 170.4, 167.8, 151.4, 132.9, 129.4, 128.2, 128.1, 126.3, 125.1, 114.4, 68.6, 58.3, 57.1, 52.1, 31.1, 30.8, 19.2, 18.9, 17.9, 17.7 ppm. MS: ES⁺: [M+Na]⁺. Accurate mass calculated: 515.1158 Found 515.1136.

***(S)*-Methyl-2-((*S*)-2-(2-((1-bromonaphthalen-2-yl)oxy)acetamido)-3-methylbutanamido)propanoate (9b):**

¹H NMR (CDCl₃): 8.22 (d, ArH, 1H, ³J_{HH} = 9.2Hz), 7.84 (d, ArH, 1H, ³J_{HH} = 8.2Hz), 7.81 (d, ArH, 1H, ³J_{HH} = 8.5Hz), 7.65 (d, NH, 1H, ³J_{HH} = 7.9Hz), 7.60 (t, ArH, 1H, ³J_{HH} = 7.9Hz), 7.45 (t, NH, 1H, J = 7.2), 7.19 (d, ArH, 1H, ³J_{HH} = 28.9Hz), 6.38 (d, NH, 1H, J = 8.5), 4.72 (s, OCH₂C=O, 2H), 4.61 (t, NHCH(CH₃), 1H, ³J_{HH} = 7.2Hz), 4.39 (dd, NHCHCH(CH₃)₂, 1H, ³J_{HH} = 6.4, 3.2Hz), 3.75 (s, OCH₃, 2H), 2.26 (m, (CH₃)₂CH, 1H), 1.42 (d, NHCHCH₃, 3H, ³J_{HH} = 7.1Hz), 1.04 (d, (CH₃)₂CH, 3H, ³J_{HH} = 3.2Hz), 1.02 (d, (CH₃)₂CH, 3H, ³J_{HH} = 3.3Hz) ppm. ¹³C NMR (CDCl₃): 1723.1, 170.1, 169.9, 167.8, 151.4, 132.9, 130.4, 129.4, 128.2, 128.1, 126.3, 125.1, 114.5, 109.9, 68.7, 58.1, 48.0, 31.0, 19.2, 18.3, 17.9 ppm. MS: ES⁺: [M+Na]⁺. Accurate mass calculated: 487.0845. Found 487.0837.

(S)-Ethyl-2-(2-(2-((1-bromonaphthalen-2-yl)oxy)acetamido)-3-methylbutanamido)acetate (9c):

¹H NMR (CDCl₃): 8.23 (d, NH, 1H, ³J_{HH} = 8.8Hz), 7.82 (dd, ArH, 2H, ³J_{HH} = 7.8, 4.9Hz), 7.62 (m, ArH, 2H), 7.45 (t, ArH, 1H, ³J_{HH} = 4.6Hz), 7.20 (d, ArH, 1H, ³J_{HH} = 8.8Hz), 6.54 (s, NH, 1H), 4.72 (s, OCH₂C=O, 2H), 4.44 (dd, NHCHCH(CH₃)₂, 1H, ³J_{HH} = 6.2, 3.8Hz), 4.07 (dd, NHCH₂C=O, 2H, ³J_{HH} = 6.9, 5.5Hz), 3.76 (s, OCH₃, 2H), 2.32 (m, (CH₃)₂CH, 1H), 1.05 (d, OCH₂CH₃, 3H, ³J_{HH} = 7.1Hz), 1.05 (d, (CH₃)₂CH, 3H, ³J_{HH} = 6.7Hz), 0.97 (d, (CH₃)₂CH, 3H, ³J_{HH} = 6.7Hz) ppm. ¹³C NMR (CDCl₃): 171.2, 170.5, 168.4, 151.7, 133.3, 130.8, 129.9, 128.6, 128.5, 126.7, 125.5, 114.8, 110.2, 69.0, 58.5, 52.9, 41.6, 31.2, 19.7, 18.3 ppm. MS: ES⁺: [M+Na]⁺. Accurate mass calculate: 473.0692 Found 473.0688.

(S)-Ethyl-2-((S)-2-(2-((1-bromonaphthalen-2-yl)oxy)acetamido)-3-methylbutanamido)-3-phenylpropanoate (9d):

¹H NMR (CDCl₃): 8.23 (d, ArH, 1H, ³J_{HH} = 8.5Hz), 7.84 (d, ArH, 1H, ³J_{HH} = 8.9Hz), 7.61 (d, ArH, 1H, ³J_{HH} = 8.1Hz), 7.56 (t, ArH, 1H, ³J_{HH} = 7.6Hz), 7.45 (t, ArH, 1H, ³J_{HH} = 8.1Hz), 7.23(d, ArH, 1H, ³J_{HH} = 6.8Hz), 7.11(d, NH, 1H, ³J_{HH} = 8.7Hz), 6.35 (d, NH, 1H, ³J_{HH} = 8.7Hz), 4.89(m, NHCH(CH₂Ph), 1H), 4.61(d, OCH₂C=O, 2H, ³J_{HH} = 6.8Hz), 4.37 (dd, NHCHCH(CH₃)₂, 1H, ³J_{HH} = 6.4, 4.3Hz), 4.17 (q, OCH₂CH₃, 2H, ³J_{HH} = 8.3, 7.6Hz), 3.12 (m, NHCH₂Ph, 2H), 2.24 (m, (CH₃)₂CH, 1H), 1.24 (t, OCH₂CH₃, 3H³J_{HH} = 7.1Hz), 0.99 (d, (CH₃)₂CH, 3H, ³J_{HH} = 6.3Hz), 0.96 (d, (CH₃)₂CH, 3H, ³J_{HH} = 7.3Hz) ppm. ¹³C NMR (CDCl₃): 171.1, 170.0, 167.7, 151.3, 135.6, 132.9, 130.4, 129.4, 129.3, 128.5, 128.2, 128.1, 127.1, 114.4, 109.8, 68.6, 61.6, 58.1, 53.0, 37.8, 30.6, 19.2, 17.7, 14.0 ppm. MS: ES⁺: [M+Na]⁺. Accurate mass calculated: 577.1314 Found 577.1289.

Deprotection of the C-terminus:

A solution of THF: water (30 mL: 5 mL) was added to the naphthalene derivative. Lithium hydroxide (0.3 g) was added. The solution was stirred overnight. After this time, distilled water (100 mL) was added, and then hydrochloric acid (1.0 M) was added drop-wise until the pH was lowered to pH 3. The resulting precipitate was collected by filtration and washed with water to give compounds (**10 – 25**) as shown in Scheme 2.1 and Table 2.3. The yield was between 64 – 83%. The impurity (an excess of the amino acid ester) was calculated by NMR spectroscopy to be between 12 – 27% for all derivatives except compounds **11, 12, 13, 15, 16, 19, 22** and **24**, which were pure. The

resulting product was purified by washing with methanol. The yield after purification was typically between 40 – 60% and the products was typically 90 – 99% pure.

(S)-3-Methyl-2-((S)-3-methyl-2-(2-(naphthalen-2-yloxy)acetamido)butanamido)butanoic acid (10):

¹H NMR (d₆-DMSO): 7.89 (d, ArH, 1H, ³J_{HH} = 8.5Hz), 7.84 (d, ArH, 1H, ³J_{HH} = 4.3Hz), 7.77 (s, ArH, 1H), 7.51 (d, ArH, 1H, ³J_{HH} = 7.9Hz), 7.49 (d, ArH, 1H, ³J_{HH} = 8.1Hz), 7.46 (t, ArH, 1H, ³J_{HH} = 6.9Hz), 7.43 (t, ArH, 1H, ³J_{HH} = 9.6Hz), 7.38 (dd, NH, 1H, ³J_{HH} = 4.4Hz), 7.22 (d, NH, 1H, ³J_{HH} = 7.9Hz), 4.81 (d, OCH₂C=O, 2H, ³J_{HH} = 6.8Hz), 4.43 (dd, NHCHCH(CH₃)₂, 1H, ³J_{HH} = 6.4, 3.2Hz), 4.12 (d, NHCHCH(CH₃)₂, 1H, ³J_{HH} = 6.4, 2.7Hz), 2.05 (m, (CH₃)₂CH, 1H), 1.83 (m, (CH₃)₂CH, 1H, ³J_{HH} = 7.2Hz), 0.88 (d, (CH₃)₂CH, 6H, ³J_{HH} = 6.5Hz), 0.82 (d, (CH₃)₂CH, 6H, ³J_{HH} = 6.9Hz) ppm. ¹³C NMR (d₆-DMSO): 173.1, 171.3, 167.6, 155.9, 134.3, 129.7, 129.0, 127.8, 127.0, 126.8, 124.2, 118.8, , 107.6, 67.0, 60.6, 57.7, 57.1, 31.3, 29.9, 19.5, 18.4, 14.4 ppm. ES⁺: [M+Na]⁺. Accurate mass calculated: 423.1896 Found 423.1894.

(S)-2-((S)-3-Methyl-2-(2-(naphthalen-2-yloxy)acetamido)butanamido)propanoic acid (11):

¹H NMR (d₆-DMSO): 8.39 (d, ArH, 1H, ³J_{HH} = 7.1Hz), 7.96 (d, ArH, 1H, ³J_{HH} = 9.1Hz), 7.84 (d, ArH, 1H, ³J_{HH} = 4.0Hz), 7.79 (d, NH, 1H, ³J_{HH} = 3.1Hz), 7.75 (d, ArH, 1H, ³J_{HH} = 8.1Hz), 7.46 (t, ArH, 1H, ³J_{HH} = 7.6Hz), 7.35 (t, ArH, 1H, ³J_{HH} = 8.1Hz), 7.27 (s, ArH, 1H), 6.7 (d, NH, 1H, ³J_{HH} = 8.6Hz), 4.71(d, OCH₂C=O, 2H, ³J_{HH} = 3.7Hz), 4.79 (d, NH, 1H, ³J_{HH} = 7.2Hz), 4.34(dd, NHCHCH(CH₃)₂, 1H, ³J_{HH} = 7.5, 3.2Hz), 4.11 (m, NHCH(CH₃), 1H), 2.02 (m, (CH₃)₂CH, 1H), 1.26 (d, CH₃, 3H, ³J_{HH} = 7.2Hz), 0.88 (d, (CH₃)₂CH, 3H, ³J_{HH} = 6.6Hz), 0.83 (d, (CH₃)₂CH, 3H, ³J_{HH} = 7.4Hz) ppm. ¹³C NMR (d₆-DMSO): 173.8, 170.3, 167.2, 155.5, 133.9, 129.3, 128.6, 127.5, 126.5, 126.4, 123.8, 118.4, 107.2, 66.6, 56.6, 47.4, 31.0, 25.0, 19.0, 17.8 ppm. ES⁺: [M+Na]⁺. Accurate mass calculated: 395.1583 Found 395.1584.

(S)-2-(3-Methyl-2-(2-(naphthalen-2-yloxy)acetamido)butanamido)acetic acid (12):

¹H NMR (d₆-DMSO): 8.44 (t, ArH, 1H, ³J_{HH} = 7.2Hz), 7.99 (d, ArH, 1H, ³J_{HH} = 10.8Hz), 7.85 (dd, ArH, 1H, ³J_{HH} = 7.0Hz), 7.75 (d, ArH, 1H, ³J_{HH} = 7.2Hz), 7.46 (t, ArH, 1H, ³J_{HH} = 8.1Hz), 7.35 (t, ArH, 1H, ³J_{HH} = 9.0Hz), 7.25 (t, ArH, NH, 2H), 4.71 (d, OCH₂C=O, 2H, ³J_{HH} = 7.2Hz), 4.30 (dd, NHCHCH(CH₃)₂, 1H, ³J_{HH} = 5.9, 3.3Hz), 3.78 (dd, NHCH₂C=O, 2H, ³J_{HH} = 7.2,

5.4Hz), 2.04 (m, (CH₃)₂CH, 1H), 0.87 (d, (CH₃)₂CH, 3H, ³J_{HH} = 7.4Hz) 0.84 (d, (CH₃)₂CH, 3H, ³J_{HH} = 6.4Hz) ppm. ¹³C NMR (d₆-DMSO): 170.95, 170.91, 167.3, 155.5, 134.0, 129.3, 128.6, 127.5, 126.6, 126.4, 123.8, 118.4, 107.2, 66.6, 57.0, 40.6, 30.7, 19.1, 17.8 ppm. ES⁺: [M+Na]⁺. Accurate mass calculated: 381.1426 Found 381.1438.

(S)-2-((R)-3-Methyl-2-(2-(naphthalen-2-yloxy)acetamido)butanamido)-3-phenyl propanoic acid (13):

¹H NMR (d₆-DMSO): 8.39 (d, ArH, 1H, ³J_{HH} = 6.9Hz), 7.89 (d, NH, 1H, ³J_{HH} = 9.3Hz), 7.87 (d, ArH, 1H, ³J_{HH} = 4.4Hz), 7.84 (d, ArH, 1H, ³J_{HH} = 4.9Hz), 7.75 (d, ArH, 1H, ³J_{HH} = 8.3Hz), 7.46 (t, ArH, 1H, ³J_{HH} = 7.4Hz), 7.36 (t, ArH, 1H, ³J_{HH} = 6.4Hz), 7.25 (d, NH, 1H, ³J_{HH} = 7.4Hz), 7.22 (s, NH, 1H), 4.68(d, OCH₂C=O, 2H, ³J_{HH} = 8.8Hz), 4.43(m, NHCH(CH₂Ph), 1H), 4.30 (dd, NHCHCH(CH₃)₂, 1H, ³J_{HH} = 6.4, 3.3Hz), 3.04 (dd, NHCH₂Ph, 1H, ³J_{HH} = 7.9, 5.3Hz), 2.88 (dd, NHCH₂Ph, 1H, ³J_{HH} = 7.9, 4.8Hz), 1.98 (m, (CH₃)₂CH, 1H), 0.83 (d, (CH₃)₂CH, 3H, ³J_{HH} = 7.7Hz), 0.79 (d, (CH₃)₂CH, 3H, ³J_{HH} = 6.4Hz) ppm. ¹³C NMR (d₆-DMSO): 173.1, 171.0, 167.6, 155.9, 137.8, 134.4, 129.8, 129.4, 129.1, 128.5, 127.9, 127.0, 126.9, 126.8, 124.2, 118.8, 107.6, 67.0, 57.2, 53.8, 36.9, 31.3, 31.1, 30.8, 19.5, 18.1 ppm. ES⁺: [M+Na]⁺. Accurate mass calculated: 471.1911 Found 471.1896.

(S)-2-((R)-2-(2-((6-Bromonaphthalen-2-yl)oxy)acetamido)-3-methyl butanemido)-3-methyl butanoic acid (14):

¹H NMR (d₆-DMSO): 8.27(d, NH, 1H, ³J_{HH} = 7.2Hz), 8.12 (s, ArH, 1H), 7.98 (d, ArH, 1H, ³J_{HH} = 9.0Hz), 7.85 (d, ArH, 1H, ³J_{HH} = 9.9Hz), 7.72 (d, NH, 1H, ³J_{HH} = 7.2Hz), 7.57 (dd, ArH, 1H, ³J_{HH} = 8.1Hz), 7.30 (s, ArH, 1H), 4.72 (d, OCH₂C=O, 2H, ³J_{HH} = 7.2Hz), 4.41 (dd, NHCHCH(CH₃)₂, 1H, ³J_{HH} = 7.2, 3.3Hz), 4.11 (d, NHCHCH(CH₃)₂, 1H), 1.17 (m, (CH₃)₂CH, 1H), 0.84 (m, (CH₃)₂CH, 6H) ppm. ¹³C NMR (d₆-DMSO): 172.7, 170.9, 167.1, 155.9, 132.6, 129.9, 129.3, 128.8, 128.7, 119.6, 116.5, 107.4, 66.7, 57.3, 56.8, 40.1, 30.9, 29.6, 19.1, 18.9, 18.0, 17.8 ppm. MS: ES⁺: [M + Na]⁺. Accurate mass calculated: 501.1013 Found 501.1001.

(S)-2-((R)-2-(2-((6-Bromonaphthalen-2-yl)oxy)acetamido)-3-methyl butanamido)propanoic acid (15):

¹H NMR (d₆-DMSO): 8.41 (d, NH, 1H, ³J_{HH} = 9.0Hz), 8.13 (s, ArH, 1H), 8.03 (d, NH, 1H, ³J_{HH} = 9.8Hz), 7.85 (d, ArH, 1H, ³J_{HH} = 8.2Hz), 7.72 (d, ArH, 1H, ³J_{HH} = 9.8Hz), 7.58 (dd,

ArH, 1H, $^3J_{\text{HH}} = 10.6\text{Hz}$), 7.30 (s, ArH, 1H, $^3J_{\text{HH}} = 9.8\text{Hz}$), 7.92 (d, NH, 1H, $^3J_{\text{HH}} = 10.6\text{Hz}$), 4.72 (d, $\text{OCH}_2\text{C}=\text{O}$, 2H, $^3J_{\text{HH}} = 6.5\text{Hz}$), 4.31 (dd, $\text{NHCHCH}(\text{CH}_3)_2$, 1H, $^3J_{\text{HH}} = 6.7, 3.6\text{Hz}$), 4.18 (t, $\text{NHCH}(\text{CH}_3)$, 1H, $^3J_{\text{HH}} = 7.4\text{Hz}$), 2.01 (m, $(\text{CH}_3)_2\text{CH}$, 1H), 1.25 (d, CH_3 , 3H, $^3J_{\text{HH}} = 8.2\text{Hz}$), 0.88 (d, $(\text{CH}_3)_2\text{CH}$, 3H, $^3J_{\text{HH}} = 8.0\text{Hz}$), 0.83 (d, $(\text{CH}_3)_2\text{CH}$, 3H, $^3J_{\text{HH}} = 7.0\text{Hz}$) ppm. ^{13}C NMR (d_6 -DMSO): 174.3, 170.8, 167.5, 156.4, 132.9, 130.2, 129.8, 129.2, 129.1, 127.4, 120.1, 116.9, 107.8, 67.0, 57.1, 47.9, 31.4, 19.5, 18.3, 17.3 ppm. ES⁺: $[\text{M}+\text{Na}]^+$. Accurate mass calculated: 473.0688 Found 473.0696.

(R)-2-(2-(2-((6-Bromonaphthalen-2-yl)oxy)acetamido)-3-methylbutanamido)acetic acid (16):

^1H NMR (d_6 -DMSO): 8.42 (t, NH, 1H, $^3J_{\text{HH}} = 5.6\text{Hz}$), 8.12 (s, ArH, 1H), 8.01 (d, ArH, 1H, $^3J_{\text{HH}} = 9.0\text{Hz}$), 7.86 (d, ArH, 1H, $^3J_{\text{HH}} = 8.7\text{Hz}$), 7.72 (d, ArH, 1H, $^3J_{\text{HH}} = 8.8\text{Hz}$), 7.58 (dd, ArH, 1H, $^3J_{\text{HH}} = 6.9\text{Hz}$), 7.31 (s, ArH, 1H), 7.29 (d, NH, 1H, $^3J_{\text{HH}} = 4.6\text{Hz}$), 4.72 (d, $\text{OCH}_2\text{C}=\text{O}$, 2H, $^3J_{\text{HH}} = 5.3\text{Hz}$), 4.30 (dd, $\text{NHCHCH}(\text{CH}_3)_2$, 1H, $^3J_{\text{HH}} = 5.5, 4.2\text{Hz}$), 3.76 (dd, $\text{NHCH}_2\text{C}=\text{O}$, 2H, $^3J_{\text{HH}} = 5.8\text{Hz}$), 2.03 (m, $(\text{CH}_3)_2\text{CH}$, 1H), 0.86 (d, $(\text{CH}_3)_2\text{CH}$, 3H, $^3J_{\text{HH}} = 6.9\text{Hz}$), 0.84 (d, $(\text{CH}_3)_2\text{CH}$, 3H, $^3J_{\text{HH}} = 7.1\text{Hz}$) ppm. ^{13}C NMR (d_6 -DMSO): 171.4, 167.6, 156.3, 133.0, 130.2, 129.7, 129.2, 129.0, 120.0, 116.9, 107.6, 67.3, 67.0, 57.4, 40.9, 31.1, 19.4, 18.2 ppm. ES⁺: $[\text{M}+\text{Na}]^+$. Accurate mass calculated: 459.0532 Found 459.0546.

(S)-2-((R)-2-(2-((6-Bromonaphthalen-2-yl)oxy)acetamido)-3-methylbutanamido)-3-phenylpropanoic acid (17):

^1H NMR (d_6 -DMSO): 8.40 (d, NH, 1H, $^3J_{\text{HH}} = 6.3\text{Hz}$), 8.38 (s, ArH, 1H), 8.20 (d, NH, 1H, $^3J_{\text{HH}} = 8.1\text{Hz}$), 8.12 (s, ArH, 1H, $^3J_{\text{HH}} = 8.1\text{Hz}$), 7.72 (d, ArH, 1H, $^3J_{\text{HH}} = 10.8\text{Hz}$), 7.57 (dd, ArH, 1H, $^3J_{\text{HH}} = 4.5\text{Hz}$), 7.28 (d, ArH, 1H, $^3J_{\text{HH}} = 9.9\text{Hz}$), 7.21 (s, ArH, 1H), 4.43 (m, $\text{NHCH}(\text{CH}_2\text{Ph})$, 1H), 4.68 (d, $\text{OCH}_2\text{C}=\text{O}$, 2H, $^3J_{\text{HH}} = 7.1\text{Hz}$), 4.29 (dd, $\text{NHCHCH}(\text{CH}_3)_2$, 1H, $^3J_{\text{HH}} = 6.3, 4.3\text{Hz}$), 3.04 (d, NHCH_2Ph , 2H, $^3J_{\text{HH}} = 6.3\text{Hz}$), 1.99 (m, $(\text{CH}_3)_2\text{CH}$, 1H), 0.82 (d, $(\text{CH}_3)_2\text{CH}$, 3H, $^3J_{\text{HH}} = 6.7\text{Hz}$), 0.77 (d, $(\text{CH}_3)_2\text{CH}$, 3H, $^3J_{\text{HH}} = 7.4\text{Hz}$) ppm. ^{13}C NMR (d_6 -DMSO): 172.6, 170.5, 166.9, 155.9, 137.4, 132.5, 129.8, 129.3, 128.9, 128.8, 128.1, 126.3, 126.7, 126.3, 119.6, 116.5, 107.3, 66.6, 56.8, 53.3, 36.5, 31.31, 31.05, 30.8, 19.08, 17.71 ppm. ES⁺: $[\text{M}+\text{Na}]^+$. Accurate mass calculated: 549.1001 Found 549.1017.

***(S)*-2-((*R*)-2-(2-((1,6-Dibromonaphthalen-2-yl)oxy)acetamido)-3-methylbutanamido)-3-methylbutanoic acid (18):**

^1H NMR (d_6 -DMSO): 8.26 (d, ArH, 1H, $^3J_{\text{HH}} = 3.5\text{Hz}$), 8.19 (d, NH, 1H, $^3J_{\text{HH}} = 9.6\text{Hz}$), 8.04 (d, ArH, 1H, $^3J_{\text{HH}} = 9.6\text{Hz}$), 7.98 (d, ArH, 1H, $^3J_{\text{HH}} = 9.6\text{Hz}$), 7.89 (d, NH, 1H, $^3J_{\text{HH}} = 10.5\text{Hz}$), 7.76 (dd, ArH, 1H, $^3J_{\text{HH}} = 7.8\text{Hz}$), 7.47 (d, ArH, 1H, $^3J_{\text{HH}} = 10.5\text{Hz}$), 4.87 (d, $\text{OCH}_2\text{C}=\text{O}$, 2H, $^3J_{\text{HH}} = 7.0\text{Hz}$), 4.47 (dd, $\text{NHCHCH}(\text{CH}_3)_2$, 1H, $^3J_{\text{HH}} = 5.2, 3.3\text{Hz}$), 4.12 (dd, $\text{NHCHCH}(\text{CH}_3)_2$, 1H, $^3J_{\text{HH}} = 6.3, 3.0\text{Hz}$), 2.04 (m, $(\text{CH}_3)_2\text{CH}$, 1H), 0.90 (d, $(\text{CH}_3)_2\text{CH}$, 3H, $^3J_{\text{HH}} = 4.3\text{Hz}$), 0.88 (d, $(\text{CH}_3)_2\text{CH}$, 3H, $^3J_{\text{HH}} = 4.8\text{Hz}$), 0.85 (d, $(\text{CH}_3)_2\text{CH}$, 6H, $^3J_{\text{HH}} = 6.8\text{Hz}$), 0.79 (d, $(\text{CH}_3)_2\text{CH}$, 6H, $^3J_{\text{HH}} = 6.8\text{Hz}$) ppm. ^{13}C NMR (d_6 -DMSO): 173.1, 171.1, 167.1, 152.9, 131.4, 131.2, 130.9, 130.4, 128.8, 128.0, 118.0, 116.6, 107.7, 68.2, 57.7, 56.7, 31.6, 29.9, 19.5, 19.4, 18.4, 17.9 ppm. ES^+ : $[\text{M}+\text{Na}]^+$. Accurate mass calculated: 579.0106 Found 579.0115.

***(S)*-2-((*R*)-2-(2-((1,6-Dibromonaphthalen-2-yl)oxy)acetamido)-3-methylbutanamido) propanoic acid (19):**

^1H NMR (d_6 -DMSO): 8.42 (d, NH, 1H, $^3J_{\text{HH}} = 6.9\text{Hz}$), 8.25 (d, ArH, 1H, $^3J_{\text{HH}} = 1.8\text{Hz}$), 8.03 (d, ArH, 1H, $^3J_{\text{HH}} = 9.0\text{Hz}$), 7.98 (d, ArH, 1H, $^3J_{\text{HH}} = 9.1\text{Hz}$), 7.89 (d, NH, 1H, $^3J_{\text{HH}} = 9.1\text{Hz}$), 7.75 (dd, ArH, 1H, $^3J_{\text{HH}} = 9.0\text{Hz}$), 7.67 (d, ArH, 1H, $^3J_{\text{HH}} = 9.1\text{Hz}$), 4.87 (d, $\text{OCH}_2\text{C}=\text{O}$, 2H, $^3J_{\text{HH}} = 5.4\text{Hz}$), 4.36 (q, $\text{NHCHCH}(\text{CH}_3)_2$, 1H, $^3J_{\text{HH}} = 5.9\text{Hz}$), 4.20 (t, $\text{NHCH}(\text{CH}_3)$, 1H, $^3J_{\text{HH}} = 7.1\text{Hz}$), 2.03 (m, $(\text{CH}_3)_2\text{CH}$, 1H), 1.27 (d, CH_3 , 3H, $^3J_{\text{HH}} = 7.3\text{Hz}$), 0.88 (d, $(\text{CH}_3)_2\text{CH}$, 6H, $^3J_{\text{HH}} = 7.8\text{Hz}$) ppm. ^{13}C NMR (d_6 -DMSO): 174.29, 170., 167.1, 152.9, 131.4, 131.2, 130.9, 130.4, 128.8, 128.0, 118.0, 116.6, 107.7, 68.1, 56.7, 47.8, 31.6, 19.4, 18.0, 17.3 ppm. ES^+ : $[\text{M}+\text{Na}]^+$. Accurate mass calculated: 550.9793 Found 550.9792.

***(R)*-2-(2-(2-((1,6-Dibromonaphthalen-2-yl)oxy)acetamido)-3-methylbutanamido) acetic acid (20):**

^1H NMR (d_6 -DMSO): 8.24 (d, ArH, 1H, $^3J_{\text{HH}} = 2.0\text{Hz}$), 8.03 (d, ArH, 1H, $^3J_{\text{HH}} = 9.3\text{Hz}$), 7.98 (d, ArH, 1H, $^3J_{\text{HH}} = 9.4\text{Hz}$), 7.86 (d, NH, 1H, $^3J_{\text{HH}} = 8.8\text{Hz}$), 7.75 (dd, ArH, 1H, $^3J_{\text{HH}} = 7.7\text{Hz}$), 7.49 (d, ArH, 1H, $^3J_{\text{HH}} = 8.8\text{Hz}$), 7.28 (d, NH, 1H, $^3J_{\text{HH}} = 8.8\text{Hz}$), 4.87 (q, $\text{NHCHCH}(\text{CH}_3)_2$, 1H, $^3J_{\text{HH}} = 7.4\text{Hz}$), 4.51 (d, $\text{OCH}_2\text{C}=\text{O}$, 2H, $^3J_{\text{HH}} = 6.6\text{Hz}$), 4.32 (dd, $\text{NHCH}_2\text{C}=\text{O}$, 2H, $^3J_{\text{HH}} = 6.4, 3.6\text{Hz}$), 2.05 (m, $(\text{CH}_3)_2\text{CH}$, 1H), 0.87 (d, $(\text{CH}_3)_2\text{CH}$, 3H, $^3J_{\text{HH}} = 3.8\text{Hz}$), 0.86 (d, $(\text{CH}_3)_2\text{CH}$, 3H, $^3J_{\text{HH}} = 8.2\text{Hz}$) ppm. ^{13}C NMR (d_6 -DMSO): 171.3, 170.8, 167.2, 153.0, 131.4, 131.2, 130.9, 130.4, 128.8, 128.0, 117.9, 116.6, 68.1, 57.2, 41.7, 31.3, 19.5, 18.1, 17.9 ppm. ES^+ : $[\text{M}+\text{Na}]^+$. Accurate mass calculated: 536.9637 Found 536.9658.

***(S)*-2-((*R*)-2-(2-((1,6-Dibromonaphthalen-2-yl)oxy)acetamido)-3-methylbutanamido)-3-phenylpropanoic acid (21):**

^1H NMR (d_6 -DMSO): 8.42 (d, NH, 1H, $^3J_{\text{HH}} = 7.5\text{Hz}$), 8.25 (d, ArH, 1H, $^3J_{\text{HH}} = 2.0\text{Hz}$), 8.03 (d, ArH, 1H, $^3J_{\text{HH}} = 9.0\text{Hz}$), 7.75 (d, ArH, 1H, $^3J_{\text{HH}} = 9.1\text{Hz}$), 7.46 (d, NH, 1H, $^3J_{\text{HH}} = 9.4\text{Hz}$), 7.36 (dd, ArH, 1H, $^3J_{\text{HH}} = 11.1\text{Hz}$), 4.83 (m, NHCH(CH₂Ph), 1H), 4.93 (d, OCH₂C=O, 2H, $^3J_{\text{HH}} = 8.8\text{Hz}$), 4.78 (dd, NHCHCH(CH₃)₂, 1H, $^3J_{\text{HH}} = 6.4, 5.4\text{Hz}$), 4.34 (dd, NHCH₂Ph, 2H, $^3J_{\text{HH}} = 6.7\text{Hz}$), 2.02 (m, (CH₃)₂CH, 1H), 0.85 (d, (CH₃)₂CH, 3H, $^3J_{\text{HH}} = 8.2\text{Hz}$), 0.80 (d, (CH₃)₂CH, 3H, $^3J_{\text{HH}} = 5.4\text{Hz}$) ppm. ^{13}C NMR (d_6 -DMSO): 173.1, 170.8, 167.0, 153.0, 137.8, 131.4, 131.2, 130.99, 130.4, 129.5, 128.8, 128.6, 128.0, 126.9, 126.7, 118.0, 116.6, 107.7, 68.1, 56.8, 53.8, 36.9, 31.5, 19.5, 18.0, 17.8 ppm. ES⁺: [M+Na]⁺. Accurate mass calculated: 627.0106, Found 627.0119.

***(S)*-2-((*R*)-2-(2-((1-Bromonaphthalen-2-yl)oxy)acetamido)-3-methylbutanamido)-3-methylbutanoic acid (22):**

^1H NMR (d_6 -DMSO): 8.22 (d, NH, 1H, $^3J_{\text{HH}} = 8.1\text{Hz}$), 8.11 (d, ArH, 1H, $^3J_{\text{HH}} = 8.1\text{Hz}$), 7.96 (d, ArH, 1H, $^3J_{\text{HH}} = 9.3\text{Hz}$), 7.89 (d, ArH, 1H, $^3J_{\text{HH}} = 9.3\text{Hz}$), 7.67 (d, NH, 1H, $^3J_{\text{HH}} = 8.1\text{Hz}$), 7.49 (t, ArH, 1H, $^3J_{\text{HH}} = 8.1\text{Hz}$), 7.42 (d, ArH, 1H, $^3J_{\text{HH}} = 10.5\text{Hz}$), 4.82 (d, OCH₂C=O, 2H, $^3J_{\text{HH}} = 6.1\text{Hz}$), 4.50 (dd, NHCHCH(CH₃)₂, 1H, $^3J_{\text{HH}} = 5.2, 2.6\text{Hz}$), 4.47 (dd, NHCHCH(CH₃)₂, 1H, $^3J_{\text{HH}} = 6.4, 2.7\text{Hz}$), 2.08 (m, (CH₃)₂CH, 1H), 0.89 (d, (CH₃)₂CH, 6H, $^3J_{\text{HH}} = 6.4\text{Hz}$), 0.85 (d, (CH₃)₂CH, 6H, $^3J_{\text{HH}} = 7.4\text{Hz}$) ppm. ^{13}C NMR (d_6 -DMSO): 172.7, 170.7, 166.8, 152.0, 132.1, 129.6, 129.2, 128.3, 128.2, 125.2, 124.6, 115.1, 107.4, 67.8, 57.3, 56.3, 31.2, 29.5, 19.1, 19.0, 18.0, 17.5 ppm. ES⁺: [M+Na]⁺. Accurate mass calculated: 501.1001. Found 501.1003.

***(S)*-2-((*R*)-2-(2-((1-Bromonaphthalen-2-yl)oxy)acetamido)-3-methylbutanamido)propanoic acid (23):**

^1H NMR (d_6 -DMSO): 8.43 (d, NH, 1H, $^3J_{\text{HH}} = 6.9\text{Hz}$), 8.11 (d, ArH, 1H, $^3J_{\text{HH}} = 8.5\text{Hz}$), 8.01 (d, NH, 1H, $^3J_{\text{HH}} = 9.0\text{Hz}$), 7.89 (d, ArH, 1H, $^3J_{\text{HH}} = 8.1\text{Hz}$), 7.66 (t, ArH, 1H, $^3J_{\text{HH}} = 8.4\text{Hz}$), 7.63 (d, ArH, 1H, $^3J_{\text{HH}} = 8.0\text{Hz}$), 7.50 (d, ArH, 1H, $^3J_{\text{HH}} = 9.1\text{Hz}$), 7.44 (d, NH, 1H, $^3J_{\text{HH}} = 9.1\text{Hz}$), 4.83 (d, OCH₂C=O, 2H, $^3J_{\text{HH}} = 6.5\text{Hz}$), 4.36 (dd, NHCHCH(CH₃)₂, 1H, $^3J_{\text{HH}} = 6.3, 5.3\text{Hz}$), 4.19 (m, NHCH(CH₃), 1H, $^3J_{\text{HH}} = 7.4\text{Hz}$), 2.04 (m, (CH₃)₂CH, 1H), 1.28 (d, CH₃, 3H, $^3J_{\text{HH}} = 8.2\text{Hz}$), 0.91 (d, (CH₃)₂CH, 3H, $^3J_{\text{HH}} = 8.6\text{Hz}$), 0.87 (d, (CH₃)₂CH, 3H, $^3J_{\text{HH}} = 8.3\text{Hz}$) ppm. ^{13}C NMR (d_6 -DMSO): 171.2, 170.0, 167.8, 151.3, 135.6, 132.9, 130.4, 129.4, 129.3,

128.5, 128.2, 128.1, 127.1, 126.3, 125.1, 114.4, 109.8, 68.6, 61.6, 58.1, 53.0, 37.8, 30.6, 19.2, 17.8, 14.0 ppm. ES⁺: [M+Na]⁺. Accurate mass calculated: 473.0698. Found 473.0688.

(R)-2-(2-(2-((1-Bromonaphthalen-2-yl)oxy)acetamido)-3-methylbutanamido)acetic acid (24):

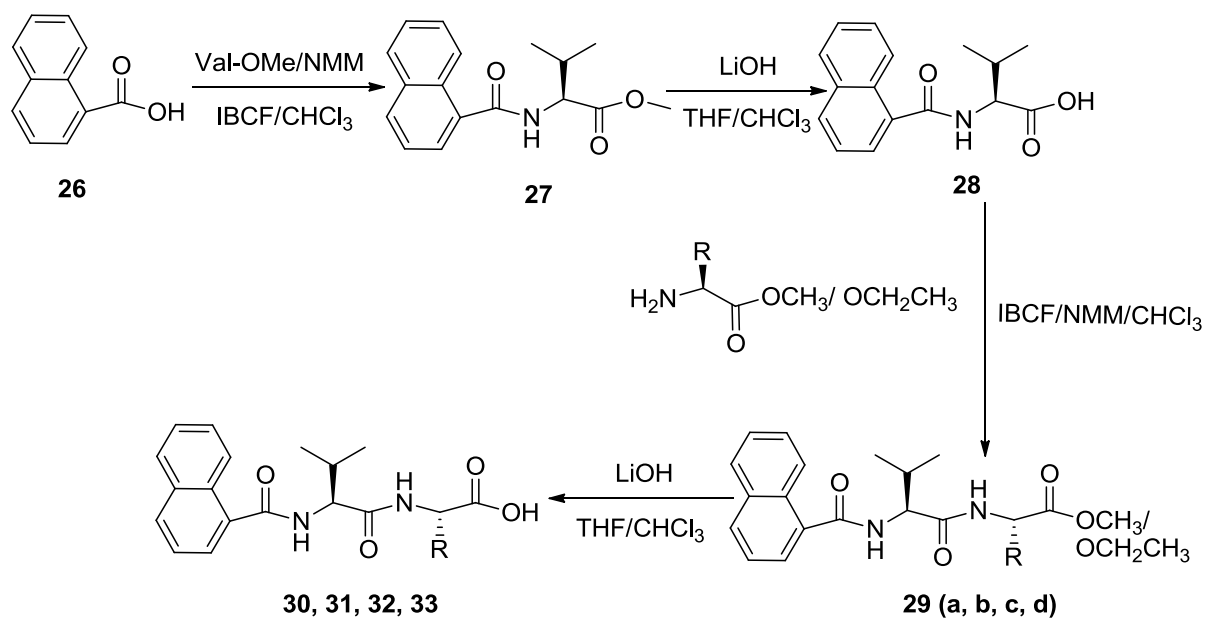
¹H NMR (d₆-DMSO): 8.90 (t, NH, 1H, ³J_{HH} = 7.3Hz), 8.53 (d, ArH, 1H, ³J_{HH} = 8.1Hz), 8.42 (d, ArH, 1H, ³J_{HH} = 8.8Hz), 8.38 (d, ArH, 1H, ³J_{HH} = 8.6Hz), 8.32 (d, ArH, 1H, ³J_{HH} = 8.6Hz), 8.08 (t, NH, 1H, ³J_{HH} = 7.8Hz), 7.90 (m, ArH, 2H), 5.29 (d, OCH₂C=O, 2H, ³J_{HH} = 8.1Hz), 4.78 (dd, NHCHCH(CH₃)₂, 1H, ³J_{HH} = 5.6, 3.2Hz), 4.21 (dd, NHCH₂C=O, 2H, ³J_{HH} = 6.4, 4.0Hz), 2.48 (m, (CH₃)₂CH, 1H), 1.33 (d, (CH₃)₂CH, 3H, ³J_{HH} = 7.2Hz), 1.30 (d, (CH₃)₂CH, 3H, ³J_{HH} = 6.9Hz) ppm. ¹³C NMR (d₆-DMSO): 171.5, 171.2, 167.4, 152.5, 132.5, 130.0, 129.7, 128.7, 128.6, 125.6, 125.0, 115.5, 107.8, 68.2, 57.1, 31.4, 19.5, 17.9 ppm. ES⁺: [M+Na]⁺. Accurate mass calculated: 459.0536 Found 459.0532.

(S)-2-((R)-2-(2-((1-Bromonaphthalen-2-yl)oxy)acetamido)-3-methylbutanamido)-3-phenylpropanoic acid (25):

¹H NMR (d₆-DMSO): 8.42(d, NH, 1H, ³J_{HH} = 7.7Hz), 8.11 (d, ArH, 1H, ³J_{HH} = 8.5Hz), 7.98 (d, NH, 1H, ³J_{HH} = 9.0Hz), 7.81 (d, ArH, 1H, ³J_{HH} = 8.7Hz), 7.67 (d, ArH, 1H, ³J_{HH} = 9.7Hz), 7.63 (t, ArH, 1H, ³J_{HH} = 5.5Hz), 7.48 (t, ArH, 1H, ³J_{HH} = 8.4Hz), 7.17 (d, ArH, 1H, ³J_{HH} = 9.0 Hz), 4.46 (m, NHCH(CH₂Ph), 1H), 1H), 4.83 (d, OCH₂C=O, 2H, ³J_{HH} = 8.9Hz), 4.35 (dd, NHCHCH(CH₃)₂, 1H, ³J_{HH} = 6.1, 4.2Hz), 3.07 (dd, NHCH₂Ph, 1H, ³J_{HH} = 8.6, 6.5Hz), 2.93 (dd, NHCH₂Ph, 1H, ³J_{HH} = 8.6, 4.5Hz), 2.02 (m, (CH₃)₂CH, 1H), 0.86 (d, (CH₃)₂CH, 3H, ³J_{HH} = 6.5Hz), 0.81 (d, (CH₃)₂CH, 3H, ³J_{HH} = 7.5Hz) ppm. ¹³C NMR (d₆-DMSO): 171.2, 170.0, 167.8, 151.3, 135.6, 132.9, 130.4, 129.4, 129.3, 128.5, 128.2, 128.1, 127.1, 126.3, 125.1, 114.4, 109.8, 68.6, 61.6, 58.1, 53.0, 37.8, 30.6, 19.2, 17.8, 14.0 ppm. MS: ES⁻: [M - H]⁻. Accurate mass calculated: 525.1025. Found: 525.1030.

From naphthalene acetic acid:

According to Chen's research, naphthalene was coupled to the amino acids using different linkers, -CH₂ and -OCH₂. Here, we have linked the naphthalene to amino acids by -CH₂ as shown in Scheme 2.2.



Scheme 2.2: The general reaction of naphthalene dipeptide synthesis based on naphthalene acetic acid ring using IBCF method.

Compound	Substituent
29	R
a	CH(CH ₃) ₂
b	CH ₃
c	H
d	CH ₂ Ph

Table 2.4: The R group of the general structure of compounds 29 (a, b, c, d) in the Scheme 2.

Dipeptides	R	Abbreviation
30	CH(CH ₃) ₂	1nap-VVOH
31	CH ₃	1nap-VAOH
32	H	1nap-VGOH
33	CH ₂ Ph	1nap-VFOH

Table 2.5: The R group of the general structure of compounds 30–33 and their abbreviations in the Scheme 2.

Standard coupling methodology:

N-Methylmorpholine (4 mL) and IBCF (3 mL) were added to 1-naphthalene acetic acid (5.0g) in chloroform (70 mL) at 0 °C. A solution of L-valine methyl ester (4.0 g, 1.5eq.) and NMM (4 mL) in chloroform was added. The solution was stirred at room temperature overnight. The solution was washed with distilled water (100 mL), hydrochloric acid (2 x 100 mL, 0.1 M), aqueous potassium carbonate (100 mL, 0.1 M), and distilled water again (4 x 100 mL) and dried with magnesium sulfate. The solvent was removed *in vacuo* to give compound **27** as shown in the Scheme 2.2. The yield was 75%. The impurities (an excess of valine methyl ester and IBCF) were calculated by NMR spectroscopy to be 35%. The resulting product was purified by washing with methanol. The yield after purification was typically 50% and the compound was 85% pure and used directly in the next step.

***(S)*-Methyl-3-methyl-2-(2-naphthalen-1-yl)acetamido)butanoate (27):**

¹H NMR (CDCl₃): 7.99 (d, ArH, 1H, ³J_{HH} = 7.1Hz), 7.88 (d, ArH, 1H, ³J_{HH} = 8.6Hz), 7.83 (d, ArH, 1H, ³J_{HH} = 7.6Hz), 7.55 (d, ArH, 1H, ³J_{HH} = 5.6Hz), 7.52 (d, ArH, 1H, ³J_{HH} = 5.8Hz), 7.48 (d, ArH, 1H, ³J_{HH} = 6.1Hz), 7.46 (s, ArH, 1H), 5.85 (d, NH, 1H, ³J_{HH} = 8.1Hz), 4.50 (q, CH₂C=O, 2H, ³J_{HH} = 14.0Hz), 4.07 (q, NHCHCH(CH₃)₂, 1H, ³J_{HH} = 6.1Hz), 1H), 3.61 (s, OCH₃, 3H), 1.97 (m, (CH₃)₂CH, 1H), 0.71 (d, (CH₃)₂CH, 6H, ³J_{HH} = 6.8Hz) ppm. ¹³C NMR (CDCl₃): 173.08, 170.36, 133.27, 132.93, 131.90, 128.27, 127.70, 126.93, 125.77, 125.55, 125.42, 124.36, 102.73, 57.14, 29.19, 17.95 ppm. MS: ES⁺ ([M+Na]⁺). Accurate mass calculated: 322.1419 Found 322.1428.

Deprotection of the C-terminus:

A solution of THF: water (30 mL: 5 mL) was added to the compound **27**. Lithium hydroxide (0.5 g) was added. The solution was stirred overnight. After this time, distilled water (100 mL) was added, and then hydrochloric acid (1.0 M) was added drop-wise until the pH was lowered to pH 3. Chloroform was added to the resulting oil of compound **28** in separating funnel and the organic phase was dried over magnesium sulfate and the solvent was removed *in vacuo*. The resulting precipitate was collected by filtration and washed with water to give compound **28** as shown in Scheme 2.2. The yield was 68%. The impurity (excess of valine methyl ester) was calculated by NMR

spectroscopy 8%. The resulting product was purified by washing with methanol to give yield of 45% and purity of 96%.

***(S)*-Methyl-2-(2-naphthalen-1-yl)acetamido)butanoic acid (28):**

^1H NMR (d_6 -DMSO): 8.38 (d, NH, 1H,), 8.13 (d, ArH, 1H,), 7.91 (d, ArH, 1H,), 7.80 (d, ArH, 1H,), 7.59 (d, ArH, 1H,), 7.51 (d, ArH, 1H,), 7.45 (s, ArH, 1H,), 7.44 (d, NH, 1H,), 4.34 (d, $\text{CH}_2\text{C}=\text{O}$, 2H, $^3\text{J}_{\text{HH}} = 12.8\text{Hz}$), 4.13 (d, $\text{NHCHCH}(\text{CH}_3)_2$, 1H), 1.98 (m, $(\text{CH}_3)_2\text{CH}$, 1H), 0.86 (m, $(\text{CH}_3)_2\text{CH}$, 6H) ppm. ^{13}C NMR (d_6 -DMSO): 173.1, 170.4, 133.3, 132.9, 131.9, 128.3, 127.7, 126.9, 125.8, 125.6, 125.4, 124.4, 102.7, 57.2, 29.2, 17.9 ppm. MS: ES^+ ($[\text{M}+\text{Na}]^+$). Accurate mass calculated: 308.1263 Found 308.1261.

Standard coupling methodology:

N-Methylmorpholine (0.6 mL) and IBCF (3 mL) were added to compound 26 (1.0 g) in chloroform (70 mL) at 0°C. A solution of *L*-phenylalanine ethyl ester hydrochloride, *L*-valine ethyl ester hydrochloride, *L*-alanine ethyl ester hydrochloride or glycine ethyl ester hydrochloride and NMM (0.6 mL) in chloroform was added. The solution was stirred at room temperature overnight. The solution was washed with distilled water (100 mL), hydrochloric acid (2 x 100 mL, 0.1 M), aqueous potassium carbonate (100 mL, 0.1 M), and distilled water again (4 x 100 mL) and dried with magnesium sulfate. The solvent was removed *in vacuo* to give compounds **29 (a - d)** as shown in the Scheme 2.2 and Table 2.4. The yield was between 27 - 56%. The impurity (an excess of the amino acid methyl ester) was calculated by NMR spectroscopy to be between 12 - 27% for all derivatives. The resulting product was purified by washing with methanol. The yield after purification was 35 - 40% and the product was typically 80 - 90% pure.

***(S)*-Methyl-2-((*S*)-3-methyl-2-(2-naphthalen-1-yl)acetamido)butanamido)butanoate (29a):**

^1H NMR (CDCl_3): 7.96 (d, ArH, 1H, $^3\text{J}_{\text{HH}} = 8.3$), 7.86 (d, ArH, 1H, $^3\text{J}_{\text{HH}} = 7.8$), 7.82 (d, ArH, 1H, $^3\text{J}_{\text{HH}} = 8.8$), 7.52 (d, ArH, 1H, $^3\text{J}_{\text{HH}} = 6.9$), 7.50 (d, ArH, 1H, $^3\text{J}_{\text{HH}} = 7.4$), 7.45 (s, ArH, 1H,), 7.42 (d, ArH, 1H, $^3\text{J}_{\text{HH}} = 8.9$), 6.33 (d, NH, 1H, $^3\text{J}_{\text{HH}} = 8.8$), 5.87 (d, NH, 1H, $^3\text{J}_{\text{HH}} = 8.3$), 4.09 (s, $\text{CH}_2\text{C}=\text{O}$, 2H), 4.41 (dd, $\text{NHCHCH}(\text{CH}_3)_2$, 1H, $^3\text{J}_{\text{HH}} = 5.4, 4.3$), 4.21 (dd, $\text{NHCHCH}(\text{CH}_3)_2$, 1H, $^3\text{J}_{\text{HH}} = 6.4, 2.1$), 3.71 (s, OCH_3 , 3H), 2.08 (m, $(\text{CH}_3)_2\text{CH}$, 1H), 1.91 (m, $(\text{CH}_3)_2\text{CH}$, 1H), 0.85 (d, $(\text{CH}_3)_2\text{CH}$, 3H, $^3\text{J}_{\text{HH}} = 7.3$), 0.82 (d, $(\text{CH}_3)_2\text{CH}$, 3H, $^3\text{J}_{\text{HH}} =$

6.3Hz), 0.75 (d, (CH₃)₂CH, 3H, ³J_{HH} = 6.3), 0.54 (d, (CH₃)₂CH, 3H, ³J_{HH} = 7.3Hz) ppm. ¹³C NMR (CDCl₃): 171.9, 171.0, 170.7, 133.9, 131.9, 130.7, 128.8, 128.3, 126.8, 126.1, 125.6, 123.6, 58.5, 57.0, 52.1, 41.6, 30.9, 30.3, 19.0, 18.8, 17.7, 17.5, 17.3 ppm. MS: ES⁺ ([M+Na]⁺). Accurate mass calculated: 421.2103 Found 421.2104.

(S)-Methyl-2-((S)-3-methyl-2-(2-naphthalen-1yl)acetamido)butanamido)propanoate (29b):

¹H NMR (CDCl₃): 7.98 (d, ArH, 1H, ³J_{HH} = 7.8Hz), 7.86 (d, ArH, 1H, ³J_{HH} = 4.9Hz), 7.81 (d, ArH, 1H, ³J_{HH} = 5.4Hz), 7.55 (d, ArH, 1H, ³J_{HH} = 3.4Hz), 7.50 (d, ArH, 1H, ³J_{HH} = 4.4Hz), 7.47 (d, ArH, 1H, ³J_{HH} = 6.4Hz), 7.44 (d, ArH, 1H, ³J_{HH} = 4.9Hz), 6.37 (d, NH, 1H, ³J_{HH} = 6.9Hz), 5.92 (d, NH, 1H, ³J_{HH} = 7.9Hz), 4.47 (m, NHCH(CH₃), 1H, ³J_{HH} = 7.8Hz), 4.20 (dd, NHCHCH(CH₃)₂, 1H, ³J_{HH} = 6.4Hz), 4.08 (d, CH₂C=O, 2H, ³J_{HH} = 12.5Hz), 3.71 (s, OCH₃, 3H), 1.94 (m, (CH₃)₂CH, 1H), 1.31 (d, CH₃, 3H, ³J_{HH} = 7.2Hz), 0.75 (d, (CH₃)₂CH, 3H, ³J_{HH} = 6.3Hz), 0.56 (d, (CH₃)₂CH, 3H, ³J_{HH} = 7.6Hz) ppm. ¹³C NMR (CDCl₃): 172.9, 171.3, 170.6, 134.3, 132.3, 131.2, 129.2, 128.9, 128.7, 127.1, 126.5, 126.0, 124.0, 61.8, 58.6, 48.4, 42.1, 31.1, 19.3, 18.5, 17.9 ppm. MS: ES⁺: [M+Na]⁺. Accurate mass calculated: 393.1790. Found 393.1802.

(S)-Ethyl-2-(3-methyl-2-(2-naphthalen-1yl)acetamido)butanamido)acetate(29c):

¹H NMR (CDCl₃): 7.96(d, ArH, 1H, ³J_{HH} = 6.4Hz), 7.88 (dd, ArH, 1H, ³J_{HH} = 6.8Hz), 7.83 (d, ArH, 1H, ³J_{HH} = 7.2Hz), 7.52 (d, ArH, 1H, ³J_{HH} = 3.1Hz), 7.49 (d, ArH, 1H, ³J_{HH} = 3.0Hz), 7.46 (s, ArH, 1H), 7.44 (d, ArH, 1H, ³J_{HH} = 2.7Hz), 6.35 (d, NH, 1H, ³J_{HH} = 6.1Hz), 5.92 (d, NH, 1H, ³J_{HH} = 5.5Hz), 4.10 (s, CH₂C=O, 2H), 4.01 (d, NHCHCH(CH₃)₂, 1H, ³J_{HH} = 8.0Hz), 3.98 (q, OCH₂CH₃, 2H, ³J_{HH} = 8.0Hz), 3.90 (d, NHCH₂C=O, 2H, ³J_{HH} = 5.4Hz), 1.94 (m, (CH₃)₂CH, 1H), 1.26 (t, OCH₂CH₃, 3H, ³J_{HH} = 7.1Hz) 0.73 (d, (CH₃)₂CH, 3H, ³J_{HH} = 8.3Hz), 0.54 (d, (CH₃)₂CH, 3H, ³J_{HH} = 7.3Hz) ppm. ¹³C NMR (CDCl₃): 172.1, 170.9, 169.3, 133.9, 131.9, 130.7, 128.9, 128.6, 128.3, 126.7, 126.1, 125.7, 123.6, 61.5, 58.3, 41.7, 41.1, 30.2, 19.0, 17.4, 14.1 ppm. MS: ES⁺: [M+Na]⁺. Accurate mass calculated: 393.1790 Found: 393.1787.

***(S)*-Ethyl-2-((*S*)-3-methyl-2-(2-naphthalen-1-yl)acetamido)butanamido)-3-phenylpropanoate(29d):**

¹H NMR (CDCl₃): 8.21 (d, ArH, 1H, ³J_{HH} = 5.9Hz), 8.11 (d, ArH, 1H, ³J_{HH} = 6.5Hz), 7.89 (d, ArH, 1H, ³J_{HH} = 8.6Hz), 7.79 (d, ArH, 1H, ³J_{HH} = 3.7Hz), 7.49 (d, ArH, 1H, ³J_{HH} = 7.4Hz), 7.42 (d, ArH, 1H, ³J_{HH} = 6.5Hz), 7.14 (d, ArH, 1H, ³J_{HH} = 7.0Hz), 6.09 (d, NH, 1H, ³J_{HH} = 8.1Hz), 5.72 (d, NH, 1H, ³J_{HH} = 9.2Hz), 4.17 (m, NHCH(CH₂Ph), 1H), 1H), 4.07 (s, CH₂C=O, 2H), 3.89 (dd, NHCHCH(CH₃)₂, 1H, ³J_{HH} = 7.3, 6.3Hz), 3.60 (q, OCH₂CH₃, 2H, ³J_{HH} = 9.3, 6.0Hz), 3.05 (dd, NHCH₂Ph, 1H, ³J_{HH} = 7.3, 6.3Hz), 2.93 (dd, NHCH₂Ph, 1H, ³J_{HH} = 7.0, 6.1Hz), 1.97 (m, (CH₃)₂CH, 1H), 1.26 (t, OCH₂CH₃, 2H, ³J_{HH} = 7.0Hz), 0.78 (d, (CH₃)₂CH, 3H, ³J_{HH} = 7.6 Hz), 0.68 (d, (CH₃)₂CH, 3H, ³J_{HH} = 6.3Hz) ppm. ¹³C NMR (CDCl₃): 171.1, 169.9, 167.4, 151.6, 135.6, 131.6, 131.4, 131.2, 130.0, 129.3, 128.6, 128.5, 128.2, 127.1, 119.1, 115.3, 109.9, 68.5, 61.6, 58.0, 53.0, 37.8, 30.8, 19.2, 17.8, 14.0 ppm. MS: ES⁺ ([M+Na]⁺). Accurate mass calculated: 483.2260. Found 483.2257.

Deprotection of the C-terminus:

A solution of THF: water (30 mL, 5 mL) was added to the compounds **29 (a – d)**. Lithium hydroxide (0.5 g) was added and the solution was stirred overnight. After this time, distilled water (100 mL) was added, and then hydrochloric acid (1.0 M) was added drop-wise until the pH was lowered to pH 3. Chloroform was added to the resulting compounds **30, 31, 32** or **33** in a separating funnel and the organic phase was dried over magnesium sulfate and the solvent was removed *in vacuo* to give compounds (**30 – 32**) as shown in Scheme 2.2 and Table 2.5. The yield was between 65 – 78%. The impurity (an excess of valine methyl ester) was calculated by NMR spectroscopy to be between 7 – 9% for all derivatives except compound **30**, which was pure and used directly in the next step of the reaction. The resulting product was purified by washing with methanol. The yield after purification was typically between 50 – 60% and the resulting products were between 96 – 98% pure.

***(S)*-3-Methyl-2-((*S*)-3-methyl-2-(2-naphthalen-1-yl)acetamido)butanamido)butanoic acid (30):**

¹H NMR (d₆-DMSO): 8.22 (d, NH, 1H, ³J_{HH} = 9.2Hz), 8.20 (d, NH, 1H, ³J_{HH} = 4.6Hz), 8.12 (s, ArH, 1H), 8.09 (d, ArH, 1H, ³J_{HH} = 8.5Hz), 7.91 (t, ArH, 1H, ³J_{HH} = 3.2Hz), 7.79 (d, NH, 1H, ³J_{HH} = 3.1Hz), 7.80 (d, ArH, 1H, ³J_{HH} = 5.9Hz), 7.49 (d, ArH, 1H, ³J_{HH} = 8.1Hz), 7.43 (d, ArH,

^1H , $^3\text{J}_{\text{HH}} = 5.3\text{Hz}$), 3.96 (s, $\text{CH}_2\text{C}=\text{O}$, 2H), 4.32 (dd, $\text{NHCHCH}(\text{CH}_3)_2$, 1H, $^3\text{J}_{\text{HH}} = 7.2, 4.3\text{Hz}$), 4.21 (dd, $\text{NHCHCH}(\text{CH}_3)_2$, 1H, $^3\text{J}_{\text{HH}} = 5.9, 3.3\text{Hz}$), 2.0 (m, $(\text{CH}_3)_2\text{CH}$, 1H), 1.98 (m, $(\text{CH}_3)_2\text{CH}$, 1H), 0.86 (d, $(\text{CH}_3)_2\text{CH}$, 6H, $^3\text{J}_{\text{HH}} = 7.3\text{Hz}$) ppm. ^{13}C NMR ($\text{DMSO } d_6$): 173.1, 171.7, 170.3, 155.91, 133.6, 133.4, 132.3, 128.6, 128.1, 127.3, 126.1, 125.9, 125.8, 124.7, 57.6, 57.5, 31.1, 31.0, 29.9, 19.5, 19.4, 18.4 ppm. MS: ES^+ ($[\text{M}+\text{Na}]^+$). Accurate mass calculated: 407.1947. Found 407.1943.

(S)-2-((S)-3-Methyl-2-(2-naphthalen-1-yl)acetamido)butanamido)propanoic acid (31):

^1H NMR (d_6 -DMSO): 8.39 (d, NH, 1H, $^3\text{J}_{\text{HH}} = 9.3\text{Hz}$), 8.28 (d, ArH, 1H, $^3\text{J}_{\text{HH}} = 6.4\text{Hz}$), 8.20 (d, NH, 1H, $^3\text{J}_{\text{HH}} = 9.8\text{Hz}$), 8.12 (dd, ArH, 1H, $^3\text{J}_{\text{HH}} = 5.9\text{Hz}$), 7.91 (dd, ArH, 1H, $^3\text{J}_{\text{HH}} = 5.8\text{Hz}$), 7.80 (t, ArH, 1H, $^3\text{J}_{\text{HH}} = 6.9\text{Hz}$), 7.51 (d, ArH, 1H, $^3\text{J}_{\text{HH}} = 4.4\text{Hz}$), 7.50 (d, ArH, 1H, $^3\text{J}_{\text{HH}} = 6.2\text{Hz}$), 7.44 (d, ArH, 1H, $^3\text{J}_{\text{HH}} = 5.3\text{Hz}$), 4.19 (dd, $\text{NHCHCH}(\text{CH}_3)_2$, 1H, $^3\text{J}_{\text{HH}} = 5.9, 4.0\text{Hz}$), 3.95 (d, $\text{OCH}_2\text{C}=\text{O}$, 2H, $^3\text{J}_{\text{HH}} = 10.6\text{Hz}$), 4.17 (m, $\text{NHCH}(\text{CH}_3)$, 1H), 1.98 (m, $(\text{CH}_3)_2\text{CH}$, 1H), 1.25 (d, CH_3 , 3H, $^3\text{J}_{\text{HH}} = 7.3\text{Hz}$), 0.86 (d, $(\text{CH}_3)_2\text{CH}$, 3H, $^3\text{J}_{\text{HH}} = 6.3\text{Hz}$), 0.84 (d, $(\text{CH}_3)_2\text{CH}$, 3H, $^3\text{J}_{\text{HH}} = 8.6\text{Hz}$) ppm. ^{13}C NMR (d_6 -DMSO): 174.3, 171.1, 170.7, 170.3, 133.6, 132.3, 128.6, 128.1, 127.3, 126.1, 126.0, 125.8, 124.7, 57.5, 47.8, 31.2, 30.2, 19.5, 18.4, 17.3 ppm. MS: ES^+ ($[\text{M}+\text{Na}]^+$). Accurate mass calculated: 379.1634 Found 379.1635.

(S)-2-(3-Methyl-2-(2-naphthalen-1-yl)acetamido)butanamido)acetic acid (32):

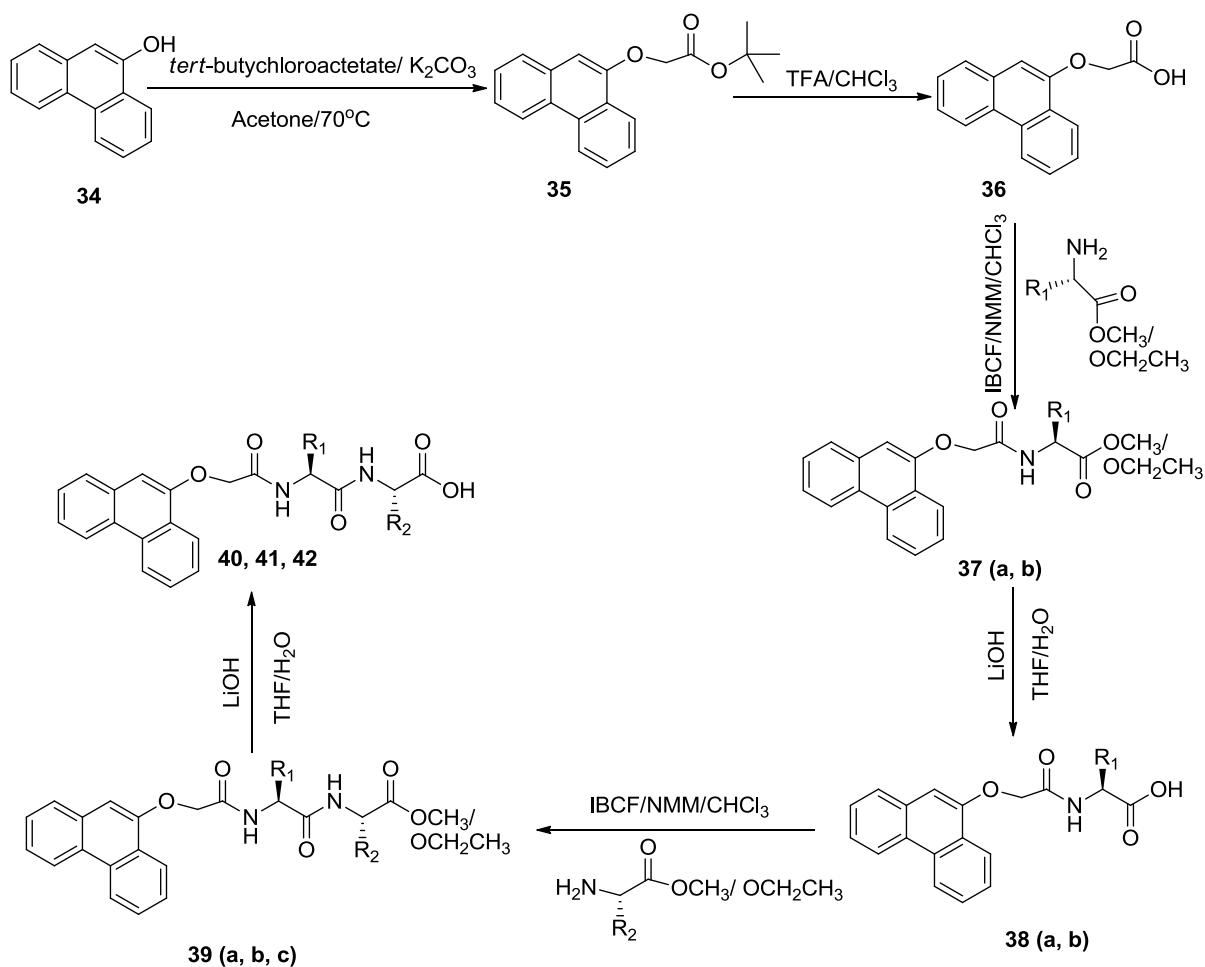
^1H NMR (d_6 -DMSO): 8.38 (dd, ArH, 1H, $^3\text{J}_{\text{HH}} = 7.8\text{Hz}$), 8.30 (d, NH, 1H, $^3\text{J}_{\text{HH}} = 5.9\text{Hz}$), 8.43 (d, NH, 1H, $^3\text{J}_{\text{HH}} = 7.8\text{Hz}$), 8.12 (m, ArH, 1H), 7.90 (d, ArH, 1H, $^3\text{J}_{\text{HH}} = 4.0\text{Hz}$), 7.80 (t, ArH, 1H, $^3\text{J}_{\text{HH}} = 5.2\text{Hz}$), 7.50 (d, ArH, 1H, $^3\text{J}_{\text{HH}} = 4.6\text{Hz}$), 7.49 (d, ArH, 1H, $^3\text{J}_{\text{HH}} = 4.6\text{Hz}$), 7.44 (s, ArH, 1H), 4.20 (dd, $\text{NHCHCH}(\text{CH}_3)_2$, 1H, $^3\text{J}_{\text{HH}} = 6.5, 5.3\text{Hz}$), 3.95 (d, $\text{CH}_2\text{C}=\text{O}$, 2H, $^3\text{J}_{\text{HH}} = 12.6\text{Hz}$), 3.78 (d, $\text{NHCH}_2\text{C}=\text{O}$, 1H, $^3\text{J}_{\text{HH}} = 5.3\text{Hz}$), 3.73 (d, $\text{NHCH}_2\text{C}=\text{O}$, 1H, $^3\text{J}_{\text{HH}} = 6.3\text{Hz}$), 2.01 (m, $(\text{CH}_3)_2\text{CH}$, 1H), 0.86 (d, $(\text{CH}_3)_2\text{CH}$, 3H, $^3\text{J}_{\text{HH}} = 4.4\text{Hz}$), 0.84 (d, $(\text{CH}_3)_2\text{CH}$, 3H, $^3\text{J}_{\text{HH}} = 3.7\text{Hz}$) ppm. ^{13}C NMR (d_6 -DMSO): 172.8, 167.6, 153.0, 131.4, 131.2, 130.9, 130.4, 128.8, 128.0, 118.0, 116.6, 107.7, 68.0, 57.0, 30.3, 19.4, 18.0 ppm. MS: ES^+ ($[\text{M}+\text{Na}]^+$). Accurate mass calculated: 365.1475. Found 365.1477.

(S)-2-((S)-3-Methyl-2-(2-naphthalen-1-yl)acetamido)butanamido)-3-phenyl propanoic acid (33):

^1H NMR (d_6 -DMSO): 8.21 (d, ArH, 1H, $^3J_{\text{HH}} = 9.1\text{Hz}$), 8.11 (dd, ArH, 1H, $^3J_{\text{HH}} = 5.0\text{Hz}$), 7.89 (dd, ArH, 1H, $^3J_{\text{HH}} = 4.0\text{Hz}$), 7.87 (t, NH, 1H, $^3J_{\text{HH}} = 4.5\text{Hz}$), 7.79 (d, ArH, 1H, $^3J_{\text{HH}} = 3.4\text{Hz}$), 7.49 (d, ArH, 1H, $^3J_{\text{HH}} = 4.0\text{Hz}$), 7.42 (s, ArH, 1H), 7.20 (d, NH, 1H, $^3J_{\text{HH}} = 6.1\text{Hz}$), 7.14 (d, ArH, 1H, $^3J_{\text{HH}} = 5.5\text{Hz}$), 4.43(m, NHCH(CH₂Ph), 1H, $^3J_{\text{HH}} = 8.1\text{Hz}$), 1H), 4.07 (s, CH₂C=O, 2H), 4.22 (dd, NHCHCH(CH₃)₂, 1H, $^3J_{\text{HH}} = 7.3, 4.3\text{Hz}$), 2.89 (dd, NHCH₂Ph, 2H, $^3J_{\text{HH}} = 9.6, 7.3\text{Hz}$), 1.97(m, (CH₃)₂CH, 1H), 0.84 (d, (CH₃)₂CH, 3H, $^3J_{\text{HH}} = 7.3\text{Hz}$), 0.78 (d, (CH₃)₂CH, 3H, $^3J_{\text{HH}} = 3.9\text{Hz}$) ppm. ^{13}C NMR (d_6 -DMSO): 173.8, 173.0, 156.6, 138.3, 133.3, 133.1, 132.2, 129.4, 128.5, 128.3, 128.0, 127.9, 127.7, 127.6, 126.7, 126.4, 126.0, 70.1, 55.7, 36.8, 30.2, 27.9, 19.5, 19.2, 19.1, 18.3 ppm. MS: ES⁺ ([M+Na]⁺). Accurate mass calculated: 455.1947 Found 455.1952.

2.2.2- Phenanthrol dipeptides:

Phenanthrol dipeptide derivatives were synthesised previously using different methods, IBCF^{12, 13} or DCC^{5, 11} methods. We synthesised dipeptides conjugated to phenanthrol using IBCF method as shown in the Scheme 2.3.



Scheme 2.3: The general reaction of 9-phenanthrene dipeptide synthesis based on 9-phenanthrol ring using IBCF method.

Compound	Substituent
37, 38	R ₁
a	CH(CH ₃) ₂
b	CH ₂ Ph

Table 2.6: The R₁ group of the general structure of compounds 37 and 38 (a, b) in the Scheme 3.

Compound	Functional group	
	R ₁	R ₂
39	R ₁	R ₂
a	CH(CH ₃) ₂	CH(CH ₃) ₂
b	CH ₂ Ph	CH ₂ Ph
c	CH(CH ₃) ₂	CH ₂ Ph

Table 2.7: The R₁ and R₂ groups of the general structure of compounds 39 (a, b, c) in the Scheme 3.

Dipeptide	R ₁	R ₂	Abbreviation
40	CH(CH ₃) ₂	CH(CH ₃) ₂	9Ph-VVOH
41	CH ₂ Ph	CH ₂ Ph	9Ph-FFOH
42	CH(CH ₃) ₂	CH ₂ Ph	9Ph-VFOH

Table 2.8: The R₁ and R₂ groups of the general structure of compounds 40–42 and their abbreviations in the Scheme 3.

Experimental section:

The phenanthrol dipeptides were prepared by the general method to prepare dipeptides used by Chen *et al*¹⁴. To a stirred a solution of 9-phenanthrol (10.0 g) and K₂CO₃ (3 eq.) in acetone (200 mL), *tert*-butyl chloroacetate (1.1 eq.) was added and the solution was refluxed at 70°C overnight. Chloroform (200 mL) was added to the resulting suspension in a separating funnel and water (100 mL) water. The organic phase was washed with water (4 x 200 mL). Then, the solution was dried with magnesium sulphate and the solvent was removed *in vacuo* to give compound **35** as shown in Scheme 2.3. The yield was 50% and the impurity (*tert*-butyl chloroacetate) was calculated by NMR spectroscopy to be around 17%. Then the resulting product was purified by washing with methanol and the yield was typically 30%. The resulting product was 93% pure.

¹H, ¹³C NMR and mass spectroscopy of the resulting products:

Tert-Butyl-2-(phenanthren-9-yloxy)acetate (35):

¹H NMR (CDCl₃): 8.57 (d, ArH, 1H, ³J_{HH} = 8.3Hz), 8.51(d, ArH, 1H, ³J_{HH} = 8.8Hz), 8.41 (d, ArH, 1H, ³J_{HH} = 8.3Hz), 7.61 (m, ArH, 3H), 7.45 (m, ArH, 2H), 6.80 (s, ArH, 1H), 4.71 (s, OCH₂C=O, 2H), 1.45 (s, C(CH₃)₃, 9H) ppm. ¹³C NMR (CDCl₃): 168.2, 152.3, 134.5, 132.9,

131.8, 127.8, 127.7, 127.6, 127.3, 127.2, 126.9, 126.8, 125.0, 123.3, 122.9, 122.8, 103.6, 82.9, 66.3, 30.1, 28.5 ppm. MS: ES⁺: [M+Na]⁺. Accurate mass calculated: 331.1325 Found 331.1334.

Removal of the *tert*-butyl protection group:

The *tert*-butyl 9-phenanthrol acetate derivative was dissolved in chloroform (30 mL), and trifluoroacetic acid (10 mL) was added, and the solution was stirred for overnight. Hexane was added to the solution, and then the resulting precipitate was collected by filtering. The resulting precipitate was collected by filtration and washed with water to give compound **36** as shown in Scheme 2.3. The resulting product was pure and used directly in the next step of the reaction. The yield was 68%.

2-(Phenanthren-9-yloxy)acetic acid (36):

¹H NMR (d₆-DMSO): 8.82 (d, ArH, 1H, ³J_{HH} = 7.8Hz), 8.72(d, ArH, 1H, ³J_{HH} = 7.9Hz), 8.35 (d, ArH, 1H, ³J_{HH} = 9.1Hz), 7.86 (d, ArH, 1H, ³J_{HH} = 9.0), 7.72 (m, ArH, 2H), 7.55 (m, ArH, 2H), 7.19 (s, ArH, 1H), 4.99 (s, OCH₂C=O, 2H), 13.7 (s, OH) ppm. ¹³C NMR (d₆-DMSO): 170.4, 155.9, 134.4, 129.7, 129.0, 127.9, 127.1, 126.8, 124.2, 118.8, 107.4, 64.9 ppm. MS ([M+Na]⁺). Accurate mass calculated: MS: CI: Low resolution [NH₄⁺] found 270.2.

Standard coupling methodology:

N-Methylmorpholine (2 eq.) and IBCF (1.1 eq.) was added to compound **36** (5.0 g) in (70 mL) chloroform at 0 °C. A solution of L-valine methyl ester or L-phenylalanine ethyl ester (1.5 eq.) and NMM (2 eq.) in chloroform was added and the solution was stirred at room temperature overnight. Then, the solution was washed with distilled water (100 mL), hydrochloric acid (2 x 100 mL, 0.1 M), aqueous potassium carbonate (100 mL, 0.1 M), and distilled water again (4 x 100 mL) and dried with magnesium sulfate. The solvent was removed *in vacuo* to give compounds **37 (a - b)** as shown in Scheme 2.3 and Table 2.6. The yield was between 59 – 69% and the resulting product for all derivatives was pure and used directly in the next step of the reaction.

***(S)*-Methyl-3-methyl-2-(2-(phenanthren-9-yloxy)acetamido)butanoate (37a):**

¹H NMR (CDCl₃): 8.69 (d, ArH, 1H, ³J_{HH} = 8.3Hz), 8.60 (d, ArH, 1H, ³J_{HH} = 6.1Hz), 8.36 (d, ArH, 1H, ³J_{HH} = 7.2Hz), 7.73 (m, ArH, 3H), 7.55 (m, ArH, 2H), 7.19 (d, NH, 1H, ³J_{HH} =

8.9Hz), 6.99 (s, ArH, 1H), 4.83(d, OCH₂C=O, 2H, ³J_{HH} = 3.1Hz), 4.70 (dd, NHCHCH(CH₃)₂, 1H, ³J_{HH} = 4.8, 4.1Hz), 3.74 (s, OCH₃, 3H), 2.24 (m, (CH₃)₂CH, 1H), 0.96 (d,(CH₃)₂CH, 3H, ³J_{HH} = 6.9Hz) , 0.89 (d,(CH₃)₂CH, 3H, ³J_{HH} = 6.9Hz) ppm. ¹³C NMR (CDCl₃): 198.3, 170.1, 166.2, 149.1, 130.3, 129.6, 125.8, 125.7, 125.3, 125.1, 124.9, 123.9, 123.2, 120.9, 120.7, 120.0, 102.4, 65.7, 54.9, 50.4, 29.5, 17.1, 15.8 ppm. MS: ES⁺: [M+Na]⁺. Accurate mass calculated: 388.1516 Found 388.1525.

(S)- Ethyl-2-(2-(phenanthren-9-yloxy)acetamido)-3-phenylpropanoate (37b):

¹H NMR (CDCl₃): 8.67 (d, NH, 1H, ³J_{HH} = 8.8Hz), 8.52 (m, ArH, 1H), 8.12 (d, ArH, 1H, ³J_{HH} = 7.8Hz), 7.73 (m, ArH, 2H), 7.57 (m, ArH, 3H), 7.11 (m, ArH, 4H), 7.03 (d, ArH, 2H, ³J_{HH} = 7.0Hz), 6.93 (s, ArH, 1H), 5.01 (m, NHCH(CH₂Ph)C=O, 1H), 4.78 (d, OCH₂C=O, 2H, ³J_{HH} = 3.2Hz), 4.19 (dq, OCH₂CH₃, 2H, ³J_{HH} = 5.2, 4.4, 2.4Hz), 3.16 (dd, NHCH(CH₂Ph)C=O, 2H, ³J_{HH} = 2.7, 3.3Hz), 1.23 (t, OCH₂CH₃, 3H, ³J_{HH} = 7.2Hz) ppm. ¹³C NMR (CDCl₃): 171.3, 169.5, 168.2, 151.3, 135.8, 132.6, 131.9, 129.6, 129.0, 128.1, 127.9, 127.6, 127.4, 127.1, 126.2, 125.5, 123.2, 122.9, 122.4, 117.7, 104.3, 67.7, 62.1, 52.9, 38.3, 14.5 ppm. MS: ES⁺: [M+Na]⁺. Accurate mass calculated: 450.1664 Found 450.1681.

Deprotection of the C-terminus:

A solution of THF: water (30 mL: 5 mL) was added to compound **37a** or **b**. Lithium hydroxide (0.5 g) was added and the solution was stirred overnight. After this time, distilled water (100 mL) was added, and then hydrochloric acid (1.0 M) was added drop-wise until the pH was lowered to pH 3. Then, the resulting precipitate was collected by filtration and washed with water to give compounds **38 (a – b)** as shown in Scheme 2.3 and Table 2.6. The yield was between 85 – 90% and the resulting product for all derivatives was pure and used directly in the next step of the reaction.

(S)-Methyl-3-methyl-2-(2-(phenanthren-9-yloxy)acetamido)butanoic acid (38a):

¹H NMR (d₆-DMSO): 8.82 (d, ArH, 1H, ³J_{HH} = 13.8Hz), 8.73 (d, NH, 1H, ³J_{HH} = 7.9Hz), 8.36 (t, ArH, 2H, ³J_{HH} = 10.9Hz), 7.76 (m, ArH, 3H), 7.57 (m, ArH, 2H), 7.17 (s, ArH, 1H), 4.94 (d, OCH₂C=O, 2H, ³J_{HH} = 6.0Hz), 4.31 (dd, NHCHCH(CH₃)₂, 1H, ³J_{HH} = 5.5, 3.0Hz), 2.17 (m, (CH₃)₂CH, 1H), 0.93 (d,(CH₃)₂CH, 6H, ³J_{HH} = 8.3Hz) ppm. ¹³C NMR (d₆-DMSO): 172.8, 167.7, 151.2, 132.2, 130.7, 127.5, 127.3, 127.2, 126.7, 125.9, 125.6, 124.7, 122.9, 122.7,

122.2, 103.5, 66.8, 56.8, 29.9, 19.2, 17.9 ppm. MS: ES⁻: [M - H]⁻. Accurate mass calculated: 350.1393 Found 350.1392.

***(S)*-2-(2-(Phenanthren-9-yloxy)acetamido)-3-phenylpropanoic acid (38b):**

¹H NMR (d₆-DMSO): 8.83 (d, ArH, 1H, ³J_{HH} = 7.3Hz), 8.74 (d, NH, 1H, ³J_{HH} = 7.3Hz), 8.39 (d, ArH, 1H, ³J_{HH} = 8.3Hz), 8.33 (dd, ArH, 1H, ³J_{HH} = 8.3, 1.3Hz), 7.76 (m, ArH, 3H), 7.57 (m, ArH, 2H), 7.24 (m, ArH, 6H), 4.82 (d, OCH₂C=O, 1H, ³J_{HH} = 13.6Hz), 4.75 (d, OCH₂C=O, 1H, ³J_{HH} = 13.6Hz), 4.60 (m, NHCH(CH₂Ph)C=O, 1H), 3.18 (dd, NHCH(CH₂Ph)C=O, 1H, ³J_{HH} = 8.5, 4.7Hz), 3.07 (dd, NHCH(CH₂Ph)C=O, 1H, ³J_{HH} = 9.5, 5.2Hz) ppm. ¹³C NMR (d₆-DMSO): 173.1, 167.9, 151.4, 137.8, 132.6, 131.1, 129.5, 128.6, 127.9, 127.8, 127.5, 126.9, 126.8, 126.4, 125.9, 125.1, 123.3, 123.1, 122.8, 104.1, 67.4, 53.5, 36.7 ppm. MS: ES⁻: [M - H]⁻. Accurate mass calculated: 398.1401 Found 398.1392.

Standard coupling methodology:

N-Methylmorpholine (1.5 eq.) and IBCF (1.1 eq.) were added to compound **38a** or **38b** (1.0g) in chloroform (70 mL) at 0°C. A solution of L-phenylalanine ethyl ester hydrochloride or L-valine ethyl ester hydrochloride (1 eq.) and NMM (1.5 eq.) in chloroform was added and the solution was stirred at room temperature overnight. Then, the solution was washed with distilled water (100 mL), hydrochloric acid (2 x 100 mL, 0.1 M), aqueous potassium carbonate (100 mL, 0.1 M), and distilled water again (4 x 100 mL) and dried with magnesium sulphate, and the solvent was removed *in vacuo* to give compounds **39 (a - b)** as shown in Scheme 2.3 and Table 2.7. The yield was between 38 - 50%. The resulting product for all derivatives was pure and used directly in the next step of the reaction, except compound **39c**. This contained an impurity (an excess of valine methyl ester) that was calculated by NMR spectroscopy to be 3%, and was purified by washing with methanol to give a yield of typically 30% and purity of 99%.

***(S)*-Methyl-3-methyl-2-((S)-3-methyl-2-(2-(phenanthren-9-yloxy)acetamido)butanamido) butanoate (39a):**

¹H NMR (CDCl₃): 8.68 (d, NH, 1H, ³J_{HH} = 8.5Hz), 8.59 (t, ArH, 1H, ³J_{HH} = 6.3Hz), 8.34 (d, ArH, 1H, ³J_{HH} = 8.1Hz), 7.72 (m, ArH, 3H), 7.55 (m, ArH, 2H), 7.30 (d, ArH, 1H, ³J_{HH} = 9.5Hz), 7.00 (s, ArH, 1H), 6.39 (d, NH, 1H, ³J_{HH} = 8.1Hz), 4.84 (s, OCH₂C=O, 2H, ³J_{HH} =

3.1Hz), 4.54 (dd, NHCHCH(CH₃)₂, 1H, ³J_{HH} = 5.2, 3.9Hz), 4.46 (dd, NHCHCH(CH₃)₂, 1H, ³J_{HH} = 6.7, 2.4Hz), 3.74 (s, OCH₃, 3H), 2.18 (m, 2x(CH₃)₂CH, 2H), 0.98 (d,(CH₃)₂CH, 3H, ³J_{HH} = 7.1Hz), 0.93 (d,(CH₃)₂CH, 3H, ³J_{HH} = 3.4Hz), 0.91 (d,(CH₃)₂CH, 3H, ³J_{HH} = 3.7Hz), 0.88 (d,(CH₃)₂CH, 3H, ³J_{HH} = 6.7Hz) ppm. ¹³C NMR (CDCl₃): 172.5, 170.9, 168.7, 151.4, 132.6, 131.9, 128.1, 127.9, 127.5, 127.4, 127.3, 126.2, 125.5, 123.2, 122.9, 104.5, 67.9, 58.6, 57.6, 52.6, 31.6, 31.5, 19.6, 19.3, 18.4, 18.1 ppm. MS: ES⁺: [M+Na]⁺. Accurate mass calculated: 487.2212 Found 487.2209.

(S)-Ethyl-2-((S)-2-(2-(phenanthren-9-yloxy)acetamido)-3-phenylpropanaimdo)-3-phenylpropanoate(39b):

¹H NMR (CDCl₃): 8.69 (d, NH, 1H, ³J_{HH} = 7.8Hz), 8.60 (m, ArH, 1H), 8.16 (d, ArH, 1H, ³J_{HH} = 8.8Hz), 7.71 (m, ArH, 3H), 7.55 (m, ArH, 2H), 7.26 (s, ArH, 1H), 7.12 (m, ArH, 8H), 6.97 (d, ArH, 2H, ³J_{HH} = 7.1Hz), 6.88 (s, ArH, 1H), 6.40 (d, NH, 1H, ³J_{HH} = 8.3Hz), 4.79 (m, NHCH(CH₂Ph)C=O, 2H), 4.70 (s, OCH₂C=O, 2H), 4.16 (dq, OCH₂CH₃, 2H, ³J_{HH} = 2.3, 4.3, 4.8Hz), 3.05 (m, NHCH(CH₂Ph)C=O, 4H), 1.23 (t, OCH₂CH₃, 3H, ³J_{HH} = 7.1Hz) ppm. ¹³C NMR (CDCl₃): 170.9, 169.9, 168.3, 150.9, 135.8, 135.6, 132.2, 131.5, 129.5, 129.3, 129.3, 129.2, 128.7, 128.6, 128.5, 127.8, 127.6, 127.2, 127.1, 127.0, 126.8, 125.7, 125.1, 122.8, 122.5, 122.1, 103.8, 67.3, 61.6, 53.7, 53.3, 53.2, 37.9, 37.7, 14.1 ppm. MS: ES⁺: [M+Na]⁺. Accurate mass calculated: 597.2383 Found 597.2365.

(S)-Ethyl-2-((S)-3-methyl-2-(2-(phenanthren-9-yloxy)acetamido)butanamido)-3-phenyl propanoate(39c):

¹H NMR (CDCl₃): 8.69 (d, NH, 1H, ³J_{HH} = 8.9Hz), 8.60 (t, ArH, 1H, ³J_{HH} = 5.3Hz), 8.35 (dd, ArH, 1H, ³J_{HH} = 5.6, 3.4Hz), 7.74 (m, ArH, 3H), 7.55 (m, ArH, 2H), 7.19 (m, ArH, 5H), 7.07 (d, ArH, 2H, ³J_{HH} = 7.9Hz), 6.98 (s, ArH, 1H), 6.41 (d, NH, 1H, ³J_{HH} = 7.8Hz), 4.88 (m, NHCH(CH₂Ph)C=O, 1H), 4.81 (d, OCH₂C=O, 1H, ³J_{HH} = 13.6Hz), 4.73 (d, OCH₂C=O, 1H, ³J_{HH} = 13.6Hz), 4.43 (dd, NHCHCH(CH₃)₂, 1H, ³J_{HH} = 5.8, 2.6Hz), 4.18 (q, OCH₂CH₃, 2H, ³J_{HH} = 7.3Hz), 3.12 (dd, NHCH(CH₂Ph)C=O, 1H, ³J_{HH} = 8.6, 5.0Hz), 3.01 (dd, NHCH(CH₂Ph)C=O, 1H, ³J_{HH} = 8.6, 5.0Hz), 2.14 (m, (CH₃)₂CH, 1H), 1.25 (t, OCH₂CH₃, 3H, ³J_{HH} = 7.3Hz), 0.94 (d,(CH₃)₂CH, 3H, ³J_{HH} = 7.5Hz), 0.84 (d, (CH₃)₂CH, 3H, ³J_{HH} = 6.5Hz) ppm. ¹³C NMR (CDCl₃): 171.2, 170.2, 168.2, 150.9, 135.6, 129.3, 128.6, 127.7, 127.6, 127.2, 126.9, 125.1, 122.8, 122.6, 122.0, 104.0, 67.4, 61.7, 57.8, 53.1, 37.8, 31.1, 19.2, 17.8, 14.2 ppm. MS: ES⁺: [M+Na]⁺. Accurate mass calculated: 549.2363 Found 549.2365.

Deprotection of the C-terminus:

A solution of THF: water (30 mL: 5 mL) was added to compound **39 (a, b or c)**. Lithium hydroxide (0.3 g) was added and the solution was stirred overnight. After this time, distilled water (100 mL) was added, and then hydrochloric acid (1.0 M) was added drop-wise until the pH was lowered to pH 3. Then, the resulting precipitate was collected by filtration and washed with water to give compounds (**40 – 42**) as shown in Scheme 2.3 and Table 2.8. The yield was between 71 – 75% and the impurity (and excess of methyl or ethyl ester) was calculated by NMR spectroscopy to be between 17 – 20% for all derivatives except compound **40**, which was pure. Then, the resulting product was purified by washing with methanol. The yield after purification was typically between 55 – 60% and the resulting products were between 89 - 95% pure.

(S)-2-((S)-2-(2-(Phenanthren-9-yloxy)acetamido)-3-phenylpropanamido)-3-phenyl propanoic acid (40):

¹H NMR (d₆- DMSO): 8.82 (d, ArH, 1H, ³J_{HH} = 8.0Hz), 8.72 (d, ArH, 1H, ³J_{HH} = 8.2Hz), 8.50 (d, NH, 1H, ³J_{HH} = 8.1Hz), 8.25 (d, ArH, 1H, ³J_{HH} = 8.3Hz), 8.15 (d, NH, 1H, ³J_{HH} = 8.3Hz), 7.74 (m, ArH, 3H), 7.56 (m, ArH, 2H), 7.21 (m, ArH, 10H), 7.10 (s, ArH, 1H), 4.72 (m, NHCH(CH₂Ph)C=O, OCH₂=O, 3H), 4.51 (dd, NHCH(CH₂Ph)C=O, 1H, ³J_{HH} = 8.2, 5.4Hz), 3.19 (m, NHCH(CH₂Ph)C=O, 2H), 2.93 (m, NHCH(CH₂Ph)C=O, 2H) ppm. ¹³C NMR (d₆-DMSO): 172.7, 170.8, 167.0, 150.9, 137.4, 137.3, 132.2, 130.7, 129.3, 129.1, 128.2, 127.9, 127.5, 127.4, 127.1, 126.6, 126.4, 126.3, 126.0, 125.5, 124.7, 122.9, 122.7, 122.3, 103.6, 66.9, 53.5, 53.2, 37.4, 36.7 ppm. MS: ES⁻: [M – H]⁻. Accurate mass was not measured because the product could not be dissolved in any solvent suitable for mass spectroscopy.

(S)-3-Methyl-2-((S)-3-methyl-2-(2-(phenanthren-9-yloxy)acetamido)butanamido) butanoic acid(41):

¹H NMR (d₆- DMSO): 8.84 (d, NH, 1H, ³J_{HH} = 8.6Hz), 8.72 (d, NH, 1H, ³J_{HH} = 8.0Hz), 8.34 (d, ArH, 1H, ³J_{HH} = 6.6Hz), 8.18 (d, ArH, 1H, ³J_{HH} = 8.1Hz), 8.10 (d, ArH, 1H, ³J_{HH} = 9.0Hz), 7.76 (m, ArH, 3H), 7.56 (m, ArH, 2H) 7.17 (s, ArH, 1H), 4.84 (d, OCH₂C=O, 2H, ³J_{HH} = 4.7Hz), 4.49 (dd, NHCHCH(CH₃)₂, 1H, ³J_{HH} = 6.2, 3.3Hz), 4.15 (dd, NHCHCH(CH₃)₂, 1H, ³J_{HH} = 5.6, 2.6Hz), 2.06 (m, 2x(CH₃)₂CH, 2H), 0.87 (d, (CH₃)₂CH, 12H) ppm. ¹³C NMR (d₆-DMSO): 172.7, 170.9, 167.1, 151.1, 132.2, 130.8, 127.5, 127.3, 127.1, 126.7, 125.9, 125.6,

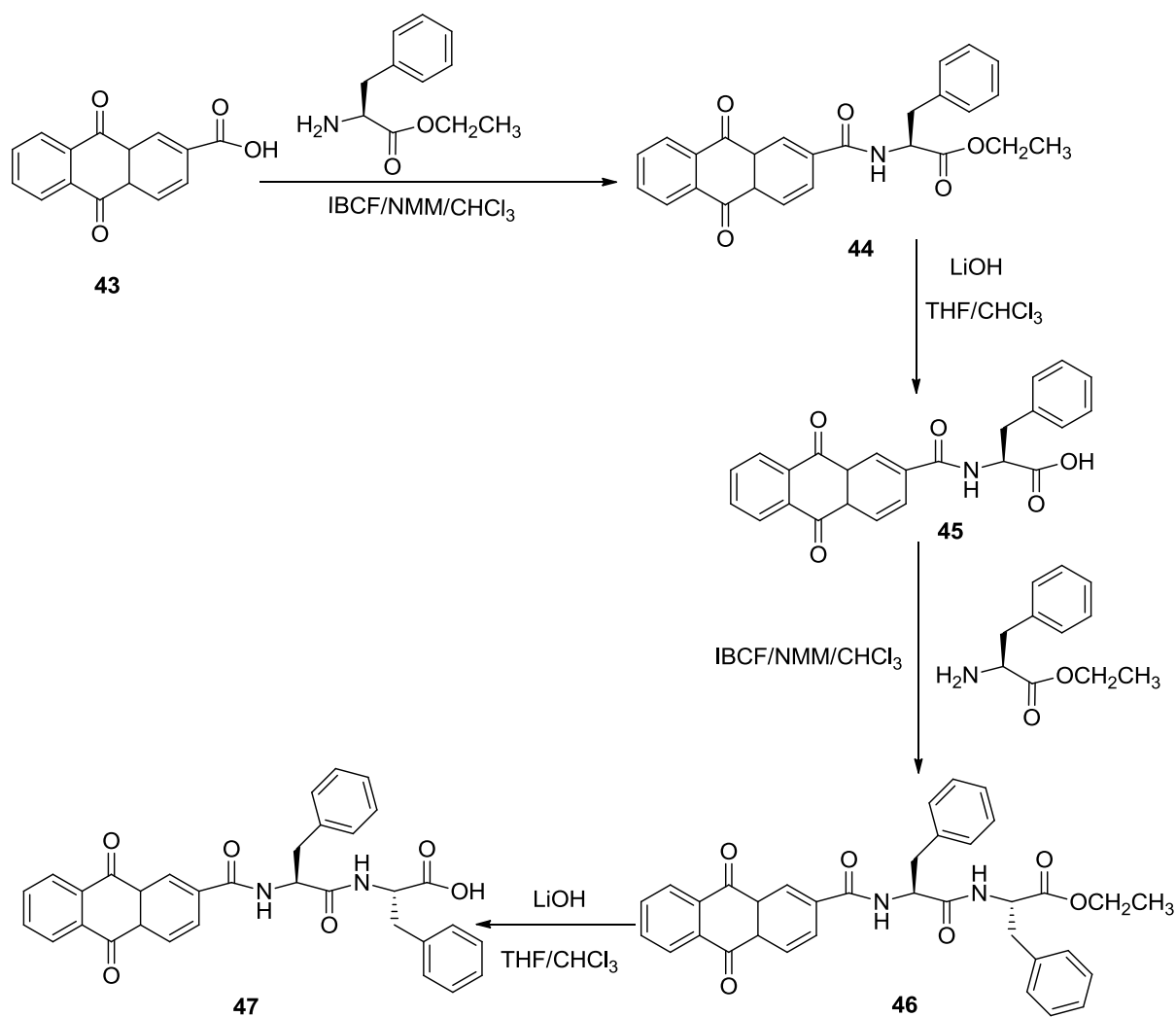
124.7, 122.9, 122.7, 122.0, 103.6, 66.9, 57.3, 56.7, 31.1, 29.6, 25.1, 19.2, 19.0, 18.0, 17.8 ppm. MS: ES⁻: [M - H]⁻. Accurate mass calculated: 449.2076 Found 449.2076.

(S)-2-((S)-3-Methyl-2-(2-(phenanthren-9-yloxy)acetamido)butanamido)-3-phenylpropanoic acid(42):

¹H NMR (d₆-DMSO): 8.82 (d, ArH, 1H, ³J_{HH} = 8.6Hz), 8.72 (d, NH, 1H, ³J_{HH} = 8.0Hz), 8.43 (d, ArH, 1H, ³J_{HH} = 7.8Hz), 8.33 (d, ArH, 1H, ³J_{HH} = 8.1Hz), 8.02 (d, NH, 1H, ³J_{HH} = 9.1Hz), 7.76 (m, ArH, 3H), 7.56 (m, ArH, 2H), 7.24 (m, ArH, 6H), 4.93(d, OCH₂=O, 2H, ³J_{HH} = 9.7Hz), 4.50 (m, NHCH(CH₂Ph)C=O, 1H), 4.38 (dd, NHCHCH(CH₃)₂, 1H, ³J_{HH} = 6.4, 4.3Hz), 3.06 (dd, NHCH(CH₂Ph)C=O, 2H, ³J_{HH} = 7.7, 5.1Hz), 2.92 (dd, NHCH(CH₂Ph)C=O, 2H, ³J_{HH} = 8.5, 6.4Hz), 2.06 (m, (CH₃)₂CH, 1H), 0.86 (d, (CH₃)₂CH, 3H, ³J_{HH} = 6.9Hz), 0.81 (d, (CH₃)₂CH, 3H, ³J_{HH} = 7.4Hz) ppm. ¹³C NMR (d₆-DMSO): 171.7, 170.6, 167.1, 151.0, 137.5, 132.2, 129.0, 128.1, 127.5, 127.3, 127.2, 126.3, 125.9, 124.7, 122.9, 103.6, 66.9, 53.5, 36.5, 30.9, 19.2, 17.6 ppm. MS: ES⁻: [M - H]⁻. Accurate mass calculated: 521.2058 Found 521.2052.

2.2.3- Anthraquinone dipeptide:

Peptides conjugated to anthraquinone were prepared elsewhere²³. Here, we have attempted to synthesise similar peptides using the IBCF method as shown in the Scheme 2.4 in order to study the hydrogelation properties and compare with other aromatic groups in Chapter 3.



Scheme 2.4: The general reaction of 2-antraquinone dipeptide synthesis based on 2-antraquinone ring using IBCF method.

Dipeptide	Abbreviation
47	2AQ-FFOH

Table 2.9: The abbreviation of compounds 47 in the Scheme 4.

Experimental section:

Standard coupling methodology:

N-Methylmorpholine (4 mL) and IBCF (3 mL) was added to anthraquinone acetic acid (5.0 g) in chloroform (70 mL) at 0°C. A solution of phenylalanine ethyl ester hydrochloride (4.0 g, 1.5 eq.) and NMM (4 mL) in chloroform was added and the solution was stirred at room temperature overnight. After this time, the solution was washed with distilled water (100 mL), hydrochloric acid (2 x 100 mL, 0.1 M), aqueous potassium carbonate (100 mL, 0.1 M), and distilled water again (4 x 100 mL) and dried with magnesium sulfate. Then, the solvent was removed *in vacuo* to give compound **44** as shown in Scheme 2.4. The yield was 40% and the impurity (an excess of phenyl alanine ethyl ester and IBCF) was calculated by NMR spectroscopy to be 28%. The resulting product was purified by washing with methanol. The yield after purification was typically 25% and the purity was 81%.

***(2S)*-2-(9,10-dioxo-4a,9,9a,10-tetrahydroanthracene-2-carboxamido)-3-phenyl propanoate (44):**

¹H NMR (CDCl₃): 8.58 (d, ArH, 1H, ³J_{HH} = 2.0Hz), 8.36 (m, ArH, 3H), 8.21 (dd, ArH, 1H, ³J_{HH} = 6.2, 2.0Hz), 7.85 (dd, ArH, 2H, ³J_{HH} = 2.5, 3.0Hz), 7.31 (m, ArH, 3H), 7.20 (d, ArH, 2H, ³J_{HH} = 6.7Hz), 6.85 (d, NH, 1H, ³J_{HH} = 7.8Hz), 5.12 (dd, NHCH(CH₂Ph)C=O, 1H, ³J_{HH} = 7.6, 5.6Hz), 4.27 (q, OCH₂CH₃, 2H, ³J_{HH} = 7.1, 7.1Hz), 3.33 (dd, NHCH(CH₂Ph)C=O, 2H, ³J_{HH} = 7.8, 6.0Hz), 1.32 (t, OCH₂CH₃, 3H, ³J_{HH} = 7.2Hz) ppm. ¹³C NMR (CDCl₃): 182.4, 182.3, 171.3, 165.1, 138.9, 135.7, 135.3, 134.5, 133.6, 133.4, 133.3, 132.8, 129.4, 128.7, 128.5, 1227.9, 127.4, 127.3, 125.4, 61.9, 61.4, 53.9, 37.9 18.9, 14.2, 14.1 ppm. MS: (ES⁺): [M+Na]⁺. Accurate mass calculated: 450.1329 Found: 450.1317.

Deprotection of the C-terminus:

A solution of THF: water (30 mL: 5 mL) was added to anthraquinone derivative. Lithium hydroxide (0.3 g) was added. The solution was stirred overnight. After this time, distilled water (100 mL) was added, and then hydrochloric acid (1.0 M) was added drop-wise until the pH was lowered to pH 3. The resulting precipitate was collected by filtration and washed with water. The resulting precipitate was collected by filtration and washed with water to give compound **45** as shown in Scheme 2.4. The yield was 75

%. The impurity (an excess of phenylalanine ethyl ester) was calculated by ¹H NMR spectroscopy to be 12%. The resulting product was purified by washing with methanol. The yield after purification was typically 50% and the purity was 90%.

(2S)-2-(9,10-Dioxo-4a,9,9a,10-tetrahydroanthracene-2-carboxamido)-3-phenylpropanoic acid (45):

¹H NMR (d₆-DMSO): 9.30 (d, NH, 1H, ³J_{HH} = 7.8Hz), 8.62 (s, ArH, 1H), 8.25 (m, ArH, 4H), 7.96 (m, ArH, 2H), 7.34 (d, ArH, 2H, ³J_{HH} = 7.3Hz), 7.28 (t, ArH, 2H, ³J_{HH} = 7.3Hz), 7.19 (t, ArH, 1H, ³J_{HH} = 6.3Hz), 4.70 (m, NHCH(CH₂Ph)C=O, 1H), 3.25 (dd, NHCH(CH₂Ph)C=O, 2H, ³J_{HH} = 8.8, 6.3Hz), 1.32 (t, OCH₂CH₃, 3H, ³J_{HH} = 7.2Hz) ppm. ¹³C NMR (d₆-DMSO): 182.5, 173.3, 165.3, 139.1, 138.4, 135.1, 135.0, 133.5, 133.4, 133.3, 129.4, 128.6, 128.5, 127.5, 127.2, 127.1, 126.8, 126.0, 67.4, 54.7, 36.5, 25.5, 19.2 ppm. MS: ES⁻: [M - H]⁻. Accurate mass calculated: 398.1043 Found: 398.1028.

Standard coupling methodology:

N-Methylmorpholine (4 mL) and IBCF (3 mL) was added to anthraquinone phenylalanine derivative (3.0 g) in chloroform (70 mL) at 0 °C. A solution of phenylalanine ethyl ester hydrochloride (4.0 g, 1.5 eq.) and NMM (4 mL) in chloroform was added and the solution was stirred at room temperature overnight. After this time, the solution was washed with distilled water (100 mL), hydrochloric acid (2 x 100 mL, 0.1 M), aqueous potassium carbonate (100 mL, 0.1 M), and distilled water again (4 x 100 mL) and dried with magnesium sulfate. Then, the solvent was removed *in vacuo* to give compound **46** as shown in Scheme 2.4. The yield was 35% and the impurity of IBCF was calculated by ¹H NMR spectroscopy to be 13%. The resulting product was purified by washing with methanol. The yield after purification was typically 20% and the purity was 92%.

2S-2-((2S)-2-(9,10-Dioxo-4a,9,9a,10-tetrahydroanthracene-2-carboxamido)-3-phenyl propanamido)-3-phenylpropanoate (46):

¹H NMR (CDCl₃): 8.56 (s, ArH, 1H), 8.34 (m, ArH, 3H), 8.16 (d, NH, 1H, ³J_{HH} = 7.8Hz), 7.84 (m, ArH, 2H), 7.28 (m, ArH, 10H), 7.01 (d, ArH, 2H, ³J_{HH} = 8.3Hz), 6.18 (d, NH, 1H, ³J_{HH} = 7.8Hz), 4.81 (m, NHCH(CH₂Ph)C=O, 2H), 4.16 (m, OCH₂CH₃, 2H), 3.12 (m, 2x NHCH(CH₂Ph)C=O, 4H), 1.24 (t, OCH₂CH₃, 3H, ³J_{HH} = 7.1Hz) ppm. ¹³C NMR (CDCl₃): 182.3,

165.2, 138.7, 135.5, 134.5, 133.4, 132.8, 129.4, 129.2, 128.9, 128.6, 128.5, 127.9, 127.5, 127.4, 127.3, 127.2, 125.8, 61.7, 54.9, 53.6, 37.9, 14.1 ppm. MS: ES⁺: [M+Na]⁺. Accurate mass calculated: 597.1989 Found: 597.2002.

Deprotection of the C-terminus:

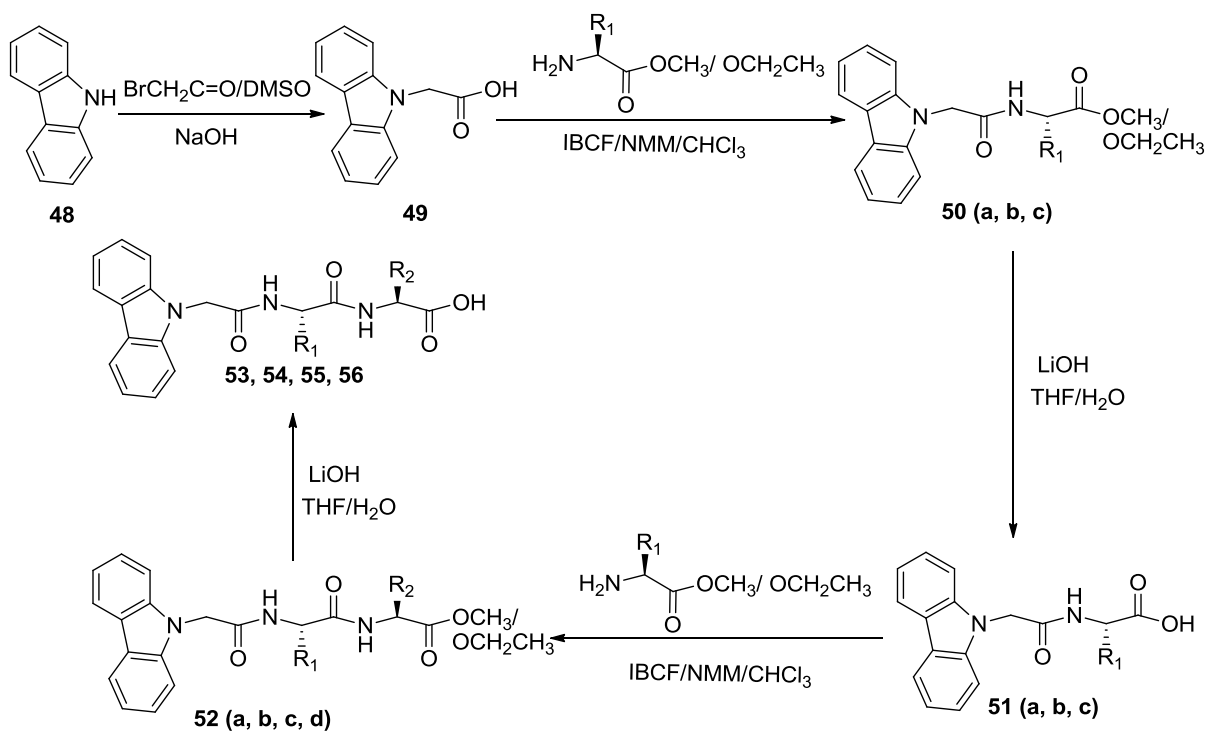
A solution of THF: water (30 mL: 5 mL) was added to compound **46**. Lithium hydroxide (0.3 g) was added. The solution was stirred overnight. After this time, distilled water (100 mL) was added, and then hydrochloric acid (1.0 M) was added drop-wise until the pH was lowered to pH 3. The resulting precipitate was collected by filtration and washed with water. The resulting precipitate was collected by filtration and washed with water to give compound **47** as shown in the Scheme 2.4. The yield was 75%. The resulting product was purified by washing with methanol. The yield after purification was typically 50% and the purity was 92%.

2S-2-((2S)-2-(9,10-Dioxo-4a,9,9a,10-tetrahydroanthracene-2-carboxamido)-3-phenyl propanamido)-3-phenylpropanoic acid (47):

¹H NMR (d₆-DMSO): 9.13 (d, NH, 1H, ³J_{HH} = 8.9Hz), 8.59 (s, ArH, 1H), 8.46 (d, NH, 1H, ³J_{HH} = 7.9Hz), 8.25 (m, ArH, 4H), 7.96 (m, ArH, 2H), 7.26 (m, ArH, 10H), 4.83 (m, NHCH(CH₂Ph)C=O, 1H), 4.48 (m, NHCH(CH₂Ph)C=O, 1H), 3.11 (m, NHCH(CH₂Ph)C=O, 2H), 2.99 (m, NHCH(CH₂Ph)C=O, 2H) ppm. ¹³C NMR (d₆-DMSO): 182.2, 172.7, 171.1, 164.7, 138.9, 138.2, 137.4, 134.7, 133.1, 133.1, 133.0, 133.2, 129.1, 128.2, 128.0, 126.9, 126.8, 126.8, 126.4, 126.2, 125.8, 54.7, 53.6, 38.9, 36.8, 36.5, 27.5 ppm. MS: ES⁻: [M - H]⁻. Accurate mass calculated: 545.1723 Found: 545.1713.

2.2.4- Carbazole dipeptides:

Carbazole dipeptide derivatives were synthesised previously using different methods, IBCF^{12, 13} or DCC^{5, 11} methods. Previous research has described the synthesis of carbazole linked with cyclic and acyclic peptoids²⁴. Also, a carbazole based organogel has been prepared previously²⁵, but there is no literature reporting dipeptides conjugated to carbazole. Therefore we have synthesised dipeptides conjugated to carbazole using the method²⁶ described in Scheme 2.5.



Scheme 2.5: The general reaction of dipeptide synthesis based on carbazole ring using IBCF method.

Compound	Substituent
50, 51	R_1
a	CH_3
b	CH_2Ph
c	$\text{CH}(\text{CH}_3)_2$

Table 2.10: The R_1 group of the general structure of compounds 50 and 51 (a, b, c, d) in the Scheme 5.

Compound	Functional group	
	R_1	R_2
52	R_1	R_2
a	CH_3	$\text{CH}(\text{CH}_3)_2$
b	CH_2Ph	CH_2Ph
c	$\text{CH}(\text{CH}_3)_2$	$\text{CH}(\text{CH}_3)_2$
d	$\text{CH}(\text{CH}_3)_2$	CH_2Ph

Table 2.11: The R_1 and R_2 group of the general structure of compound 52 (a, b, c, d) in the Scheme 5.

Dipeptide	R ₁	R ₂	Abbreviation
53	CH ₃	CH(CH ₃) ₂	Carb-AVOH
54	CH ₂ Ph	CH ₂ Ph	Carb-FFOH
55	CH(CH ₃) ₂	CH(CH ₃) ₂	Carb-VVOH
56	CH(CH ₃) ₂	CH ₂ Ph	Carb-VFOH

Table 2.12: The R₁ and R₂ group of the general structure of compounds 53-56 and their abbreviations in the Scheme 5.

Experimental section:

Carbazole acetic acid synthesis:

Carbazole (8.35 g, 0.05 moles) was dissolved in dimethyl sulfoxide (30 mL) and ground NaOH (6.0 g, 0.15 moles) was added to the solution. The mixture was heated to 85°C for 30 minutes to give a dark brown solution. Bromoacetic acid (8.34 g, 0.06 moles) was added to the solution in portions for 30 minutes. The resulting solution was stirred overnight, and then poured into 200 mL of cold distilled water. The precipitate was filtered under vacuum. HCl (1.0 M) was added drop-wise to the filtrate to reach pH 3 – 4. Then, the resulting precipitate was collected by filtration and washed with water to give compound 49 as shown in the Scheme 2.5²⁷. The yield was 75 % and the resulting product was pure and used directly in the next step of the reaction.

Carbazole acetic acid (49):

¹H NMR (d₆-DMSO): 8.16 (d, ArH, 2H³J_{HH} = 7.7Hz), 7.56(d, ArH, 2H³J_{HH} = 8.2Hz), 7.45 (t, ArH, 2H³J_{HH} = 7.1Hz), 7.22 (t, ArH, 2H³J_{HH} = 7.8Hz), 5.24 (s, NCH₂C=O, 2H), 13.70 (s, OH) ppm. ¹³C NMR (d₆-DMSO): 170.6, 140.8, 126.1, 122.6, 120.5, 119.5, 109.6, 44.3 ppm. MS (CI): [NH₄]⁺ 243.24.

Standard coupling methodology:

N-Methylmorpholine (1.5 eq.) and IBCF (1 eq.) was added to carbazole acetic acid (4.0 g, 0.017 mole) in chloroform (150 mL) at 0 °C. A solution of alanine methyl ester (1 eq.) and NMM (1.5 eq.) in chloroform was added and the solution was stirred at room temperature overnight. Then, the solution was washed with distilled water (2 x 100 mL), hydrochloric acid (100 mL, 0.1 M), aqueous potassium carbonate (100 mL, 0.1 M),

and distilled water again (2 x 100 mL) and dried with magnesium sulfate, and the solvent was removed *in vacuo* to give compounds **50 (a – c)** as shown in Scheme 2.5 and Table 2.10. The yield was between 51 – 67% and the impurity (an excess of valine methyl ester) was calculated by ¹H NMR spectroscopy to be between 8 – 15% of all derivatives, except compound **50a**, which was pure and used directly in the next step of the reaction. Then, the resulting product was purified by washing with methanol to give yield between 40 – 50% and the purity was typically between 93 – 97%.

(R)-Methyl-2-(2-(9H-carbazol-9-yl)acetamido)propanoate (50a):

¹H NMR (CDCl₃): 8.11 (d, ArH, 2H, ³J_{HH} = 6.7Hz), 7.49 (t, ArH, 2H, ³J_{HH} = 7.7Hz), 7.37 (d, ArH, 2H, ³J_{HH} = 9.2Hz), 7.31 (t, ArH, 2H, ³J_{HH} = 8.7Hz), 7.25 (s, CDCl₃), 6.08 (d, NH, 1H, ³J_{HH} = 7.5Hz), 4.92 (s, NCH₂C=O, 2H), 4.59 (m, NHCH(CH₃)C=O, 1H), 3.60 (s, OCH₃, 3H), 1.21 (d, NHCH(CH₃)C=O, 3H, ³J_{HH} = 7.2Hz) ppm. ¹³C NMR (CDCl₃): 172.4, 167.9, 140.5, 126.3, 123.6, 120.2, 118.8, 108.7, 52.4, 47.9, 47.2, 17.9 ppm. MS: ES⁺: ([M+Na]⁺). Accurate mass calculated: 333.1215 Found: 333.1222.

(R)-Ethyl-2-(2-(2-(9H-carbazole-9-yl)acetamido)-3-phenylpropanoate (50b):

¹H NMR (CDCl₃): 8.11 (d, ArH, 2H, ³J_{HH} = 7.7Hz), 7.46 (t, ArH, 2H, ³J_{HH} = 7.8Hz), 7.31 (d, ArH, 2H, ³J_{HH} = 6.9Hz), 7.26 (d, ArH, 3H, ³J_{HH} = 8.1Hz), 7.06 (t, ArH, 1H, ³J_{HH} = 7.7Hz), 6.94 (t, ArH, 2H, ³J_{HH} = 7.2Hz), 6.62 (d, ArH, 2H, ³J_{HH} = 8.7Hz), 5.87 (d, NH, 1H, ³J_{HH} = 5.6Hz), 4.89 (s, NCH₂C=O, 2H), 4.80 (d, NHCH(CH₂Ph)C=O, 1H, ³J_{HH} = 6.5Hz), 4.01 (q, OCH₂CH₃, 2H, ³J_{HH} = 7.1Hz), 2.94 (dd, NHCH(CH₂Ph)C=O, 1H, ³J_{HH} = 8.2, 5.1Hz), 2.82 (dd, NHCH(CH₂Ph)C=O, 1H, ³J_{HH} = 7.2, 6.1Hz), 1.07 (t, OCH₂CH₃, 3H, ³J_{HH} = 7.1Hz) ppm. ¹³C NMR (CDCl₃): 170.8, 168.1, 140.5, 135.38, 129.2, 128.8, 127.3, 126.8, 123.8, 120.9, 120.7, 108.9, 61.8, 53.1, 47.3, 37.8, 14.3 ppm. MS: ES⁺: ([M+Na]⁺). Accurate mass calculated: 423.1685 Found: 423.1700.

(R)-Methyl-2-(2-(9H-carbazol-9-yl)acetamido)-3-methylbutanoate (50c):

¹H NMR (CDCl₃): 8.13 (d, ArH, 2H, ³J_{HH} = 7.8Hz), 7.51 (t, ArH, 2H, ³J_{HH} = 8.1Hz), 7.39 (d, ArH, 2H, ³J_{HH} = 8.5Hz), 7.32 (t, ArH, 2H, ³J_{HH} = 8.1Hz), 7.26 (s, NH, 1H), 4.97 (d, NCH₂C=O, 2H, ³J_{HH} = 2.8Hz), 4.49 (dd, NHCH(CH₃)₂C=O, 1H, ³J_{HH} = 5.6, 4.0Hz), 3.55 (s, OCH₃, 3H), 1.96 (m, CH(CH₃)₂, 1H), 0.72 (d, CH(CH₃)₂, 3H, ³J_{HH} = 7.1Hz). 0.46 (d, CH(CH₃)₂, 3H, ³J_{HH} = 7.3Hz) ppm. ¹³C NMR (CDCl₃): 171.8, 169.5, 168.5, 140.7, 126.9, 123.9, 121.1, 109.2,

57.3, 52.5, 47.5, 31.1, 19.4, 19.3, 17.6 ppm. MS: ES⁺: ([M+Na]⁺). Accurate mass calculated: 361.1542 Found: 361.1528.

Deprotection of the C-terminus:

A solution of THF: water (30 mL: 5 mL) was added to compound **50 (a, b or c)**. Lithium hydroxide (0.3 g) was added and the solution was stirred overnight. After this time, distilled water (100 mL) was added, and then hydrochloric acid (1.0 M) was added drop-wise until the pH was lowered to pH 3. The resulting precipitate was collected by filtration and washed with water to give compounds **51 (a – c)** as shown in Scheme 2.5 and Table 2.10. The yield was between 84 – 87% and the resulting products for all derivatives were pure and used directly in the next step of the reaction.

(R)-2-(2-(9H-Carbazol-9-yl)acetamido)propanoic acid (51a):

¹H NMR (d₆-DMSO): 8.74 (d, NH, 1H, ³J_{HH} = 7.4Hz), 8.15 (d, ArH, 2H, ³J_{HH} = 7.5Hz), 7.54 (d, ArH, 2H, ³J_{HH} = 8.2Hz), 7.42 (t, ArH, 2H, ³J_{HH} = 8.2Hz), 7.21(t, ArH, 2H, ³J_{HH} = 7.8Hz), 5.08(d, NCH₂C=O, 2H, ³J_{HH} = 16.8Hz), 4.26 (m, NHCH(CH₃)C=O, 1H), 1.30 (d, NHCH(CH₃)C=O, 3H, ³J_{HH} = 7.2Hz) ppm. ¹³C NMR (d₆-DMSO): 173.9, 167.3, 140.5, 125.6, 122.2, 120.1, 118.9, 109.4, 47.6, 45.2, 17.3 ppm. MS: ES⁻: [M – H]⁻. Accurate mass calculated: 319.1059 Found: 319.1063.

(R)-Ethyl-2-(2-(2-(9H-Carbazole-9-yl)acetamido)-3-phenylpropanoate (51b):

¹H NMR (d₆-DMSO): 8.71 (d, ArH, 1H, ³J_{HH} = 11.8Hz), 8.12 (d, ArH, 2H, ³J_{HH} = 7.7Hz), 7.37 (d, ArH, 4H, ³J_{HH} = 3.67Hz), 7.28 (m, ArH, 5H), 7.18 (m, ArH, 2H), 5.01(q, NCH₂C=O, 2H, ³J_{HH} = 17.0Hz), 4.49(m, NHCH(CH₂Ph)C=O, 1H), 3.11 (dd, NHCH(CH₂Ph)C=O, 1H, ³J_{HH} = 9.2, 5.2Hz), 2.91 (dd, NHCH(CH₂Ph)C=O, 1H, ³J_{HH} = 8.2, 4.0Hz) ppm. ¹³C NMR (d₆-DMSO): 172.7, 167.4, 140.5, 137.4, 129.2, 128.2, 126.5, 125.6, 122.1, 120.0, 118.9, 109.3, 53.5, 45.2, 36.8 ppm. MS: ES⁻: [M – H]⁻. Accurate mass calculated: 371.1396 Found: 371.1398.

(R)-2-(2-(9H-Carbazol-9-yl)acetamido)-3-methylbutanoic acid (51c):

¹H NMR (d₆-DMSO): 8.60 (d, NH, 1H, ³J_{HH} = 8.8Hz), 8.15 (d, ArH, 2H, ³J_{HH} = 7.8Hz), 7.56 (d, ArH, 2H, ³J_{HH} = 8.8Hz), 7.43 (t, ArH, 2H, ³J_{HH} = 7.1Hz), 7.21 (t, ArH, 2H, ³J_{HH} = 7.8Hz), 5.17 (q, NCH₂C=O, 2H, ³J_{HH} = 16.6, 13.7Hz), 4.20 (dd, NHCH(CH₃)₂C=O, 1H, ³J_{HH} = 5.6, 3.7Hz), 2.11 (m, CH(CH₃)₂, 1H), 0.92 (d, CH(CH₃)₂, 3H, ³J_{HH} = 7.0Hz), 0.90 (d, (CH₃)₂CH,

3H, $^3J_{\text{HH}} = 7.3\text{Hz}$) ppm. ^{13}C NMR (d_6 -DMSO): 172.8, 167.7, 168.5, 140.5, 125.6, 122.1, 120.1, 118.9, 109.3, 57.1, 45.1, 29.9, 19.1, 17.9 ppm. MS: ES⁻: [M - H]⁻. Accurate mass calculated: 323.1406 Found: 323.1396.

Standard coupling methodology:

N-Methylmorpholine (1.5 eq.) and IBCF (1 eq.) were added to compound **51 (a, b, or c)** (1.0 g) in chloroform (100 mL) at 0 °C. A solution of L-valine methyl ester hydrochloride, L-phenylalanine ethyl ester hydrochloride or L-alanine methyl ester hydrochloride (1eq.) and NMM (1.5eq.) in chloroform was added and the solution was stirred at room temperature overnight. Then, the solution was washed with distilled water (2 x 100 mL), hydrochloric acid (100 mL, 0.1 M), aqueous potassium carbonate (100 mL, 0.1 M), and distilled water again (2 x 100 mL) and dried with magnesium sulfate, and the solvent was removed *in vacuo* to give compounds **52 (a - d)** as shown in Scheme 2.5 and Table 2.11. The yield was between 50 - 75% and the impurity (an excess of valine methyl ester) was calculated by ^1H NMR spectroscopy to be between 5 - 6% for all derivatives except compounds **52a** and **52b**, which were pure and used directly in the next step of the reaction. Then, the resulting product was purified by washing with methanol. The yield after purification was between 25 - 40% and the resulting product was between 98 - 99% pure.

(R)-Methyl-2-((R)-2-(2-(9H-carbazole-9-yl)acetamido)propanamido)-3-methylbutanoate (52a):

^1H NMR (CDCl_3): 8.11 (d, ArH, 2H, $^3J_{\text{HH}} = 6.9\text{Hz}$), 7.48 (t, ArH, 2H, $^3J_{\text{HH}} = 7.1\text{Hz}$), 7.32 (m, ArH, 4H), 7.25(s, CDCl_3), 6.47 (d, NH, 1H, $^3J_{\text{HH}} = 8.2\text{Hz}$), 6.06 (d, NH, 1H, $^3J_{\text{HH}} = 6.2\text{Hz}$), 4.94(s, $\text{NCH}_2\text{C}=\text{O}$, 2H), 4.52 (m, $\text{NHCH}(\text{CH}_3)\text{C}=\text{O}$, 1H), 4.41 (dd, $\text{NHCHCH}(\text{CH}_3)_2$, 1H, $^3J_{\text{HH}} = 5.5\text{Hz}$), 3.72 (s, OCH_3 , 3H), 2.10 (m, $(\text{CH}_3)_2\text{CH}$, 1H), 1.17 (d, $\text{NHCH}(\text{CH}_3)\text{C}=\text{O}$, 3H, $^3J_{\text{HH}} = 7.0\text{Hz}$), 0.85 (d, $\text{NHCHCH}(\text{CH}_3)_2$, 3H, $^3J_{\text{HH}} = 6.9\text{Hz}$), 0.84 (d, $(\text{CH}_3)_2\text{CH}$, 3H, $^3J_{\text{HH}} = 7.4\text{Hz}$) ppm. ^{13}C NMR (CDCl_3): 172.1, 171.1, 168.6, 168.3, 140.5, 126.5, 123.6, 120.7, 120.5, 108.4, 57.1, 52.2, 48.7, 47.1, 31.1, 18.9, 17.6 ppm. MS: ES⁺: ([M+Na]⁺). Accurate mass calculated: 432.1899 Found: 432.1908.

(R)-Ethyl-2-((R)-2-(2-(9H-carbazole-9-yl)acetamido)-3-phenylpropanamido)-3-phenyl propanoate (52b):

¹H NMR (CDCl₃): 8.13 (d, ArH, 2H, ³J_{HH} = 6.2Hz), 7.42 (t, ArH, 2H, ³J_{HH} = 8.8Hz), 7.31 (t, ArH, 2H, ³J_{HH} = 8.8Hz), 7.26 (CDCl₃), 7.16 (m, ArH, 5H), 7.05 (t, ArH, 1H, ³J_{HH} = 8.8Hz), 6.94 (t, ArH, 2H, ³J_{HH} = 8.8Hz), 6.83 (d, ArH, 2H, ³J_{HH} = 9.7Hz), 6.63 (d, ArH, 2H, ³J_{HH} = 7.1Hz), 6.21 (d, NH, 1H, ³J_{HH} = 7.9Hz), 5.84 (d, NH, 1H, ³J_{HH} = 8.8Hz), 4.84 (d, NCH₂C=O, 2H, ³J_{HH} = 6.2Hz), 4.64 (m, NHCH(CH₂Ph)C=O, 1H), 4.14 (q, OCH₂CH₃, 2H, ³J_{HH} = 9.7Hz), 2.99 (dd, NHCH(CH₂Ph)C=O, 1H, ³J_{HH} = 7.2, 6.2Hz), 2.80 (m, NHCH(CH₂Ph)C=O, 2H), 2.69 (dd, NHCH(CH₂Ph)C=O, 1H, ³J_{HH} = 8.2, 6.2Hz), 1.22 (t, OCH₂CH₃, 3H, ³J_{HH} = 7.1Hz) ppm. ¹³C NMR (CDCl₃): 170.9, 169.5, 168.3, 140.1, 135.7, 135.3, 129.2, 128.9, 128.6, 128.4, 127.1, 126.9, 126.7, 123.5, 120.7, 120.5, 108.4, 61.6, 53.8, 53.3, 46.9, 37.9, 37.1, 14.1 ppm. MS: ES⁺: [M+Na]⁺. Accurate mass calculated: 570.2369 Found: 570.2363.

(R)-Methyl-2-((R)-2-(2-(9H-carbazol-9-yl)acetamido)-3-methylbutanamido)-3-methyl butanoate (52c):

¹H NMR (d₆-DMSO): 8.09 (d, ArH, 2H, ³J_{HH} = 8.8Hz), 7.46(t, ArH, 2H, ³J_{HH} = 8.6Hz), 7.34(d, NH, 1H, ³J_{HH} = 8.6Hz), 7.28 (t, ArH, 2H, ³J_{HH} = 7.5Hz), 6.54 (d, NH, 1H, ³J_{HH} = 8.2Hz), 6.12(d, NH, 1H, ³J_{HH} = 8.7Hz), 4.94 (d, NCH₂C=O, 2H, ³J_{HH} = 8.5Hz), 4.41(dd, NHCH(CH₃)C=O, 1H, ³J_{HH} = 5.4, 4.4Hz), 4.29 (dd, NHCHCH(CH₃)₂, 1H, ³J_{HH} = 6.4, 3.3Hz), 3.70 (s, OCH₃, 3H), 2.07 (m, (CH₃)₂CH, 1H), 1.93 (m, (CH₃)₂CH, 1H), 0.84 (d, CH(CH₃)₂, 3H, ³J_{HH} = 7.4Hz), 0.80 (d, CH(CH₃)₂, 3H, ³J_{HH} = 6.4Hz), 0.76 (d, CH(CH₃)₂, 3H, ³J_{HH} = 7.7Hz), 0.53 (d, CH(CH₃)₂, 3H, ³J_{HH} = 7.4Hz) ppm. ¹³C NMR (CDCl₃): 172.1, 170.3, 168.5, 140.3, 126.5, 126.3, 125.8, 123.5, 120.8, 120.4, 119.3, 110.6, 108.5, 94.0, 58.6, 57.0, 52.2, 46.9, 31.0, 30.2, 19.1, 18.9, 17.7, 17.5 ppm. MS (ES⁺): ([M+Na]⁺). Accurate mass calculated: 460.2223 Found: 460.2212.

(R)-Ethyl-2-((R)-2-(2-(9H-carbazol-9-yl)acetamido)-3-methylbutanamido)-3-phenyl propanoate (52d):

¹H NMR (CDCl₃): 8.14 (d, ArH, 2H, ³J_{HH} = 8.5Hz), 7.49 (t, ArH, 2H, ³J_{HH} = 8.8Hz), 7.34 (dd, ArH, 4H, ³J_{HH} = 8.8, 8.8Hz), 7.22 (t, ArH, 3H, ³J_{HH} = 2.8Hz), 6.96(m, ArH, 2H), 6.04(d, NH, 1H, ³J_{HH} = 8.8Hz), 5.82 (d, NH, 1H, ³J_{HH} = 8.1Hz), 4.97 (d, NCH₂C=O, 2H, ³J_{HH} = 2.4Hz), 4.70 (m, NHCH(CH₂Ph)C=O, 1H), 4.16 (m, NHCH(CH₂Ph)C=O, OCH₂CH₃, 3H), 3.05 (dd, NHCH(CH₂Ph)C=O, 1H, ³J_{HH} = 6.3, 7.1Hz), 2.83 (dd, NHCH(CH₂Ph)C=O, 1H, ³J_{HH} = 7.8,

7.3Hz), 1.87 (m, (CH₃)₂CH, 1H), 1.23 (t, OCH₂CH₃, 3H, ³J_{HH} = 8.1Hz), 0.69 (d, CH(CH₃)₂, 3H, ³J_{HH} = 8.1Hz), 0.31(d, CH(CH₃)₂, 3H, ³J_{HH} = 6.3Hz) ppm. ¹³C NMR (CDCl₃): 171.1, 169.6, 168.3, 140.2, 135.7, 129.2, 127.1, 126.6, 123.5, 120.8, 120.5, 108.5, 99.9, 61.6, 58.2, 52.9, 47.0, 37.9, 30.0, 19.0, 17.1, 14.1 ppm. MS ES⁺: [M+Na]⁺. Accurate mass calculated: 522.2372 Found: 522.2369.

Deprotection of the C-terminus:

A solution of THF: water (30 mL: 5 mL) was added to the carbazole derivative. Lithium hydroxide (0.3 g) was added and the solution was stirred overnight. After this time, distilled water (100 mL) was added, and then hydrochloric acid (1.0 M) was added drop-wise until the pH was lowered to pH 3. The resulting precipitate was collected by filtration and washed with water to give compounds (**53 – 56**) as shown in Scheme 2.5 and Table 2.12. The yield was between 69 – 80% and the impurity (an excess of valine methyl ester) was calculated by ¹H NMR spectroscopy to be between 4 – 5% for all derivatives except compounds **53** and **55**, which were pure and used directly in the next step of the reaction. Then, the resulting product was purified by washing with methanol. The yield after purification was between 50 – 55% and the resulting product was between 97 – 98% pure.

(R)-2-((R)-2-(2-(9H-Carbazole-9-yl)acetamido)propanamido)-3-methylbutanoic acid (53):

¹H NMR (d₆-DMSO): 8.63 (d, NH, 1H, ³J_{HH} = 7.7Hz), 8.14(d, ArH, 2H, ³J_{HH} = 7.7Hz), 8.01(d, NH, 1H, ³J_{HH} = 8.4Hz), 7.53 (d, ArH, 2H, ³J_{HH} = 8.2Hz), 7.42(t, ArH, 2H, ³J_{HH} = 7.1Hz), 7.20(t, ArH, 2H, ³J_{HH} = 7.8Hz), 5.10(d, NCH₂C=O, 2H, ³J_{HH} = 13.8Hz), 4.47(m, NHCH(CH₃)C=O, 1H), 4.14(dd, NHCHCH(CH₃)₂, 1H, ³J_{HH} = 6.4, 5.6Hz), 2.03 (m, (CH₃)₂CH, 1H) 1.27 (d, NHCH(CH₃)C=O, 3H, ³J_{HH} = 7.0Hz), 0.85 (d, CH(CH₃)₂, 3H, ³J_{HH} = 7.5Hz), 0.83 (d, CH(CH₃)₂, 3H, ³J_{HH} = 6.4Hz) ppm. ¹³C NMR (d₆-DMSO): 172.8, 172.2, 167.0, 140.6, 125.6, 122.1, 120.1, 118.9, 109.4, 57.1, 47.9, 45.2, 30.0, 19.0, 18.5, 17.8 ppm. MS: ES⁻: [M – H]⁻. Accurate mass calculated: 418.1743 Found 418.1749.

(R)-2-((R)-2-(2-(9H-Carbazole-9-yl)acetamido)-3-phenylpropanamido)-3-phenyl propanoic acid (54):

¹H NMR (d₆-DMSO): 8.58 (d, NH, 1H, ³J_{HH} = 8.7Hz), 8.51 (d, NH, 1H, ³J_{HH} = 7.7Hz), 8.10 (d, ArH, 2H, ³J_{HH} = 7.6Hz), 7.35 (t, ArH, 2H, ³J_{HH} = 6.0Hz), 7.22 (m, ArH, 14H), 4.94 (q, NCH₂C=O, 2H, ³J_{HH} = 16.8Hz), 4.63 (m, NHCH(CH₂Ph)C=O, 1H), 4.47 (m, NHCH(CH₂Ph)C=O, 1H), 3.07 (m, NHCH(CH₂Ph)C=O, 2H), 2.92 (dd, NHCH(CH₂Ph)C=O, 1H, ³J_{HH} = 7.9, 6.2Hz), 2.77 (dd, NHCH(CH₂Ph)C=O, 1H, ³J_{HH} = 8.2, 3.2Hz) ppm. ¹³C NMR (d₆-DMSO): 172.7, 171.1, 166.9, 140.4, 137.5, 137.4, 129.3, 129.1, 128.2, 128.0, 126.4, 126.3, 125.5, 122.0, 119.9, 118.8, 109.3, 53.5, 53.4, 45.1, 37.9, 36.6 ppm. MS: ES⁻: [M - H]⁻. Accurate mass calculated: 518.2080 Found: 518.2095.

(R)-2-((R)-2-(2-(9H-Carbazol-9-yl)acetamido)-3-methylbutanamido)-3-methyl butanoic acid (55):

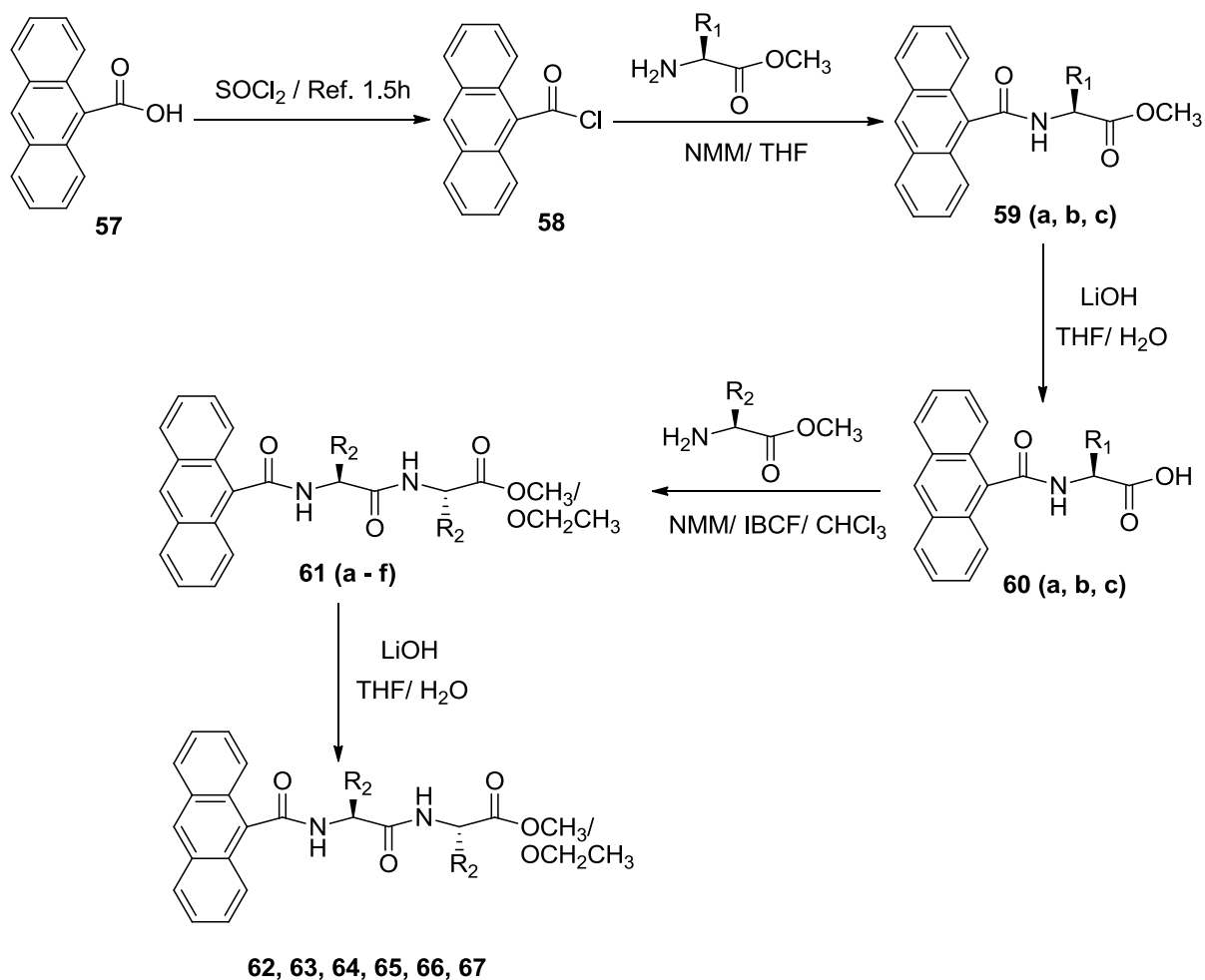
¹H NMR (d₆-DMSO): 8.44 (d, NH, 1H, ³J_{HH} = 9.6Hz), 8.14(d, ArH, 3H, ³J_{HH} = 7.7Hz), 8.01(d, NH, 1H, ³J_{HH} = 8.4Hz), 7.55 (d, ArH, 2H, ³J_{HH} = 8.3Hz), 7.43 (t, ArH, 2H, ³J_{HH} = 7.1Hz), 7.21(t, ArH, 2H, ³J_{HH} = 7.7Hz), 5.22 (q, NCH₂C=O, 2H, ³J_{HH} = 16.6, 18.9Hz), 4.41(dd, NHCH(CH₃)C=O, 1H, ³J_{HH} = 6.2, 3.7Hz), 4.14 (dd, NHCHCH(CH₃)₂, 1H, ³J_{HH} = 5.8, 2.5Hz), 2.03 (m, (CH₃)₂CH, 2H) 0.87 (d, CH(CH₃)₂, 12H, ³J_{HH} = 6.8Hz) ppm. ¹³C NMR (d₆-DMSO): 172.8, 171.1, 167.3, 161.6, 151.3, 140.5, 125.6, 122.1, 120.1, 118.9, 109.4, 78.8, 57.3, 45.2, 31.1, 29.5, 19.2, 19.1, 18.1, 17.9 ppm. MS: ES⁻: [M - H]⁻. Accurate mass calculated: 446.5620 Found: 446.5620.

(R)-2-((R)-2-(2-(9H-Carbazol-9-yl)acetamido)-3-methylbutanamido)-3-phenyl propanoic acid (56):

¹H NMR (d₆-DMSO): 8.42 (d, NH, 1H, ³J_{HH} = 7.7Hz), 8.36 (d, NH, 1H, ³J_{HH} = 9.2Hz), 8.15 (d, ArH, 2H, ³J_{HH} = 7.7Hz), 7.53 (d, ArH, 2H, ³J_{HH} = 8.2Hz), 7.43 (t, ArH, 2H, ³J_{HH} = 7.1Hz), 7.23 (m, ArH, 7H), 5.13 (q, NCH₂C=O, 2H, ³J_{HH} = 22.9, 16.2Hz), 4.46 (m, NHCH(CH₂Ph)C=O, 1H), 4.29 (dd, NHCHCH(CH₃)₂, 1H, ³J_{HH} = 6.0, 3.5Hz), 3.06 (dd, NHCH(CH₂Ph)C=O, 1H, ³J_{HH} = 8.9, 5.2Hz), 2.90(dd, NHCH(CH₂Ph)C=O, 1H, ³J_{HH} = 9.5, 4.6Hz), 2.01 (m, (CH₃)₂CH, 1H), 0.85 (d, CH(CH₃)₂, 3H, ³J_{HH} = 3.8Hz), 0.84 (d, CH(CH₃)₂, 3H, ³J_{HH} = 4.0Hz) ppm. ¹³C NMR (d₆-DMSO): 203.0, 172.8, 170.8, 167.2, 140.5, 137.5, 129.0, 128.2, 126.4, 125.6, 122.1, 120.1, 118.9, 109.3, 78.8, 56.9, 53.4, 45.2, 31.1, 19.2, 17.8 ppm. MS: ES⁻: [M - H]⁻. Accurate mass calculated: 470.2075 Found: 470.2080.

2.2.5- Anthracene dipeptides:

Dipeptides conjugated to anthracene by a C=O linker have not been synthesised previously. The method²⁶ of the synthesis is described in Scheme 2.6.



Scheme 2.6: The general reaction of dipeptide synthesis based on 9-anthracene ring using IBCF method.

Compound	Substituent
59, 60	R ₁
a	CH(CH ₃) ₂
b	CH ₃
c	H

Table 2.13: The R₁ group of the general structure of compounds 59 and 60 (a, b, c, d) in the Scheme 2.6.

Compound	Functional group	
	R ₁	R ₂
61	R ₁	R ₂
a	CH(CH ₃) ₂	CH(CH ₃) ₂
b	CH(CH ₃) ₂	H
c	CH(CH ₃) ₂	CH ₂ Ph
d	CH ₃	CH ₃
e	CH ₃	CH(CH ₃) ₂
f	H	CH ₂ Ph

Table 2.14: The R₁ and R₂ group of the general structure of compound 61 (a - f) in the Scheme 2.6.

Dipeptide	R ₁	R ₂	Abbreviation
62	CH(CH ₃) ₂	CH(CH ₃) ₂	9anth-VVOH
63	CH(CH ₃) ₂	H	9anth-VGOH
64	CH(CH ₃) ₂	CH ₂ Ph	9anth-VFOH
65	CH ₃	CH ₃	9anth-AAOH
66	CH ₃	CH(CH ₃) ₂	9anth-AVOH
67	H	CH ₂ Ph	9anth-GFOH

Table 2.15: The R₁ and R₂ group of the general structure of compounds 62–67 and their abbreviations in the Scheme 2.6.

Experimental section:

Preparation of anthracene acid chloride (58):

Anthracene acetic acid (2.22g, 0.01mol) was refluxed in thionyl chloride (30mL) for 1.5 hours. An excess of thionyl chloride was evaporated *in vacuo* and completely removed by washing the result product with toluene (10 mL) three times²⁶. Then, the resulting precipitate was collected by filtration and washed with water to give compound **58** as shown in Scheme 2.6. The yield was 83 % and the resulting product was pure and used directly in the next step of the reaction.

First coupling step:

Anthracene acid chloride was dissolved in THF (80 mL). A solution of L-valine methyl ester hydrochloride, L-alanine methyl ester hydrochloride or glycine methyl ester hydrochloride, THF and NMM was added drop-wise to a solution of anthracene at room temperature and the mixture was stirred at room temperature overnight. The solution was washed with distilled water (100 mL), hydrochloric acid (2 x 100 mL, 0.1 M), aqueous potassium carbonate (100 mL, 0.1 M), and distilled water again (4 x 100 mL) and dried with magnesium sulfate, and the solvent was removed *in vacuo* to give compounds **59 (a - c)** as shown in Scheme 2.6 and Table 2.13. The yield was between 60 - 72% and the impurity (an excess of valine methyl ester, IBCF) was calculated by NMR spectroscopy to be between 8 - 13% for all derivatives except compound **59b**, which was pure and used directly in the next step of the reaction. Then, the resulting product was purified by washing with methanol. The yield after purification was between 45 - 50% and the resulting product was between 88 - 95% pure.

***(S)*-Methyl-2-(anthracene-9-carboxamido)-3-methylbutanoate (59a):**

^1H NMR (CDCl_3): 8.44 (s, ArH, 1H), 8.08 (s, ArH, 2H), 7.96 (d, ArH, 2H, $^3J_{\text{HH}} = 8.1\text{Hz}$), 7.45 (m, ArH, 4H), 6.38 (d, NH, 1H, $^3J_{\text{HH}} = 9.3\text{Hz}$), 5.02 (dd, $\text{NHCH}(\text{CH}_3)_2\text{C}=\text{O}$, 1H, $^3J_{\text{HH}} = 5.2, 4.8\text{Hz}$), 3.78 (s, OCH_3 , 3H), 2.38 (m, $\text{CH}(\text{CH}_3)_2$, 1H), 1.10 (d, $\text{CH}(\text{CH}_3)_2$, 3H, $^3J_{\text{HH}} = 7.6\text{Hz}$), 0.91 (d, $\text{CH}(\text{CH}_3)_2$, 3H, $^3J_{\text{HH}} = 6.7\text{Hz}$) ppm. ^{13}C NMR (CDCl_3): 172.6, 170.0, 131.8, 131.5, 129.4, 128.9, 128.6, 127.2, 125.9, 125.7, 125.5, 68.4, 58.2, 52.7, 45.3, 31.3, 26.0, 21.8, 19.8, 18.3, 17.6 ppm. MS: ES^+ : $[\text{M}+\text{Na}]^+$. Accurate mass calculated: 358.1420 Found 358.1419.

***(S)*-Methyl-2-(anthracene-9-carboxamido)propanoate (59b):**

^1H NMR (CDCl_3): 8.43 (s, ArH, 1H), 8.08 (s, ArH, 2H), 7.94 (d, ArH, 2H, $^3J_{\text{HH}} = 8.8\text{Hz}$), 7.44 (m, ArH, 4H), 6.47 (d, NH, 1H, $^3J_{\text{HH}} = 7.3\text{Hz}$), 5.02 (m, $\text{NHCHCH}_3\text{C}=\text{O}$, 1H), 3.78 (s, OCH_3 , 3H), 1.59 (d, $\text{NHCHCH}_3\text{C}=\text{O}$, 3H, $^3J_{\text{HH}} = 7.4\text{Hz}$) ppm. ^{13}C NMR (CDCl_3): 173.5, 169.5, 131.5, 131.4, 128.9, 128.8, 128.6, 128.1, 127.2, 125.9, 125.4, 53.0, 49.1, 30.7, 18.7 ppm. MS: ES^+ $[\text{M}+\text{Na}]^+$. Accurate mass calculated: 330.1107 Found 330.110.

Methyl-2-(anthracene-9-carboxamido)acetate (59c):

¹H NMR (CDCl₃): 8.44 (s, ArH, 1H), 8.11 (d, ArH, 2H, ³J_{HH} = 8.8Hz), 7.95 (d, ArH, 2H, ³J_{HH} = 8.8Hz), 7.45 (m, ArH, 4H), 6.44 (s, NH, 1H), 4.42 (d, NHCH₂C=O, 2H, ³J_{HH} = 6.2Hz), 3.79 (s, OCH₃, 3H) ppm. ¹³C NMR (CDCl₃): 183.2, 169.3, 142.4, 134.1, 133.9, 133.5, 130.8, 129.6, 129.2, 128.6, 127.6, 127.3, 126.2, 122.4, 121.6, 120.7, 119.8, 117.1, 52.4, 42.1, 41.6, 40.7 ppm. MS: ES⁺: [M+Na]⁺. Accurate mass calculated: 316.0955 Found 316.0950

Deprotection of the C-terminus:

A solution of THF: water (30 mL: 5 mL) was added to compound **59 (a, b or c)**. Lithium hydroxide (0.3 g) was added and the solution was stirred overnight. After this time, distilled water (100 mL) was added, and then hydrochloric acid (100 mL, 1.0 M) was added drop wise until the pH was lowered to pH 3. Then, the resulting precipitate was collected by filtration and washed with water to give compounds **60 (a – c)** as shown in Scheme 2.6 and Table 2.13. The yield was between 52 – 73% and the impurity (an excess of valine methyl ester) was calculated by ¹H NMR spectroscopy to be between 4 – 12% for all derivatives except compound **60b**, which was pure and used directly in the next step of the reaction. Then, the resulting product was purified by washing with methanol. The yield after purification was between 30 – 55% and the resulting product was typically between 89 – 97% pure.

(S)-2-(anthracene-9-carboxamido)-3-methylbutanoic acid (60a):

¹H NMR (d₆-DMSO): 9.08 (d, ArH, 1H, ³J_{HH} = 7.8Hz), 8.66 (s, ArH, 1H), 8.24 (m, ArH, 1H), 8.13 (m, ArH, 2H), 7.96 (d, NH, 1H, ³J_{HH} = 7.8Hz), 7.55 (d, ArH, 4H, ³J_{HH} = 5.6Hz), 4.59 (t, NHCH(CH₃)₂C=O, 1H, ³J_{HH} = 7.3Hz), 2.24 (m, CH(CH₃)₂, 1H), 1.08 (d, CH(CH₃)₂, 3H, ³J_{HH} = 8.1Hz), 1.00 (d, CH(CH₃)₂, 3H, ³J_{HH} = 6.3Hz) ppm. ¹³C NMR (d₆-DMSO): 173.0, 168.9, 133.1, 130.7, 128.6, 128.3, 128.1, 127.7, 127.4, 127.0, 126.3, 126.0, 125.8, 125.5, 125.2, 66.9, 58.4, 29.1, 25.1, 19.4, 18.3 ppm. MS: ES⁻: [M – H]⁻. Accurate mass calculated: 344.1261 Found 344.1263.

(S)-2-(anthracene-9-carboxamido)propanoic acid (60b):

¹H NMR (d₆-DMSO): 9.18 (d, NH, 1H, ³J_{HH} = 6.6Hz), 8.67 (s, ArH, 1H), 8.37 (d, ArH, 1H, ³J_{HH} = 6.6Hz), 8.13 (d, ArH, 2H, ³J_{HH} = 6.8Hz), 7.98 (d, ArH, 1H, ³J_{HH} = 8.0Hz), 7.56 (dd, ArH, 4H, ³J_{HH} = 4.5, 3.3Hz), 4.66 (m, NHCHCH₃C=O, 1H), 1.45 (d, NHCHCH₃C=O, 3H, ³J_{HH} =

7.4Hz) ppm. ^{13}C NMR (d_6 -DMSO): 174.5, 168.6, 133.2, 131.0, 128.7, 128.5, 128.1, 127.6, 126.7, 126.5, 126.2, 125.9, 125.7, 79.5, 67.4, 48.7, 25.5, 17.1 ppm. MS: ES⁻: [M - H]⁻. Accurate mass calculated: 292.0964 Found 292.0974.

2-(anthracene-9-carboxamido)acetic acid (60c):

^1H NMR (d_6 -DMSO): 9.19 (t, NH, 1H, $^3\text{J}_{\text{HH}} = 6.0\text{Hz}$), 8.67 (s, ArH, 1H), 8.22 (m, ArH, 2H), 8.13 (m, ArH, 2H), 7.56 (m, ArH, 4H), 4.13 (d, $\text{NHCH}_2\text{C}=\text{O}$, 2H, $^3\text{J}_{\text{HH}} = 6.0\text{Hz}$) ppm. ^{13}C NMR (d_6 -DMSO): 171.3, 168.8, 134.5, 133.0, 132.7, 130.6, 130.5, 128.6, 128.2, 127.5, 127.3, 127.0, 126.7, 126.3, 125.6, 124.8, 41.2 ppm. MS: ES⁻: [M - H]⁻. Accurate mass calculated: 278.0818 Found 278.0817.

Standard coupling methodology:

N-Methylmorpholine (1.5 eq.) and IBCF (1 eq.) were added to compound **60 (a, b or c)** (1.0 g) in chloroform (100 mL) at 0 °C. A solution of L-phenylalanine ethyl ester hydrochloride, L-alanine methyl ester hydrochloride, L-valine methyl ester hydrochloride or glycine methyl ester hydrochloride (1.0 eq.) and NMM (1.5 eq.) in chloroform was added and the solution was stirred at room temperature overnight. Then, the solution was washed with distilled water (2 x 100 mL), hydrochloric acid (100 mL, 0.1 M), aqueous potassium carbonate (100 mL, 0.1 M), and distilled water again (2 x 100 mL) and dried with magnesium sulfate, and the solvent was removed *in vacuo* to give compounds **61 (a - f)** as shown in Scheme 2.6 and Table 2.14. The yield was between 33 - 78% and the impurity (an excess of valine methyl ester and IBCF) was calculated by ^1H NMR spectroscopy to be between 18 - 25% for all derivatives except compound **61a**, which was pure and used directly in the next step of the reaction. Then, the resulting product was purified by washing with methanol. The yield after purification was between 20 - 60% and the resulting product was between 85 - 94% pure.

(S)-Methyl-2-((S)-2-(anthracene-9-carboxamido)-3-methylbutanamido)-3-methylbutanoate (61a):

^1H NMR (CDCl_3): 8.52 (s, ArH, 1H), 8.08 (d, ArH, 2H, $^3\text{J}_{\text{HH}} = 10.0\text{Hz}$), 8.03 (d, ArH, 2H, $^3\text{J}_{\text{HH}} = 7.4\text{Hz}$), 7.52 (m, ArH, 4H), 6.59 (dd, NH, 2H, $^3\text{J}_{\text{HH}} = 7.1, 8.6\text{Hz}$), 4.79 (dd, $\text{NHCH}(\text{CH}_3)_2\text{C}=\text{O}$, 1H, $^3\text{J}_{\text{HH}} = 7.1, 2.1\text{Hz}$), 4.70 (dd, $\text{NHCH}(\text{CH}_3)_2\text{C}=\text{O}$, 1H, $^3\text{J}_{\text{HH}} = 5.0, 4.4\text{Hz}$),

3.80 (s, OCH₃, 3H), 2.31(m, 2x CH(CH₃)₂, 2H), 1.66 (d, CH(CH₃)₂, 6H, ³J_{HH} = 7.6, 8.2Hz), 1.08 (d, CH(CH₃)₂, 3H, ³J_{HH} = 6.8Hz), 1.03 (d, CH(CH₃)₂, 3H, ³J_{HH} = 6.8Hz) ppm. ¹³C NMR (CDCl₃): 172.1, 170.9, 131.2, 131.0, 128.5, 128.4, 128.1, 126.9, 125.5, 124.9, 59.7, 57.3, 52.2, 31.1, 30.9, 19.5, 19.0, 18.7, 17.7 ppm. MS: ES⁺([M+Na]⁺). Accurate mass calculated: 457.2112 Found 457.2103.

(S)-Methyl-2-(2-(anthracene-9-carboxamido)-3-methylbutanamido)acetate (61b):

¹H NMR (CDCl₃): 8.93 (d, NH, 1H, ³J_{HH} = 8.6Hz), 8.65(s, ArH, 1H), 8.60 (t, ArH, 1H, ³J_{HH} = 6.5Hz), 8.13 (d, ArH, 3H, ³J_{HH} = 7.5Hz), 7.94 (d, NH, 2H, ³J_{HH} = 8.8Hz), 7.54 (d, ArH, 4H, ³J_{HH} = 7.5Hz), 4.73 (dd, NHCH(CH₃)₂C=O, 1H, ³J_{HH} = 6.3, 3.3Hz), 4.10 (d, NHCH₂C=O, 1H, ³J_{HH} = 6.3Hz), 4.03 (d, NHCH₂C=O, 1H, ³J_{HH} = 5.3Hz), 3.69 (s, OCH₃, 3H), 2.13 (m, CH(CH₃)₂, 1H), 1.08 (d, CH(CH₃)₂, 3H, ³J_{HH} = 7.3Hz), 1.01 (d, CH(CH₃)₂, 3H, ³J_{HH} = 6.3Hz) ppm. ¹³C NMR (CDCl₃): 171.4, 170.3, 169.5, 131.5, 131.4, 128.9, 128.5, 127.3, 125.9, 125.4, 59.6, 52.8, 45.3, 31.3, 19.9, 18.8 ppm. MS: ES⁺: [M+Na]⁺. Accurate mass calculated: 415.1644. Found 415.1634.

(S)-Ethyl-2-((S)-2-(anthracene-9-carboxamido)-3-methylbutanamido)-3-phenylpropanoate (61c):

¹H NMR (CDCl₃): 8.51 (s, ArH, 1H), 8.03 (d, ArH, 2H, ³J_{HH} = 9.0Hz), 7.51 (m, ArH, 4H), 7.28 (m, ArH, 6H), 6.64 (d, NH, 1H, ³J_{HH} = 9.5Hz), 6.50 (d, NH, 1H, ³J_{HH} = 8.6Hz), 5.00 (d, NHCH(CH₂Ph)C=O, 1H, ³J_{HH} = 8.8Hz), 4.78 (dd, NHCH(CH₃)₂C=O, 1H, ³J_{HH} = 8.6, 2.6Hz), 4.20 (q, OCH₂CH₃, 2H, ³J_{HH} = 7.1, 7.1Hz), 3.23 (d, NHCH(CH₂Ph)C=O, 2H, ³J_{HH} = 6.0Hz), 2.29(m, CH(CH₃)₂, 1H), 1.29 (t, OCH₂CH₃, 3H, ³J_{HH} = 7.1Hz), 1.15 (d, CH(CH₃)₂, 3H, ³J_{HH} = 6.7Hz) 1.07 (d, CH(CH₃)₂, 3H, ³J_{HH} = 6.8Hz) ppm. ¹³C NMR (CDCl₃): 171.6, 170.7, 170.1, 136.0, 131.6, 131.5, 129.7, 129.1, 129.0, 128.9, 128.5, 127.7, 127.3, 125.9, 125.4, 66.2, 62.0, 59.7, 53.8, 38.5, 31.6, 19.8, 18.8, 15.7, 14.5 ppm. MS: ES⁺: [M+Na]⁺. Accurate mass calculated: 519.2263 Found 519.2260.

(S)-Methyl-2-((S)-2-(anthracene-9-carboxamido)propanamido)propanoate (61d):

¹H NMR (CDCl₃): 8.51 (s, ArH, 1H), 8.10 (d, ArH, 2H, ³J_{HH} = 8.2Hz), 8.04 (d, ArH, 2H, ³J_{HH} = 7.6Hz), 7.53 (m, ArH, 4H), 6.87 (d, NH, 1H, ³J_{HH} = 7.8Hz), 6.63 (d, NH, 1H, ³J_{HH} = 7.3Hz), 5.01 (m, NHCHCH₃C=O, 1H), 4.70 (m, NHCHCH₃C=O, 1H), 3.81 (s, OCH₃, 3H), 1.63 (d, NHCHCH₃C=O, 3H, ³J_{HH} = 7.3Hz), 1.53 (d, NHCHCH₃C=O, 3H, ³J_{HH} = 7.1Hz) ppm. ¹³C NMR

(CDCl₃): 170.9, 169.2, 167.5, 128.9, 128.6, 126.6, 126.2, 124.8, 123.5, 122.7, 50.5, 47.4, 46.2, 16.3, 15.9 ppm. MS: ES⁺: [M+Na]⁺. Accurate mass calculated: 401.1483 Found 401.1477.

(S)-Methyl-2-((S)-2-(anthracene-9-carboxamido)propanamido)-3-methylbutanoate (61e):

¹H NMR (CDCl₃): 8.50 (s, ArH, 1H), 8.09 (d, ArH, 2H, ³J_{HH} = 8.1Hz), 8.03 (d, ArH, 2H, ³J_{HH} = 7.8Hz), 7.50 (m, ArH, 4H), 6.85 (d, NH, 1H, ³J_{HH} = 8.8Hz), 6.65 (d, NH, 1H, ³J_{HH} = 7.1Hz), 5.02 (m, NHCHCH₃C=O, 1H), 4.64 (dd, NHCH(CH₃)₂C=O, 1H, ³J_{HH} = 5.1, 4.0Hz), 3.80 (s, OCH₃, 3H), 2.29 (m, NHCH(CH₃)₂C=O, 1H), 1.63 (d, NHCHCH₃C=O, 3H, ³J_{HH} = 7.6Hz), 1.05 (d, NHCH(CH₃)₂C=O, 3H, ³J_{HH} = 7.3Hz), 1.01 (d, (CH₃)₂CH, 3H, ³J_{HH} = 6.9Hz) ppm. ¹³C NMR (CDCl₃): 172.6, 172.1, 170.0, 134.5, 131.4, 129.1, 128.9, 128.5, 127.6, 127.3, 125.9, 125.2, 123.2, 57.9, 52.7, 50.2, 31.8, 31.7, 19.4, 19.3, 18.4, 18.2 ppm. MS: ES⁺: [M+Na]⁺. Accurate mass calculated: 429.1801 Found 429.1790.

(S)-Ethyl-2-(2-(anthracene-9-carboxamido)acetamido)-3-phenylpropanoate (61f):

¹H NMR (CDCl₃): 8.48 (s, ArH, 1H), 8.03 (m, ArH, 3H), 7.49 (m, ArH, 3H), 7.28 (m, ArH, 5H), 7.18 (d, ArH, 2H, ³J_{HH} = 7.5Hz), 6.87 (s, NH, 1H), 6.71 (d, NH, 1H, ³J_{HH} = 8.4Hz), 4.87 (dd, NHCH(CH₂Ph)C=O, 1H, ³J_{HH} = 8.2, 6.9Hz), 4.37 (dd, NHCH₂C=O, 2H, ³J_{HH} = 7.3, 7.1Hz), 4.20 (q, OCH₂CH₃, 2H, ³J_{HH} = 7.1, 7.1Hz), 3.20 (d, NHCH(CH₂Ph)C=O, 1H, ³J_{HH} = 6.9Hz), 3.13 (d, NHCH(CH₂Ph)C=O, 1H, ³J_{HH} = 8.3Hz), 1.26 (t, OCH₂CH₃)₂, 3H, ³J_{HH} = 7.1Hz) ppm. ¹³C NMR (CDCl₃): 171.6, 170.5, 168.5, 136.0, 131.4, 131.2, 129.8, 129.0, 128.9, 128.8, 128.5, 128.1, 127.6, 127.3, 125.9, 125.4, 62.1, 53.9, 43.9, 38.3, 19.4, 14.5 ppm. MS: ES⁺: [M+Na]⁺. Accurate mass calculated: 477.1802 Found 477.1709.

Deprotection of the C-terminus:

A solution of THF: water (30 mL: 5 mL) was added to the compounds **61 (a, b, c, d, e or f)**. Lithium hydroxide (0.3 g) was added and the solution was stirred overnight. After this time, distilled water (100 mL) was added, and then hydrochloric acid (1.0 M) was added drop-wise until the pH was lowered to pH 3. The resulting precipitate was collected by filtration and washed with water to give compounds **(62 – 67)** as shown in Scheme 2.6 and Table 2.15. The yield was between 60 – 77% and the impurity (excess of valine methyl ester) was calculated by NMR spectroscopy to be between 3 – 12% of all

derivatives. Then, the resulting product was purified by washing with methanol. The yield after purification was between 30 – 35% and the resulting product was typically between 90 – 99% pure.

(S)-2-((S)-2-(Anthracene-9-carboxamido)-3-methylbutanamido)-3-methylbutanoic acid (62):

¹H NMR (d₆-DMSO): 8.93 (d, NH, 1H, ³J_{HH} = 9.1Hz), 8.66 (s, ArH, 1H), 8.11 (m, ArH, NH, 4H), 7.95 (m, ArH, 1H), 7.54 (m, ArH, 4H), 4.69 (t, NHCH(CH₃)₂C=O, 1H, ³J_{HH} = 8.2Hz), 4.32 (dd, NHCH(CH₃)₂C=O, 1H, ³J_{HH} = 5.9, 2.5Hz), 2.14(m, 2x CH(CH₃)₂, 2H), 1.05 (d, NHCH(CH₃)₂, 3H, ³J_{HH} = 7.4Hz), 0.99 (d, NHCH(CH₃)₂, 6H, ³J_{HH} = 6.2Hz), 1.03 (d, NHCH(CH₃)₂, 3H, ³J_{HH} = 6.8Hz) ppm. ¹³C NMR (d₆-DMSO): 171.4, 170.3, 169.5, 131.5, 131.4, 128.9, 128.5, 127.3, 125.9, 125.4, 59.6, 52.8, 45.3, 31.3, 19.9, 18.8 ppm. MS: ES⁻: [M – H]⁻. Accurate mass calculated: 419.1961 Found 419.1971.

(S)-2-(2-Anthracene-9-carboxamido)-3-methylbutanamido)acetic acid (63):

¹H NMR (d₆-DMSO): 8.90 (d, NH, 1H, ³J_{HH} = 8.8Hz), 8.65 (s, ArH, 1H), 8.43 (t, NH, 1H, ³J_{HH} = 7.1Hz), 8.13 (d, ArH, 3H, ³J_{HH} = 6.3Hz), 7.96 (m, ArH, 1H), 7.54 (d, ArH, 4H, ³J_{HH} = 6.3Hz), 4.62 (t, NHCH(CH₃)₂C=O, 1H, ³J_{HH} = 7.8Hz), 4.06 (dd, NHCH₂C=O, 1H, ³J_{HH} = 5.6, 3.6Hz), 3.90 (dd, NHCH₂C=O, 1H, ³J_{HH} = 5.8, 11.6Hz), 2.14 (m, CH(CH₃)₂, 1H), 1.03 (d, NHCH(CH₃)₂, 3H, ³J_{HH} = 8.1Hz), 0.97 (d, NHCH(CH₃)₂, 3H, ³J_{HH} = 4.1Hz) ppm. ¹³C NMR (d₆-DMSO): 171.4, 171.2, 168.3, 134.6, 133.2, 133.0, 130.6, 128.3, 128.1, 127.6, 127.3, 126.9, 126.7, 126.2, 125.9, 125.4, 125.2, 58.9, 40.7, 29.8, 19.4, 18.6 ppm. MS: ES⁻: [M – H]⁻. Accurate mass calculated: 377.1512 Found 377.1501.

(S)-2-((S)-2-(Anthracene-9-carboxamido)-3-methylbutanamido)-3-phenylpropanoic acid (64):

¹H NMR (d₆-DMSO): 8.80 (d, NH, 1H, ³J_{HH} = 8.6Hz), 8.64 (s, ArH, 1H), 8.32 (s, ArH, 3H), 8.12 (d, ArH, 2H, ³J_{HH} = 6.0Hz), 7.95 (d, NH, 1H, ³J_{HH} = 9.2Hz), 7.53 (m, ArH, 3H), 7.34 (d, ArH, 2H, ³J_{HH} = 7.6Hz), 7.28 (t, ArH, 2H, ³J_{HH} = 6.8Hz), 7.22 (t, ArH, 1H, ³J_{HH} = 8.6Hz), 4.62 (m, NHCH(CH₂Ph)C=O, NHCH(CH₃)₂C=O, 2H), 3.17 (dd, NHCH(CH₂Ph)C=O, 1H, ³J_{HH} = 8.7, 4.8Hz), 2.99 (dd, NHCH(CH₂Ph)C=O, 1H, ³J_{HH} = 9.2, 4.8Hz), 2.08 (m, CH(CH₃)₂, 1H), 0.99 (d, NHCH(CH₃)₂, 3H, ³J_{HH} = 6.8Hz), 0.96 (d, CH(CH₃)₂, 3H, ³J_{HH} = 7.4Hz) ppm. ¹³C NMR (d₆-DMSO): 172.9, 170.9, 168.2, 137.5, 134.5, 133.2, 130.6, 129.1, 128.4, 128.2, 127.5, 127.3,

127.0, 126.7, 126.4, 126.2, 125.8, 125.1, 64.9, 58.9, 53.4, 38.9, 36.8, 30.1, 25.1, 19.3, 18.6, 15.1 ppm. MS: ES⁻: [M - H]⁻. Accurate mass calculated: 467.1964 Found 467.1971.

(S)-2-((S)-2-(Anthracene-9-carboxamido)propanamido)propanoic acid (65):

¹H NMR (d₆-DMSO): 9.00 (d, NH, 1H, ³J_{HH} = 6.5Hz), 8.65 (s, ArH, 1H), 8.39 (s, ArH, 1H), 8.33 (d, NH, 1H, ³J_{HH} = 7.3Hz), 8.12 (d, ArH, 2H, ³J_{HH} = 8.1Hz), 7.96 (m, ArH, 1H), 7.55 (m, ArH, 4H), 7.76 (m, NHCHCH₃C=O, 1H), 4.38 (m, NHCHCH₃C=O, 1H), 1.40 (d, 2xNHCHCH₃C=O, 6H, ³J_{HH} = 4.9Hz) ppm. ¹³C NMR (d₆-DMSO): 174.6, 172.7, 168.4, 133.3, 130.9, 128.7, 128.4, 128.1, 127.5, 127.1, 126.7, 126.5, 125.9, 125.6, 49.2, 47.9, 17.9, 17.6 ppm. MS: ES⁻: [M - H]⁻. Accurate mass calculated: 387.1317 Found 387.1321.

(S)-2-((S)-2-(Anthracene-9-carboxamido)propanamido)-3-methylbutanoic acid (66):

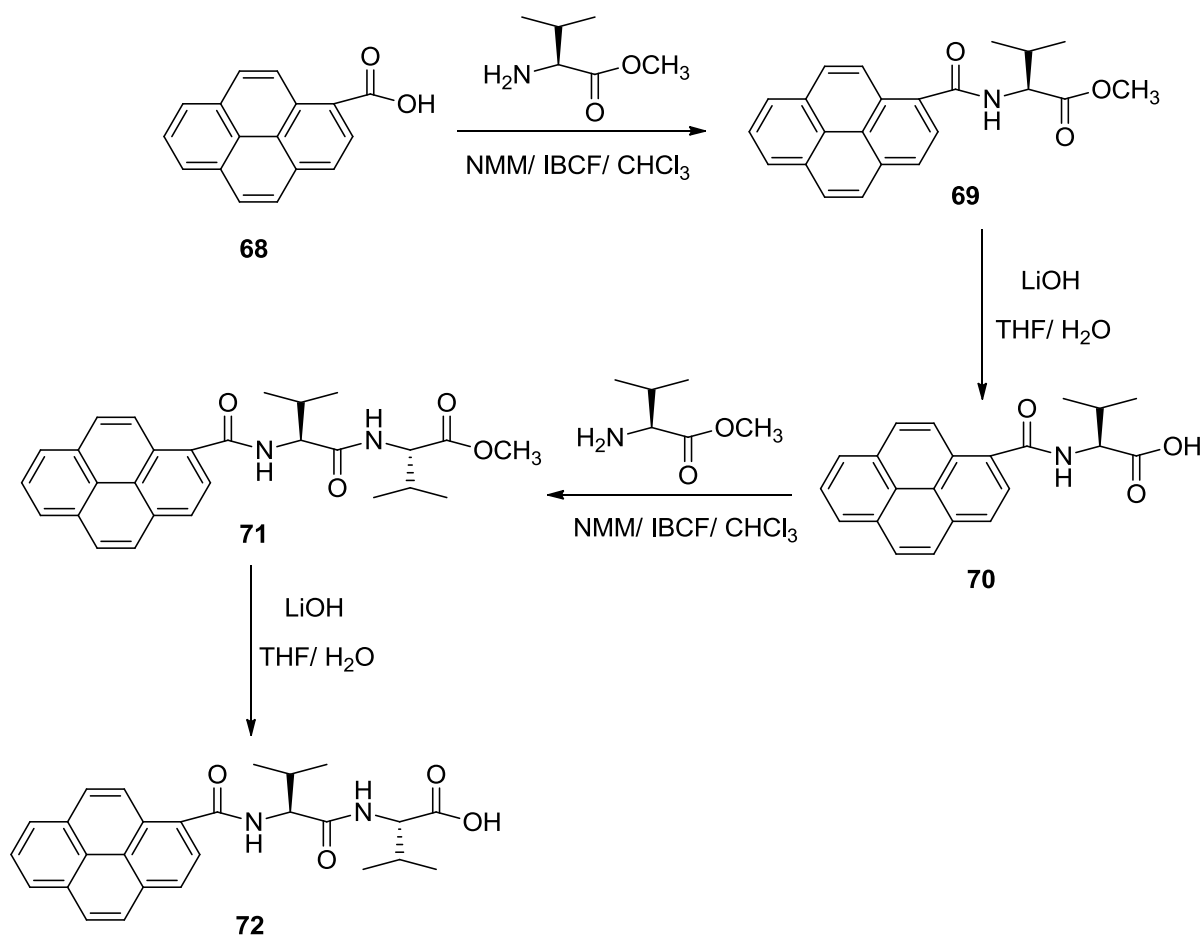
¹H NMR (d₆-DMSO): 9.01 (d, NH, 1H, ³J_{HH} = 8.5Hz), 8.65 (s, ArH, 1H), 8.28 (m, ArH, 1H), 8.12 (m, ArH, 2H), 8.08 (d, NH, 1H, ³J_{HH} = 8.7Hz), 7.95 (m, ArH, 2H), 7.55 (m, ArH, 3H), 4.82 (t, NHCHCH₃C=O, 1H, ³J_{HH} = 7.8Hz), 4.31 (dd, NHCH(CH₃)₂C=O, 1H, ³J_{HH} = 5.3, 3.2Hz), 2.15 (m, NHCH(CH₃)₂C=O, 1H), 1.37 (d, NHCHCH₃C=O, 3H, ³J_{HH} = 7.4Hz), 0.99 (d, NHCH(CH₃)₂C=O, 3H, ³J_{HH} = 4.3Hz), 0.97 (d, CH(CH₃)₂, 3H, ³J_{HH} = 4.2Hz) ppm. ¹³C NMR (d₆-DMSO): 182.5, 173.0, 172.7, 168.0, 134.6, 133.0, 132.9, 130.6, 127.1, 126.7, 125.5, 57.2, 48.9, 30.0, 29.2, 19.1, 17.9, 17.7 ppm. MS: ES⁻: [M - H]⁻. Accurate mass calculated: 391.1643 Found 391.1658.

(S)-2-(2-(Anthracene-9-carboxamido)acetamido)-3-phenylpropanoic acid (67):

¹H NMR (d₆-DMSO): 8.97 (t, NH, 1H, ³J_{HH} = 5.5Hz), 8.65 (s, ArH, 1H), 8.41 (d, NH, 1H, ³J_{HH} = 7.9Hz), 8.22 (m, ArH, 2H), 8.12 (m, ArH, 2H), 7.54 (m, ArH, 4H), 7.31 (d, ArH, 4H, ³J_{HH} = 4.4Hz), 7.23 (m, ArH, 1H), 4.59 (m, NHCH(CH₂Ph)C=O, 1H), 4.13 (dd, NHCH₂C=O, 2H, ³J_{HH} = 9.8, 6.1Hz), 3.16 (dd, NHCH(CH₂Ph)C=O, 1H, ³J_{HH} = 8.5, 5.7Hz) ppm. ¹³C NMR (d₆-DMSO): 172.9, 168.8, 168.6, 137.4, 134.6, 132.9, 130.6, 129.2, 128.2, 128.1, 127.4, 127.2, 126.7, 126.5, 126.2, 125.8, 125.5, 64.9, 53.7, 41.9, 38.9, 36.9, 15.1 ppm. MS: ES⁻: [M - H]⁻. Accurate mass calculated: 425.1512 Found 425.1501.

2.2.6- Pyrene dipeptides:

Peptides amphiphile conjugated to pyrene have been synthesised using different methods elsewhere²⁸. Also, Zhang *et al.* have synthesised dipeptide based pyrene²⁹. Here, we have synthesised 1-pyrene dipeptide using the IBCF method as shown in Scheme 2.7.



Scheme 2.7: The general reaction of dipeptide synthesis based on 1-pyrene ring using IBCF method.

Dipeptide	Abbreviation
72	Py-VVOH

Table 2.16: The abbreviation of compounds 72 in the Scheme 2.7.

Experimental section:

Standard coupling methodology:

N-Methylmorpholine (4 mL) and IBCF (3 mL) was added to pyrene carboxylic acid (5.0 g) in chloroform (70 mL) chloroform at 0 °C. A solution of L-valine methyl ester hydrochloride (4.0 g, 1.5 eq.) and NMM (4 mL) in chloroform was added and the solution was stirred at room temperature overnight. Then, the solution was washed with distilled water (100 mL), hydrochloric acid (2 x 100 mL, 0.1 M), aqueous potassium carbonate (100 mL, 0.1 M), and distilled water again (4 x 100 mL) and dried with magnesium sulfate, and the solvent was removed *in vacuo* to give compound **69** as shown in Scheme 2.7. The yield was 50% and the impurity (an excess of valine methyl ester) was calculated by ¹H NMR spectroscopy to be 10%. Then, the resulting product was purified by washing with methanol. The yield after purification was typically 25% and the resulting product was 95% pure.

(S)-Methyl-3-methyl-2-(pyrene-1-carboxamido)butanoate (**69**):

¹H NMR (CDCl₃): 8.63 (d, ArH, 1H, ³J_{HH} = 8.8Hz), 8.24 (d, ArH, 2H, ³J_{HH} = 8.1Hz), 8.18 (m, ArH, 6H), 6.63 (d, NH, 1H, ³J_{HH} = 8.8Hz), 5.01 (dd, NHCH(CH₃)₂C=O, 1H, ³J_{HH} = 5.1, 4.3Hz), 3.84 (s, OCH₃, 3H), 2.41 (m, CH(CH₃)₂, 1H), 1.15 (d, CH(CH₃)₂, 3H, ³J_{HH} = 6.3Hz), 1.04 ppm (d, CH(CH₃)₂, 3H, ³J_{HH} = 7.1Hz) ppm. ¹³C NMR (CDCl₃): 173.0, 170.2, 133.2, 131.7, 131.1, 130.9, 129.3, 129.2, 129.1, 127.6, 126.8, 126.3, 126.2, 125.2, 125.1, 124.8, 58.1, 52.8, 32.0, 19.7, 18.4 ppm. MS: ES⁺: [M+Na]⁺. Accurate mass calculated: 382.1428 Found 382.1419.

Deprotection of the C-terminus:

A solution of THF: water (30 mL: 5 mL) was added to the compound **69**. Lithium hydroxide (0.3 g) was added and the solution was stirred overnight. After this time, distilled water (100 mL) was added, and then hydrochloric acid (1.0 M) was added dropwise until the pH was lowered to pH 3. Then, the resulting precipitate was collected by filtration and washed with water to give compound **70** as shown in Scheme 2.7. The yield was 77% and the impurity (an excess of valine methyl ester) was calculated by ¹H NMR spectroscopy to be 20%. Then, the resulting product was purified by washing with

methanol. The yield after purification was typically 35% and the resulting product was 87% pure.

***(S)*-3-Methyl-2-(pyrene-1-carboxamido)butanoic acid (70):**

^1H NMR (d_6 - DMSO): 8.87 (d, NH, 1H, $^3J_{\text{HH}} = 8.8\text{Hz}$), 8.49 (d, ArH, 1H, $^3J_{\text{HH}} = 9.5\text{Hz}$), 8.36 (m, ArH, 3H), 8.25(m, ArH, 3H), 8.13 (m, ArH, 2H), 4.51 (dd, $\text{NHCH}(\text{CH}_3)_2\text{C}=\text{O}$, 1H, $^3J_{\text{HH}} = 6.3, 2.3\text{Hz}$), 2.26 (m, $\text{CH}(\text{CH}_3)_2$, 1H), 1.06 (d, $\text{CH}(\text{CH}_3)_2$, 3H, $^3J_{\text{HH}} = 6.9\text{Hz}$), 1.05 (d, $\text{CH}(\text{CH}_3)_2$, 3H, $^3J_{\text{HH}} = 7.3\text{Hz}$) ppm. ^{13}C NMR (d_6 - DMSO): 173.6, 169.8, 132.2, 131.9, 131.1, 130.6, 128.6, 128.4, 128.2, 127.6, 126.9, 126.2, 126.0, 125.8, 125.1, 124.7, 124.1, 124.0, 58.8, 29.8, 19.8, 18.9 ppm. MS: ES $^-$: [M – H] $^-$. Accurate mass calculated: 344.1288 Found 344.1287.

Standard coupling methodology:

N-Methylmorpholine (4 mL) and IBCF (3 mL) was added to compound **70** (3.0 g) in chloroform (70 mL) at 0 °C. A solution of L-valine methyl ester hydrochloride (4.0 g, 1.5 eq.) and NMM (4 mL) in chloroform was added and the solution was stirred at room temperature overnight. Then, the solution was washed with distilled water (100 mL), hydrochloric acid (2 x 100 mL, 0.1 M), aqueous potassium carbonate (100 mL, 0.1 M), and distilled water again (4 x 100 mL) and dried with magnesium sulfate, and the solvent was removed *in vacuo* to give compound **71** as shown in Scheme 2.7. The yield was 53% and the impurity (an excess of valine methyl ester) was calculated by ^1H NMR spectroscopy to be 10%. Then, the resulting product was purified by washing with diethyl ether. The yield after purification was typically 20% and the resulting product was 92% pure.

***(S)*-Methyl-3-methyl-2-((*S*)-3-methyl-2-(pyrene-1-carboxamido)butanamido)butanoate (71):**

^1H NMR (CDCl_3): 8.61 (d, ArH, 1H, $^3J_{\text{HH}} = 9.3\text{Hz}$), 8.25 (d, ArH, 2H, $^3J_{\text{HH}} = 7.4\text{Hz}$), 8.16 (m, ArH, 4H), 8.07 (m, ArH, 2H), 6.85 (d, NH, 1H, $^3J_{\text{HH}} = 9.1\text{Hz}$), 6.60 (d, NH, 1H, $^3J_{\text{HH}} = 8.5\text{Hz}$), 4.75 (dd, $\text{NHCH}(\text{CH}_3)_2\text{C}=\text{O}$, 1H, $^3J_{\text{HH}} = 6.0, 2.7\text{Hz}$), 4.65 (dd, $\text{NHCH}(\text{CH}_3)_2\text{C}=\text{O}$, 1H, $^3J_{\text{HH}} = 4.8, 3.9\text{Hz}$), 3.79 (s, OCH_3 , 3H), 2.35 (m, $\text{CH}(\text{CH}_3)_2$, 1H), 2.28 (m, $\text{CH}(\text{CH}_3)_2$, 1H), 1.17 (d, $\text{CH}(\text{CH}_3)_2$, 3H, $^3J_{\text{HH}} = 7.2\text{Hz}$), 1.16 (d, $\text{CH}(\text{CH}_3)_2$, 3H, $^3J_{\text{HH}} = 8.2\text{Hz}$), 1.00 (d, $\text{CH}(\text{CH}_3)_2$, 3H, $^3J_{\text{HH}} = 6.2\text{Hz}$), 0.96 (d, $\text{CH}(\text{CH}_3)_2$, 3H, $^3J_{\text{HH}} = 7.2\text{Hz}$) ppm. ^{13}C NMR (CDCl_3): 172.5, 171.6,

170.4, 133.1, 131.5, 131.1, 130.7, 129.2, 129.2, 129.2, 129.1, 127.5, 126.8, 126.3, 126.2, 125.2, 125.1, 124.7, 124.6, 59.8, 57.8, 52.6, 31.8, 31.5, 19.8, 19.4, 18.9, 18.2 ppm. MS: ES⁺: [M+Na]⁺. Accurate mass calculated: 481.2108 Found 481.2103.

Deprotection of the C-terminus:

A solution of THF: water (30 mL: 5 mL) was added to the compound **71**. Lithium hydroxide (0.3 g) was added and the solution was stirred overnight. After this time, distilled water (100 mL) was added, and then hydrochloric acid (1.0 M) was added drop-wise until the pH was lowered to pH 3. Then, the resulting precipitate was collected by filtration and washed with water to give compound **72** as shown in Scheme 2.7. The yield was 73% and the impurity was THF. The resulting product was purified by washing with methanol. The yield after purification was typically 45% and the resulting product was 85% pure.

***(S)*-3-methyl-2-((*S*)-3-methyl-2-(pyrene-1-carboxamido)butanamido)butanoic acid (**72**):**

¹H NMR (d₆-DMSO): 8.76 (d, NH, 1H, ³J_{HH} = 8.6Hz), 8.46 (d, NH, 1H, ³J_{HH} = 9.2Hz), 8.35 (t, ArH, 3H, ³J_{HH} = 7.8Hz), 8.26 (m, ArH, 3H), 8.13 (m, ArH, 3H), 4.60 (t, NHCH(CH₃)₂C=O, 1H, ³J_{HH} = 7.6Hz), 4.28 (dd, NHCH(CH₃)₂C=O, 1H, ³J_{HH} = 6.7, 4.2Hz), 2.16 (m, 2xCH(CH₃)₂, 2H), 1.05 (d, CH(CH₃)₂, 3H, ³J_{HH} = 7.1Hz), 1.03 (d, CH(CH₃)₂, 3H, ³J_{HH} = 7.7Hz), 0.97 (d, CH(CH₃)₂, 6H, ³J_{HH} = 6.8Hz) ppm. ¹³C NMR (d₆-DMSO): 172.5, 171.6, 170.4, 133.1, 131.5, 131.1, 130.7, 129.2, 129.2, 129.2, 129.1, 127.5, 126.8, 126.3, 126.2, 125.2, 125.1, 124.7, 124.6, 59.8, 57.8, 52.6, 31.8, 31.5, 19.8, 19.4, 18.9, 18.2 ppm. MS: ES⁻: [M - H]⁻. Accurate mass calculated: 443.1969 Found 443.1971.

DCC coupling method:

We have attempted to synthesise some peptide derivatives such as compounds **75** and **77** using a different coupling method (using DCC) in an effort to increase the yield or decrease the amount of impurity, but this method was not successful. The yield was low (typically 18%) and there was lots of impurity. The experimental of the DCC method was similar to IBCF method, but we used DCC as coupling agent and dimethyl amino pyridine (DMAP) as a catalyst. The reaction was carried out in dichloromethane instead of chloroform. An example synthesis is described below:

A DMAP (0.1 g) was added to a solution of the anthraquinone or pyrene derivative (1.0 g) in DCM (70 mL). Then, a DCC (1 eq.) was added. A solution of valine methyl ester hydrochloride (1 eq.) and NMM (1 eq.) in DCM (30 mL) was added in ice bath. The solution was stirred overnight at room temperature. After this time, the solution was washed with distilled water (100 mL), hydrochloric acid (2 x 100 mL, 0.1 M), aqueous potassium carbonate (100 mL, 0.1 M), and distilled water again (4 x 100 mL) and dried with magnesium sulfate, and the solvent was removed *in vacuo*.

2.3- Result and Discussion:

Peptides can be synthesised by coupling the carboxyl group (*C*-terminus) of one amino acid to the amino group (*N*-terminus) of another¹⁻³. Here, we have synthesised 35 dipeptides conjugated to different aromatic rings. 20 Dipeptides were linked to a naphthalene ring with different linkers and different substituents, 6 dipeptides linked to anthracene, 4 dipeptides linked to carbazole, 1 dipeptide linked to anthraquinone and 1 dipeptide linked to pyrene. We have used different methods in the first step of the reaction to prepare different linkers such as reacting with *tert*-butyl chloroacetate, thionyl chloride or bromoacetic acid and we have used the IBCF method to couple the carboxyl group of the aromatic ring to the *N*-terminus of the first amino acid. We have synthesised this large library of dipeptides in order to study their ability to form hydrogels and study their properties for some applications which is discussed in more detail in Chapter 3.

2.3.1- Dipeptides synthesis:

Naphthalene dipeptide synthesis

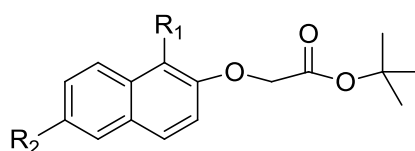
Naphthalene dipeptides derivatives were synthesised by using two methods. A first method was the method of Chen *et al.*¹⁴ This starts from naphthol derivatives. The second method started from naphthalene acetic acid derivatives. The difference between the methods is that the first method used *tert*-butyl chloroacetate to react with naphthol derivatives and then the *tert*-butyl group was removed using trifluoroacetic acid. In the first coupling step, the resulting product was reacted with valine methyl ester hydrochloride. In the second method, naphthalene acetic acid derivatives were coupled with the first amino ester (valine methyl ester hydrochloride) without using *tert*-butyl chloroacetate. The results showed that the dipeptides conjugated to the

aromatic ring with different linker groups have different ability to form gels. These results agreed with Chen's research³⁰, where they reported that using different linkers, -CH₂ and -OCH₂ to couple naphthalene ring to the amino acid can affect the ability of a dipeptide to form a hydrogel.

The reaction mechanism of dipeptides conjugated to naphthol was as following:

Deprotonation of the naphthol derivatives:

Naphthol derivatives were deprotonated by potassium carbonate, followed by nucleophilic attack of the deprotonated naphthalene derivative on chloro-*tert*-butylacetate to give compounds **2(a, b, c, d)** (Fig. 2.1). The *tert*-butyl group was removed using trifluoroacetic acid (TFA) in chloroform.

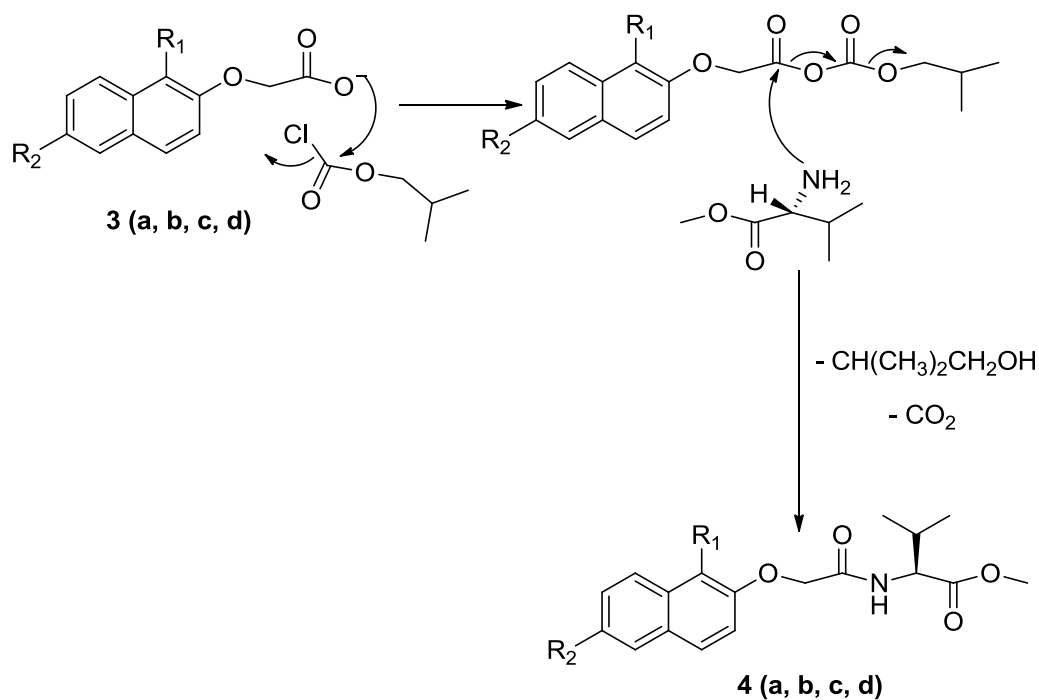


2 (a, b, c, d)
a= R₁= H, R₂= H
b= R₁= H, R₂= Br
c= R₁= Br, R₂= Br
d= R₁= Br, R₂= H

Figure 2.1: The general structure of compound 2 (a, b, c, d).

Coupling step reaction mechanism for two methods:

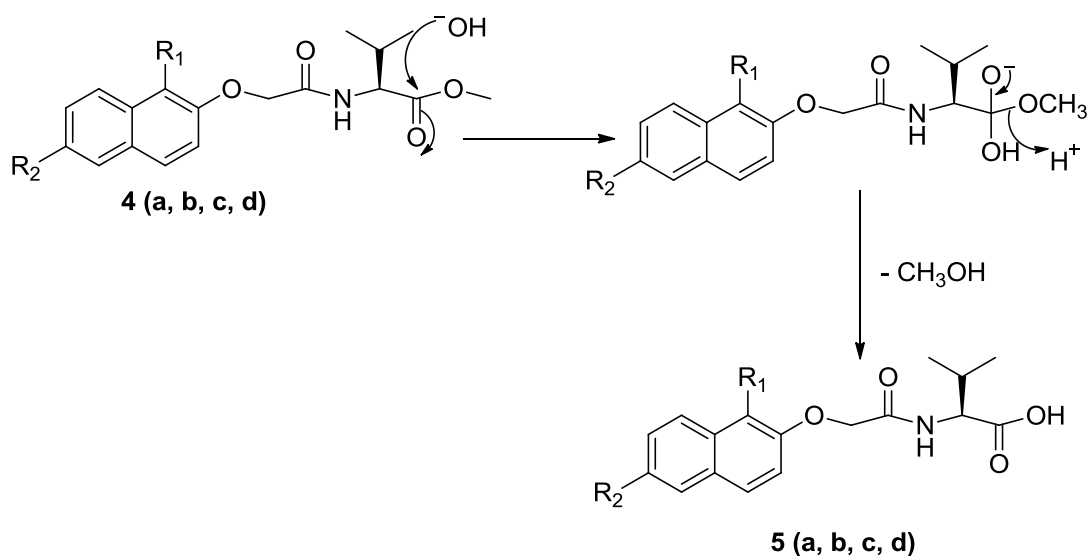
Compounds **3 (a, b, c, d)** were synthesised by coupling with the first amino acid (valine methyl ester hydrochloride) using IBCF and *N*-methylmorpholine (NMM) in chloroform. NMM was used to free the amino group from the corresponding hydrochloride salt. IBCF was used as the coupling agent. The reaction proceeded by the nucleophilic attack of the amino acid on to the activated carboxylic acid as shown in Scheme 2.8.



Scheme 2.8: The reaction mechanism of the coupling step of the amino acid conjugated to naphthalene ring.

Deprotection reaction mechanism:

Lithium hydroxide was used to deprotect the resulting products of the first coupling step at room temperature overnight. The product was isolated using 1.0M HCl to lower the pH to pH 3 and so precipitate the carboxylic acid as shown in Scheme 2.9.



Scheme 2.9: The deprotection reaction mechanism between the resulting product of the first amino acid and the base (lithium hydroxide).

According to Chen *et al.* the naphthalene dipeptides can be used as a hydrogelators^{14, 18}. Chen *et al.* synthesised naphthalene dipeptides from 6-bromonaphthol using different amino acids in the first coupling step. Here, twenty naphthalene dipeptide derivatives were synthesised from 1-bromo-2-naphthol, 6-bromo-2-naphthol, 1,6-dibromo-2-naphthol, 2-naphthol and 1-naphthalene acetic acid (Fig. 2.2). In general, the yields of the deprotection step were good (65 – 73%), whereas in the first and the second coupling steps the yield was low (between 35 to 40% for all derivatives). We tried to increase the yield by using a different coupling method (DCC^{5, 19} instead of IBCF^{5, 13, 14}). The result showed that the yield of the coupling step using DCC method was lower (20%) than when using the IBCF method. Therefore, we instead attempted to change the equivalents of the reactants in the IBCF method, the equivalents of the amino acid and of IBCF. The yields increased for the first coupling step when the equivalents of valine methyl ester hydrochloride and IBCF were increased from one equivalent to 1.5 and the equivalents of IBCF changed from one to 1.1. By this optimisation, the yield in the first coupling step was raised to between 73 to 76%. This modification in protocol was also used for the second coupling step, but the yield was not found to increase. The lack of improvement for this second coupling could be due to the steric hindrance of the dipeptide.

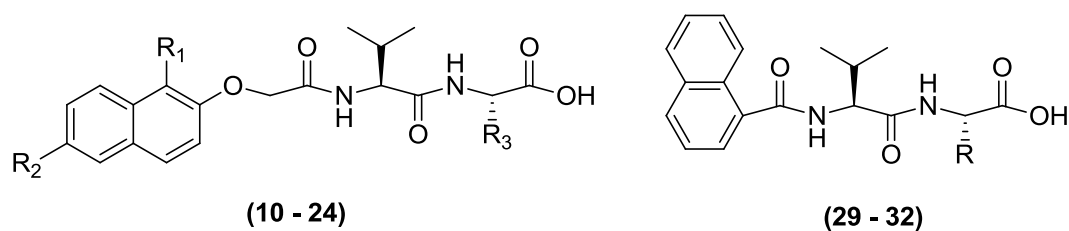


Figure 2.2: The general structure of twenty dipeptides that synthesised. Structure of compounds 10 - 24 refer to dipeptides based on 2-naphthol, 1-bromonaphthol, 6-bromonaphthol and 1,6dibromonaphthol. Structure of compounds 29 - 32 refer to dipeptides based on 1-naphthalene acetic acid.

9-Phenanthrol dipeptide synthesis:

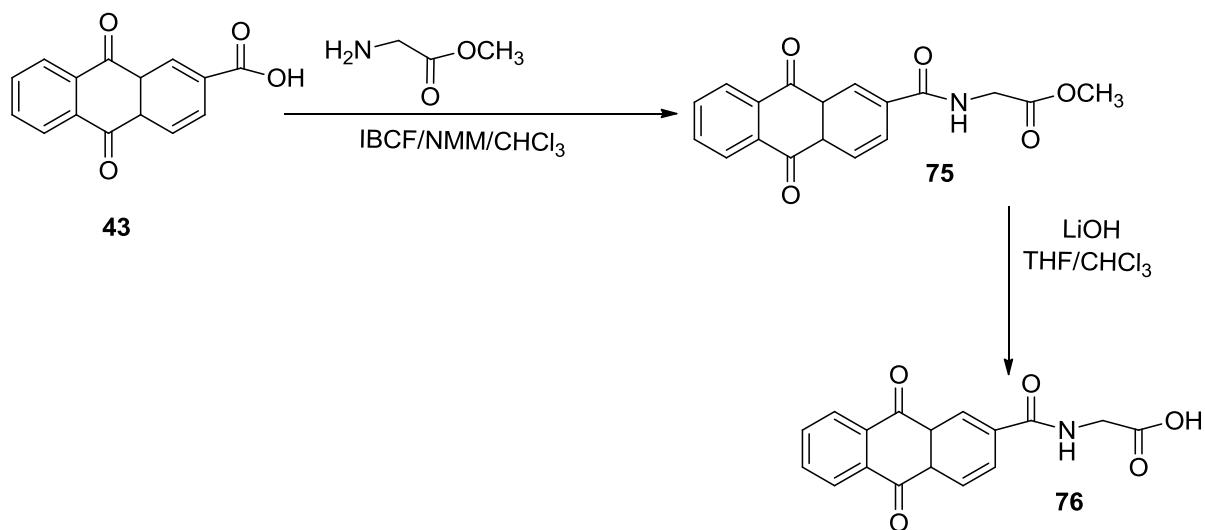
We have used the same procedure that we used to prepare naphthalene dipeptide derivatives to prepare dipeptides linked to phenanthrol, with the same linker between the aromatic group and the amino acid. 9-Phenanthrol was reacted with *tert*-butyl chloroacetate in acetone in the presence of K₂CO₃ to give *tert*-butyl phenanthrol derivative, followed by a deprotecting step using trifluoroacetic acid in chloroform, and then the resulting product was coupled with the first amino acid.

The yields of the coupling steps and the deprotection steps were between 71 – 75 %. We obtained a white or off-white solid product in all steps. We synthesised three dipeptide derivatives, **40**, **41** and **42**. ¹H, ¹³C NMR and mass spectroscopic analysis produced evidence of the success the reaction. Almost all compounds in the coupling and deprotection steps were pure, so we used the product directly for the second step of the next reaction. Exceptions were **35**, **39c**, **41** and **42** where we removed impurities by washing with methanol. The yield however decreased after purification to typically 40 – 60%.

2-Anthraquinone dipeptide synthesis:

The protocol of the synthesis of naphthalene dipeptide derivatives was used again to prepare anthraquinone dipeptides, but we directly coupled the first amino acid, rather than using an –OCH₂ linker. Here, unlike for the naphthalene examples, we carried out the coupling reaction using phenylalanine because it has been used in much research previously¹⁷ and reported as a good hydrophobic amino acid to form a strong hydrogels. We repeated the coupling and deprotection steps and we synthesised one dipeptide from anthraquinone, compound **47**. The yield of the last step of the reaction to obtain the dipeptide **47** was 75%. We attempted to synthesise other peptides with a different amino acid, glycine methyl ester. The reaction was successful as shown by the ¹H NMR spectroscopy result after purification with methanol (Fig. 2.3). However, the yield of compound **75** in this step was very low (27%) (Scheme 2.10) and the impurities (IBCF, starting material) were very difficult to remove in this stage of the synthesis. We tried changing the equivalents of some reactants, such as the amount of glycine methyl ester from 1 equivalent to 1.5 equivalents, but this modification of the method did not increase the yield and did not remove the impurity. Moreover, we attempted changing

the method by using DCC coupling method, but the impurities increased and the yield decreased to 18%.



Scheme 2.10: Reaction of anthraquinone to obtain compounds 75 and 76.

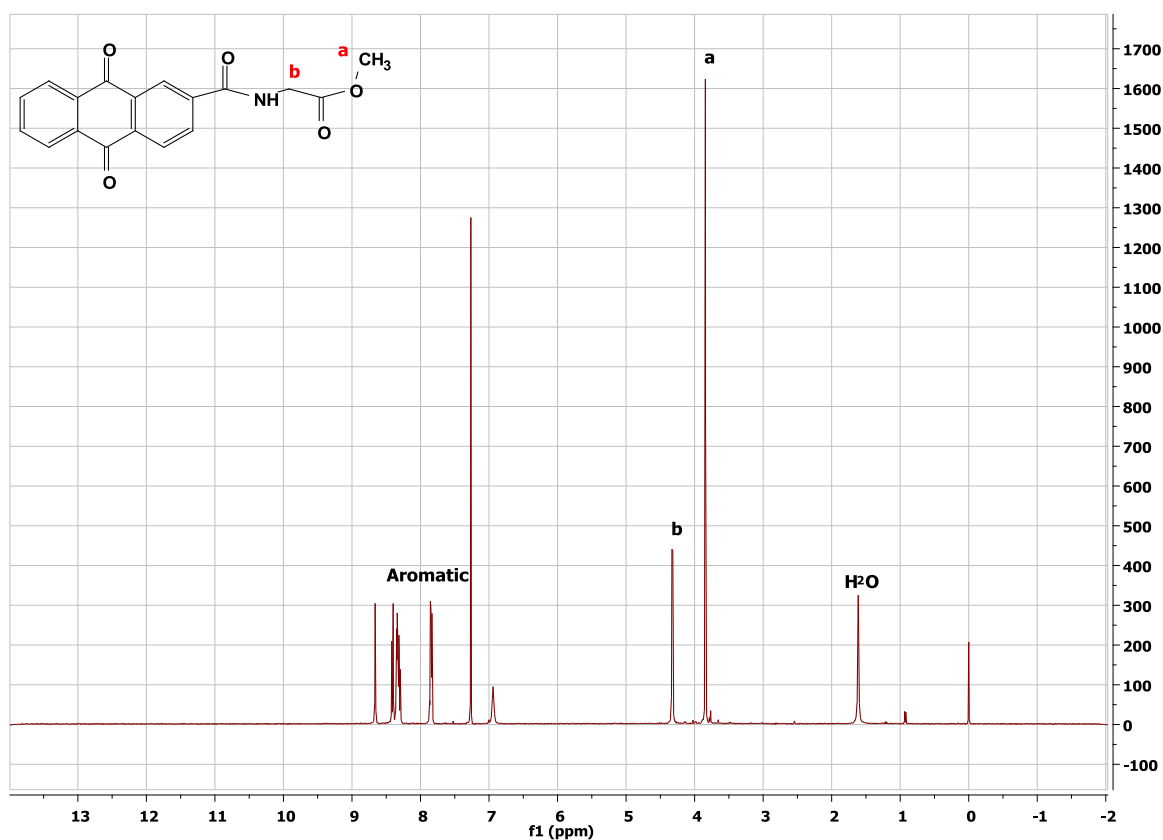


Figure 2.3: An example of ¹H NMR spectroscopy of compound 75.

When we attempted the deprotection step to obtain compound **76** (Scheme 2.10), there were impurities as shown in the ^1H NMR data (Fig. 2.4). We noted some impurity in the aromatic area (7 – 9ppm). We noted that there were 2 extra protons in the aromatic area, but the identity of the impurity is not clear. We tried to purify the product by washing with organic solvents (methanol, hexane, ethyl acetate or diethyl ether) that have different polarity, but they did not remove the impurity. Furthermore, we tried to purify the product by using crystallisation from toluene, ethanol or ethyl acetate, but also this did not purify the compound **76**. We have repeated the coupling and deprotection step with glycine four times, but we obtained the same result and we failed to synthesise more peptides from these aromatic groups.

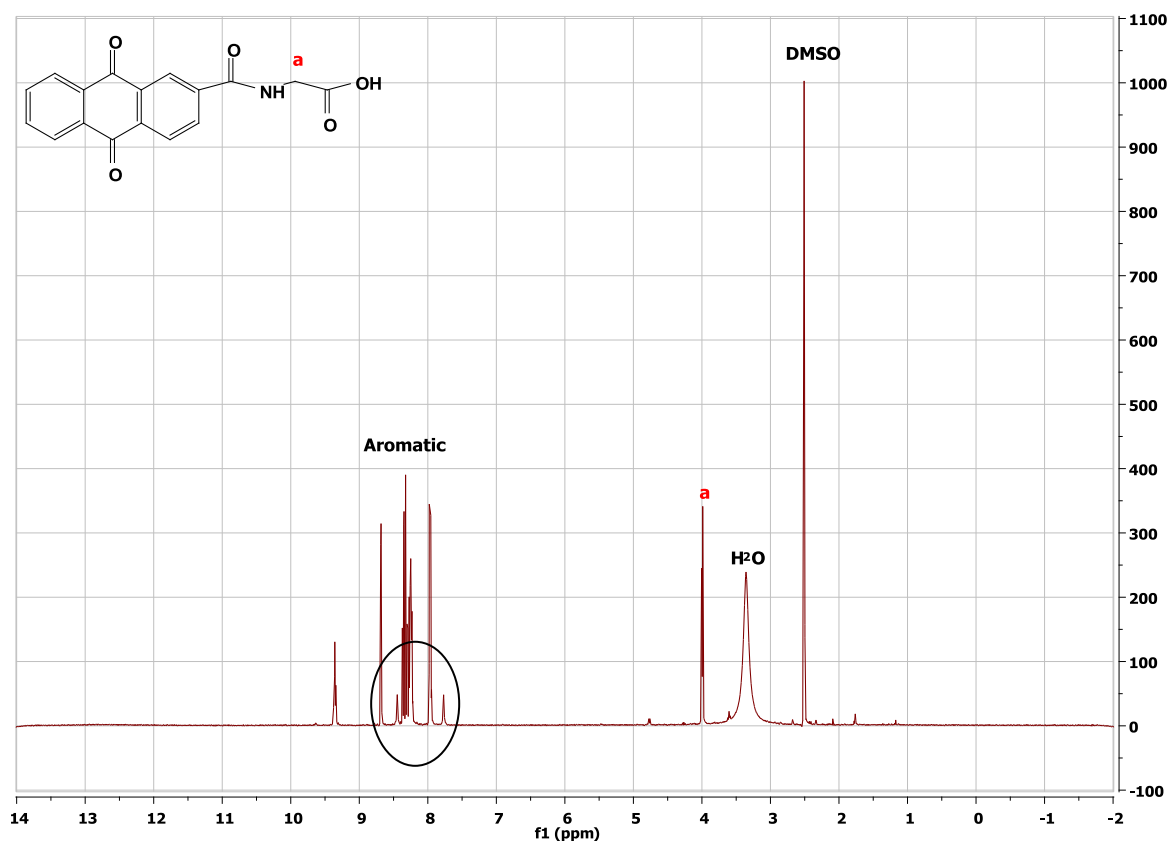
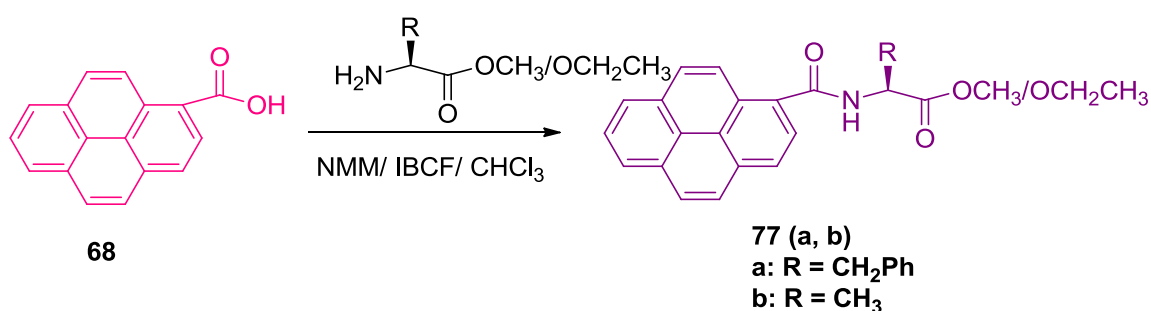


Figure 2.4: An example of ^1H NMR spectroscopy of compound **76**. Circles are the impurities (excess of aromatic protons at 8 – 8.5ppm)

1-Pyrene dipeptide synthesis:

We have synthesised pyrene dipeptide derivatives using the same protocol as for the synthesis of naphthalene dipeptide derivatives. Again, we directly coupled the amino acids to the ring without a $-OCH_2$ linker. We synthesised one pyrene dipeptide, compound **72**. The yield of the last step to obtain compound **72** was 73%. We have tried to synthesise other peptides using different amino acid sequences such as phenylalanine ethyl ester or alanine methyl ester to obtain compounds **77a** or **77b** (Scheme 2.11), but the yield was very low in the first coupling step (25 and 27% respectively) and the impurities (excess of phenylalanine ethyl ester, alanine methyl ester, IBCF) were again very difficult to remove from the first coupling of the synthesis. Figure 2.5 shows an example of a 1H NMR spectrum of **77a**. We attempted to change the synthesis method by using DCC coupling method, but the impurity increased and there were impurities that it has not removed. The yield was lower (18%) than for the IBCF method. Again, we tried varying the reaction conditions; the equivalents of some reactants such as phenylalanine ethyl ester, alanine methyl ester, or IBCF to try and lower the amounts of impurity, but changing these conditions did not decrease the impurity or increase the yield.



Scheme 2.11: The reaction of pyrene carboxylic acid to obtain compounds 77a and 77b.

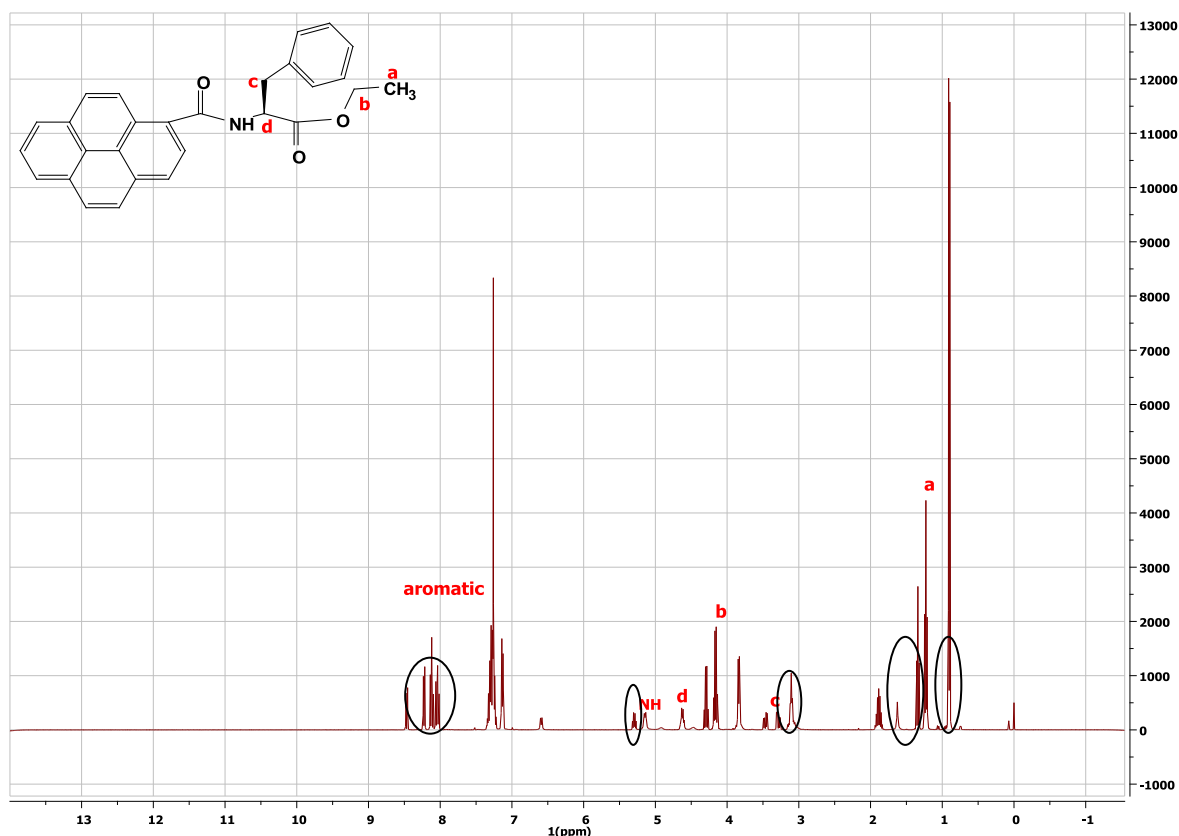
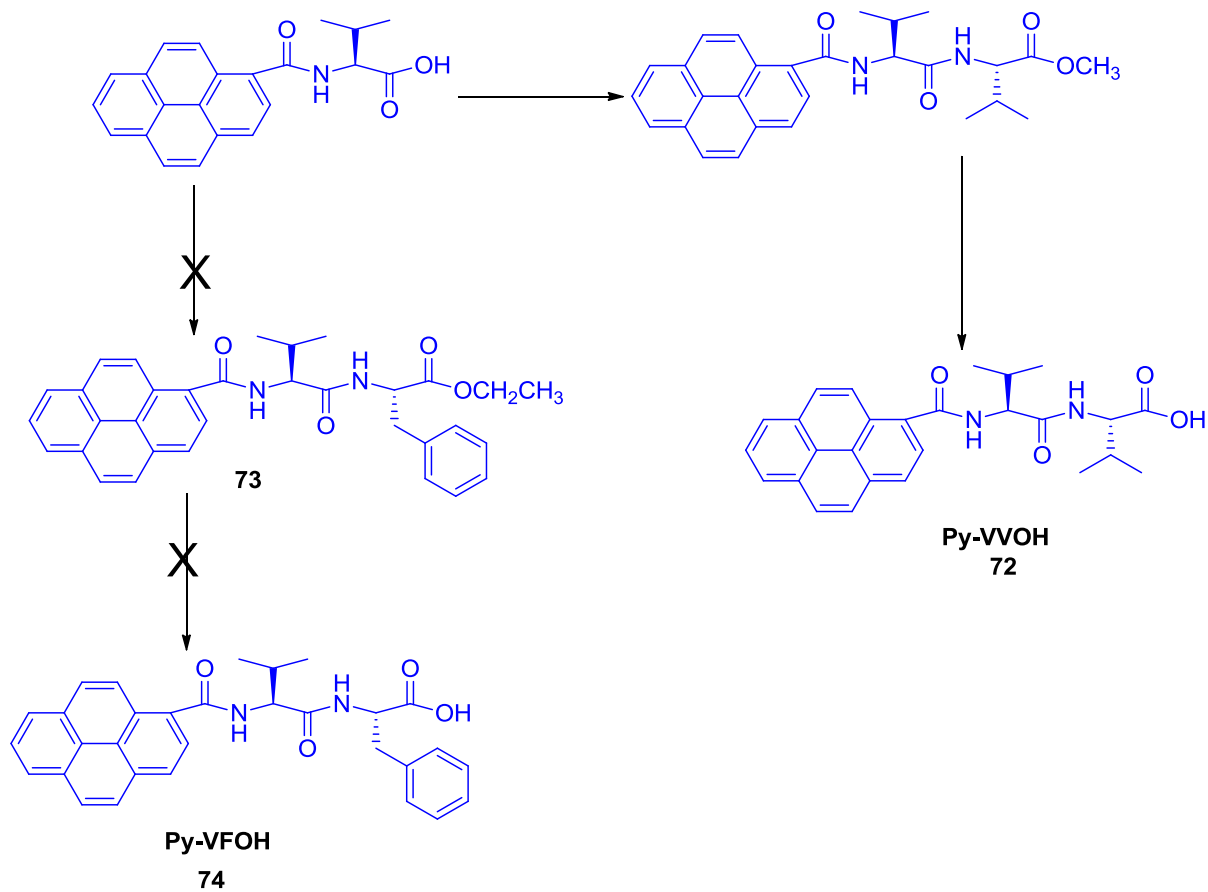


Figure 2.5: The ^1H NMR spectrum of 77a with some impurities. Circled are the impurities (excess of ethyl ester at 1.4ppm and 4.3ppm, IBCF at 0.9, 3ppm, NH at 5.3ppm and aromatic protons at 8 – 8.5ppm).

Furthermore, we tried to synthesise compound **74**, but the last step of the reaction (the second deprotection step) was not successful (Scheme 2.12). There was a lot of impurity such as excess of phenylalanine and some pyrene carboxylic acid either had not reacted or was formed during the deprotection step. Figure 2.6 shows the ^1H NMR spectrum of **73**. We tried different purification methods, for example washing with organic solvents (methanol or diethyl ether) and crystallisation with hexane or toluene, but these methods were not successful. Also the yield was low (25%). Although we tried to synthesise **73** many times by changing reaction conditions such as the equivalent of IBCF and phenylalanine ethyl ester as we did for the naphthalene derivatives, no improvement was found.



Scheme 2.12: The successful synthesis reaction of compound 72 and unsuccessful synthesis reaction of compound 74.

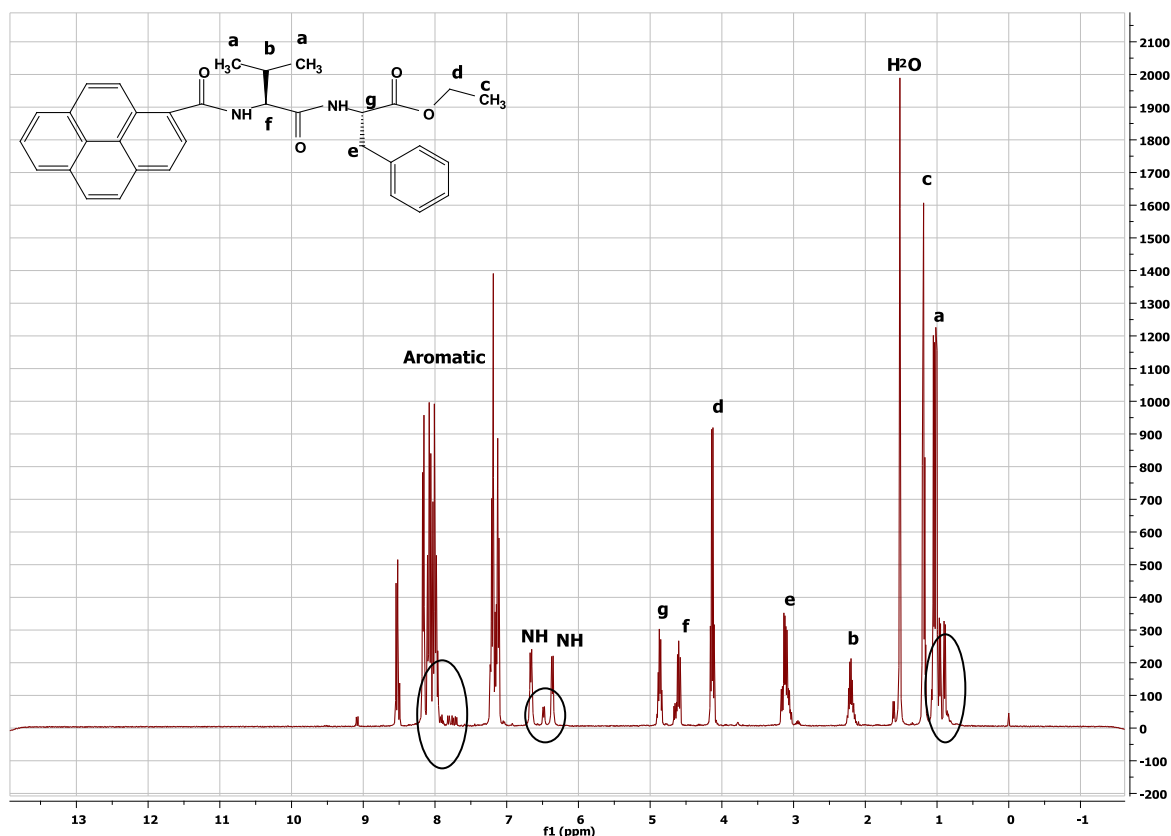
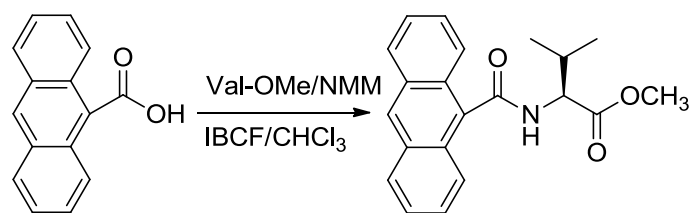


Figure 2.6: The ^1H NMR spectrum of compound 73 showing some impurities. This NMR is after purification by washing with some solvents. Circled are the impurities (excess of valine at 0.5 – 1ppm, NH at 6.5ppm and aromatic protons at 7.5 – 8ppm).

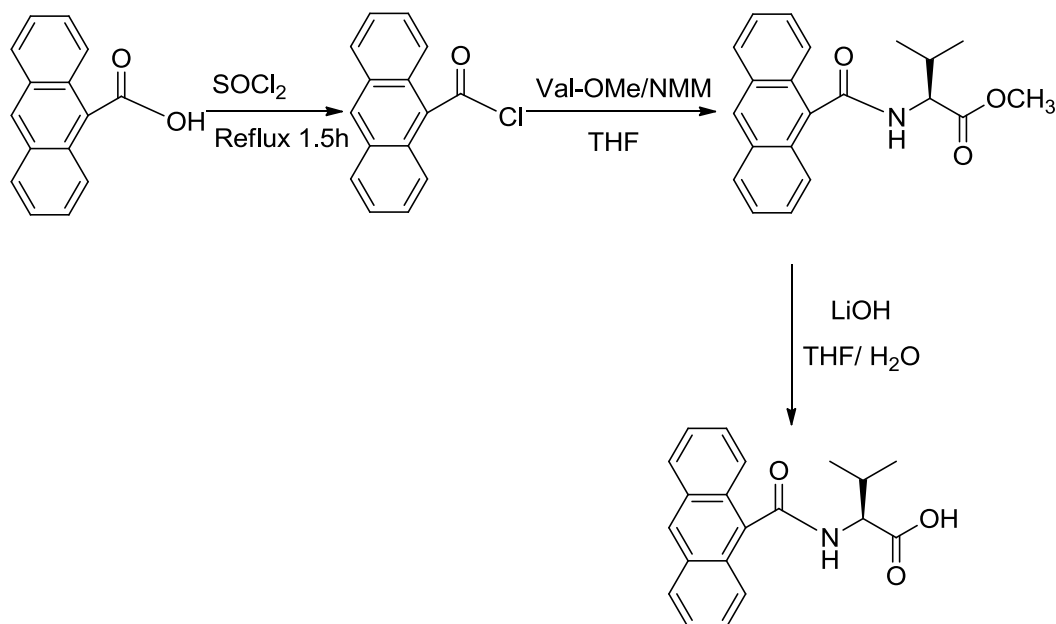
9-Anthracene dipeptide synthesis:

We attempted to synthesise 9-anthracene dipeptide derivatives using the IBCF method by coupling 9-anthracene carboxylic acid with the first amino acid. However, unlike for the pyrene and anthraquinone examples described above, the reaction was not successful (Scheme 2.13). This may be a result of the steric clash between the anthracene ring and the amino acid. To the best of our knowledge, there are no literature examples of a successful coupling reaction between 9-anthracene carboxylic acid and an amino acid. For this reason we examined another strategy. Kim *et al.* have used thionyl chloride to react with 9-anthracene carboxylic acid to prepare 9-anthracene acid chloride²⁶. We have used this reaction to convert the carboxylic acid to the acid chloride and tried to react the acid chloride with the first amino acid. The reaction was successful as determined by NMR spectroscopy.



Scheme 2.13: The unsuccessful coupling reaction between 9-anthracene and valine methyl ester hydrochloride.

After the second coupling and deprotection steps, the dipeptide derivatives were formed in good yield (60 – 70%). Scheme 2.14 shows an example of the successful reaction of 9-anthracene with thionyl chloride followed by coupling with the first amino acid. We have synthesised 6 dipeptide derivatives with different sequences: compounds **62**, **63**, **64**, **65**, **66** and **67**.



Scheme 2.14: An example of a successful reaction of anthracene dipeptide synthesis after react the anthracene carboxylic acid with thionyl chloride to give anthracene acid chloride.

We have tried to synthesise 9-anthracene dipeptide derivatives using phenylalanine in the first coupling of the reaction again because it has been reported before as a good hydrophobic amino acid likely lead to hydrogelation¹⁷. The reaction was successful for the first coupling and deprotection steps, but in both steps the yield was very low (less

than 20%) and we found that there were significant impurities such as anthracene chloride, phenylalanine ethyl ester and unknown impurities. We attempted purification of the resulting product in three steps and using different methods, by crystallization with ethanol, toluene or ethyl acetate and washing with organic solvents (diethyl ether, hexane or methanol that have different polarity). The most effective solvent was found to be methanol. We washed the product three times with methanol, but even then we could not remove all impurities. This purification method by washing with methanol was successful with 9-anthracene peptide conjugated to different amino acid such as compound **63**. Figures 2.7 and 2.8 show the ^1H NMR spectra before and after purification of **63** with methanol respectively.

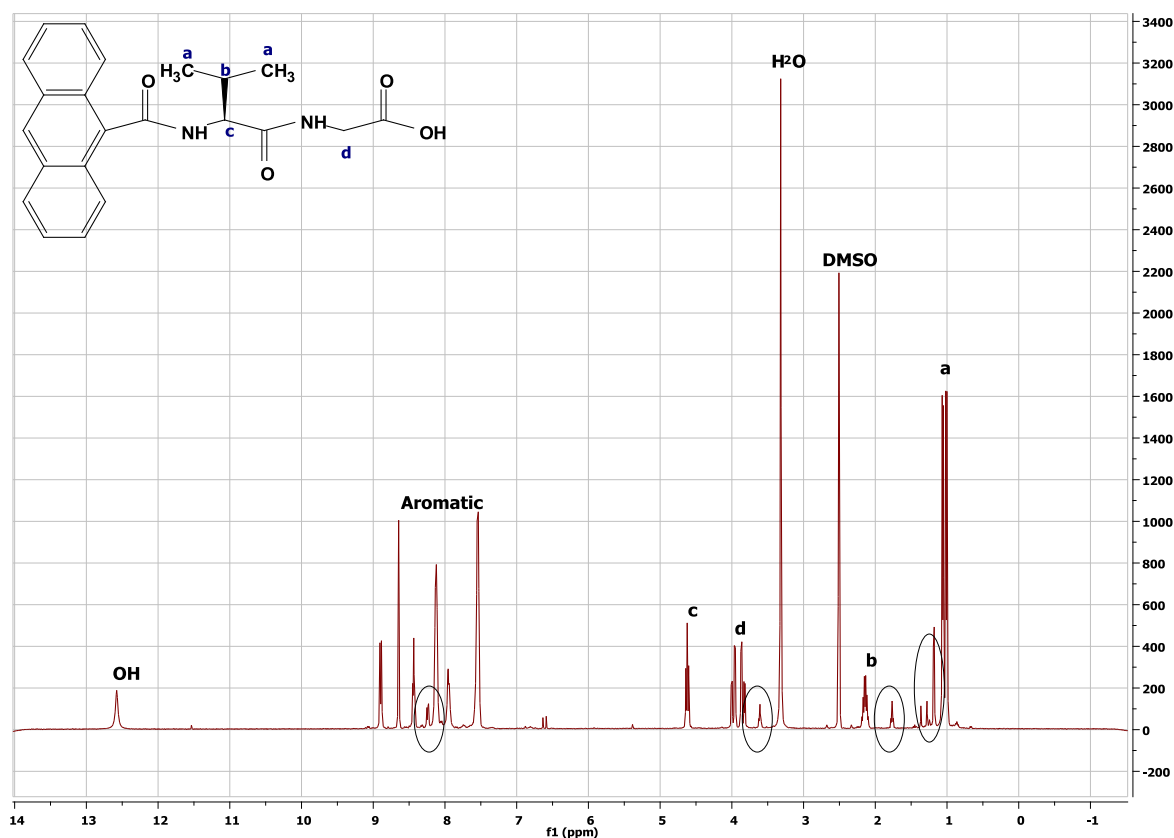


Figure 2.7: The ^1H NMR spectrum of compound **63 before purification. Circled are the impurities (excess of valine at 1 – 1.5ppm, THF at 0.7ppm and 3.6ppm and aromatic protons at approximately 8.3ppm).**

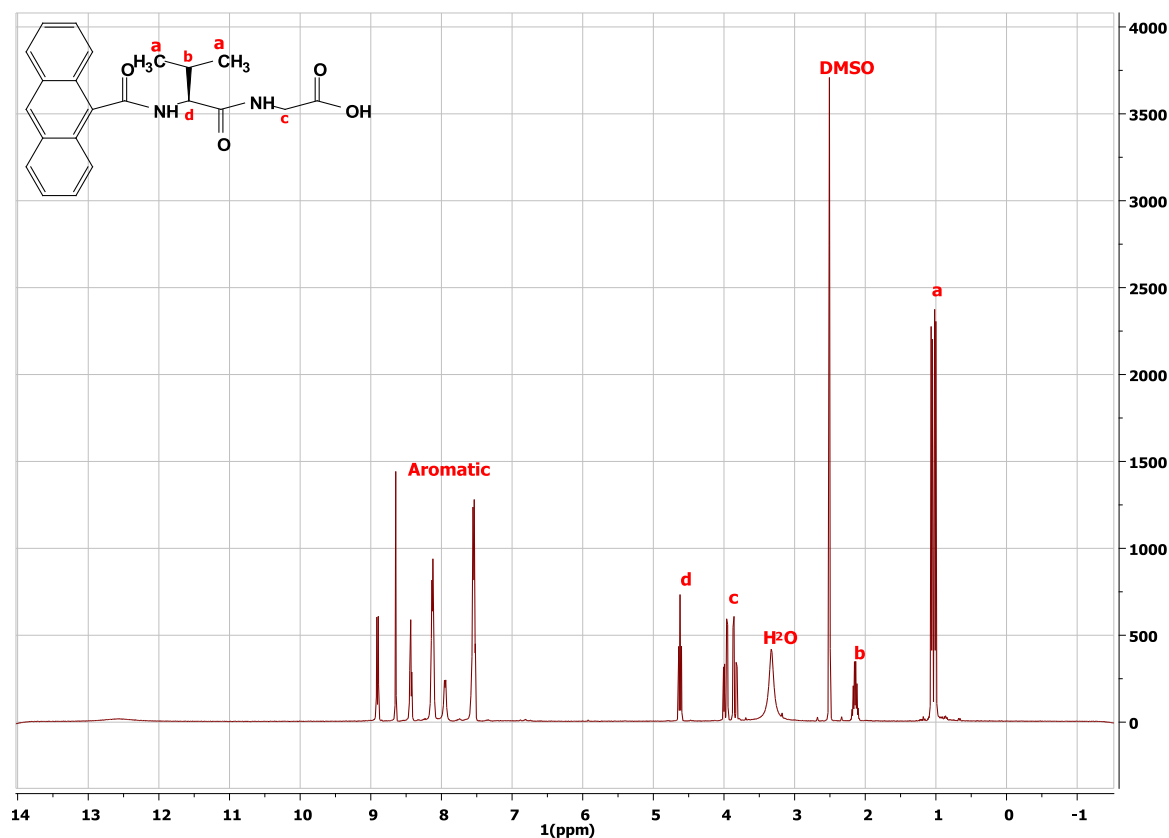
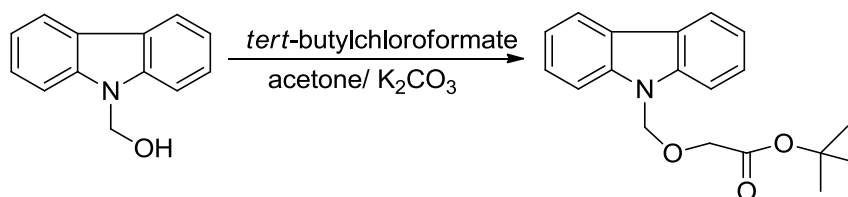


Figure 2.8: The ^1H NMR spectrum of compound 63 after purification with MeOH.

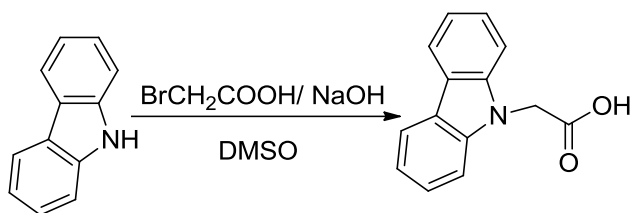
Carbazole dipeptide synthesis:

We have used two different starting materials to synthesise carbazole dipeptide derivatives, 9-carbazole methanol and carbazole. 9-Carbazole methanol was reacted with *tert*-butyl chloroacetate in acetone in the presence of K_2CO_3 at 70°C overnight (Scheme 2.15). However, this reaction was not successful. Instead, we recovered the starting material as determined by ^1H NMR and ^{13}C NMR spectroscopy. The failure of the reaction may result from the instability between N and O. We therefore tried to find another carbazole derivative from which to synthesise dipeptides.



Scheme 2.15: The unsuccessful reaction between 9-carbazole methanol and *tert*-butylchloroformate.

Following a literature procedure, carbazole was reacted with bromoacetic acid in DMSO in the presence of NaOH¹¹ to give carbazole acetic acid derivative in a good yield (83%) as shown in the Scheme 2.16. The resulting product was coupled with the first amino acid using the IBCF method^{13, 14} followed by deprotection, a second coupling and second deprotection step to give four carbazole dipeptide derivatives, **53**, **54**, **55**, and **56**.



Scheme 2.16: A successful reaction between carbazole and bromoacetic acid.

From the results we noted that the yield was good (between 67 – 80 %), where the highest yield obtained was for compound **54** (80%) and the lowest yield was for compound **56** (67%). The products contained few impurities, which were purified using washes with diethyl ether and methanol. We obtained white or off-white solid products in all steps.

2.4- Conclusion:

Peptides can be synthesised by coupling the carboxylic group of the C-terminus of one amino acid to the *N*-terminus of another. Here, we have synthesised a range of new dipeptides conjugated to various aromatic groups such as naphthalene, anthracene, anthraquinone, pyrene, carbazole and phenanthrol. We have used different methods for the first step of the reaction before the coupling step. We have synthesised 35 dipeptides conjugated to different aromatic groups. 20 dipeptides were synthesized from naphthalene ring with different substituents and different linker between the aromatic ring and amino acid sequence, 6 dipeptides from 9-anthracene ring, 4 dipeptides from 9-carbazole ring, 3 dipeptides from 9-phenanthrol, 1 dipeptide from 1-pyrene ring and 1 dipeptide from 2-anthraquinone ring. The yields were good (between 51 – 83%) for all dipeptides. We failed to synthesise some dipeptides because we had difficulty to purify them and their yields were very low (such as compounds **74** and **76**). We have synthesised a large number of dipeptides with different hydrophobicity and different aromatic group in order to study their ability to form gel and study their mechanical properties which we will discuss that in details in Chapter 3.

Table 2.17 shows the summary of the yield and the purities of all conjugated dipeptides that synthesised. From the table 2.17, we noted that the purity was excellent for almost dipeptide derivatives except compound 72; where it has more impurities which may affect its hydrogelation properties.

Dipeptide	Yield %	Purity %
10	40	90
11	60	95
12	57	97
13	55	98
14	59	94
15	60	98
16	50	99
17	48	97
18	60	99
19	57	96
20	58	95
21	49	98
22	60	99
23	56	99
24	59	98
25	60	99
30	50	96
31	54	97
32	60	99
33	60	98
40	55	89
41	59	94
42	60	95
47	50	92
53	50	97
54	66	98
55	56	98
56	67	97
62	30	90
63	34	96
64	35	99
65	33	98
66	35	97
67	35	99
72	45	85

Table 2.17: the yield and the purity of the all dipeptide synthesised.

2.5- References:

1. F. C. McKay and N. F. Albertson, *Journal of the American Chemical Society*, 1957, **79**, 4686-4690.
2. C. A. G. N. Montalbetti and V. Falque, *Tetrahedron*, 2005, **61**, 10827-10852.
3. D. J. Adams and P. D. Topham, *Soft Matter*, 2010, **6**, 3707-3721.
4. D. J. Adams and I. Young, *Journal of Polymer Science Part A: Polymer Chemistry*, 2008, **46**, 6082-6090.
5. J. C. Sheehan and G. P. Hess, *Journal of the American Chemical Society*, 1955, **77**, 1067-1068.
6. D. P. M. Löwik, L. Ayres, J. Smeenk and J. M. Hest, *Synthesis of Bio-Inspired Hybrid Polymers Using Peptide Synthesis and Protein Engineering*, Springer Berlin Heidelberg, 2006.
7. R. Vegners, I. Shestakova, I. Kalvinsh, R. M. Ezzell and P. A. Janmey, *Journal of Peptide Science*, 1995, **1**, 371-378.
8. B. Adhikari and A. Banerjee, *Chemistry – A European Journal*, 2010, **16**, 13698-13705.
9. R. B. Merrifield, *Journal of the American Chemical Society*, 1963, **85**, 2149-2154.
10. M. A. Gauthier and H.-A. Klok, *Chemical Communications*, 2008, 2591-2611.
11. Y. Zhang, H. Gu, Z. Yang and B. Xu, *Journal of the American Chemical Society*, 2003, **125**, 13680-13681.
12. D. J. Adams, M. F. Butler, W. J. Frith, M. Kirkland, L. Mullen and P. Sanderson, *Soft Matter*, 2009, **5**, 1856-1862.
13. K. U. Prasad, M. A. Iqbal and D. W. Urry, *International Journal of Peptide and Protein Research*, 1985, **25**, 408-413.
14. L. Chen, K. Morris, A. Laybourn, D. Elias, M. R. Hicks, A. Rodger, L. Serpell and D. J. Adams, *Langmuir*, 2009, **26**, 5232-5242.
15. K. U. Prasad, T. L. Trapane, D. Busath, G. Szabo and D. W. Urry, *Journal of Protein Chemistry*, 1982, **1**, 191-202.
16. D. J. Adams, L. M. Mullen, M. Berta, L. Chen and W. J. Frith, *Soft Matter*, 2010, **6**, 1971-1980.
17. J. Raeburn, G. Pont, L. Chen, Y. Cesbron, R. Levy and D. J. Adams, *Soft Matter*, 2012, **8**, 1168-1174.
18. D. J. Adams, *Macromolecular Bioscience*, 2011, **11**, 160-173.
19. Z. Yang, G. Liang, M. Ma, Y. Gao and B. Xu, *Journal of Materials Chemistry*, 2007, **17**, 850-854.
20. G. Liang, Z. Yang, R. Zhang, L. Li, Y. Fan, Y. Kuang, Y. Gao, T. Wang, W. W. Lu and B. Xu, *Langmuir*, 2009, **25**, 8419-8422.
21. Z. Yang, G. Liang and B. Xu, *Chemical Communications*, 2006, **7**, 738-740.
22. D. Wu, J. Zhou, J. Shi, X. Du and B. Xu, *Chemical Communications*, 2014, **50**, 1992-1994.
23. K. H. Scott L Jones, Pall Thordarson and Francois Ladouceur, *Journal of Physics: Condensed Matter*, 2010, **22**, 1-7.
24. J. B. Bremner, J. A. Coates, P. A. Keller, S. G. Pyne and H. M. Witchard, *Tetrahedron*, 2003, **59**, 8741-8755.
25. X. Yang, R. Lu, P. Xue, B. Li, D. Xu, T. Xu and Y. Zhao, *Langmuir*, 2008, **24**, 13730-13735.
26. J. Kim, T. Morozumi and H. Nakamura, *Tetrahedron*, 2008, **64**, 10735-10740.
27. Y.-P. Tian, X.-J. Zhang, J.-Y. Wu, H.-K. Fun, M.-H. Jiang, Z.-Q. Xu, A. Usman, S. Chantrapromma and L. K. Thompson, *New Journal of Chemistry*, 2002, **26**, 1468-1473.
28. M. O. Guler, R. C. Claussen and S. I. Stupp, *Journal of Materials Chemistry*, 2005, **15**, 4507-4512.
29. Y. Zhang, Z. Yang, F. Yuan, H. Gu, P. Gao and B. Xu, *Journal of the American Chemical Society*, 2004, **126**, 15028-15029.
30. L. Chen, S. Revel, K. Morris, L. C. Serpell and D. J. Adams, *Langmuir*, 2010, **26**, 13466-13471.

CHAPTER 3

Hydrogel Formation And Their Properties

3- Hydrogel formation and their properties

3.1- Introduction:

Supramolecular hydrogels are formed by the self-assembly of hydrogelators¹. These supramolecular hydrogels contain a network of nanofibres and water (Fig. 3.1)². Hydrogels were defined by Flory in 1974 as “a coherent colloidal system of at least two components, exhibiting mechanical properties characteristic of a solid, where both the dispersed component and the dispersion medium extend themselves continuously throughout the system”³. The amount of water in hydrogels is often more than 97%⁴. Nowadays, supramolecular hydrogels have been used in many applications such as drug delivery^{5, 6}, tissue engineering⁵⁻⁷, cell culturing⁸ and energy transfer⁹. They have also been used in chemical sensing agents¹⁰. Currently, dipeptides with suitable functional groups have a wide interest for use as hydrogelators. For example, dipeptides conjugated to aromatic group such as naphthalene or Fmoc have been used to form hydrogels¹¹.

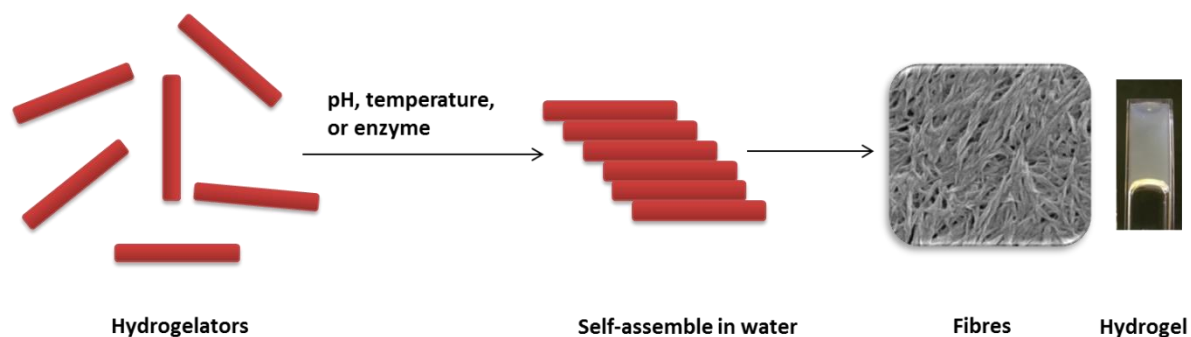


Figure 3.1: Self-assembly of hydrogelators to form hydrogel.

Hydrogel preparation:

Supramolecular hydrogels are an emerging class of soft materials which are usually formed by the self-assembly of some small organic molecules. Supramolecular dipeptide hydrogels can be prepared by several different approaches. The main method used to prepare hydrogels is to dissolve the hydrogelators into an aqueous solution and then change the temperature¹², pH¹³, or add an enzyme to start molecular self-assembly in

water, resulting in hydrogelation. For example, Zhao *et al.* have shown hydrogelation by chemical or enzymatic conversion^{14, 15} such as phosphorylation of tyrosine¹. In this Chapter, we discuss the hydrogelation of a range of dipeptides.

3.2- Experimental Section:

3.2.1- *Gel formation (Hydrogels based on dipeptide derivatives):*

Hydrogels based on naphthalene, phenanthrol, anthraquinone, pyrene and carbazole dipeptide derivatives were prepared using different methods, solvent method (DMSO: water) or the pH switch method (GdL method)¹⁶, which are described below.

1- pH switch method (GdL method):

10 mg of dipeptide derivative were suspended in deionized water (2 mL) and an equimolar amount of NaOH (0.1 M) was added to the solution to dissolve the dipeptide. The solution was stirred for about 30 minutes or until a clear solution was formed. The pH of the solution was measured to be about 10 to 12. Measured quantities of glucono- δ -lactone (GdL) were added to the solutions to control the pH to form gels. The samples were left to stand overnight to form hydrogels before measurement.

2- Solvent switch (DMSO: water):

The dipeptide derivatives (10 mg) were dissolved in 100 μ L DMSO and then deionized water (1.9 mL) was added to give a final concentration of dipeptide of 5 mg/mL. The samples were left to stand overnight.

We have used a variation on the DMSO: water method where we used water of different pH to study their effect on the hydrogelation. Previous research illustrated that hydrogels using this method cannot be formed at high pH¹⁷⁻²⁰, while other research reported that hydrogels can be formed at high pH using a different method in the presence of salts²¹.

Dipeptide derivatives (10 mg) were dissolved in 100 μ L DMSO and then made up to 2 mL with acetate buffer solutions of pH 3, 4, 5, 6 (1.9 mL), which were prepared as shown below (Table 1), were added to give a final concentration of dipeptide of 5 mg/mL. The samples were left overnight to form gels.

Buffer solution preparation:

Acetate buffer solutions of pH 3, 4, 5 and 6 were prepared by mixing 0.1 M acetic acid with 0.1 M sodium acetate in different ratios²² as shown in Table 3.1.

pH	Vol. of 0.1 M acetic acid	Vol. of 0.1 M sodium acetate
3	982.3 mL	17.7 mL
4	847.0 mL	153.0 mL
5	357.0 mL	643.0 mL
6	52.2 mL	947.8 mL

Table 3.1: The proportions of 0.1M of acetic acid and 0.1 M of sodium acetate that were used to prepare acetate buffer solutions of pH 3, 4, 5 and 6.

3.2.2- pH and pK_a measurements:

An FC200pH probe (HANNA instruments) with a 6 mm x 10 mm conical tip was used to measure pH of the dipeptide derivatives. We utilised the GdL method to prepare the samples, whilst constantly measuring the pH (at a concentration of 5mg/ mL of dipeptide). We recorded the changes in the pH every 60 s overnight at room temperature.

To determine the pK_a, water (5 mL) was added to the dipeptide derivatives (25 mg), and then an equimolar amount of NaOH (0.1 M) was added to the solutions. The pK_a was determined using titration by adding a 0.1 M HCl (10 – 40 μ L) every 5 minutes. The solution was stirred during the titration to prevent the formation of hydrogels²³.

3.2.3- Rheology studies:

Rheology is a method that was developed to characterise materials that possess both classical liquid-like and solid-like properties²⁴. Rheology can measure and link the properties of deformation of the solid state and flow of the liquid state. Rheology measures G' and G''. G' refers to the storage modulus, which is a material's ability to store energy, giving it solid-like properties. G'' refers to the loss modulus, which demonstrates the material's ability to dissipate energy, giving it liquid-like properties. G' is an order of magnitude larger than G'' when a material is considered to be a rigid hydrogel²⁵.

The rheology was studied for dipeptides that formed hydrogels using different methods for the preparation of hydrogels. 2 mL of the peptide solution as described above to prepare hydrogel was placed in a sample tube. The samples left to stand overnight to form hydrogel. After forming hydrogels, the rheology was studied using an Anton Paar Physica MCR101 rheometer. All tests were performed at room temperature. Frequency sweeps at constant strain (0.5 %) were measured between 1 rad s⁻¹ and 100 rad s⁻¹ using a cup and vane geometry. The measurements of G' and G'' with gelation were carried out at constant frequency (10 rad/s) at 25°C. Rheological data was acquired for each of the successful hydrogelators and compared.

3.2.4- *Fourier-transform Infra-Red Spectroscopy (FT-IR):*

FT-IR spectroscopy is a technique that studies the absorption of infra-red light. It measures the absorbed light by the sample to produce peaks at specific wavelength. The absorption peaks correspond to the frequencies of vibration between specific bonds in the material. This result identifies important functional groups that should be present in the product such as carbonyl groups, carboxylic acids and amide bonds²⁶. Infra-red spectra of hydrogels were collected using a TENSOR series Bruker FT-IR spectrometer, at 2cm⁻¹ resolution averaging 64 scans. Samples were prepared in D₂O, adding 1.9 mL of D₂O to dipeptide dissolved in 100 µL DMSO. Samples were left for a minimum of twelve hours to form hydrogels. The hydrogels were transferred onto the IR plates without damaging the supramolecular structure. We also prepared samples using the GdL method in D₂O, H₂O in both the wet and dry gel states as well as the as-synthesised dipeptide. The FT-IR was carried out by Lin Chen, University of Liverpool.

3.2.5- *Scanning electron microscopy (SEM):*

SEM images were recorded using a Hitachi S-4800 FE-SEM at 3 KeV. Diced silicon wafers (Agar) were used to deposit a portion of the hydrogels, prepared as described previously (the hydrogel of compound **40** was prepared in GdL method). The hydrogel was allowed to stand on the silicon wafer while it was air-dried for 1 hour. The silicon wafers were placed on aluminium stubs with an Agar adhesive tape. A 5 nm gold layer was used deposited with a sputter coating machine for 1 minute at 5 mA current. To avoid charging, a low voltage SEM was used (0.5 to 1 keV) at a 1.5 to 3 mm working

distance with the deceleration mode. The SEM was carried out by Andre Zamith Cardoso, University of Liverpool.

3.3- Result and discussion:

3.3.1- *Hydrogel and Rheology:*

3.3.1.1- Hydrogelation of naphthalene dipeptides:

The ability of naphthalene dipeptides to form hydrogels was studied previously using different methods^{2, 23, 27, 28}. Here, we have used a solvent switch method (DMSO: water) and the GdL method because they have been used previously as effective methods to form hydrogels with combinations of different aromatic groups and amino acids, naphthalene and Fmoc dipeptides^{23, 29}. Here, we attempted to use these methods with dipeptides containing different aromatic groups and different hydrophobicity to study the formation of hydrogels and compared the data with that previous collected. The first method used was a solvent method (DMSO: water). In this method, 100 μ L of DMSO was added to 10 mg of dipeptide derivative. Then, 1.9 mL H₂O was added to the solution. We have also used this method with buffered water (pH 3, 4, 5 or 6) in order to study the formation of hydrogels at different pH. The other method we used to form the gels is the GdL (glucono- δ -lactone) method¹⁶. Here, the self-catalysed hydrolysis of GdL in water lowers the pH of the solution slowly³⁰. The hydrolysis mechanism opens the lactone ring, producing gluconic acid which donates protons to the dipeptides, allowing non-covalent interactions to dominate and self-assembly to occur.

We are interested in the different methods of forming gels as these can be used to change the properties of the final material¹¹. In the solvent switch method, the self-assembly starts quickly after adding the water to the solution of peptide in DMSO and the hydrogel can form in a few minutes. This method might be useful for drug delivery application because it can be used to form an injectable hydrogel.³¹ On the other hand, in the GdL method, the formation of a hydrogel occurs after few hours. This method is useful to study and understand the self-assembly process and the mechanical properties of the hydrogel.¹⁹ The solvent switch method at different pH was used for compounds **10 – 25** (Fig. 3.2). Some dipeptides formed hydrogels and others did not using the solvent switch method with different acetate buffers. The results of these methods are

Sample name	pH 3		pH 4		pH 5		pH 6	
	G' (Pa)	G'' (Pa)	G' (Pa)	G'' (Pa)	G' (Pa)	G'' (Pa)	G' (Pa)	G'' (Pa)
Compound (11)	-	-	-	-	-	-	-	-
Compound (10)	-	-	-	-	-	-	-	-
Compound (12)	22100	5100	14200	3000	-	-	-	-
Compound (13)	4000	200	2000	100	3000	300	3100	400
Compound (14)	-	-	-	-	-	-	20000	4000
Compound (15)	6200	600	6000	500	-	-	-	-
Compound (16)	12000	3000	24000	7300	20000	4000	6000	600
Compound (17)	21000	00	2000	3000	14000	2000	15000	3000

Table 3.2: The G' and G'' using pH switch method at pH 3, 4, 5, 6 for 2-naphthol and 6-bromo-naphthol derivatives. (-) refers to dipeptides that did not form gels. G' and G'' were measured using frequency sweep at 10 rad/s.

Table 3.3 shows the results of the formation of the hydrogels using the solvent switch and GdL methods. It can be clearly seen that eleven dipeptides out of nineteen formed hydrogels using GdL method, while nine dipeptides formed hydrogels using the solvent switch method. In the GdL method, the pH was measured (before adding GdL) to be between 10 and 12 for the solution of dipeptide derivatives. After adding GdL and forming hydrogels, the pH was measured to be between 3 and 4. The pH drop allows the formation of gels¹⁹. Other research reported that hydrogels can be formed at high pH using a different method (adding calcium salts)²¹.

Table 3.3 also shows that some dipeptides formed transparent gels and others formed turbid gels. The factors that cause the turbidity could be the molecular structure of the dipeptides. For example, dipeptides that formed turbid hydrogels have high molecular structure, while dipeptides that formed transparent gels have low molecular structure (Fig. 3.3). This may due to the aggregation of the peptides that have high molecular structure into larger structures, which lead to increase in light scattering, leading to form a turbid hydrogel. Also, the turbidity can be affected by the concentration of the dipeptide. We noted that when we decrease the concentration of the hydrogelators, the turbidity decreased, presumably due to a decrease in the aggregation of the fibres.



Figure 3.3: Examples of hydrogel images that formed a turbid and transparent gel. Compound 17 (Left) formed a turbid gel and compound 12 (Right) formed a transparent using the GdL method. It shows the effect of the molecular structure on the turbidity.

Furthermore, it can be seen that any change in the peptide structure such as substitution position or order of amino acid sequence can affect and change the ability of the molecules to form a hydrogel. For instance, if we compare between dipeptides that have similar amino acids and different numbers or different substitution positions of a bromine atom, we note that they have different gelation results. For example, compound **14**, **18** and **22**, where compound **14** (bromine at position 6 on the naphthalene ring) did not form hydrogel, while compound **18** (where there are bromines at position 1 and 6) and **22** (the bromine at position 1) formed a turbid hydrogels using the solvent switch method. As a result, it can be clearly seen that a small change in the peptide structure can affect and change the formation of the hydrogel. Also, as described above, we noted that the hydrophobicity did not correlate to hydrogel formation. For instance, compound **12** formed a turbid hydrogel, whereas compound **20** and **25** which are more hydrophobic than **12** did not form hydrogel using the solvent switch method. These results agreed with other examples that discussed in the previous research²⁹. Furthermore, Chen's group¹⁹ have prepared similar naphthalene dipeptide hydrogel with different amino acid sequence using the GdL method. For example, their results showed that 2-napFVOH and 6Br-napFVOH formed turbid hydrogels, which are similar to our results that showed compounds **13** and **17** which they have similar structure and different amino acid sequence formed also turbid hydrogels. Also, precipitate was formed from compound **11**, while a crystal was formed from Chen's compound which has different amino acid sequence (2-napAV)¹⁹.

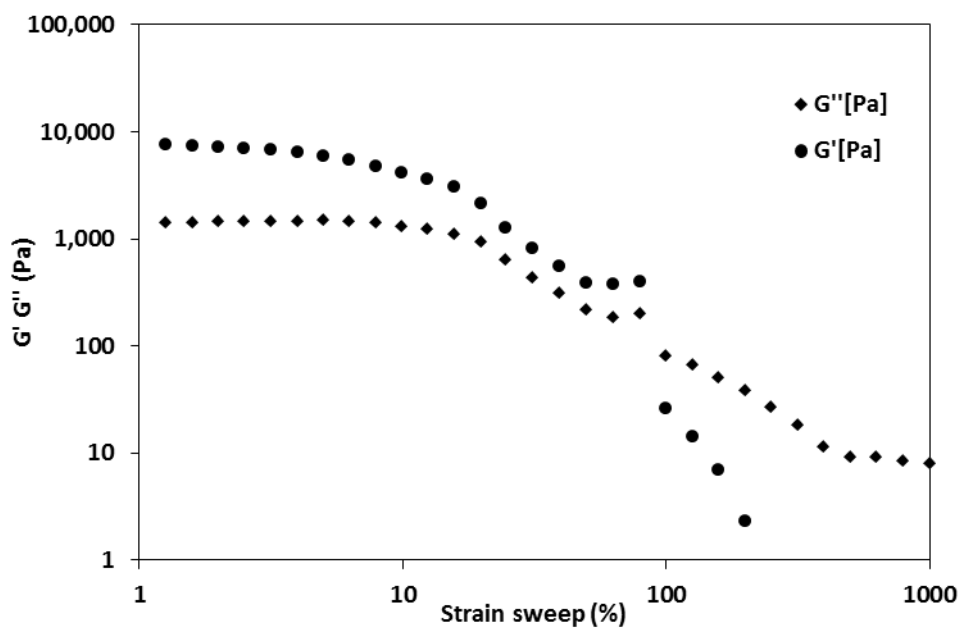
It is clear that all the dipeptides that form gels with the solvent switch method also form gels with the GdL method. However, dipeptides **15**, **25** and **30** all only form gels with the GdL method. It is still not clear why some peptides formed gel using only the GdL method. However, we expect that the method of preparing the hydrogel can modify the properties of the hydrogel formed¹¹.

Dipeptide	Gel formation DMSO: H ₂ O		Gel formation GdL		Molecular weight	LogP
Compound 10	-	Precipitate	-	Precipitate	400.36	1.390
Compound 11	-	Precipitate	-	Precipitate	372.31	0.619
Compound 12	√	Turbid Gel	√	Transparent Gel	358.46	0.832
Compound 13	√	Turbid Gel	√	Turbid Gel	448.45	2.080
Compound 14	-	Precipitate	-	Transparent Gel	479.36	2.140
Compound 15	-	Precipitate	√	Turbid Gel	451.31	1.360
Compound 16	√	Transparent Gel	√	Transparent Gel	437.46	1.570
Compound 17	√	Turbid Gel	√	Turbid Gel	527.45	2.820
Compound 18	√	Turbid Gel	√	Turbid Gel	558.20	2.920
Compound 19	√	Turbid Gel	√	Turbid Gel	530.21	2.141
Compound 20	-	Precipitate like gel	√	Turbid Gel	516.18	2.354
Compound 21	√	Turbid Gel	√	Turbid Gel	606.30	3.602
Compound 22	√	Turbid Gel	√	Turbid Gel	479.36	1.520
Compound 23	√	Turbid Gel	√	Turbid Gel	451.31	1.400
Compound 24	√	Transparent Gel	√	Transparent Gel	437.46	1.620
Compound 25	-	Precipitate	√	Transparent Gel	527.45	2.870
Compound 30	-	Precipitate	√	Turbid Gel	384.47	1.490
Compound 31	-	Precipitate	-	Precipitate	356.44	0.717
Compound 32	√	Transparent Gel	-	Gel precipitate	342.39	0.932
Compound 33	√	Turbid Gel	√	Transparent Gel	432.51	2.178

Table 3.3: Dipeptides that formed gels and did not form gels using GdL method and DMSO: water method. (-) means did not form gels, (√) means formed gels. This is a qualitative observation.

We have also studied the rheology of the gels that are formed using frequency sweeps and the strain sweeps to demonstrate the mechanical properties of the formation of the hydrogel at different conditions. Figure 3.4 (a, b) shows example data for **16**. The hydrogels were prepared using the GdL method at concentration of 5 mg/mL of the dipeptide. Figure 3.4 (a) shows the strain sweep. The data shows that the gel still has solid-like properties until a strain of about 5% and the deformation of the gel starts after this point. Here, we can see a fast drop of G' and this indicates that after this point, the hydrogel has more liquid-like properties than solid-like properties, indicating breakdown of the structure of the hydrogel. A crossover point at a strain of about 5% is typical for this kind of hydrogel²³. Figure 3 (b) shows the frequency sweep of the same hydrogel. From Figure 3.4 (b), it can be seen that the hydrogel has strong solid-like properties, with a G' of over 10^4 Pa. G'' was approximately 10^3 Pa. As expected for this kind of hydrogel^{18, 23, 27, 32}, both G' and G'' were relatively independent of frequency. This data shows that compound **16** is a good hydrogelator. Furthermore, we noted that the G' is different in the strain and frequency sweep, although the data for the same hydrogelator. These differences might be simply because we have prepared two different samples of the same hydrogelator, one to measure the strain sweep and the other to measure the frequency sweep. This may lead to errors in the preparation.

(a)



(b)

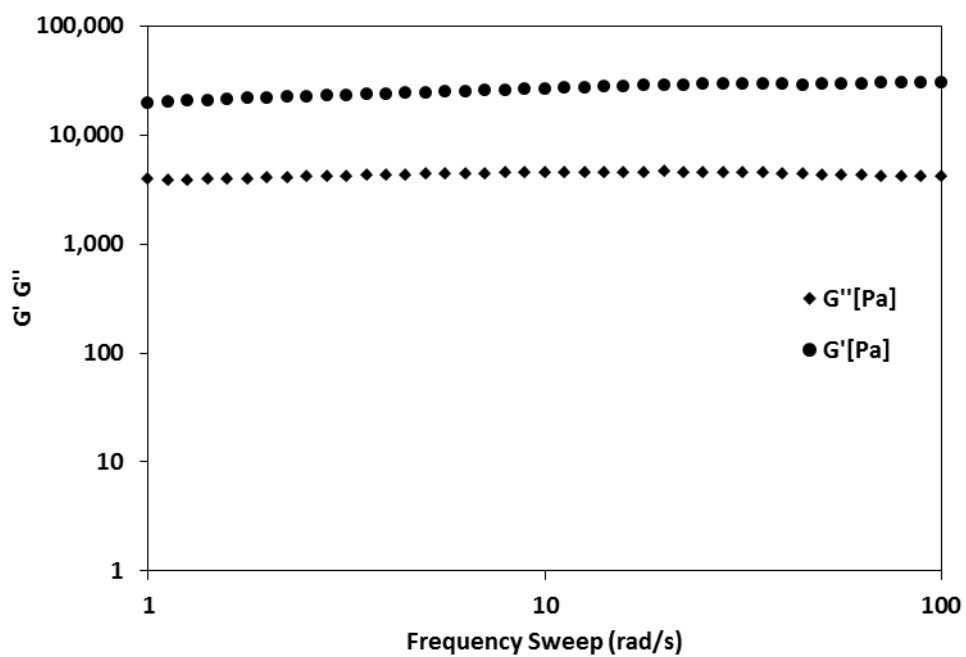


Figure 3.4: An example of studying the mechanical properties of compound 16. (a) strain sweep (b) Frequency sweep.

Table 3.4 shows the rheology studies for the dipeptides that formed hydrogels (Table 3.4 reports the G' and G'' values). G' and G'' for compound **20** were low, although a gel was still formed.

In some cases, the rheology was very different for the gels prepared by the different methods. For example, compound **17** formed a turbid gel with both methods, but has higher G' when the gel is formed by the GdL method than by the solvent switch method (27 kPa and 14 kPa respectively). However, the G' of the gel formed from **12** was 26 kPa using the GdL method and 25 kPa using the solvent switch method, showing that the GdL method does not always result in stronger gels. Figure 3.5 shows examples of some dipeptides that formed gels using the GdL method and the solvent switch method where transparent gels are formed. Transparency will be a key parameter for uses in energy transfer (see Chapter 4).

Peptides	GdL		DMSO	
	G' (Pa)	G'' (Pa)	G' (Pa)	G'' (Pa)
Compound 12	26000	6000	25000	6000
Compound 13	6000	300	6000	1000
Compound 16	23000	4000	16000	3000
Compound 17	27000	3000	14000	2000
Compound 18	4000	400	5000	4000
Compound 19	6000	800	1400	200
Compound 20	2000	300	20	15
Compound 21	3000	400	92000	11000
Compound 22	3000	200	8000	400
Compound 23	300	40	1000	130
Compound 24	7000	1000	12000	2000
Compound 25	15000	3000	-	-
Compound 32	3000	300	1000	200
Compound 33	60000	7000	5000	500

Table 3.4: G' and G'' of the dipeptides that have formed hydrogels using GdL and DMSO methods.

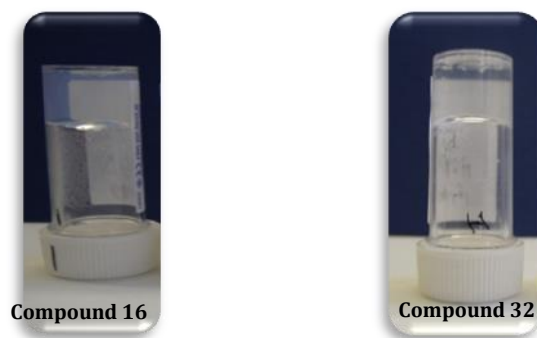
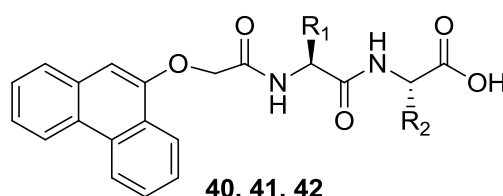


Figure 3.5: (left): Hydrogel image of compound 16 using the GdL method. (Right): hydrogel image of compound 32 using the solvent switch method.

3.3.1.2- Hydrogelation of phenanthrol dipeptides:

Hydrogels based on phenanthrol dipeptide derivatives were prepared using the different strategies as shown in Figure 3.6. Table 3.5 shows hydrogelation results of phenanthrol dipeptide derivatives. From the results, it can be seen that compound **41** formed a turbid gel using GdL method and a gel mixed with water was formed using DMSO: water method. Compound **42** formed turbid gels using both methods, whereas compound **40** formed transparent gels by both methods. These results agreed with the observations for the naphthalene dipeptides (above) that the more hydrophobic peptides may lead to more turbid hydrogel. Table 3.6 shows the rheology results (G' and G'') of phenanthrol hydrogels formed by both methods. From Table 6, we note that the strongest gel formed by both methods was compound **40**. Also, we can see that compound **41** formed a hydrogel using the GdL method, whereas it did not form a hydrogel using the solvent switch method. This agreed with previous work which illustrated that the way of preparing gel is not correlated to the formation of the gel³³.



- 40:** $R_1=CH(CH_3)_2$, $R_2=CH(CH_3)_2$
41: $R_1=CH_2Ph$, $R_2=CH_2Ph$
42: $R_1=CH(CH_3)_2$, $R_2=CH_2Ph$

Figure 3.6: The general structure of phenanthrol dipeptides

Dipeptide	Gel formation DMSO: H ₂ O	Gel formation GdL
Compound 40	Transparent Hydrogel	Transparent Hydrogel
Compound 41	Turbid hydrogel	Mix gel with water
Compound 42	Turbid hydrogel	Turbid hydrogel

Table 3.5: Phenanthrol hydrogel form in GdL and in DMSO: water.

Dipeptide	GdL		DMSO	
	G' (Pa)	G'' (Pa)	G' (Pa)	G'' (Pa)
Compound 40	24000	3000	2000	300
Compound 41	700	60	-	-
Compound 42	2000	200	2000	90

Table 3.6: G' and G'' of phenanthrol hydrogels in GdL and DMSO: Water method. (-) means did not form hydrogel and the rheology did not measure.

For all of these gels, the structure is thought to be a result of the formation of fibres by the self-assembly of the dipeptides. To show that this is also the case here, we examined the hydrogel of compound **40** using scanning electron microscopy (SEM) of the hydrogel of compound **40** (prepared using the GdL method at peptide concentration of 5 mg/mL). We have chosen this hydrogel because the dipeptides hydrogels based phenanthrol ring has not been studied before and chosen compound **40** because we examined the other phenanthrol hydrogel and they did not form a good fibres comparing to compound **40**. The hydrogel was allowed to stand on the silicon wafer while it was air-dried for 1 hour. Figure 3.7 shows an example SEM image indicating that this hydrogelator formed fibres. Further work might be concentrated on other conjugated dipeptide hydrogels and also may use Cryo-SEM for different conjugated dipeptide hydrogels to ensure that the samples are completely dried by using the freeze-dry treatment.

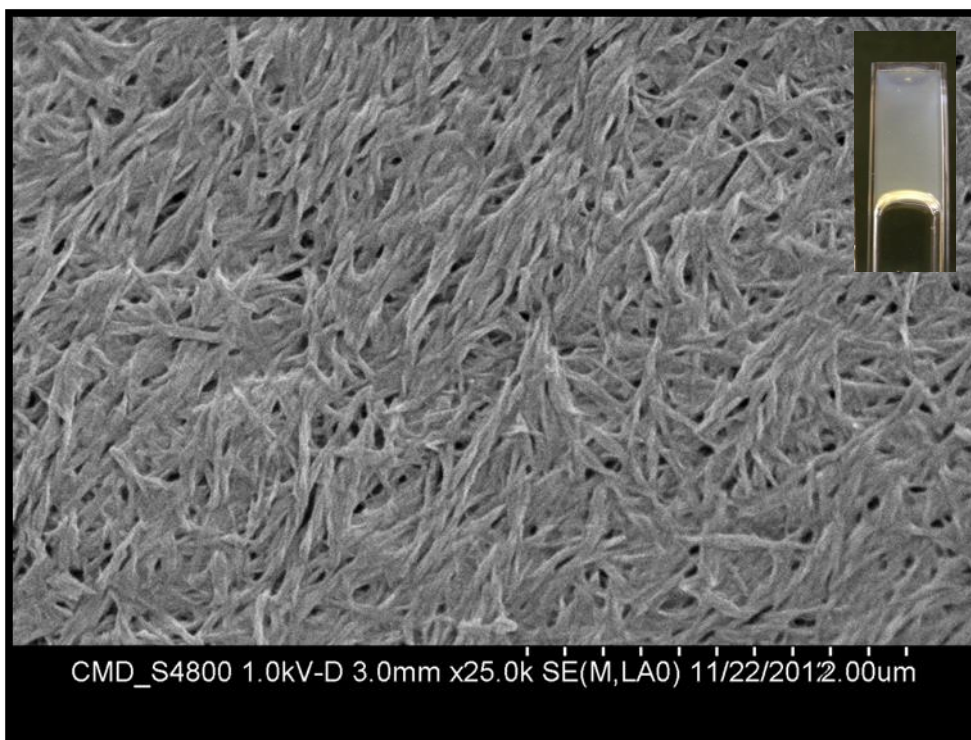


Figure 3.7: SEM image of compound 40 showing the fibre form after the gelation. Inset is the hydrogel image of the peptide in GdL at concentration of 5mg/ mL.

3.3.1.3- Hydrogelation of anthraquinone dipeptides:

Hydrogels were also formed from anthraquinone dipeptide derivatives with the same two methods. The general structure of the dipeptide is shown in Figure 3.8. Table 3.7 shows the gel formation and the rheology results of compound 47. From the results, we note that G' of the gel formed from compound 47 prepared using GdL was higher than the G' of the gel formed by the solvent switch method. Overall, looking at the naphthalene and phenanthrol dipeptide hydrogel data, it appears that the GdL method can result in stronger gels than the solvent switch method. However, the hydrogels formed from 47 by both methods were not very strong, having a lower G' and G'' comparing to the other functionalised dipeptides above.

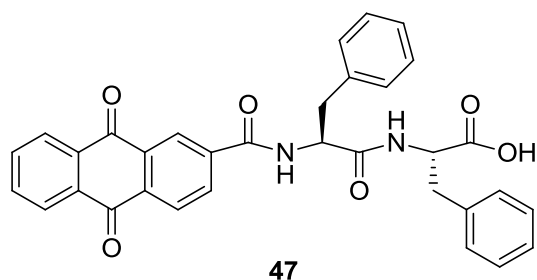


Figure 3.8: The chemical structure of compound 47.

Dipeptide	Gel formation		GdL		DMSO	
	GdL	DMSO	G' (Pa)	G'' (Pa)	G' (Pa)	G'' (Pa)
Compound 47	Turbid Gel	Turbid Gel	6000	800	2000	100

Table 3.7: Hydrogel formation and rheology results of compound 47.

3.3.1.4- Hydrogelation of carbazole dipeptides:

Hydrogels based on carbazole dipeptide derivatives were prepared using the two different strategies. The general structure of the dipeptides is shown in Figure 3.9. Table 3.8 shows the hydrogel formation results of the carbazole derivatives and the G' and G'' for the resulting gels. From the results, we can see that none of the carbazole derivatives formed gels using the solvent switch method, except compound **55** which formed a turbid gel. Using the GdL method, all derivatives formed gels. Here, we noted that changing the method of preparing the hydrogel affected the formation of the hydrogel result. This result agreed with other research that reported changing the solvent and the way of preparing the hydrogel can lead to gel or non-gel formed and also can change their mechanical properties¹¹. This might be due to changing the condition of the preparing the hydrogel and changing the kinetic of the hydrogel formation. Compounds **51a** and **53** formed transparent gels, whereas **54**, **55** and **56** formed turbid gels. The turbidity was lower when we decreased the concentration from 5 mg/mL to 2 mg/mL (compound **54**) and to 0.5 mg/mL (compound **55**). The rheology results show that compound **53** formed the strongest gel (G' of 44 kPa) while compound **51a** formed the weakest gel (G' of 6000 Pa). Also, it can be clearly seen that when we decreased the concentration, the strength of the hydrogel decreased. For example, the G' of compound

54 that formed a turbid gel at 5 mg/mL was 4000 Pa, which decreased to 500 Pa when we decreased the concentration to 2 mg/mL to form a transparent gel. A dependence of G' on the concentration is expected³¹. As the concentration is lowered, we would expect less fibres to be formed and so a weaker network. Similarly, the turbidity of the gel formed using compound **55** was decreased when we decreased the concentration from 5 mg/mL to 0.5 mg/mL. As a result, it can be seen that decreasing the concentration leads to the formation of a weaker, but more transparent hydrogel. Figure 3.10 shows an example of hydrogel formation using carbazole derivatives and both methods (compound **53** and **54** using the GdL method and the solvent switch method).

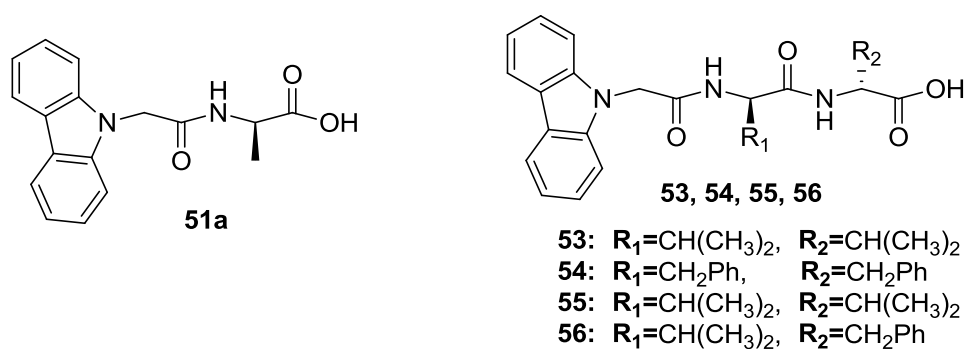


Figure 3.9: The general structure of carbazole dipeptides.

Dipeptide	Gel formation DMSO: H ₂ O	Gel formation GdL	G' (GdL) (Pa)	G'' (GdL) (Pa)
Compound 51a	Mix gel with water	Transparent Gel	6000	700
Compound 53	Mix gel with water	Transparent Gel	44000	6000
Compound 54	Mix gel with water	Turbid at 5mg/mL	3700	400
		Transparent at 2mg/mL	500	30
Compound 55	Turbid Gel	Turbid Gel at 5mg/mL	41000	6000
Compound 56	Precipitate	Turbid Gel	26000	4000

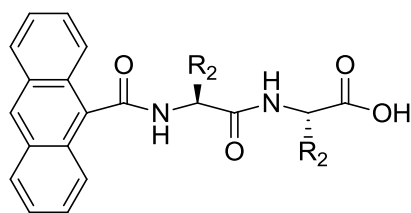
Table 3.8: The hydrogel formation by GdL and by the solvent switch method and the rheology results.



Figure 3.10: An example of hydrogel formation of carbazole derivatives in both methods.

3.3.1.5- Hydrogelation of anthracene dipeptides:

Hydrogels based on anthracene dipeptide derivatives (Fig. 3.11) were prepared using the two different strategies. Hence, we attempted to prepare 12 hydrogels from 6 dipeptides functionalised with an anthracene ring. However, none of the anthracene derivatives were able to form a gel using either method. Instead, they formed precipitates or turbid solutions (i.e. a soft precipitate like powder that suspended in the solution). Figure 3.12 shows examples of attempting to prepare hydrogels using both methods at a dipeptide concentration of 5 mg/mL, that lead to precipitate or turbid solutions. Table 3.9 summarises the hydrogelation results of anthracene dipeptide derivatives. The reason for this lack of gelation may be the lack of flexibility between the anthracene ring and the amino acid that prevent forming non-covalent interaction such as hydrogen bonding leading to non formation of fibres and non-hydrogel. Other work has synthesised dipeptide-based anthracenes⁹, but with a different linker between the anthracene ring and the amino acid sequences and this peptide formed a hydrogel (Fig. 3.13). From Figures 3.11 and 3.13, we can see that dipeptides 66 and 75 have the same aromatic group and the same amino acid sequences, but different linker. As reported previously¹⁹, the linker can affect the formation of the hydrogel. We noted that compound 75 has OCH₂ linker between the aromatic group and the amino acid sequence which leads to flexibility between the aromatic group and the amino acid sequence, hence lead to the formation of the hydrogel. In contrast, compound 66 does not have linker, therefore it leads to non-gel formed due to the lack of flexibility.



62, 63, 64, 65, 66, 67

62: $R_1 = \text{CH}(\text{CH}_3)_2$, $R_2 = \text{CH}(\text{CH}_3)_2$
63: $R_1 = \text{CH}(\text{CH}_3)_2$, $R_2 = \text{H}$
64: $R_1 = \text{CH}(\text{CH}_3)_2$, $R_2 = \text{CH}_2\text{Ph}$
65: $R_1 = \text{CH}_3$, $R_2 = \text{CH}_3$
66: $R_1 = \text{CH}_3$, $R_2 = \text{CH}(\text{CH}_3)_2$
67: $R_1 = \text{H}$, $R_2 = \text{CH}_2\text{Ph}$

Figure 3.11: The general structure of anthracene dipeptides.

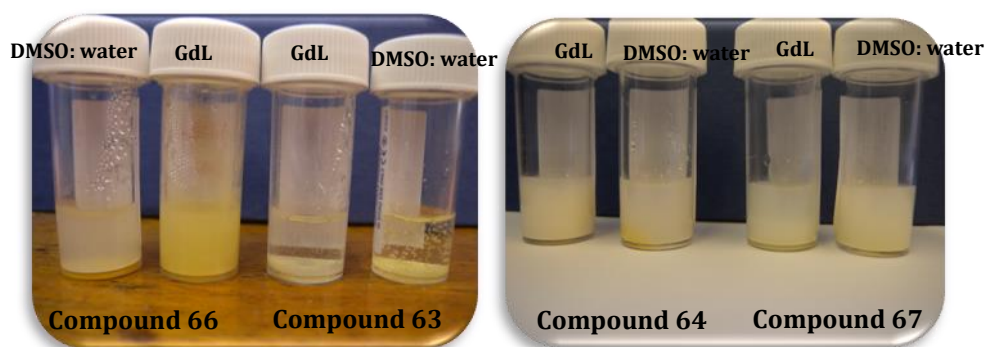
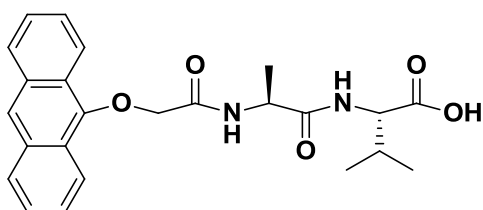


Figure 3.12: Examples of non-hydrogel images of anthracene derivatives using the GdL and solvent switch methods.



Compound 75

Figure 3.13: The general structure of anthracene dipeptide that formed hydrogel¹⁹.

Dipeptide	Gel formation GdL	Gel formation Water: DMSO
Compound 62	Precipitate	Precipitate
Compound 63	Precipitate	Precipitate
Compound 64	Turbid solution	Turbid solution
Compound 65	Precipitate	Precipitate
Compound 66	Turbid solution	Turbid solution
Compound 67	Turbid solution	Turbid solution

Table 3.9: hydrogelation results based on anthracene derivatives using the GdL and solvent switch methods.

We hypothesised that the lack of gel formation might be due to either the final pH or the kinetics of gel formation. Hence, we have attempted to prepare hydrogels from the anthracene dipeptides by changing the concentration of the GdL. However, no gels were formed. For example, compound **66** formed turbid solutions and **63** formed precipitates at all GdL concentrations (Fig. 3.14).

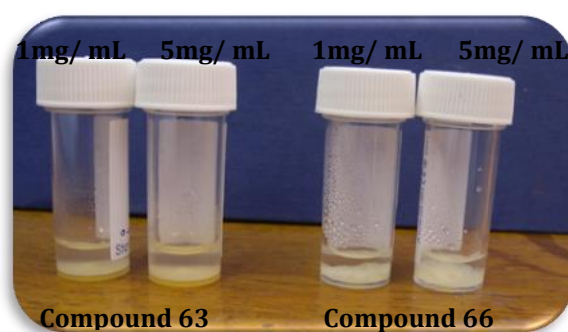


Figure 3.14: An example of precipitate solutions of compound 63 with different concentrations of GdL.

We have tried to study the formation of crystals from the anthracene dipeptides because the crystal structure may provide insights of the stability of the interactions as the gel can form fibres²⁰. We attempted to recrystallise anthracene dipeptides **63**, **66**, **64** and **67** from different solvents such as methanol, ethyl acetate or diethyl ether in order to study the crystal structure. Unfortunately, no crystals were formed. Instead, they formed precipitates (for example, **63** or **64**, Fig. 3.15).

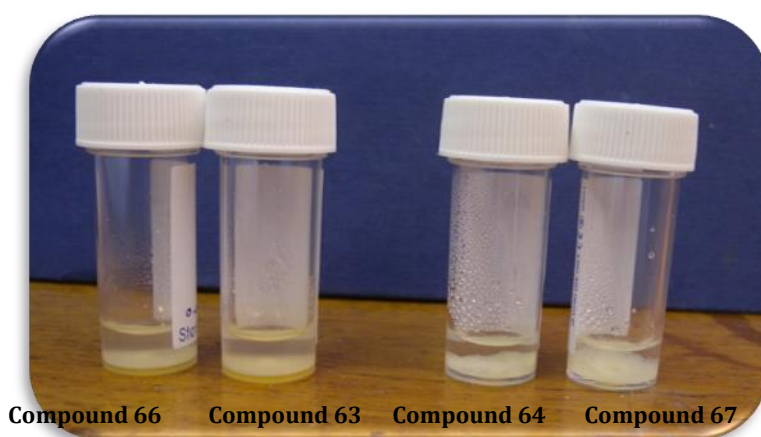


Figure 3.15: Examples of recrystallisation images of anthracene derivatives with methanol.

3.3.1.6- Hydrogelation of pyrene dipeptides:

Hydrogels based on pyrene dipeptide derivatives were previously prepared using different approaches¹⁸. Zhang *et al.*³⁴ illustrated an increase of the mechanical properties of hydrogels that formed via self-assembly in water by using a method based on molecular recognition. A weak hydrogel (pyrene-D-Ala-D-Ala) was formed with a storage modulus (G') of 120 Pa. The strength of pyrene hydrogel increased when vancomycin was added to a G' of 160000 Pa. Furthermore, when the L-Ala-L-Ala was used, it formed hydrogel with ten times lower in G' over the gelator alone. Here, we have prepared pyrene dipeptides with a different linker compared to Zhang *et al.* The general structure of compound **72** is shown in Figure 3.16. We prepared hydrogels from compound **72** with different concentration of dipeptides using the GdL method and the solvent switch method at different ratios of DMSO: water. This was to study the turbidity of the resulting gels, because one of the aims of this project was to study the fluorescence in order to study energy transfer between dipeptides linked to different aromatic groups which are discussed in Chapter 4. Compound **72** formed turbid gels at a concentration of 5 mg/mL. However, at lower concentrations, a transparent hydrogel was formed. Similarly, we attempted to change the ratio of DMSO to water for the same reason. Table 3.10 shows the results for the GdL with different concentrations of dipeptides (5 mg/ mL to 0.5 mg/ mL) and the solvent switch method at different ratio of DMSO: Water (0.1:1.9 to 0.05:1.95) with a constant concentration of dipeptide. From the results, we can see that the turbidity increases when we increase the concentration of

dipeptide or when we increase the ratio of DMSO to water. Figure 3.17 (a) shows photographs of the hydrogel formed by compound **72** at different concentrations of dipeptide to study the turbidity. Figure 3.17 (b) shows the G' of compound **72** at a concentration of 5 mg/mL and 0.5 mg/mL. It can be clearly seen that as expected the G' of the gel formed at a concentration of 5 mg/mL is higher than that of the gel formed at a concentration of 0.5 mg/mL. Table 3.11 shows the rheology results of compound **72** using both methods and different concentrations of dipeptides in GdL (5 mg/mL to 0.5 mg/mL) and different ratio of DMSO: Water (0.1:1.9 to 0.05:1.95). From the results, we can see here compound **72** formed stronger turbid hydrogel at high concentration of dipeptide using the GdL method (at 5 mg/mL, the G' is 25000 Pa) than using the solvent switch method at high ratio of DMSO: Water (at a ratio of 0.1:1.9, the G' is 14000 Pa). Also, by decreasing the concentration or the ratio of DMSO, the turbidity decreased and a weaker gel was formed.

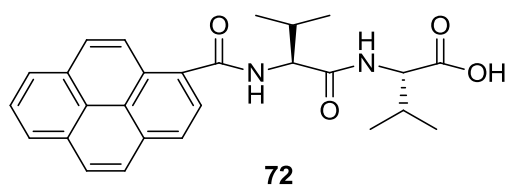


Figure 3.16: The chemical structure of compound 72.

Compound 72	Gel formation
DMSO: water (0.1:1.9)	Turbid Gel
DMSO: water (0.05:1.95)	Transparent Gel
DMSO: water (0.03:1.97)	Transparent Gel
GdL /5 mg/mL	Turbid Gel
GdL /2 mg/mL	Turbid Gel
GdL /1 mg/mL	Turbid Gel
GdL /0.5 mg/mL	Transparent Gel

Table 3.10: Hydrogel form of compound 72 using the GdL and solvent switch methods with different concentration.

(a)



(b)

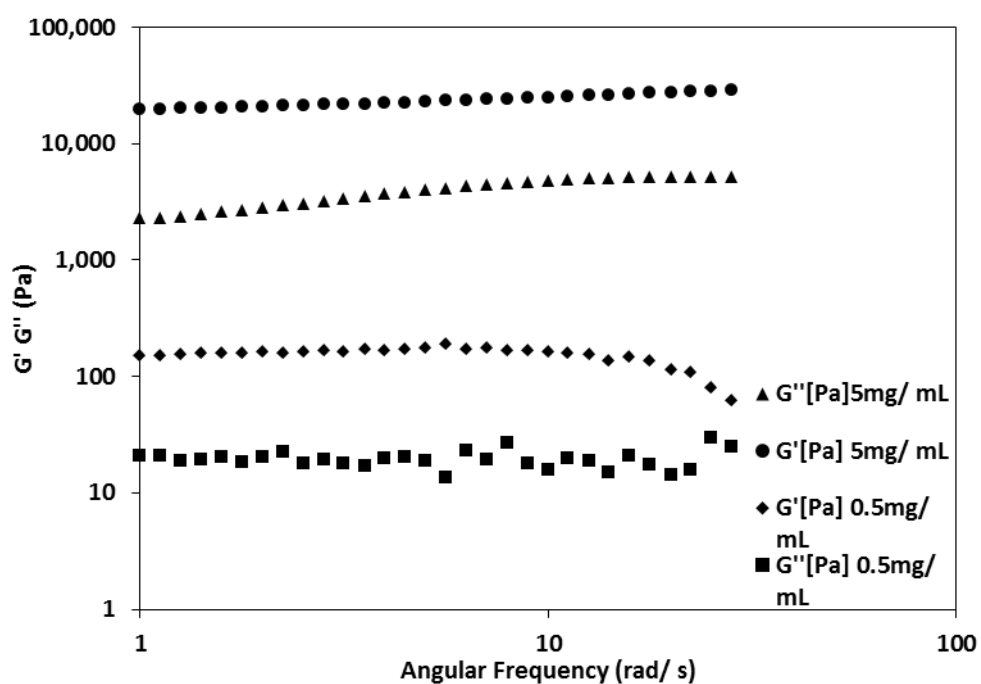


Figure 3.17: (a) Hydrogel images of compound 72 from left to right using the solvent switch method (0.1:1.9), and using the GdL method with different concentrations of dipeptide (5 mg/ mL to 0.5 mg/ mL). (b) The rheological data for gels formed from compound 72 at concentration of 5 mg/ mL and 0.5 mg/ mL.

Compound 72	G' (Pa)	G'' (Pa)
DMSO: water (0.1:1.9)	14000	2600
DMSO: water (0.03: 1.97)	20	20
DMSO: water (0.05: 1.95)	10	3
GdL (5 mg/mL)	25000	5000
GdL (2 mg/mL)	4000	600
GdL (1 mg/mL)	600	60
GdL (0.5 mg/mL)	200	20

Table 3.11: The rheology results of compound 72 in both methods with different concentrations of dipeptides and different ratio of DMSO: water.

In the cases of the other dipeptides examined, the gels were stable with time. However, we observed that the pyrene dipeptide gels were not stable. We have measured the rheology with time for compound **72** at a concentration of 5 mg/mL as shown in the Figure 3.18. The data shows that the hydrogelation process started after 45 minutes, where G' starts to dominate over G'' . After 1 hour, the hydrogel has formed and there is a plateau in both the G' and G'' . However, it can be clearly seen that the hydrogel became unstable after about 2 hours where we can see the instability of G' and G'' during the hydrogelation process. After about 8 hours, the deformation has occurred as a result of the instability of the hydrogel, leading to a decrease in the solid like properties and deformation of the hydrogel. As a result, this hydrogel has unusual mechanical properties for its hydrogelation process over the time, as it shows instability after a certain time.

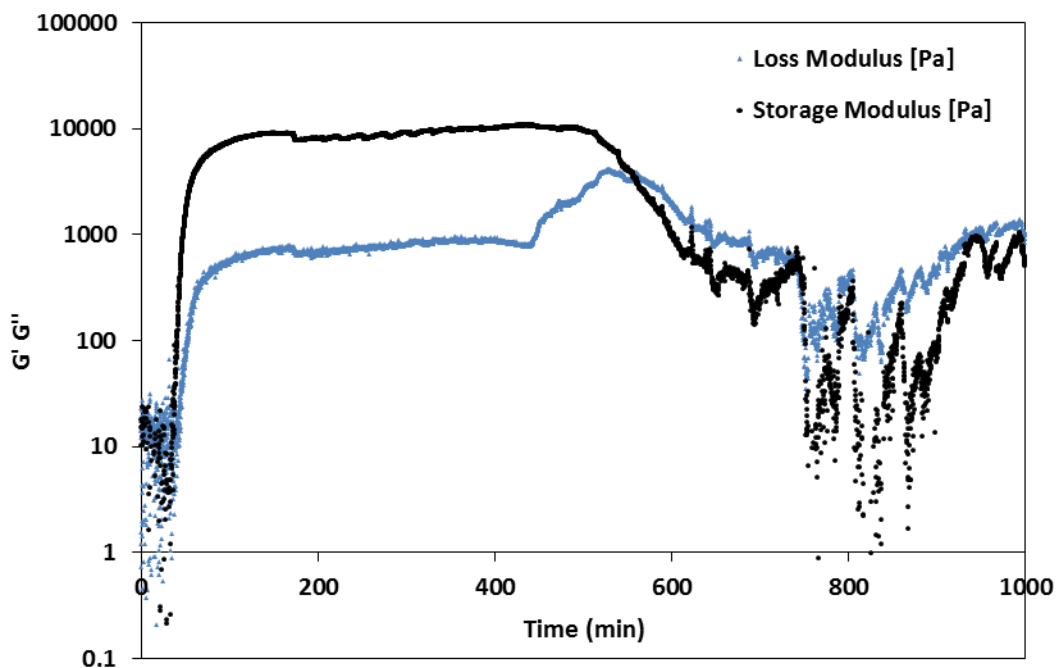


Figure 3.18: Time sweep of compound 72 that shows the formation of the hydrogel with time. It can be seen that after about 1 hour the hydrogel has formed because at this time the ratio between G' and G'' has increased, and this means that increasing the solid like properties leading to the formation of the hydrogel. Then, the hydrogel has deformed after about 8 hours.

3.3.2- pH and pK_a measurements:

For similar dipeptides, it has been reported that the hydrogels form when the pH decrease below the pK_a ^{12, 19, 23, 35}. pK_a is the acid dissociation constant also known as the acidity constant and is a quantitative measure of the strength of an acid in solutions. pK_a is defined according to Henderson-Hasselbalch equation where:

$$pH = pK_a + \log \frac{[A^-]}{[HA]}$$

Previous research has shown that the pK_a decreases with an increase in temperature for naphthalene dipeptides and it increases with an increase in hydrophobicity^{12, 19, 23, 35}. We have utilized a measurement method of measuring the pK_a via titration with 0.1 M HCl. Hydrochloric acid is used to decrease the pH from a high pH (approximately 10 – 12) to low pH (about 3). Figures 3.19 and 3.20 show examples of titration results of compounds **17** and **22** to determine the pK_a (chosen as examples of peptides with the same aromatic group, but with different number of substituents and different

hydrophobicity). From Figure 3.19 and 3.20, the apparent pK_a of the material can be established. The data shows the initial pH after dissolution to be 11.2 and 11.6 respectively for these two dipeptides. On addition of HCl, the pH drops rapidly to a plateau at pH 7.0 and 6.2 respectively. This is the buffering region, where the pK_a of the dipeptide is reached. The pH is then shown to drop over time until pH 3, where equilibrium is reached.

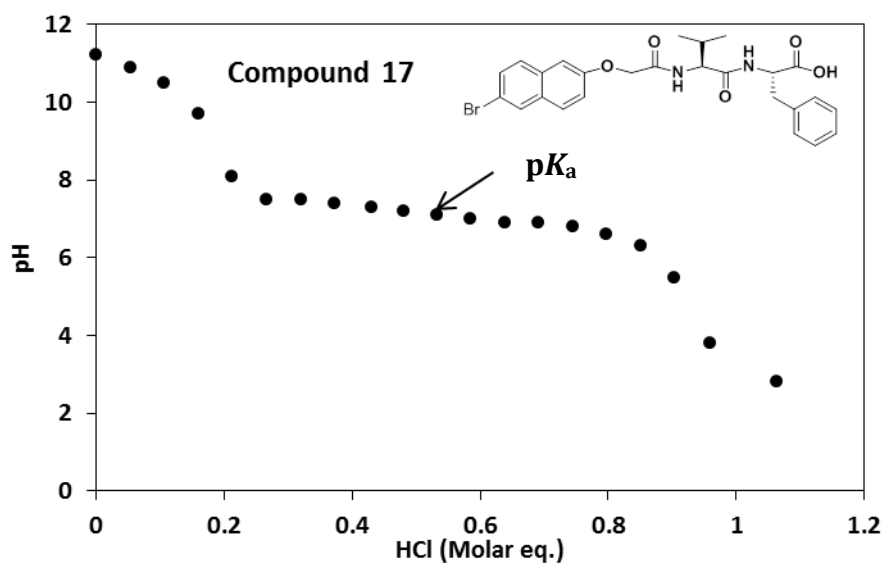


Figure 3.19: The titration of compound 17 to determine the pK_a .

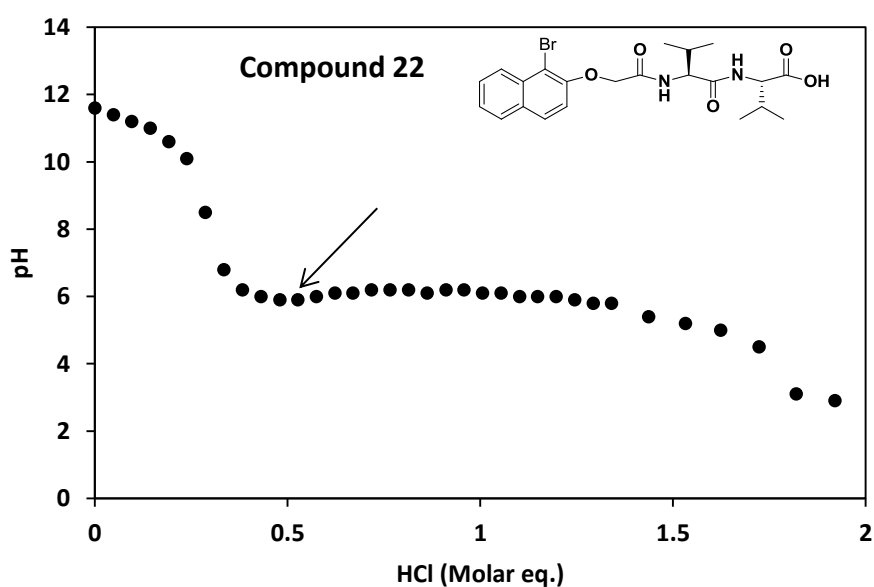


Figure 3.20: The titration of compound 22 to determine the pK_a .

Not all cases showed a single pK_a . For example, Figure 3.21 shows the pK_a of compound **14** again measured by adding 0.1 M HCl. The data show the initial pH after dissolution to be 12. After the first addition of HCl, the pH drops slowly to about 10.6 where a first plateau reached. This is the buffering region, where might be the pK_a 1 of the dipeptide is reached. The pH then drops until pH 6.5, where is the second plateau reached (pK_a 2). Then the pH continues dropping until pH 3.0, where equilibrium is reached. According to other work,¹² two different pK_a are possible. This is because there might be different structures formed as the pH decreases. Here, the data imply that there are two apparent pK_a s, pK_a 1 at 10.6 and pK_a 2 at 6.5, although it is not clear where is the exact pK_a . Formally, the pK_a should be the point where 50% of the molecules are deprotonated. From Figure 3.21, this is at pH 6.5, which is pK_a 2. These two pK_a s might arise from the possibility of forming artefacts that resulting from the formation of a hydrogel during the titration process.

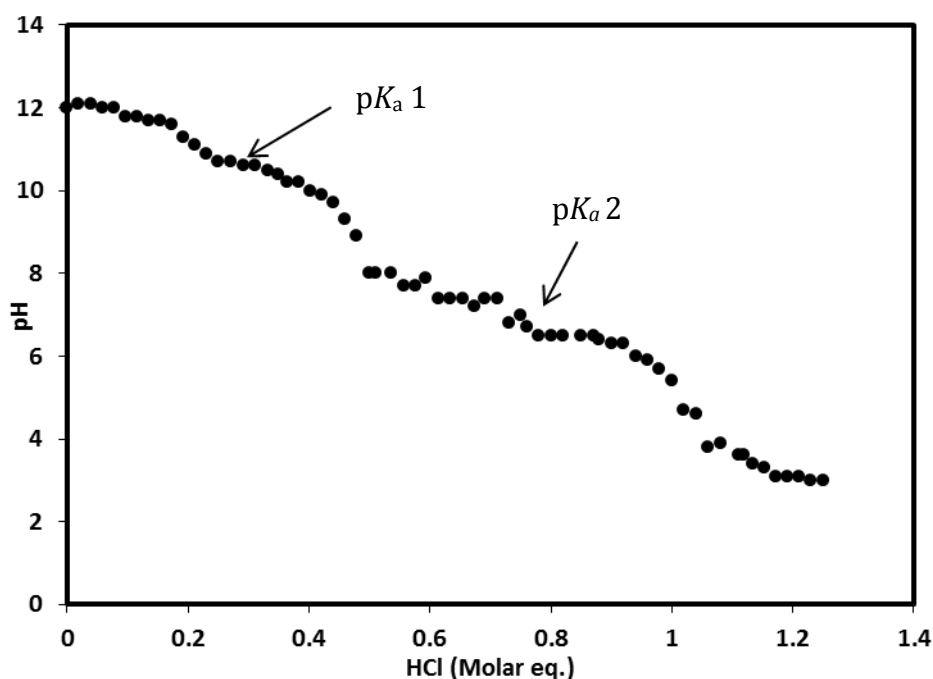


Figure 3.21: The changes in the pH on adding HCl to measure the pK_a of compound **14**.

Another way of measuring the pK_a is to add GdL to the solution. This should help minimise artefacts from gelation. Figure 3.22 shows decreasing the pH over time of compound **14** on adding GdL. Here, we note that the pH dropped quickly, with no sign of

a plateau at pH 10.6. However, it can be noted that there is correlation between Figure 3.21 and 3.22. After adding the GdL, the pH buffers at approximately 6.5, very close to the value of pK_a 2 in Figure 3.21. The lack of an observable pK_a 1 may be due to fewer artefacts from the pH measurement or may be due to a slightly different process when the pH is changed with GdL instead of HCl.

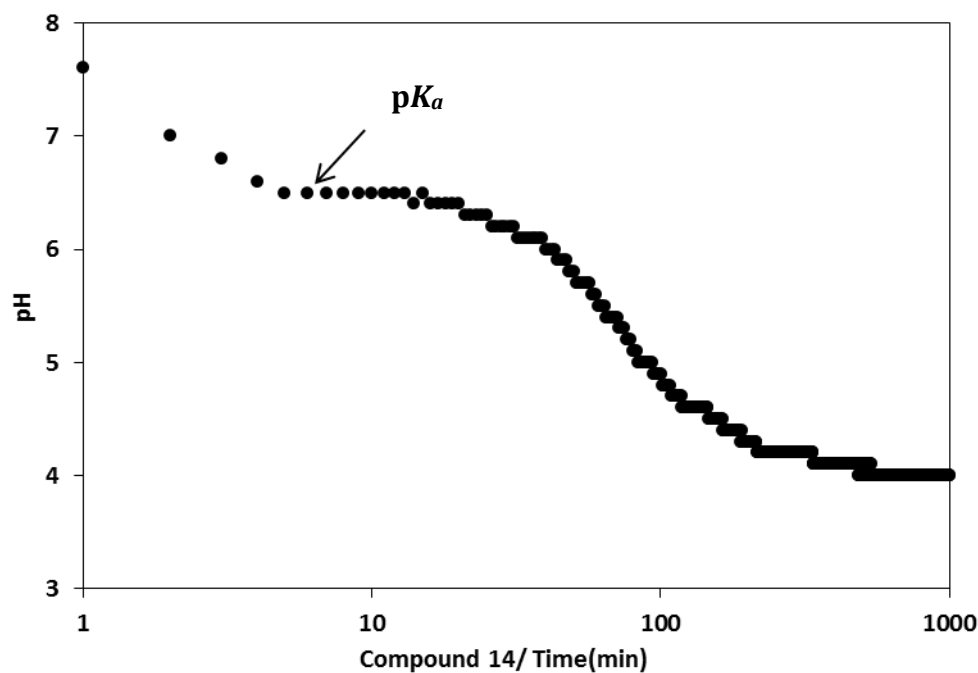


Figure 3.22: An example of pH measurement over the time for compound 14 for 24 hours where the pH is changed using GdL.

Other research has determined that there is a correlation between the apparent pK_a and the hydrophobicity of each dipeptide^{12, 19, 35}. As an extension to these findings, it was interesting to discuss whether the conjugated dipeptides with different aromatic groups and different substituents formed here exhibit similar behaviour. Hence, the determination of the pK_a of the other dipeptides was carried out and analysed in the same manner as dipeptide **17**, **22** and **14** (Figures 3.19, 3.20, and 3.21). Tables 3.12 shows the pK_a measured and logP that calculated mathematically³⁶ for the dipeptides. We can see that the pK_a increases with increasing of logP for almost dipeptides.

Peptide	LogP	pK _a	Peptide	LogP	pK _a
10	1.390	5.7	32	0.932	4.6
11	0.619	5.0	33	2.178	5.8
12	0.832	5.4	40	5.478	7.4
13	2.080	5.5	41	6.842	7.3
14	2.183	pK _a 1 = 10.6 pK _a 2 = 6.5	42	6.160	7.5
15	1.404	5.7	47	1.474	6.6
16	1.617	6.3	53	0.976	6.1
17	2.865	7.0	54	3.119	5.6
18	2.920	7.0	55	1.755	7.5
19	2.141	7.4	56	2.437	7.7
20	2.354	6.6	62	2.540	5.7
21	3.602	6.6	63	1.974	5.0
22	1.520	6.2	64	3.222	5.8
23	0.741	6.0	65	0.981	5.6
24	2.202	7.0	66	1.761	7.7
25	0.955	6.3	67	2.614	5.7
30	1.490	7.4	72	2.688	7.4
31	0.717	4.8			

Table 3.12: The pK_a and logP measurements³⁶ of dipeptides.

Figure 3.23 shows that there is a general increase of the pK_a with increasing of logP for the substituted naphthalene dipeptides, which have bromine substituent with different positions at the 1, 6 and 1,6- position and have different linker between the naphthalene ring and the amino acid sequence, -CH₂, -OCH₂. Figure 3.24 shows data for the other dipeptides conjugated to different aromatic rings such as carbazole, anthracene, anthraquinone, pyrene and phenanthrol that form hydrogels. This group of dipeptides covers a wide range of hydrophobicities and pK_a. There is an apparent relationship between these two factors and this agrees with the results of Chen *et al.*¹⁹ However, there seems to be a critical value of logP. Above this value (about 2.5), there is no

further increase in the pK_a . This shows that there are two values; one shows an increase in the pK_a with the increase of $\log P$, indicating to a linear relationship between the pK_a and the $\log P$, hence a correlation between the hydrophobicity and the pK_a , agreeing with previous work¹⁹, where it is reported a linear relationship between pK_a and $\log P$ ¹⁹. Other value shows no more increase in the pK_a above the value of about 2.5. This result above this value is shown for compound **20**, **21**, and **25**. These compounds have different substituents (**21**, **25**) and different amino acid sequences (**20**, **21**, or **20**, **25**), although they have similar pK_a and $\log P$ values. This shows that these conjugated dipeptides with different aromatic groups and different substituents formed here have similar behaviour. Also the data in Figure 3.24 show that changing the aromatic ring follow the same trend for the correlation between the pK_a and $\log P$. Furthermore, a linear regression to data for the dipeptides with r^2 of 0.3661 (Fig. 3.23) and 0.3086 (Fig. 3.24) shows that it is not close to fit the data. As a result, this correlation between pK_a and $\log P$ may give the choice of appropriate gelator, although it is still unclear whether it can form gel or not.

It must first be noted that the pK_a of the terminus of each dipeptide is a lot higher than what is expected for the amino acids. For example, the pK_a for the $-\text{COOH}$ of a glycine unit is agreed to be around 2³⁵. As shown in Table 3.12, compound **16**, which has a glycine terminus, has an apparent pK_a of 6.3. This observation can be explained by the hydrophobic interactions that come from the different amino acids used. The shift of the pK_a observed in water arises from the competition for fully hydrated shells between polar groups and hydrophobic groups in close proximity, as postulated by Urry *et al.*³⁵ It therefore makes sense in relation to these data that as hydrophobicity of the side chain increases, this competition increases, and hence a more positive shift in pK_a is acquired. Elsewhere, the use of such hydrophobic groups is demonstrated by Tang *et al.* by creating an Fmoc diphenylalanine compound which gels water at physiological pH.³⁷ Increase the π - π stacking of the fluorenyl and phenylalanine side chains is the main contributor to hydrophobic interaction in this case, enabling favourable self-assembly at a pH of 7.

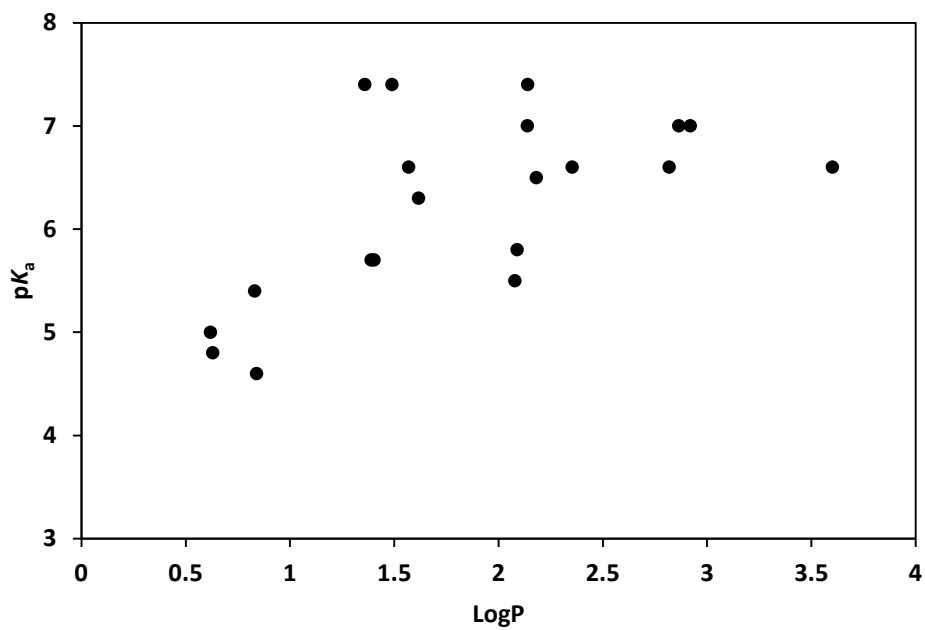


Figure 3.23: The pK_a and $\log P$ for naphthalene dipeptides (data shown in Table 3.12).

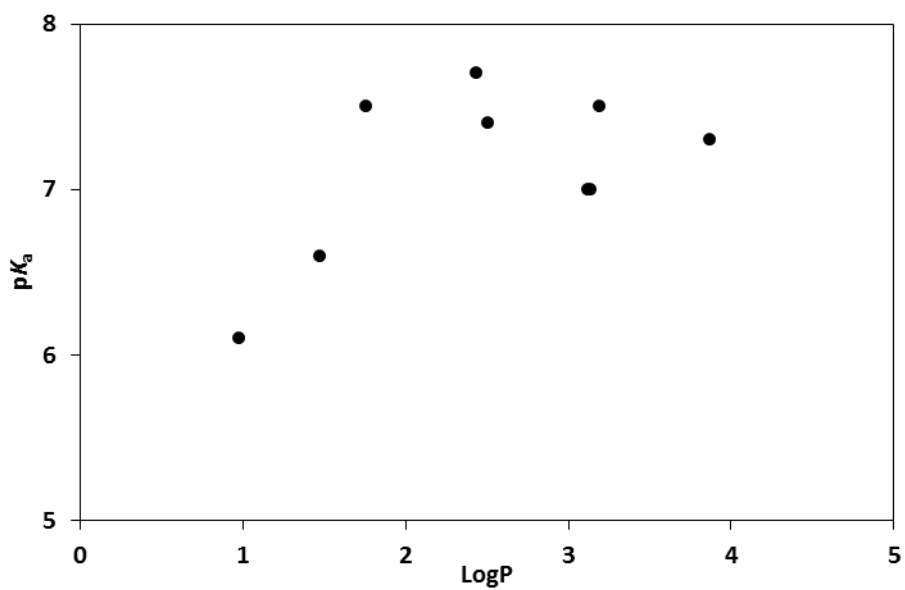


Figure 3.24: The pK_a and $\log P$ of other conjugated dipeptides (carbazole, anthraquinone, phenanthrol, pyrene and anthracene) (data shown in Table 3.12).

3.3.3- FT-IR of Hydrogels:

For most of this Chapter, we have been interested in whether gels are formed. However, an important question is how these gels are formed. Infra-Red spectroscopy (FT-IR) has been used to determine the secondary structure of peptides and proteins^{12, 19, 23, 38}. The secondary structure of a peptide can be defined as the three-dimensional form it takes as a result of non-covalent interaction³⁹. Both β -sheets and α -helices are examples of secondary structure. The conformations of peptides are largely decided by the degrees of freedom they enjoy around the C-NH and C-C=O bond^{40, 41}.

Here, we studied the FT-IR spectroscopy of dipeptide hydrogels to determine the functional groups (carboxylate and amide group) and to study the presence of β -sheet structure. β -sheet structure has been suggested before as one of the driving forces for self-assembly of this type of dipeptide, with previous work demonstrating the presence of antiparallel β -sheets^{13, 41}.

Samples were prepared for FT-IR by preparing a gel at a concentration of 5 mg/mL suspension in DMSO with D₂O (the ratio between DMSO and D₂O was 0.1: 1.9). Deuterated solvents were used to avoid the water absorption band combining with the amide I band.³⁸ Samples were left overnight to complete hydrogelation. Figure 3.25 shows the IR spectra of compounds **18**, **40**, and **72**. The spectra show the assignment of peaks due to the self-assembly of three conjugated dipeptides that have the same amino acid sequence (valine amino acid) and different aromatic groups, naphthalene, phenanthrol and pyrene to study β -sheet structure. IR spectroscopy shows different peaks, the most significant peaks are between 1600 cm⁻¹ to 1700 cm⁻¹ where the C=C bonds, amide and carboxyl groups occur²⁶. From the spectra we can see that the peaks between 1600cm⁻¹ to 1650cm⁻¹ are different. This is because the hydrogelators have different aromatic groups, where at these wavenumbers C=C stretch of aromatic groups occurs. This IR result illustrates that these peaks may indicate to the presence of antiparallel β sheets, hence it provided evidence to determine that the self-assembly of the peptides resulted in the formation of β sheets via the H-bonding interactions of the dipeptide backbones leading to the formation of the hydrogel as described elsewhere^{12, 13}.

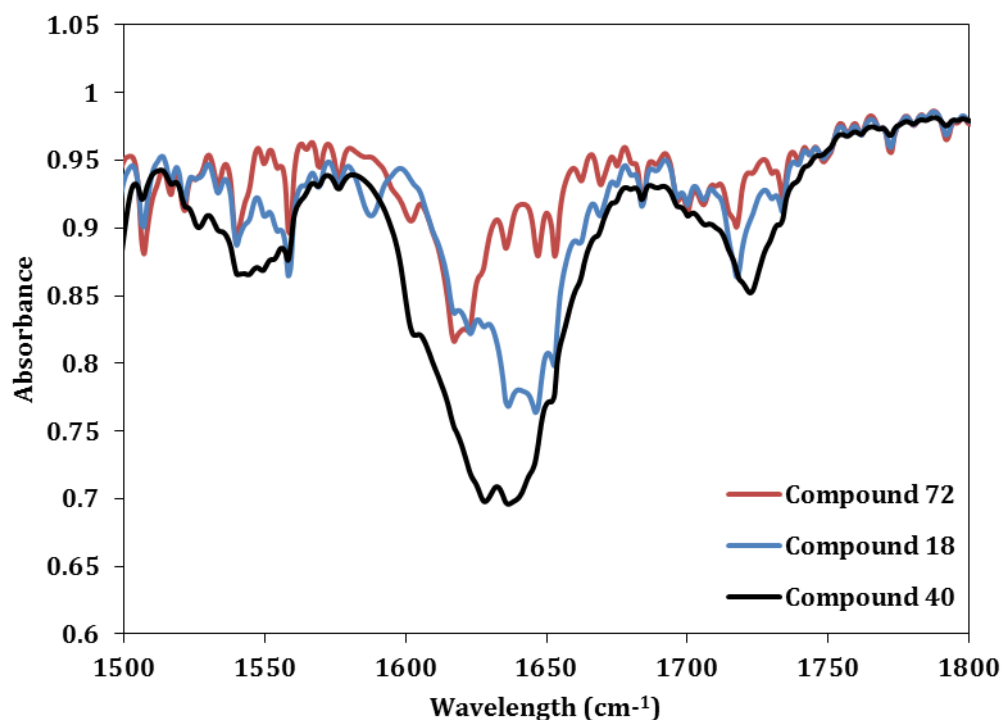


Figure 3.25: IR spectroscopy of three dipeptides conjugated to naphthalene (compound 18), pyrene (compound 72) and phenanthrol ring (compound 40).

Samples of compound **51a** were prepared for FT-IR at a concentration of 5 mg/mL in D₂O or H₂O at pH 11. Sufficient GdL was then added to ensure each hydrogel had an end pH point of between 3 and 3.3, and samples were left overnight to complete hydrogelation. IR was measured for these samples wet and also after drying the gel. The data were compared to the data from the as-synthesised peptide to study the presence of β -sheets. Figure 3.26 shows the IR spectroscopy results of compound **51a** in D₂O, H₂O wet and dry gel and the powder of dipeptide. The Figure shows the peaks that occur between 1600 and 1700 cm⁻¹. From the Figures we can see two peaks in D₂O at 1640 cm⁻¹ and at 1656 cm⁻¹ which one assigns to the amide groups. In contrast, these peaks cannot be seen in H₂O because there is a broad peak of OH occurs at the same wavenumbers. Also, in the powder state there are no peaks between 1600 and 1700 cm⁻¹ because there is no self-assembly. This result may indicate the presence of antiparallel β -sheets, which implies to the packing arrangement on the assembly.

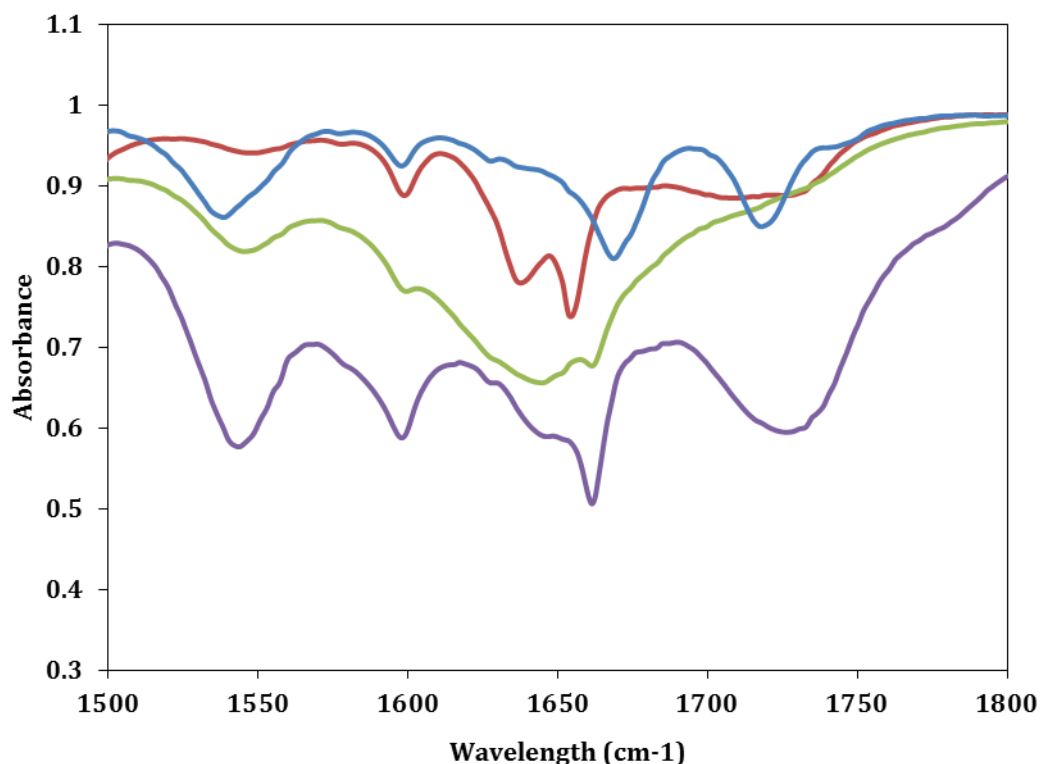


Figure 3.26: The IR spectroscopy of compound 51a in D₂O (Red) and in H₂O wet gel (green), dry gel (purple) and powder peptide (blue).

3.4- Conclusion:

Different functionalised dipeptides can be used as hydrogelators such as naphthalene, phenanthrol, pyrene, carbazole and anthraquinone dipeptide derivatives. The mechanical properties of these hydrogels have been studied. It is still not clear why some peptides formed gel and others not. Although the method of preparing hydrogel is not correlated with the formation of the gel, changing the method can modify the properties of the hydrogel formed. In conclusion, the results showed that the small change in the structure of the hydrogelator can affect the formation of the hydrogel and the method of how to prepare hydrogel is not relevant with the formation of the hydrogel. Moreover, the results showed that there is a correlation between the pK_a and the hydrophobicity of the peptides. Here we established that the hydrophobicity increases with the increase of the pK_a . Although it is still not clear why some peptides can form hydrogel and others not, these kind of dipeptides conjugated to different aromatic groups have different properties and can be used for number of different applications such as energy transfer and drug delivery, as we will discuss in the next Chapters.

Figure 3.27a shows the data plotted the logP against the success of gelation. From the Figure, we noted that there is no correlation between the logP and the formation of the hydrogel, although perhaps there is a tendency for the molecules with a higher logP to form gels. Figure 3.27b shows the data plotted with molecular weight. From the Figure, it seems to be more strongly suggest that those molecules with a higher molecular weight tend to form gels. Since the higher molecular weight molecules tend to be those incorporating phenylalanine as one of the amino acids in the dipeptide sequence, we then studied this as a factor (Fig. 3.27c). When neither amino acid in the dipeptide is a phenylalanine, there is a 55% chance that the molecule will form a gel. However, when either of the amino acids is phenylalanine, there is a 91% chance that the molecule will form a gel. If we discount structures based on anthracene dipeptides which did not form gel, then 100 % of the molecules formed gels. This does take into account the purity, where this factor can affect the gelation results. Therefore, this results show that incorporating phenylalanine into the dipeptide is a good way of maximising the chance of forming a gel. However, even this should be treated as a rule of thumb as we note that there are related dipeptides such as Fmoc-GF that do not gel.^{42, 43}

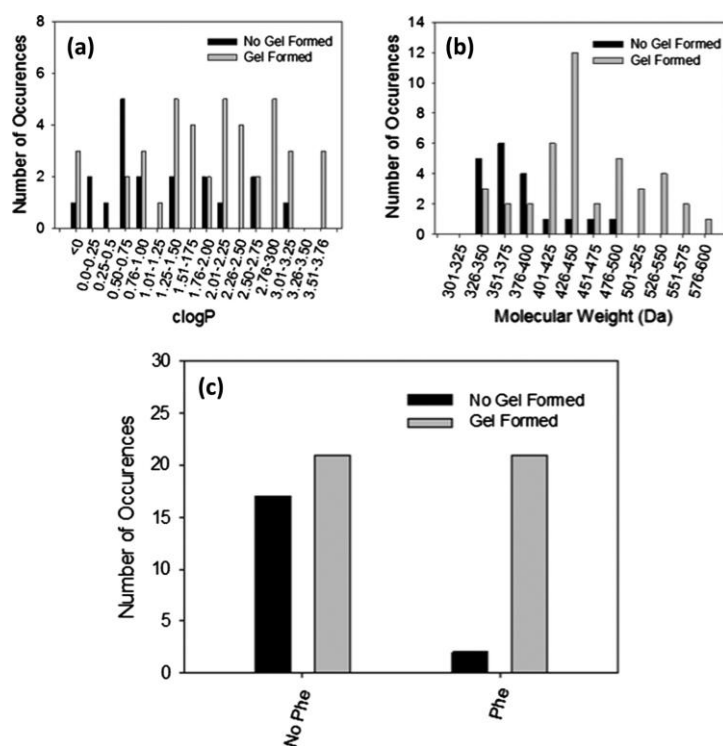


Figure 3.27: Histogram showing the ability of a dipeptide to form a gel or not based on (a) clogP or (b) molecular weight. (c) Shows the number of dipeptides that form gels or not that do not (left) or do (right) contain phenylalanine as one of the amino acids.

3.5- References:

1. F. Zhao, Y. Gao, J. Shi, H. M. Browdy and B. Xu, *Langmuir*, 2010, **27**, 1510-1512.
2. Z. Yang, G. Liang, M. Ma, Y. Gao and B. Xu, *Journal of Materials Chemistry*, 2007, **17**, 850-854.
3. P. J. Flory, *Faraday Discussions of the Chemical Society*, 1979, **68**, 14-25.
4. Z. Yang and B. Xu, *Journal of Materials Chemistry*, 2007, **17**, 2385-2393.
5. W. T. Truong, Y. Su, J. T. Meijer, P. Thordarson and F. Braet, *Chemistry – An Asian Journal*, 2011, **6**, 30-42.
6. S. Banerjee, R. K. Das and U. Maitra, *Journal of Materials Chemistry*, 2009, **19**, 6649-6687.
7. Y. Wang, Z. Zhang, L. Xu, X. Li and H. Chen, *Colloids and Surfaces B: Biointerfaces*, 2013, **104**, 163-168.
8. G. Cheng, V. Castelletto, R. R. Jones, C. J. Connon and I. W. Hamley, *Soft Matter*, 2011, **7**, 1326-1333.
9. L. Chen, S. Revel, K. Morris and D. J. Adams, *Chemical Communications*, 2010, **46**, 4267-4269.
10. S. Yamaguchi, I. Yoshimura, T. Kohira, S.-I. Tamaru and I. Hamachi, *Journal of the American Chemical Society*, 2005, **127**, 11835-11841.
11. D. J. Adams and P. D. Topham, *Soft Matter*, 2010, **6**, 3707-3721.
12. C. Tang, A. M. Smith, R. F. Collins, R. V. Ulijn and A. Saiani, *Langmuir*, 2009, **25**, 9447-9453.
13. A. M. Smith, R. J. Williams, C. Tang, P. Coppo, R. F. Collins, M. L. Turner, A. Saiani and R. V. Ulijn, *Advanced Materials*, 2008, **20**, 37-41.
14. J.-B. Guilbaud, E. Vey, S. Boothroyd, A. M. Smith, R. V. Ulijn, A. Saiani and A. F. Miller, *Langmuir*, 2010, **26**, 11297-11303.
15. H. Wang, C. Ren, Z. Song, L. Wang, X. Chen and Z. Yang, *Nanotechnology*, 2010, **21**, 1-5.
16. D. J. Adams, M. F. Butler, W. J. Frith, M. Kirkland, L. Mullen and P. Sanderson, *Soft Matter*, 2009, **5**, 1856-1862.
17. Y. Zhang, H. Gu, Z. Yang and B. Xu, *Journal of the American Chemical Society*, 2003, **125**, 13680-13681.
18. Y. Zhang, Z. Yang, F. Yuan, H. Gu, P. Gao and B. Xu, *Journal of the American Chemical Society*, 2004, **126**, 15028-15029.
19. L. Chen, S. Revel, K. Morris, L. C. Serpell and D. J. Adams, *Langmuir*, 2010, **26**, 13466-13471.
20. K. A. Houton, K. L. Morris, L. Chen, M. Schmidtman, J. T. A. Jones, L. C. Serpell, G. O. Lloyd and D. J. Adams, *Langmuir*, 2012, **28**, 9797-9806.
21. L. Chen, T. O. McDonald and D. J. Adams, *RSC Advances*, 2013, **3**, 8714-8720.
22. <http://delloyed.50megs.com/moreinf/Buffers.html>.
23. L. Chen, K. Morris, A. Laybourn, D. Elias, M. R. Hicks, A. Rodger, L. Serpell and D. J. Adams, *Langmuir*, 2009, **26**, 5232-5242.
24. H. H. Barnes, JF. Walters, K., *An introduction to rheology*, 1989.
25. Y. Y. Li, Q. Deng, M. Y. Cui, J. and Jiang, B., *Chinese Journal of Polymer Science.*, 2009, **27**, 335 - 341.
26. B. Stuart, *Infrared Spectroscopy: Fundamentals and applications*, 2004.
27. Z. Yang, G. Liang and B. Xu, *Chemical Communications*, 2006, **7**, 738-740.
28. G. Liang, Z. Yang, R. Zhang, L. Li, Y. Fan, Y. Kuang, Y. Gao, T. Wang, W. W. Lu and B. Xu, *Langmuir*, 2009, **25**, 8419-8422.
29. D. J. Adams, *Macromolecular Bioscience*, 2011, **11**, 160-173.
30. Y. Pocker and E. Green, *Journal of the American Chemical Society*, 1973, **95**, 113-119.
31. A. Mahler, M. Reches, M. Rechter, S. Cohen and E. Gazit, *Advanced Materials*, 2006, **18**, 1365-1370.
32. D. Wu, J. Zhou, J. Shi, X. Du and B. Xu, *Chemical Communications*, 2014, **50**, 1992-1994.

33. J. Raeburn, A. Zamith Cardoso and D. J. Adams, *Chemical Society Reviews*, 2013, **42**, 5143-5156.
34. M. O. Guler, R. C. Claussen and S. I. Stupp, *Journal of Materials Chemistry*, 2005, **15**, 4507-4512.
35. D. W. Urry, S. Q. Peng, T. M. Parker, D. C. Gowda and R. D. Harris, *Angewandte Chemie-International Edition in English*, 1993, **32**, 1440-1442.
36. <http://www.molinspiration.com>.
37. C. Tang, A. M. Smith, R. F. Collins, R. V. Ulijn and A. Saiani, *Langmuir*, 2009, **25**, 9447-9453.
38. J. T. Pelton and L. R. McLean, *Anal Biochem*, 2000, **277**, 167-176.
39. U. Koert, *Angew Chem Int Edit*, 1997, **36**, 1836-1837.
40. L. L. Porter and G. D. Rose, *P Natl Acad Sci USA*, 2011, **108**, 109-113.
41. C. Tang, R. Ulijn and A. Saiani, *The European Physical Journal* 2013, **36**, 1-11.
42. V. Jayawarna, M. Ali, T. A. Jowitt, A. F. Miller, A. Saiani, J. E. Gough and R. V. Ulijn, *Advanced Materials*, 2006, **18**, 611-614.
43. D. J. Adams, L. M. Mullen, M. Berta, L. Chen and W. J. Frith, *Soft Matter*, 2010, **6**, 1971-1980.

CHAPTER 4

Fluorescence And Energy Transfer

4- Fluorescence and energy transfer:

4.1- Introduction:

Hydrogels have been used in different applications such as drug delivery¹, cell culturing² and energy transfer³⁻⁶. Suitably protected dipeptides such as naphthalene peptides can be used as a fluorescent hydrogelators^{3, 7}. According to previous research, energy transfer between organised aromatic groups has been utilised in different applications such as light-harvesting^{4, 5, 8} and molecular electronics^{3, 8, 9}. One of the main strategies of organising the chromophores is to use materials that self-assemble to give organogels (gels which contain organic solvent)⁶. When the fibre-forming molecules contain a suitable donor chromophore, these fibres can be used to transfer energy to acceptor chromophores¹⁰. For example, cationic glutamate derivatives have been assembled with anionic naphthalene and anthracene-based fluorophores and used to prepare light-harvesting hydrogels^{3, 11}. In addition, it has been found there can be energy transfer between a naphthalene-based hydrogelators and a dansyl molecule^{3, 12}. Chen *et al.* illustrated that when the acceptor chromophore was incorporated in the aromatic groups, efficient energy transfer occurred. For example, they showed that there is an increase in fluorescence on formation of β -sheets between the dipeptides, because the dye incorporates within these β -sheets. The same authors also used another system where both donor and acceptor were functionalised dipeptides conjugated to different aromatic groups (donor is naphthalene dipeptide derivative and the acceptor is anthracene dipeptide derivative³). They reported that energy transfer occurred between naphthalene-diphenylalanine and a dansyl derivative leading to emission at 485 nm. In addition, there was emission at 355 nm from naphthalene diphenylalanine alone. Also, a transparent self-supporting hydrogel at a concentration of 2.2 mM and at pH of 4 was formed from this naphthalene diphenylalanine and dansyl derivative (Fig. 4.1)³. They also reported that there is energy transfer between naphthalene and anthracene derivatives^{3, 11}. Elsewhere, MacPhee *et al.* showed energy transfer between donor and acceptor chromophores conjugated to fibre-forming peptides¹³.

Supratim *et al.* reported that pyrene conjugated to glutamate derivatives formed a gel in benzene and cyclohexane, whereas a porphyrin functionalised derivative did not form gel. They also reported that energy transfer from pyrene to porphyrin occurred when

the gel of the pyrene-glutamate containing the porphyrin was prepared¹⁴. Furthermore, efficient transfer of excitation energy during nano-structures has been evidenced in an anthracene light-harvesting matrix doped with less than 1 mol% of a tetracene energy trap by Alexandre *et al.*¹⁵ They have shown that anthracenes, tetracenes and pentacenes self-assemble into stable nano-structures due to a 2,3-bis-*n*-alkoxy substitution. The fibres forming these 3-D supramolecular networks could be aligned with intense magnetic fields or mechanically, creating these materials of interest for different applications¹⁵. Moreover, pyrene conjugated to oligopeptides has been reported to give rise to fluorescent hydrogels¹⁶.

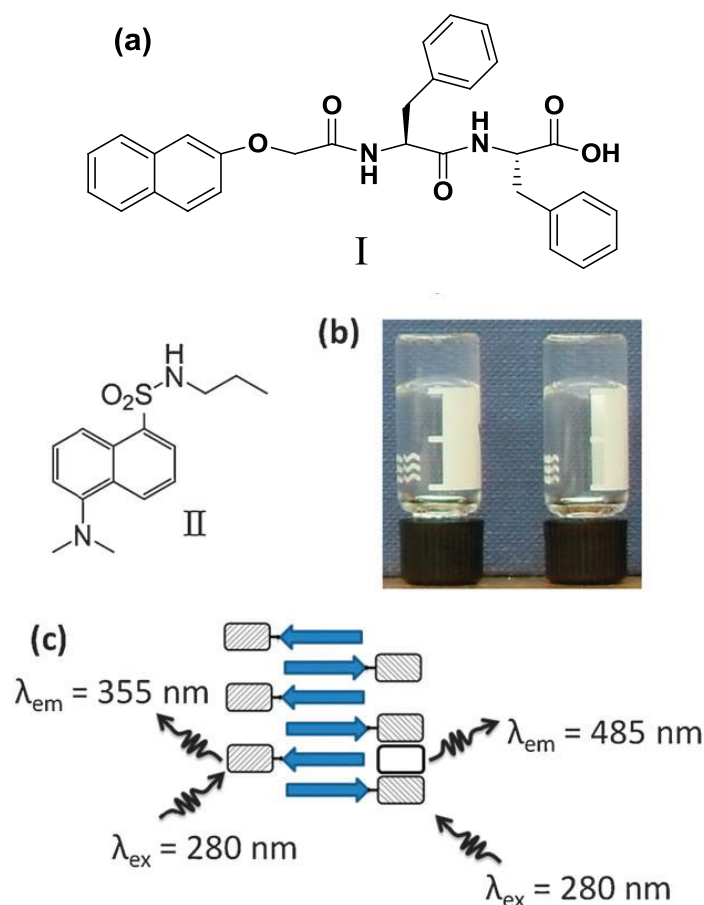


Figure 4.1: (a) Structure of naphthalene-diphenylalanine (I) and dansyl derivative (II). (b) I form a transparent self-supporting hydrogel at a concentration of 2.2 mM and at pH of 4 (left). A transparent self-supporting gel was also formed in the presence of II (0.084 mM). (c) Energy transfer occurs between I and II leading to emission at 485 nm in addition to emission at 355 nm from I alone. From Chen *et al.*³

In this Chapter, we have used our functionalised dipeptides that were described in Chapters 2 and 3. The aromatic groups that we used to functionalise the dipeptides are

9-anthracene carboxylic acid, 2-anthraquinone carboxylic acid, 1-pyrene carboxylic acid, carbazole and 9-phenanthrol. We prepared dipeptides from these starting materials using the three different approaches as explained in Chapter 2. In this Chapter, we describe a fluorescence study of the functionalised dipeptides that formed transparent hydrogels, with the aim of studying energy transfer between two different aromatic pairs such as naphthalene and anthracene, naphthalene and pyrene, anthracene and carbazole, and naphthalene and anthraquinone. These pairs were chosen on the basis of their excitation and emission wavelengths.

4.1.1- Mechanism of energy transfer:

Energy transfer can happen via two mechanisms:

4.1.1.1- Förster energy transfer:

Förster energy transfer is a mechanism that describes transfer energy (not electron transfer) between two compounds, one called the donor and the other called the acceptor. Here, the donor is excited by a photon from its ground state (S_0), which then relaxes to its excited singlet state (S_1). Then, the energy is transferred to the acceptor, resulting in excitation of the acceptor¹⁷⁻¹⁹. The excited acceptor then emits a photon and returns to its ground state (Fig. 4.2). The main conditions required for energy transfer are: 1) the donor and the acceptor must be in close proximity (typically 1 – 10 nm) and 2) the emission spectrum of the donor must overlap with the excitation spectrum of the acceptor (Fig. 4.3).

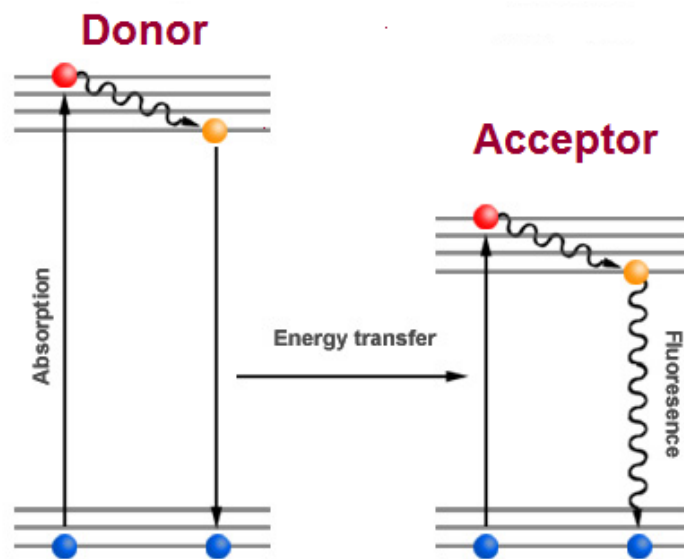


Figure 4.2: shows the Förster energy transfer mechanism¹⁹.

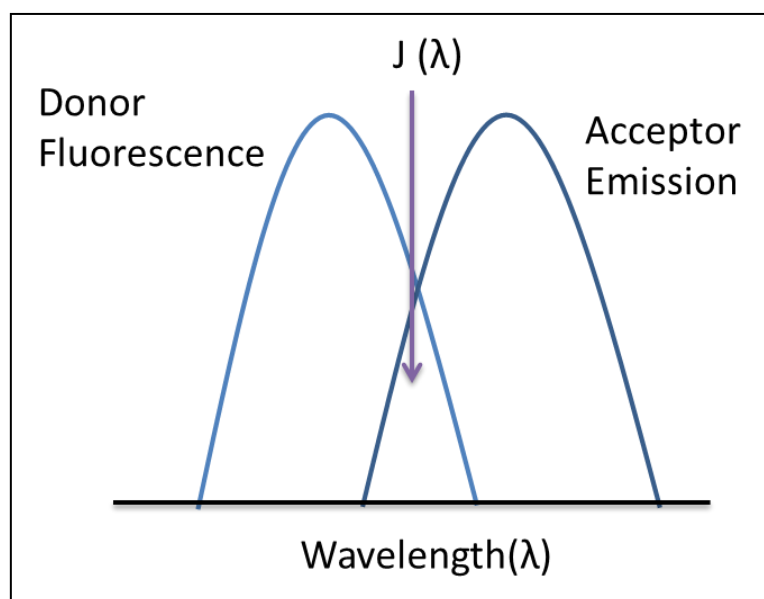


Figure 4.3: shows the overlap between the donor and acceptor to transfer energy.

4.1.1.2- Dexter energy transfer:

Dexter energy transfer is also called short range or exchange energy transfer. Here, the electron in its excited state transfers from the donor to the acceptor via a non-radiative process (without emitting a photon)²⁰. Here, the main condition for energy transfer is a wave function overlap.

The differences between Förster and Dexter energy transfer are the length scale and the underlying mechanism. In the Dexter mechanism, the energy transfer occurs between donor in its excited state (D^*) and the acceptor in its ground state (A) by exchange of an electron between the donor and the acceptor without the emission of a photon (non-radiative) resulting in return the donor to its ground state (D) and the excitation of the acceptor to its excited state (A^*) (Fig. 4.4). In the Förster mechanism, the energy transfer between donor and acceptor occurs via the emission of a photon¹⁷.

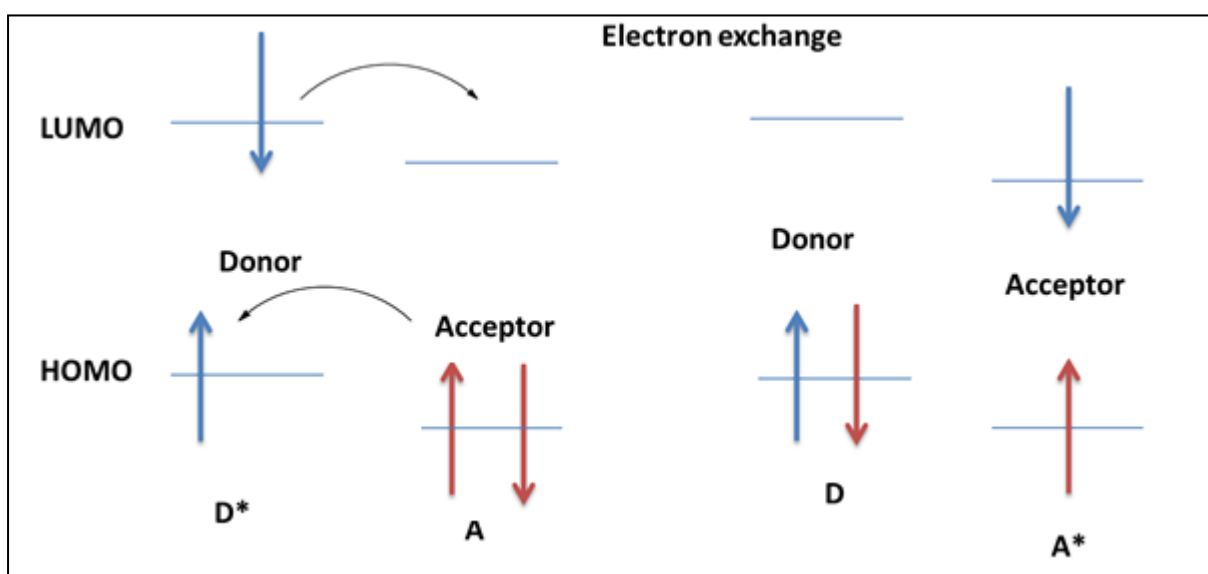


Figure 4.4: shows the Dexter energy transfer mechanism.

4.2- Experimental section:

4.2.1- Fluorescence studies:

Fluorescence studies the emitted light from a material. Here, fluorescence spectroscopy was carried out using a Perkin Elmer luminescence spectrometer LS55. Gels were prepared by two methods. In the DMSO: Water method, 10 mg of the peptide was dissolved in 100 μ L of DMSO and then 1.9 mL of deionised water was added to the mixture in 1.0 cm path-length cuvette made out of PMMA. The sample was left to form hydrogel at room temperature overnight. In the GdL method, an equimolar amount of 0.1 M NaOH was added to a solution of a dipeptide (10 mg) in 2 mL water (at concentration of 5 mg/mL) and placed in the 1.0 cm path-length cuvette. For the peptides that formed a turbid hydrogel at the concentration of 5 mg/mL, we decreased

the peptide concentration to 2 mg/mL (e.g. compound **54**) and to 0.5 mg/mL (compound **72**). The initial pH in all cases was about 10 to 12. Measured quantities of GdL were then added to the solutions.

Emission spectra were recorded for each gel at different excitation wavelengths (between 265 nm – 360 nm). We also studied the change in fluorescence of some peptide such as compound **72** with time using the GdL method. Here, emission spectra were recorded every 60 seconds for the first hour after GdL addition and then every 30 minutes for 18 hours. The emission spectra were collected between 250–600 nm by excitation at 265 nm. The slit widths of the emission and excitation were between 5 mm, and the scan speed used to collect the spectra was 100 nm/ min.

4.2.2- Energy transfer in hydrogels and organogels:

The transfer of energy from donor in its excited state to an acceptor is known as Förster resonance energy transfer (FRET)¹⁷. According to previous research, hydrogels based dipeptides conjugated to an aromatic group can transfer energy from donor to acceptors³. It has been reported that energy transfer occurs between naphthalene dipeptides and dansyl or anthracene dipeptide, where the naphthalene acts as a donor and the dansyl and anthracene as acceptors. Energy transfer occurs when dipeptides start to self-assemble. This happens when fibres form at low pH. Other research reported that chromophore-based organogels can be used as a scaffold for energy transfer and light harvesting systems^{8, 21}. Following this research, we have been preparing hydrogels based on naphthalene, carbazole, anthraquinone, pyrene and phenanthrol dipeptides derivatives to study fluorescence and energy transfer. We report the fluorescence studies and the energy transfer between different aromatic groups functionalising the dipeptides by preparing hydrogels containing two different aromatic hydrogelators. For example, we have prepared hydrogels containing two hydrogelators functionalised with naphthalene and pyrene moiety, as naphthalene dipeptides can emit light at 355 nm and pyrene dipeptides are excited by light at 355 nm.

4.2.2.1- Mix two dipeptides:

We have prepared stock solution of peptide 1 at different concentrations and then we added different amounts (10 µL–20 µL) of a stock solution of peptide 2 at different

concentrations to peptide 1 for total volume of 2 mL of the mixture. Then we added GdL (0.016g) to the mixture and leave it overnight to form gel (Table 4.1).

Mix two dipeptides	Peptide 1 conc. of the stock solution (mM)	Peptide 2 conc. of the stock solution (mM)	Amount of peptide 2 added to the mixture. (μ L)	Total amount of the mixture. (mL)	conc. of the mixture in the gel (mM)
12 + 62	14	12, 5, 1	10	2	14
25 + 72	4, 2	1	10, 20	2	4, 2
54 + 62	4	12, 5, 1	10	2	4
72 + 62	1	12	10	2	1
40 + 62	11	12, 5, 1	10	2	11

Table 4.1: Shows the different concentrations and the amount added to prepare hydrogel containing two dipeptides.

4.2.2.2- Mix dipeptide and dansyl:

We have prepared stock solution of dipeptide derivative at different concentrations and then we added different amounts (10 μ L–20 μ L) of a stock solution of dansyl derivative at different concentrations to the dipeptide for total volume of 2mL of the mixture. Then we added GdL (0.016g) to the mixture and allowed it to stand overnight to form gel (Table 4.2).

Dipeptide with dansyl	Peptide conc. of the stock solution (mM)	Dansyl conc. of the stock solution (mM)	Amount of dansyl added to the mixture. (μ L)	Total amount of the mixture. (mL)	Conc. of the mixture in the gel (mM)
40 + dansyl	11	3.4	10	2	11
54 + dansyl	4	10	20	2	4

Table 4.2: Shows the different concentrations and the amount added to prepare hydrogel containing dipeptides and dansyl derivative.

4.3- Results and discussion:

4.3.1- Fluorescence study:

The fluorescence of dipeptide hydrogels such as Fmoc or naphthalene dipeptide hydrogels was previously studied^{3, 22, 23}. Here, we have studied the fluorescence of each functionalised dipeptides before forming the hydrogel (i.e. in the solution state) and after gelation (the gel state) using both gelation methods (i.e. the GdL and the DMSO: Water methods). We measured the fluorescence at different excitation wavelengths (265, 285, 300, and 360 nm) and compared between different aromatic groups. The reason for this measurement is to know if the different aromatic groups can emit light at the same wavelength or not; to use them as a donors or acceptors depends on their excitation and emission, because to transfer energy between donor and acceptor, the emission of the donor should overlap the excitation of the acceptor (if not, there will be no energy transfer occur between them). We also studied the fluorescence of some peptides such as compound **72** and compound **16** (Fig. 4.5) with time before and after adding GdL as examples to study their fluorescence during the hydrogelation process.

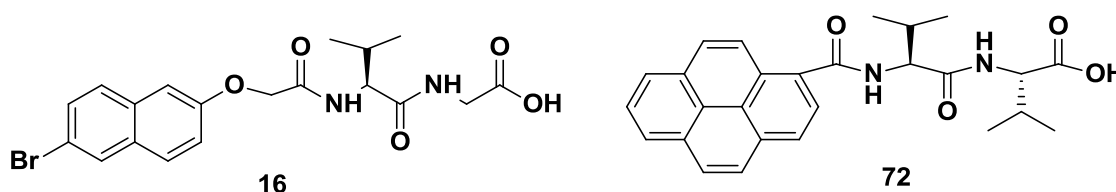


Figure 4.5: The chemical structure of compound 16 and 72.

Fluorescence study of dipeptides hydrogels:

We have studied the fluorescence using both methods (the GdL and DMSO: water methods) of the dipeptide hydrogel conjugated to phenanthrol only (**38b**, **40**), because only these hydrogels formed transparent hydrogel using both methods. In order to study the fluorescence, the hydrogel should be transparent to allow the light to pass through the sample; where the aggregation of the peptides increases in the turbid gel leads to affect the fluorescence results. Other conjugated dipeptides that we have studied their fluorescence formed a transparent hydrogel just by using the GdL method. We have prepared hydrogels at concentrations of the dipeptides of 5 mg/mL. The chemical structure of compounds **38b**, **40**, and **62** are shown in Figure 4.6. Figure 4.7

shows the fluorescence spectra of compound **38b** after forming hydrogels using both methods. From Figure 4.7, we can see that the hydrogel has a similar emission spectrum in both methods when excited at 265 nm. The intensity at the maximum emission wavelength of 380 nm was about 600 units. The fluorescence of a related peptide hydrogel, compound **40**, was also similar when formed by both methods. The intensity at the maximum emission wavelength of 380 nm was 520 units when gelled by the DMSO: water method and 558 units when gelled by the GdL method (Fig. 4.8). These data indicates that the method of forming the gel does not significantly affect the fluorescence of the phenanthrol ring. Also, we can see that the data in Figure 4.8 is less noisy than that in Figure 4.7. This is due to using different scan speeds during the measurements. Although here, using different methods does not affect the fluorescence result of the hydrogel, it affects the results of their mechanical properties (see Chapter 3), where it has been reported that changing the method can change the mechanical properties of the hydrogel formed⁷.

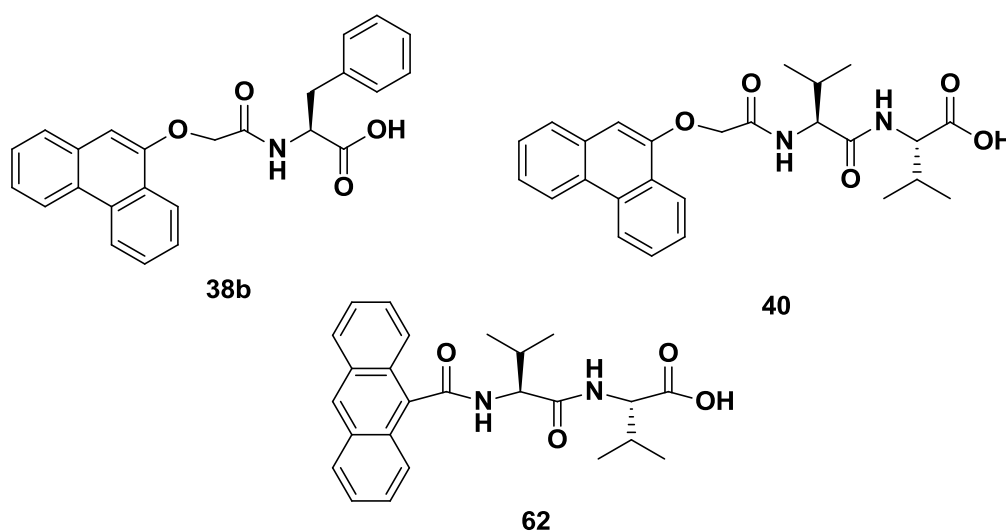


Figure 4.6: The chemical structure of compounds **38b**, **40**, and **62**.

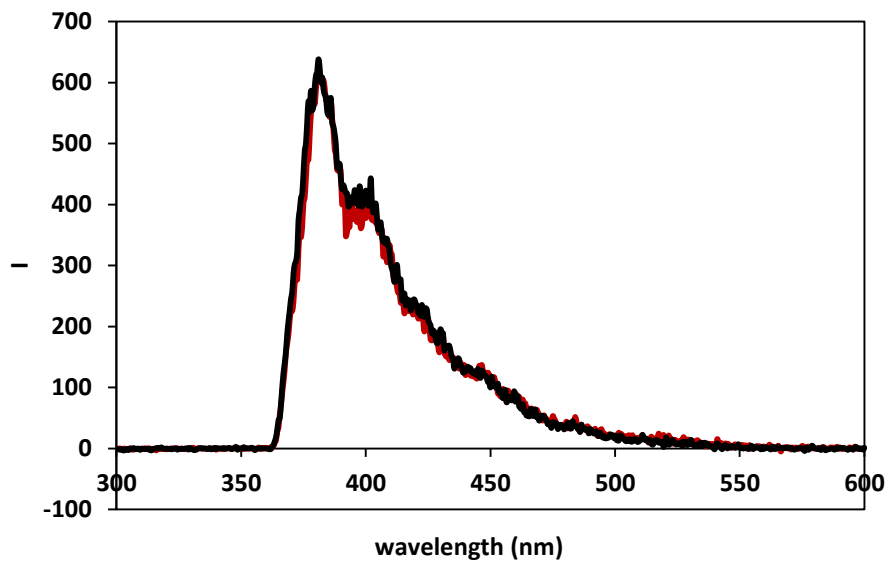


Figure 4.7: The emission spectra of compound 38b after gelation using the DMSO: Water (red) and GdL method (black). The excitation wavelength was 265 nm.

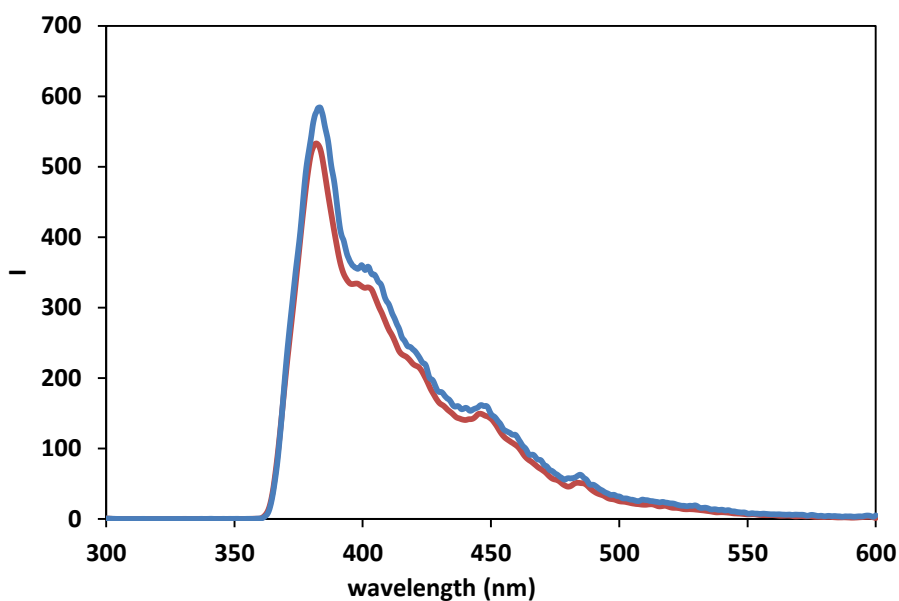


Figure 4.8: The emission spectra of compound 40 after gelation using the both methods, DMSO: Water (red) and GdL method (blue). The excitation wavelength was 265 nm.

Change in fluorescence with the gelation:

We studied the fluorescence of dipeptides functionalised with each aromatic group in solution and in the gel state. We followed the change of the fluorescence over time and after the self-assembly of the peptide. We have studied the emission of dipeptide conjugated to different aromatic groups before gelation (i.e. in the solution state) and

after forming a gel to compare between both states. The chemical structures of naphthalene and carbazole dipeptide derivatives are shown in the Figure 4.9. Figures 4.10, 4.11 and 4.12 show the emission results for compounds **12**, **72** and **56**, respectively in the solution and gel states when excited at 265 nm. From the Figures, it can be clearly seen that the intensity in the solution state is higher than that after forming gel. For example, the intensities of compound **12** at the maximum wavelength (353 nm) in the solution state and the gel state are 880 and 732 units respectively (Fig. 4.10). The decrease in the intensity after forming a hydrogel may be due to the self-quenching between the molecules due to an increase in the concentration of the dipeptide caused by the packing and stacking of the aromatic rings. This result is similar to that from other research on the fluorescence of Fmoc-dipeptides, where it has been shown that a red shift occurred and broad peak after gelation due to self-assembly and forming π - π stacking interactions between naphthalene rings^{24, 25}. Zhang *et al.*²⁵ also demonstrated that the intensity decreased after gelation due to the quenching and this result agrees with our data. This self-quenching occurs when the naphthalene rings π - π stack. Similarly, we noted that the intensity of compound **72** before gelation at the maximum wavelength of 410 nm was more than 1000 units (unfortunately, the LS55 has a maximum capacity of 1000 units), which decreased to 600 units after forming a hydrogel (Fig. 4.11).

Figure 4.12 shows the fluorescence results of the carbazole derivative (**56**). The data show different emission results from other conjugated dipeptides. After forming a hydrogel, a blue shift (decrease in wavelength) occurred. This blue shift might be indicating the formation of parallel orientations of carbazole moieties to give H-type aggregates^{26, 27}. This result has not been reported before for dipeptides hydrogels. Also, the emission spectrum shows decrease in the intensity after gelation (947 units in solution state and 800 units in the gel state) at the emission maximum wavelength of 365 nm. The decrease in the intensity after forming a hydrogel may again be due to self-quenching.

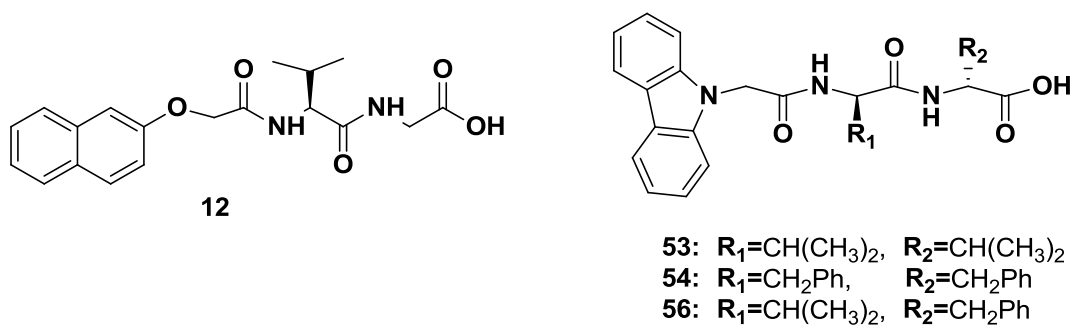


Figure 4.9: The chemical structure of compounds 12, 53, 54, and 56.

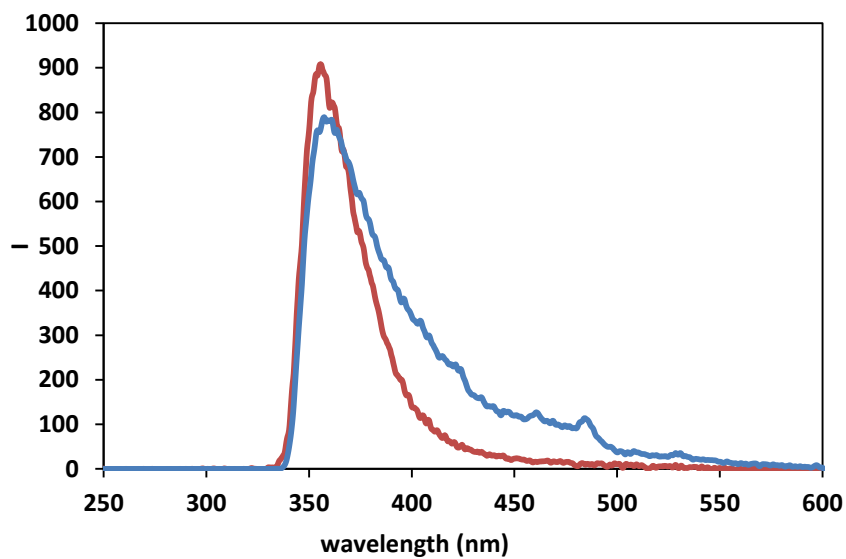


Figure 4.10: The emission spectra of compound 12 in solution (red) and the gel state (blue), showing a red shift after forming a gel, indicating to π - π stacking interactions. The excitation wavelength was 265 nm.

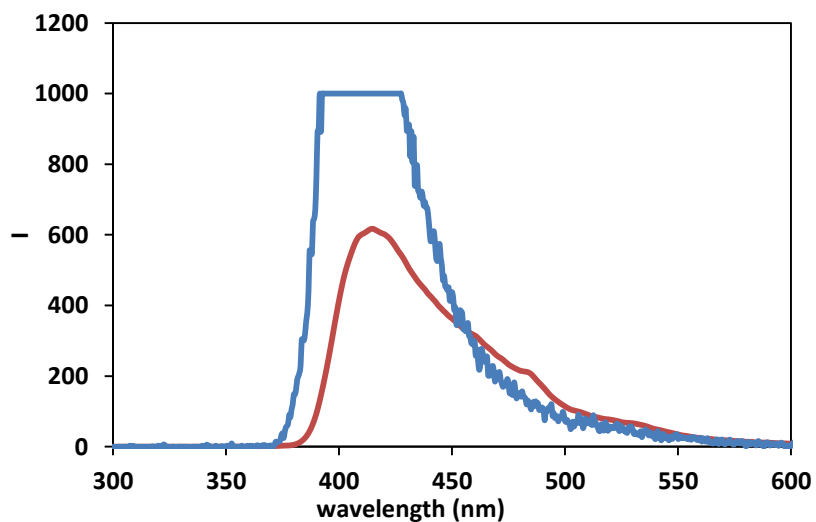


Figure 4.11: The emission spectra of pyrene dipeptide derivative in solution (blue) and in the gel state (red). The excitation wavelength was 265 nm.

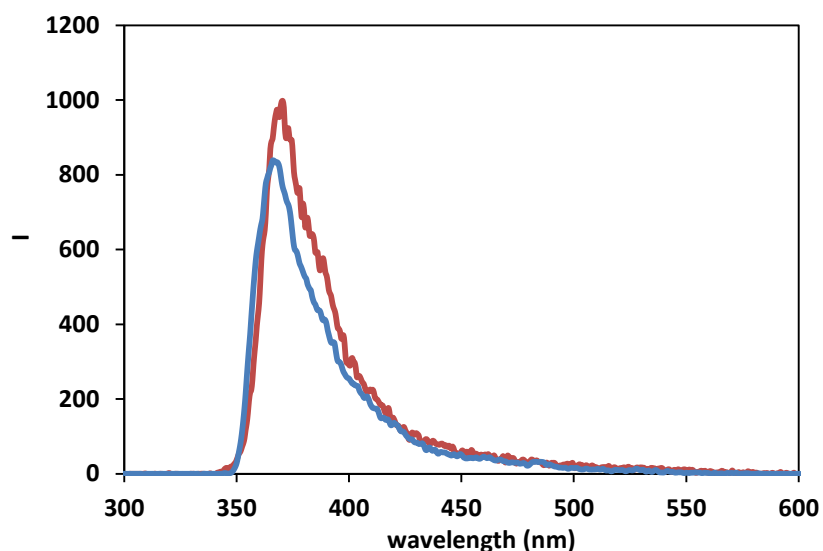


Figure 4.12: The emission spectrum of a carbazole dipeptide derivative in solution (red) and in the gel state (blue). The excitation wavelength was 265 nm.

Figure 4.13 (a) shows the intensity at 350 nm that were collected for the compound **16** that formed a transparent hydrogel using the GdL method at a concentration of 5 mg/mL over time. From Figure 4.13(a), we note that the fluorescence increased very quickly at early times after adding the GdL. Moreover, we noted that two plateaus occurred during the pH decrease. This implies that the assembly of the molecules occurs by two stages. This result agreed with previous work, where it was reported that two plateau occurred during the hydrogelation process, indicating that the self-assembly occurs by two stages²³. This was explained by the formation of fibres, followed by the aggregation of these fibres. Figure 4.13(b) shows the fluorescence emission spectra of the same hydrogel, 60 minutes after adding GdL, after 6 hours and after forming the hydrogel overnight. From Figure 4.13(b), we can see an increase of the intensity over the time. This is might be resulting from the differences in the environment at high and low pH; where the fibres have formed indicating the formation of the hydrogel, agreeing with previous research; where also has shown an increase of the fluorescence intensity when the pH decreased³.

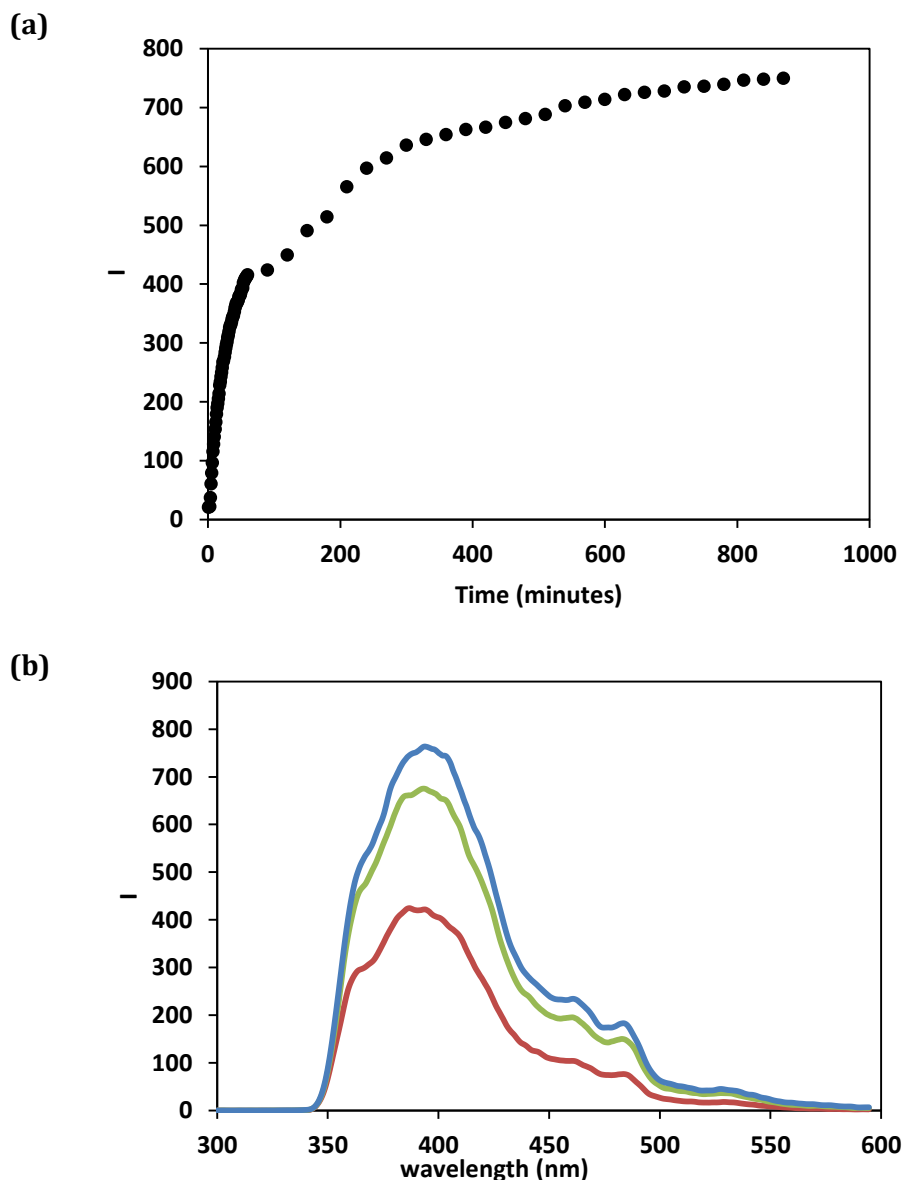


Figure 4.13: (a) The emission intensity at 350 nm of compound 16 over time after adding GdL. (b) The emission spectra (after 60 minutes of adding GdL (red), 6 hours after adding GdL (green) and after forming the hydrogel (blue)). The excitation wavelength was 265 nm.

Figure 4.14 shows the emission spectra of compound 72, which formed a transparent hydrogel using the GdL method at a concentration of 0.5 mg/mL. The compound emitted light at 450 nm when excited at 339 nm. The Figure 4.14 shows the spectra before adding GdL, 60 minutes after adding GdL and after 24 hours. We note that there was a decrease in the intensity after the addition of GdL, again probably due to self-quenching.

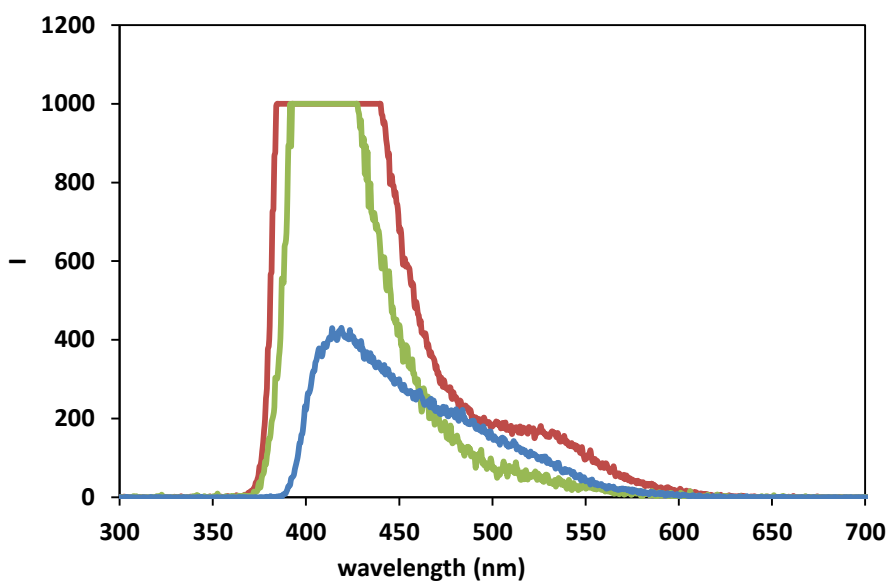
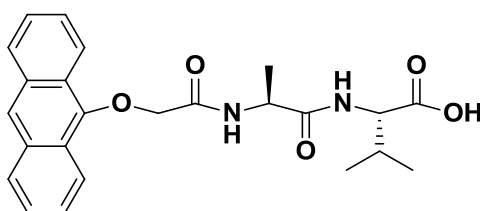


Figure 4.14: The emission spectra of compound 72 at concentration of 0.5 mg/mL, before adding GdL (red), after 60 minutes of adding GdL (green) and after forming a hydrogel overnight (blue). The excitation wavelength was 339 nm.

We also studied the emission of anthracene, phenanthrol and carbazole dipeptides at different excitation wavelengths (285 nm, 300 nm, and 360 nm) to understand their fluorescence properties and to know if they can be used for energy transfer. For instance, phenanthrol dipeptides (compound **40**) can emit light at 370 nm when excited at 285 nm as shown in Figure 4.16, while the maximum emission of the carbazole derivative (compound **56**) is 365 nm when excited at 285 nm as shown in Figure 4.17. Thus, energy transfer is unlikely to occur between naphthalene and carbazole derivatives, because they can emit light at the same excitation wavelength. Figures 4.16, 4.17 and 4.18 show the fluorescence results of compound **40** (Fig. 4.6), **56** (Fig. 4.9) and **75** (Fig. 4.15) respectively (all formed transparent hydrogels using the GdL method at concentrations of 5 mg/mL, 1 mg/mL and 5 mg/mL respectively), at different excitation wavelengths (285, 300, and 360 nm). From these data, we note that all the aromatic rings can emit light at the same excitation wavelength. For this reason, energy transfer might not occur between these aromatic groups. For example, Figure 4.16 shows the results of compound **40** when excited at different wavelengths. It can be seen that there are differences in the intensity at the maximum emission wavelength of 380 nm; the intensity increases as the excitation wavelength is increased. Also, from Figure 4.17 we

note that the intensity of compound **56** increased with increasing excitation wavelength. This increase of the intensity with an increase of the excitation wavelength is due to an increase of absorbing photons, because the molecule is excited by absorbing a photon from its ground state to its excited state, therefore at high excitation, the molecule absorbs more photons leading to increase the intensity. Also increasing the absorption of the photon could lead to shift of the peaks, therefore to the overlap of the peaks.



Compound 75

Figure 4.15: The chemical structure of compound 75.

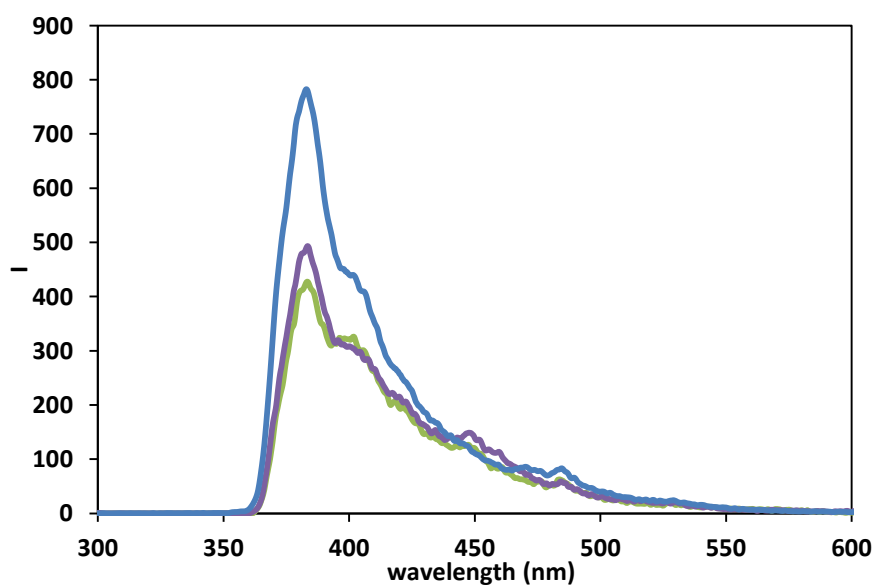


Figure 4.16: The emission spectra of compound 40 in the gel state at different excitation wavelengths (at 285 nm (green), 300 nm (purple), and at 360 nm (blue)).

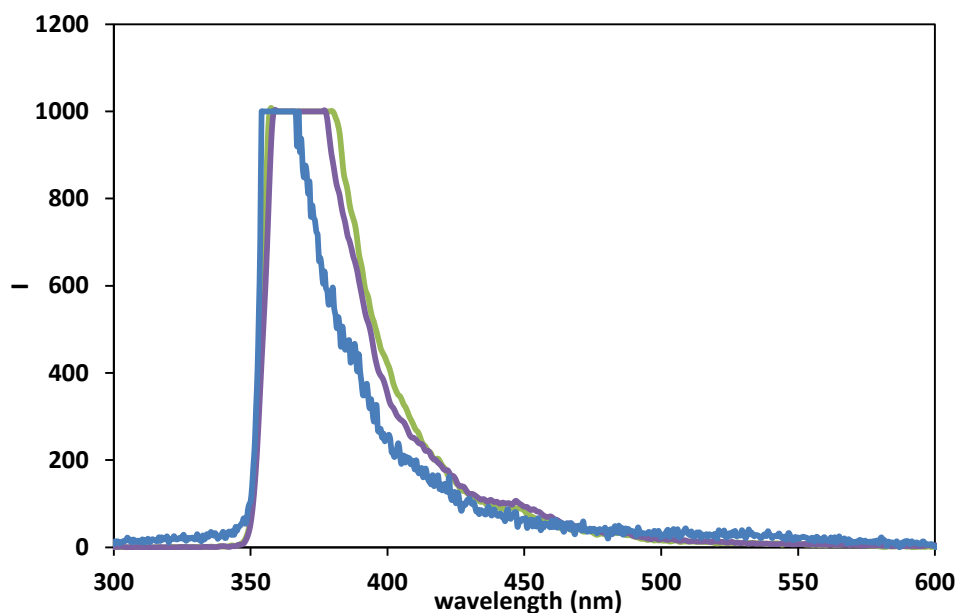


Figure 4.17: The emission spectra of compound 56 in the gel state at different excitations wavelengths (at 285 nm (green), 300 nm (purple), and at 360 nm (blue)).

Similarly, Figure 4.18 shows the emission results of compound **75** at excitations of 285 nm, 300 nm and 360 nm; hence the carbazole can emit light at the excitation wavelength of phenanthrol and anthracene. We have studied the emission at different excitation wavelengths for different aromatic groups because we attempted to find which aromatic ring can be used as a donor and which one can be used as an acceptor in order to study the energy transfer. From the above results, we can see that phenanthrol, anthracene, and carbazole dipeptides hydrogel are unlikely to be good pairs for energy transfer as the emission of the donor does not overlap the excitation of the acceptor.

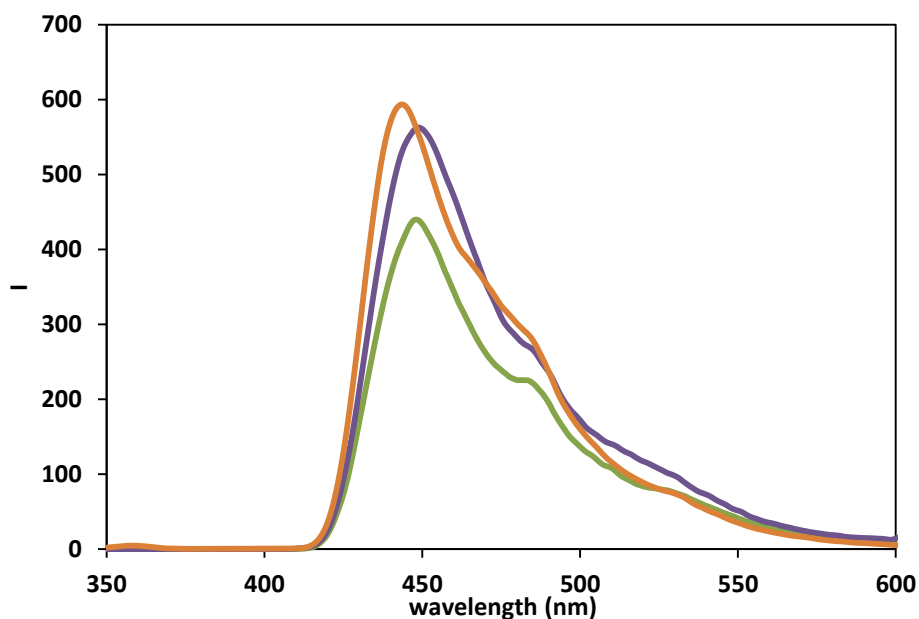


Figure 4.18: The emission spectra of compound 75 at pH 4 and at different excitation wavelengths (at 285 nm (green), 300 nm (purple), and at 360 nm (orange)).

We also compared the fluorescence spectra of peptides conjugated to carbazole, naphthalene, phenanthrol and pyrene at the same excitation wavelength (265 nm) (Fig. 4.19). From this Figure, we can see that all the functionalised dipeptides emitted light when excited at 265 nm. Moreover, we have compared the emission spectra of different dipeptides conjugated to the same aromatic group, carbazole (compounds **53**, **54**, and **56**) (Fig. 4.20). It can be clearly seen that changing the amino acids does affect the fluorescence results, because the dipeptide sequences have changed the properties of the carbazole, where they have different intensity and different fluorescence spectra, although they can be emitted at the same excitation wavelength. As a result, we can see that any small change in the hydrogelator by modifying the aromatic group or amino acid sequence can affect its molecular packing, hence affect its fluorescence properties.

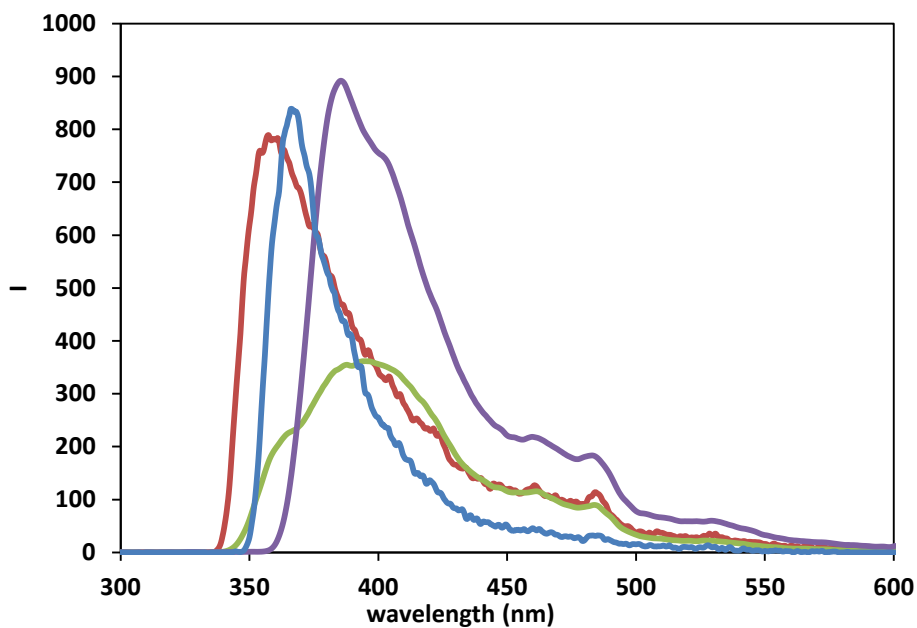


Figure 4.19: The emission spectra of dipeptides hydrogels based on different aromatic groups on excitation at 265 nm in the gel state;. The figure shows the fluorescence of compound 12 (red), compound 40 (purple), compound 56 (blue), and compound 72 (green).

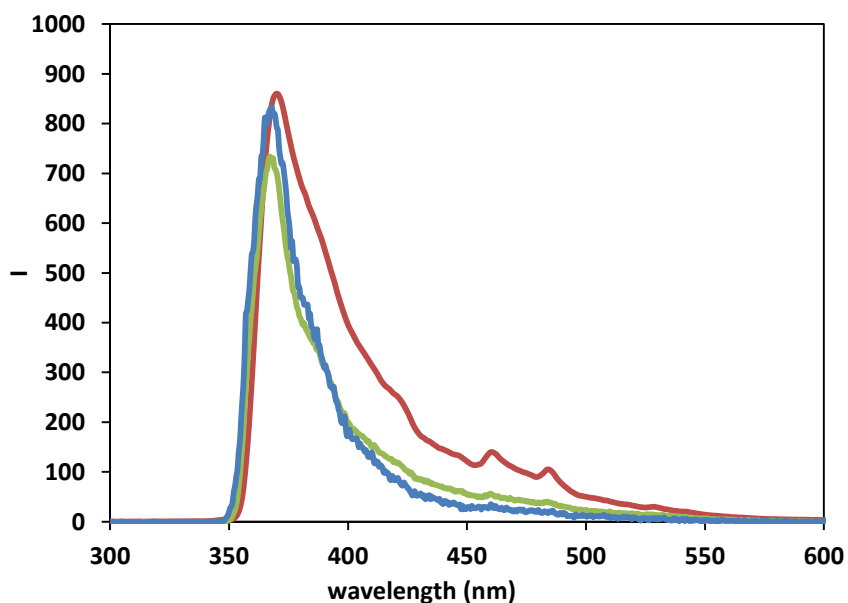


Figure 4.20: The emission spectra of carbazole hydrogels that have different amino acid sequence, compound 53 (red), compound 54 (green), and compound 56 (blue) in the gel state.

4.3.2- Energy transfer in hydrogels and organogels:

According to a previous research which illustrated that energy transfer occurred between naphthalene dipeptides and anthracene hydrogelators^{3, 15} or dansyl compounds³, we prepared hydrogels based on dipeptides conjugated to different aromatic rings to study fluorescence and energy transfer. We prepared hydrogels of two components of hydrogelators using the GdL method such as naphthalene and pyrene to study transfer energy from naphthalene (donor) to pyrene (acceptor) (as naphthalene can emit light at 355 nm and pyrene can be excited by light at 355 nm). However, the results showed no evidence of energy transfer (Fig. 4.22). We have tried with other aromatic groups such as phenanthrol and anthracene or naphthalene and carbazole (data are shown below in more detail, Figure 4.23 – 4.27), but there was no energy transfer, because for successful energy transfer between two aromatic groups, the emission of the donor must overlap the excitation of the acceptor. Also, the energy transfer depends on the distance between the donor and the acceptor. Here, from the results we attempted to find aromatic groups that can overlap each other, where one can be used as a donor and the other as an acceptor.

- **Mix two peptides:**

Previous research demonstrated that when two molecules are mixed to form a gel, these molecules may coassembly, self assemble randomly or self-sort²⁸. In a self-sorting system, the molecules separate between self and non-self. This system requires specific interaction or choice of molecules. Mixing two dipeptides such as Fmoc-dipeptide hydrogel system was demonstrated before²⁹. Other research has been reported that the self-sorting system can be achieved thermally³⁰ or by molecular trigger (where the order of the gelation can be controlled)^{31, 32}. Thermal self-sorting has been achieved by heating the solution containing two hydrogelators above the temperature required to allow dissolution of the hydrogelators completely, and then cooling the solution, where one hydrogelator assembles at a higher temperature than the other; hence the hydrogelation results in a self-sorted network³⁰. The molecular triggered self-sorting system has been demonstrated by choosing two hydrogelators that have different pK_a and assembly carried out using the GdL method^{31, 32}. The pK_a of the dipeptides is correlated to the hydrophobicity of the molecule³³. This can provide a molecular gelation trigger, where the assembly of the dipeptide start to occurs at the apparent pK_a .

Morris *et al.* showed that self-sorting of two gelators that have different pK_a can occur; where one gelator can assemble at higher pH than the other³¹. Here, mixing two dipeptides that have different pK_a using the GdL method may also result in self-sorted hydrogel. For example, mixing two dipeptides, **72** and **25**, which have different pK_a of 7.4 and 5.7 respectively (see Chapter 3) may lead to self-sorted system because **72** could self-assemble at higher pH than **25**. Similarly, the self-sorting system could occur between **12** and **62** or **40** and **62**, which also have different pK_a of 7.4 (**12**, **40**) and 5.7 (**62**).

We have studied the potential energy transfer between two peptides by preparing hydrogel containing two peptides such as naphthalene and anthracene, naphthalene and pyrene, carbazole and anthracene, pyrene and anthracene or phenanthrol and anthracene, using the GdL method. Figures 4.22 and 4.23 show energy transfer studies between two dipeptides conjugated to different aromatic groups. Figure 4.22 shows the results of the attempted energy transfer between compound **25** (Fig. 4.21) and compound **72**. Here, we added 0.01 mmol / 0.02 mmol of the pyrene dipeptide (**72**) to 4 mmol / 8 mmol naphthalene dipeptide. From Figure 4.22, we can see that there is no evidence for energy transfer occurring between naphthalene and pyrene because the data show just the emission peak of the naphthalene dipeptide when the system was excited at 265 nm. On increasing the amount of pyrene and changing the concentration of naphthalene dipeptide, the results were similar. This absence of energy transfer here might be due to the very low amount of pyrene dipeptide added compared to the naphthalene dipeptides.

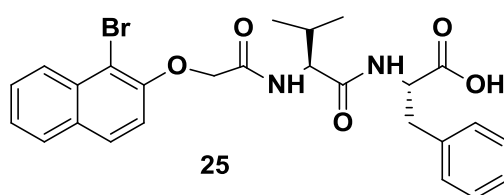


Figure 4.21: The chemical structure of compound **25**.

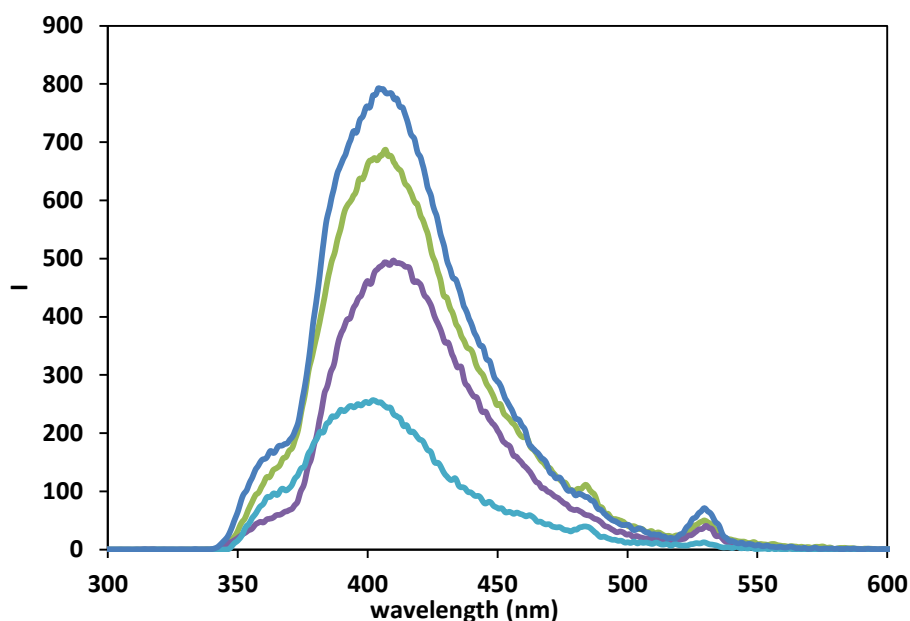


Figure 4.22: The data show the emission spectra of the energy transfer study between naphthalene and pyrene derivative. 10 μ L of compound 72 (1 mM) was added to 4 mM of compound 25 (light blue), 20 μ L to 4 mM of compound 25 (green), 10 μ L to 2 mM of compound 25 (blue colour), and 20 μ L to 2 mM of compound 25 (purple).

Figure 4.23 shows the energy transfer study between naphthalene and anthracene. We added 0.12 mmol / 0.05 mmol / 0.01 mmol of anthracene dipeptide (acceptor) to 28 mmol of naphthalene dipeptide (donor) and left the solution overnight to form hydrogel after adding GdL. Then, we studied the energy transfer on excitation at 265 nm (Fig. 4.23). The Figure shows the emission spectra of naphthalene dipeptide alone and the emission spectrum of the mixture of naphthalene and anthracene dipeptides at different concentrations of anthracene dipeptides to compare the emission spectrum between the naphthalene dipeptide alone and the mixture. The Figure does not show the emission spectrum of anthracene dipeptide alone because the anthracene dipeptide derivatives that we have synthesised did not form gels, while the mixture of this dipeptide with naphthalene dipeptide formed gel. From the Figure 4.23, we noted that the fluorescence data shows two emission peaks at 410 nm and at 371 nm. This is might be indicating to the overlapped emission peaks of naphthalene dipeptide and anthracene dipeptide, because we can see that the emission peak of the naphthalene dipeptide alone occurs in the wavelength (356 nm) that close to the small peak occurring in the emission spectrum of the mixture (at 371 nm) (with a small shift for the mixture that might be due to the

changing of the fluorescence properties after mixing two dipeptides). This may be implying that energy transfer occurred between these aromatic groups.

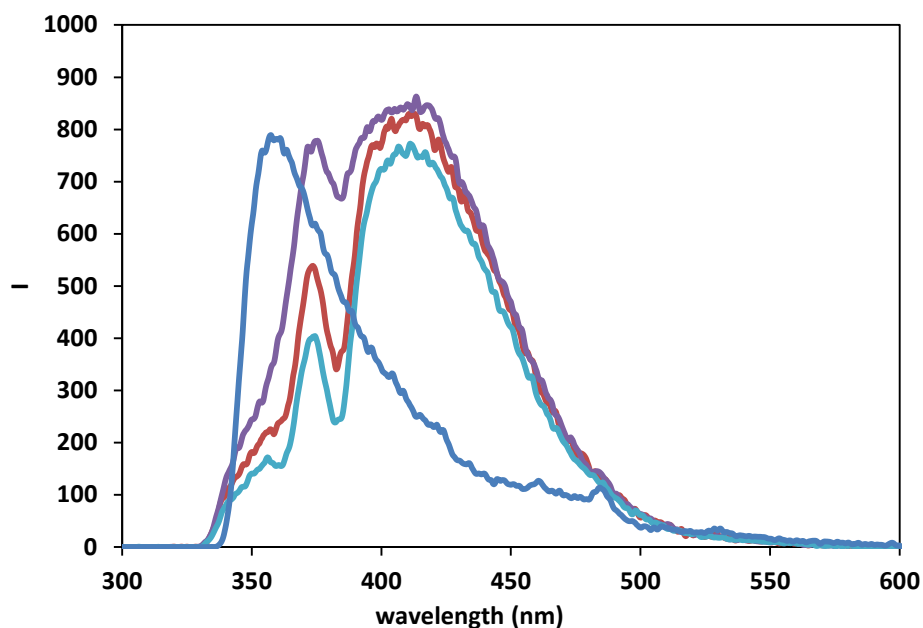


Figure 4.23: Energy transfer study between naphthalene and anthracene dipeptide derivatives in the gel state. The Figure shows the emission spectrum of the mixture dipeptides of compound 12 at concentration of 14 mM and different concentration of compound 62 (12 mM (light blue), 5 mM (red) and 1 mM (purple)) that was added to compound 12. Also it shows the emission spectrum of naphthalene dipeptide alone (blue) between its emission spectrum and the overlapped spectrum.

Figure 4.24 shows the energy transfer study between carbazole dipeptide (donor) and anthracene dipeptide (acceptor). We added 0.12 mmol / 0.05 mmol of anthracene dipeptide to 8 mmol of carbazole dipeptide. Also the Figure shows the emission spectrum of carbazole dipeptide alone to compare between the fluorescence of dipeptide hydrogel alone and the mixture (the emission spectrum of anthracene dipeptide alone was not studied because anthracene dipeptide derivatives did not form gels). From the Figure 4.24, we can see that there are two small peaks occurred at 365 nm and 387 nm. These two peaks might be arise from the overlapped emission peaks of carbazole dipeptide and anthracene dipeptide, because, it can be seen that the emission spectrum of the carbazole dipeptide alone showed one peak at the same wavelength of the small peak occurring in the emission spectrum of the mixture at 365 nm. This may implying that energy transfer might be occurred between these aromatic groups, but

the figure does not show clear peaks due to adding low amount of anthracene compared to the amount of carbazole.

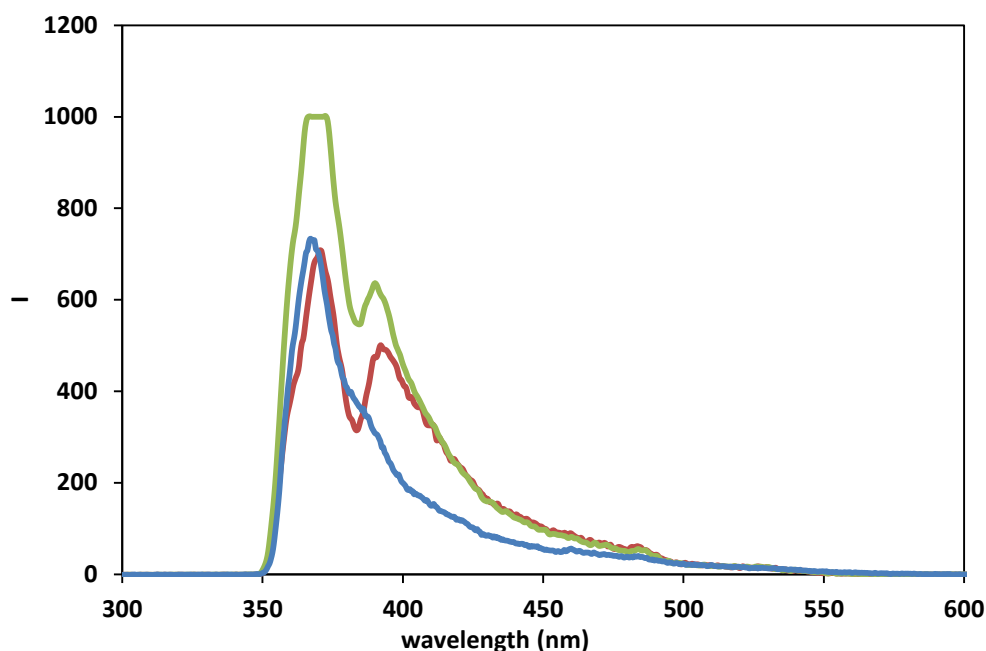


Figure 4.24: Energy transfer study between carbazole and anthracene dipeptide derivative in the gel state. Compound 54 was used at a concentration of 4 mM and different concentration of compound 62 was added; 12 mM (red) and 5mM (green). Also it shows the emission spectrum of carbazole dipeptide alone (blue) to compare between its emission spectrum and the overlapped spectrum

We also compared the fluorescence behaviour of compounds **54**, **72** and the mixed gelators on excitation of 265 nm (Fig. 4.25). From the Figure we can see that the emission spectrum of carbazole dipeptide alone occurs at different wavelength from pyrene dipeptide alone spectrum when they excited at the same wavelength (265 nm) and the emission spectrum of the mixture shows just one broad peak. This is indicating to that there is no energy transfer between the carbazole and pyrene dipeptides.

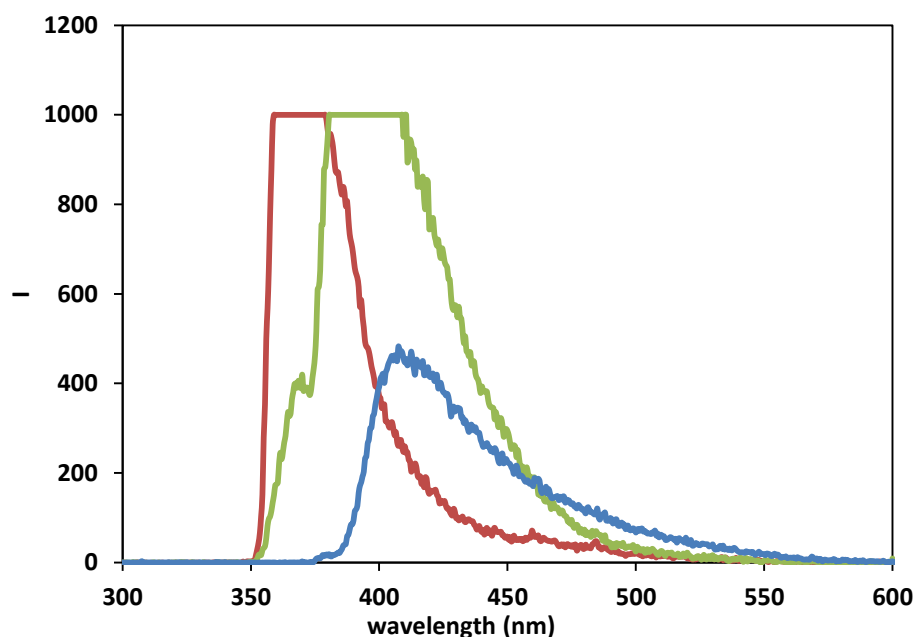


Figure 4.25: Emission spectra for compound 54 (red), compound 72 (blue), and the mixed of 54 and 72 (green) in the gel state.

Furthermore, energy transfer was studied between compound **72** (donor) and compound **62** (acceptor) at excitation of 265 nm (Fig. 4.26). We added 0.12 mmol of anthracene dipeptide to 2 mmol of pyrene dipeptide and left the solution overnight to form hydrogel after adding GdL. The Figure 4.26 also shows the emission spectrum of pyrene dipeptide alone to compare between its emission spectrum and the emission spectrum of the mixed dipeptides to illustrate whether energy transfer between pyrene and anthracene dipeptides occurs or not. From the Figure 4.26, we noted that there are two emission peaks resulting from mixing pyrene and anthracene dipeptides. One peak occurs at 410 nm, and the other peak at 522 nm. Also, the emission spectrum of the pyrene dipeptide alone shows one peak at the same wavelength (at 410 nm) of one peak for the emission spectrum of the mixture. The two overlapped peaks that result from the mixture might indicate to the occurrence of energy transfer between the pyrene dipeptide and anthracene dipeptide.

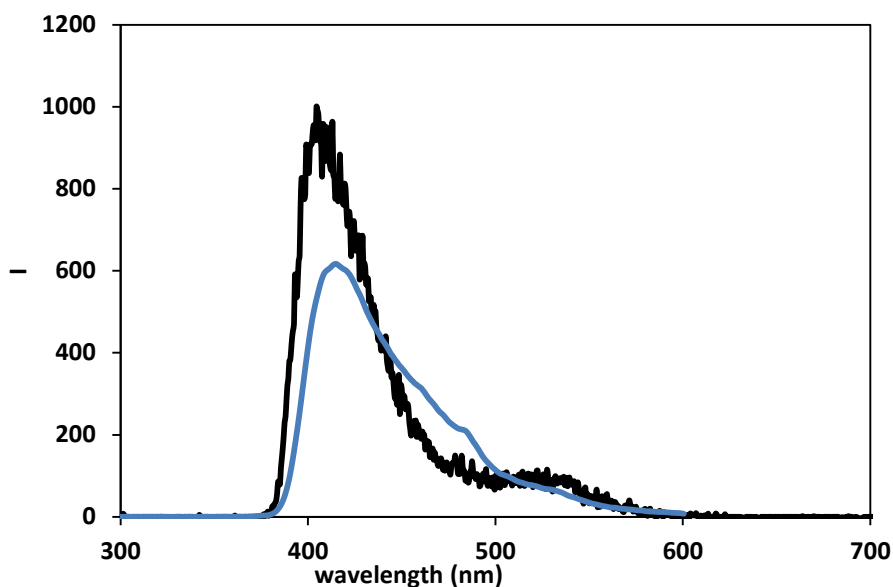


Figure 4.26: Energy transfer study between pyrene and anthracene dipeptide derivative (black) and emission spectrum of pyrene dipeptide alone (blue) in the gel state.

Figure 4.27 shows the energy transfer study between compound **40** as a donor and compound **62** as an acceptor. We added 0.12 / 0.05 mmol of anthracene dipeptide to 22 mmol of phenanthrol dipeptide and left the solution overnight to form hydrogel after adding GdL. It also shows the emission spectrum of phenanthrol dipeptide hydrogel alone (the emission spectrum of anthracene dipeptide did not study because the anthracene dipeptide derivative did not form hydrogel alone as we explained above). From the Figure 4.27, we can see that there are two peaks at about 370 nm and 398 nm resulting from the emission spectrum of the mixed dipeptide hydrogel. Also we noted that the emission spectrum of phenanthrol dipeptide alone occurs in the same wavelengths with two peaks at similar wavelengths (at 380 nm and 395 nm). Therefore, we demonstrated that the energy transfer might not be occurring between phenanthrol and anthracene because the amount of anthracene dipeptide that added was very low compared to the amount of the other dipeptide (phenanthrol dipeptide).

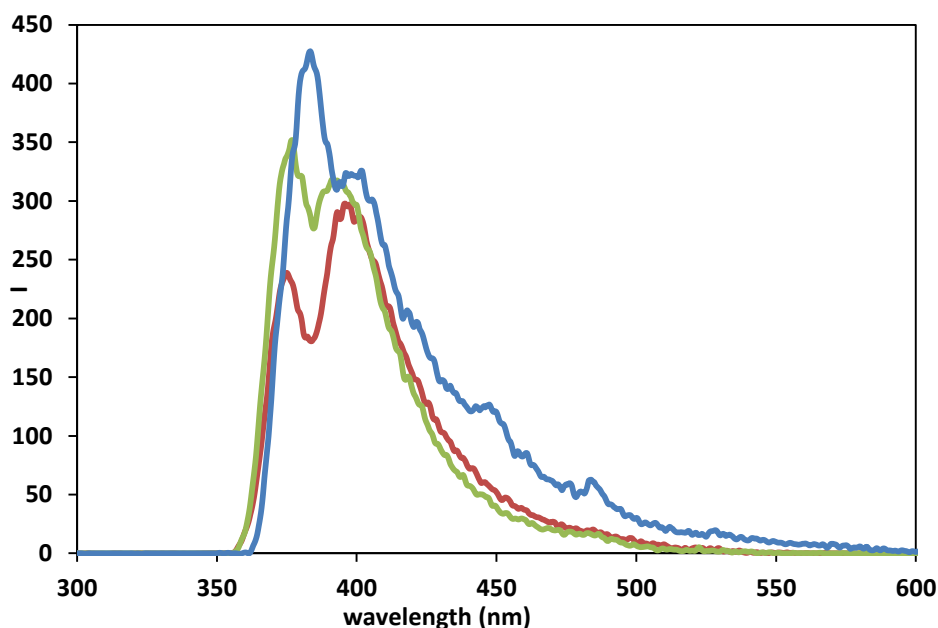


Figure 4.27: Energy transfer study between phenanthrol and anthracene dipeptide derivative in the gel state at different concentrations of anthracene (12 mM (red), 5 mM (green)). The Figure also shows the emission spectrum of phenanthrol dipeptide alone (blue).

- **Mix peptide with dansyl:**

We also attempted to study energy transfer between dipeptide derivatives (donor) and dansyl derivative (acceptor) because the energy transfer between naphthalene dipeptides and dansyl derivative was successfully studied previously³. Here, we have tried with different functionalised dipeptide as a donor.

Figure 4.29 shows energy transfer study between compound **40** as a donor and a dansyl derivative (Fig. 4.28) as an acceptor. Here, we added 0.034 mmol of dansyl derivative to 22 mmol of phenanthrol dipeptide derivative. From the Figure 4.29, we note that there are two emission peaks, one between 350 nm and 450 nm (which is similar to the emission spectrum of compound **40** alone) and another broad peak between 470 nm and 600 nm, which is similar to the spectrum of dansyl derivative. This result indicates that the dansyl derivative has been incorporated into the gel fibres, hence the energy transfer occurred between the phenanthrol dipeptide and dansyl derivative.

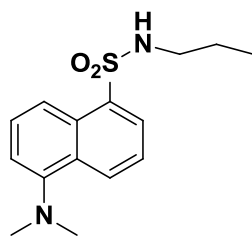


Figure 4.28: The chemical structure of the dansyl derivative used here.

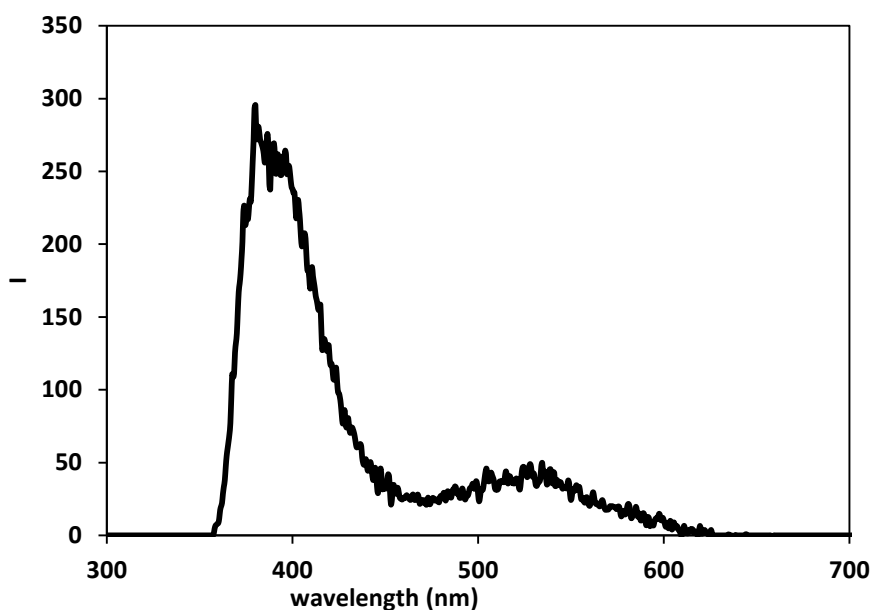


Figure 4.29: Energy transfer study between phenanthrol and dansyl derivative at concentration of 3.4 mM in the gel state. The excitation wavelength was 265 nm.

Furthermore, we studied the energy transfer between a carbazole derivative (compound **54** at concentration of 4 mM) and a dansyl derivative (at concentration of 10 mM) using an excitation wavelength of 265nm over time with amounts of 20 μ L of the dansyl solution added to the carbazole solution (Fig. 4.30). We added 0.2 mmol of dansyl derivative to 8 mmol of carbazole dipeptide derivative and left the solution overnight to form hydrogel after adding equivalent amount of GdL. The Figure shows the emission spectrum results before adding GdL and at different times after adding GdL. From the Figure 4.30, it can be seen that energy transfer occurred between the carbazole dipeptide and dansyl derivative; two emission peaks were present. We also note that the intensity of emission spectrum was high before adding GdL and then decreased with time to reach the lowest intensity after forming gel (after 19 hours), again due to self-quenching. As a result, we note that although all functionalised

dipeptides can emit light on excitation at the same wavelength, energy transfer has occurred between some derivatives, pyrene and anthracene, phenanthrol and dansyl, and between carbazole and dansyl. Other mixture that showed no energy transfer occurred might result from the low amount of the acceptor that added compared to the amount of the donor.

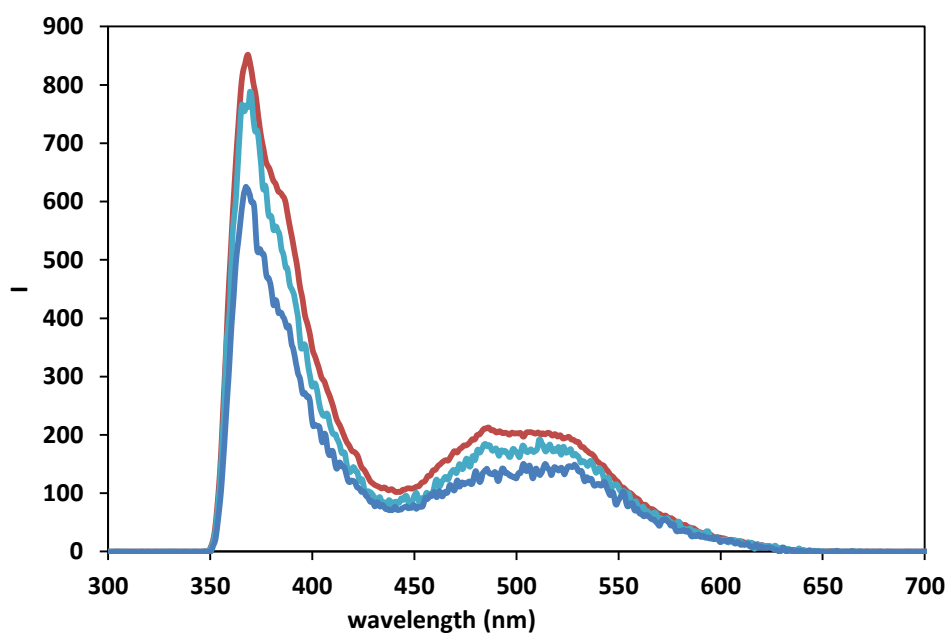


Figure 4.30: Energy transfer study between carbazole and dansyl derivatives (add 20 μ L of the concentration of 10mM), overnight (before adding GdL (red), after 60 minutes (light blue), after forming hydrogel (after 19hours) (blue).

Furthermore, the quantum yield (QY) of this system has not been measured (QY is the ratio between the number of photons emitted to the number of photons absorbed). For the clear occurrence of energy transfer, the QY of the donor must be high. Here, if we compare the known QY of one aromatic ring (donor) to other aromatic ring (acceptor), we might assume the efficiency of the QY on the energy transfer. For example, the QY of pyrene is (0.32) and the QY of anthracene is (0.32³⁴) and so QY of the both rings is similar. This value of the QY is high and may be indicative that the loss of the energy in the gel state is very low; hence, the efficiency of the energy transfer might be affected³⁵.

Moreover, according to our results, it can be seen that the efficiency of the energy transfer might be affected by the system of how the hydrogel formed, self-sorting or a random system formed (Fig. 4.31). Here, there are two different components to form hydrogel in order to study energy transfer, one containing dipeptide and dansyl and the other containing two functionalised dipeptides. In the system containing dansyl, the energy transfer is probably not affected by how the hydrogel formed, because the dansyl is hydrophobic molecule and it will 'stick' to the other hydrophobic environment and energy transfer then occurs between them. On the other hand, whether energy transfer between two dipeptides may depend on the type of the self-assembly system formed, i.e. if a self-sorting or a random system occurs. If a self-sorting results from the hydrogelation of two dipeptides, it is difficult to know if energy transfer can occur or not. The fibres resulted from the self-sorting might be close enough to each other to transfer energy between two aromatic units or they might not. In contrast, if the hydrogelation result in a random fibres formed, this may refer to the possibility of transfer energy between dipeptides because the efficiency of the energy transfer depends on the distance between the dipeptide fibres and from this we hypothesise that energy transfer will occur if two mixed components form a random fibre. It is still unclear whether the mixing of two peptides can be self-sorted or forms random fibres, and this may give expand to this project to be studied in more details.

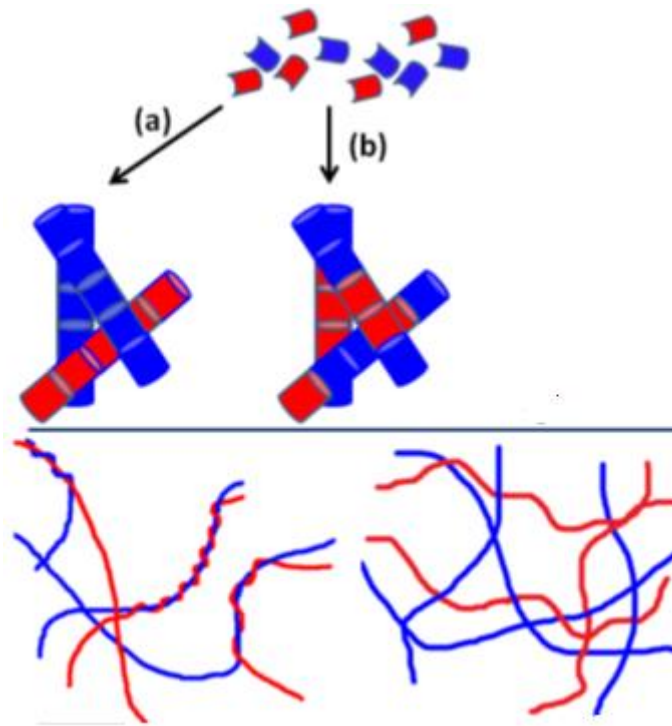


Figure 4.31: Top: Schematic of possible assembly of two LMWG into fibres. (a) Self-sorting; (b) random co-assembly. Bottom: Two hypothetical networks formed from a self-sorted system, where entanglement of the self-sorted fibres occurs (left) or an interpenetrated network forms (right)³².

4.4- Conclusion:

In conclusion, we synthesised peptides conjugated to different aromatic group such as pyrene, carbazole, 2-anthraquinone and 9-anthracene as explained in Chapter 2. Hydrogels have been prepared from these dipeptides. In this Chapter, we carried out a fluorescence study of the dipeptides that formed transparent hydrogels in order to study potential energy transfer between two different aromatic groups. The fluorescence of naphthalene, pyrene, anthracene, phenanthrol and carbazole dipeptides was studied. The results showed that all dipeptides conjugated to different aromatic groups can emit light at the same excitation with different fluorescence properties. Previous research illustrated that energy transfer occurred between naphthalene dipeptides and anthracene hydrogelators or dansyl compounds³. We carried out similar work using different functionalised dipeptides hydrogels to study the energy transfer. As a result, energy transfer has occurred between some dipeptide derivatives (pyrene and anthracene dipeptides), and between dipeptide and dansyl derivative (phenanthrol and dansyl, and carbazole and dansyl). These results indicated that energy transfers can occur between two dipeptides hydrogel or between dipeptide and dansyl derivative. In other cases, no evidence for energy transfer was found. This may imply that the packing of the fibres is important for energy transfer and this should be the focus of future work.

Table (4.3) shows the summary of the pairing that successfully transferred energy. The successful energy transfer occurred between pyrene and anthracene dipeptide derivatives, phenanthrol dipeptide and dansyl derivative, and carbazole dipeptide and dansyl derivative.

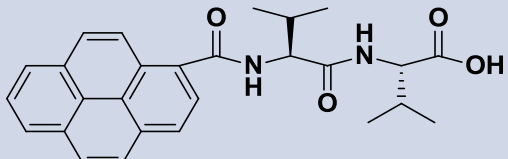
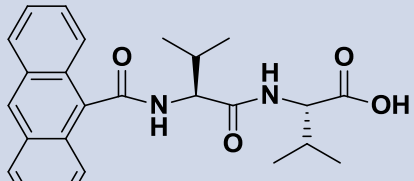
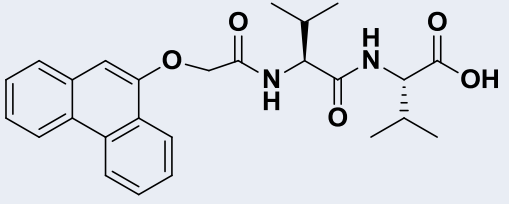
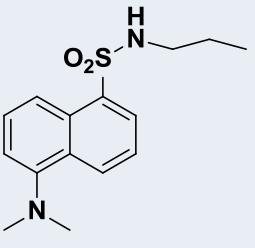
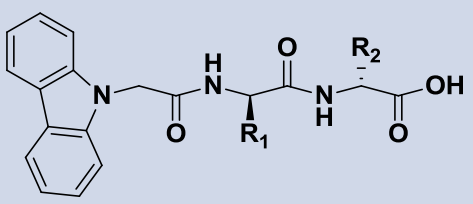
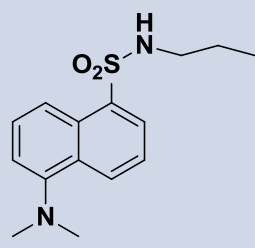
Donor	Acceptor
 <p style="text-align: center;">72</p>	 <p style="text-align: center;">62</p>
 <p style="text-align: center;">40</p>	 <p style="text-align: center;">Dansyl</p>
 <p style="text-align: center;">54</p>	 <p style="text-align: center;">Dansyl</p>

Table 4.3: The summary of the pairing that successfully transferred energy

4.5- References:

1. W. T. Truong, Y. Su, J. T. Meijer, P. Thordarson and F. Braet, *Chemistry – An Asian Journal*, 2011, **6**, 30-42.
2. G. Cheng, V. Castelletto, R. R. Jones, C. J. Connon and I. W. Hamley, *Soft Matter*, 2011, **7**, 1326-1333.
3. L. Chen, S. Revel, K. Morris and D. J. Adams, *Chemical Communications*, 2010, **46**, 4267-4269.
4. K. V. Rao, K. K. R. Datta, M. Eswaramoorthy and S. J. George, *Angewandte Chemie International Edition*, 2011, **50**, 1179-1184.
5. K. V. Rao, K. K. R. Datta, M. Eswaramoorthy and S. J. George, *Chemistry – A European Journal*, 2012, **18**, 2184-2194.
6. V. D. Rao, K. Eswaramoorthy, M. and George, S. , *Angew. Chem. Int. Ed.*, 2010, **49**, 1-7.
7. D. J. Adams and P. D. Topham, *Soft Matter*, 2010, **6**, 3707-3721.
8. A. Ajayaghosh, V. K. Praveen and C. Vijayakumar, *Chemical Society Reviews*, 2008, **37**, 109-122.
9. L. Zang, Y. Che and J. S. Moore, *Accounts of Chemical Research*, 2008, **41**, 1596-1608.
10. D. Rizkov, J. Gun, O. Lev, R. Sicsic and A. Melman, *Langmuir*, 2005, **21**, 12130-12138.
11. T. Nakashima and N. Kimizuka, *Advanced Materials*, 2002, **14**, 1113-1116.
12. M. Montalti, L. S. Dolci, L. Prodi, N. Zaccheroni, M. C. A. Stuart, K. J. C. van Bommel and A. Friggeri, *Langmuir*, 2006, **22**, 2299-2303.
13. K. J. Channon, G. L. Devlin and C. E. MacPhee, *Journal of the American Chemical Society*, 2009, **131**, 12520-12521.
14. S. Banerjee, R. K. Das and U. Maitra, *Journal of Materials Chemistry*, 2009, **19**, 6649-6687.
15. A. L. Olive, A. Guerzo, C. Belin, J. Reichwagen, H. Hopf and J.-P. Desvergne, *Research on Chemical Intermediate*, 2008, **34**, 137-145.
16. B. Adhikari, J. Nanda and A. Banerjee, *Chemistry – A European Journal*, 2011, **17**, 11488-11496.
17. C. B. Murphy, Y. Zhang, T. Troxler, V. Ferry, J. J. Martin and W. E. Jones, *The Journal of Physical Chemistry B*, 2004, **108**, 1537-1543.
18. T. W. J. Gadella Jr, G. N. M. van der Krogt and T. Bisseling, *Trends in Plant Science*, 1999, **4**, 287-291.
19. S. A. Hussain, *Science Journal of Physics*, 2012, **2012**, 1-4.
20. H.-C. Chen, C.-Y. Hung, K.-H. Wang, H.-L. Chen, W. S. Fann, F.-C. Chien, P. Chen, T. J. Chow, C.-P. Hsu and S.-S. Sun, *Chemical Communications*, 2009, **27**, 4064-4066.
21. K. V. Rao, A. Jain and S. J. George, *Journal of Materials Chemistry C*, 2014, **2**, 3055-3064.
22. B. Adhikari and A. Banerjee, *Soft Matter*, 2011, **7**, 9259-9266.
23. L. Chen, K. Morris, A. Laybourn, D. Elias, M. R. Hicks, A. Rodger, L. Serpell and D. J. Adams, *Langmuir*, 2009, **26**, 5232-5242.
24. C. Tang, R. Ulijn and A. Saiani, *The European Physical Journal* 2013, **36**, 1-11.
25. Y. Zhang, H. Gu, Z. Yang and B. Xu, *Journal of the American Chemical Society*, 2003, **125**, 13680-13681.
26. S. Das, S. L. de Rooy, A. N. Jordan, L. Chandler, I. I. Negulescu, B. El-Zahab and I. M. Warner, *Langmuir*, 2011, **28**, 757-765.
27. A. S. Weingarten, R. V. Kazantsev, L. C. Palmer, M. McClendon, A. R. Koltonow, P. S. Samuel Amanda, D. J. Kiebal, M. R. Wasielewski and S. I. Stupp, *Nature Chemistry*, 2014, **6**, 964-970.
28. L. E. Buerkle and S. J. Rowan, *Chemical Society Reviews*, 2012, **41**, 6089-6102.
29. W. Helen, P. de Leonardis, R. V. Ulijn, J. Gough and N. Tirelli, *Soft Matter*, 2011, **7**, 1732-1740.
30. M. M. Smith and D. K. Smith, *Soft Matter*, 2011, **7**, 4856-4860.
31. K. L. Morris, L. Chen, J. Raeburn, O. R. Sellick, P. Cotanda, A. Paul, P. C. Griffiths, S. M. King, R. K. O'Reilly, L. C. Serpell and D. J. Adams, *Nature Communications* 2013, **4**, 1-6.

32. C. Colquhoun, E. R. Draper, E. G. B. Eden, B. N. Cattoz, K. L. Morris, L. Chen, T. O. McDonald, A. E. Terry, P. C. Griffiths, L. C. Serpell and D. J. Adams, *Nanoscale*, 2014, **6**, 13719-13725.
33. L. Chen, S. Revel, K. Morris, L. C. Serpell and D. J. Adams, *Langmuir*, 2010, **26**, 13466-13471.
34. A. G. L. O. Jean-Pierre Desvergne, Neralagatta M. Sangeetha, Jens Reichwagen, Henning Hopf and André Del Guerso, *Pure Appl. Chem.*, 2006, **78**, 2333-2339.
35. A. Del Guerso, A. G. L. Olive, J. Reichwagen, H. Hopf and J.-P. Desvergne, *Journal of the American Chemical Society*, 2005, **127**, 17984-17985.

CHAPTER 5

Controlled Release

5- The controlled release:

5.1- Introduction:

Hydrogels are a 3D dimensional network that can be prepared using different methods¹⁻¹². Of relevance to this Thesis are hydrogels prepared using LMWG dipeptides^{13, 14}. These hydrogels have been used in some biomedical applications such as cell culturing^{15, 16} and drug delivery¹⁷⁻¹⁹. Drug delivery systems such as injections, tablets or sprays must deliver the correct dose of the drug in an efficient manner. Often, a controlled release is needed so that the drug is effective for a reasonable period of time. In a drug delivery system, the concentration of the drug increases to reach the maximum peak and then it falls off so that another dose needs to maintain the effective of the drug. If the concentration of the drug increases above the maximum range, this may cause the toxicity. Also, if the concentration of the drug falls below the minimum level, the drug will be ineffective²⁰. To control and maintain the effective level of drugs, we have to study new controlled release systems.

Drug delivery in hydrogels has had great attention since the 1960s²¹. Although the first hydrogels that were prepared were not suitable for the purpose of controlled release because some of them were toxic, it is possible that the LWMG gels based on peptides may be appropriate to be used as a scaffold because they are easy to remove and release when no longer needed. Some examples of LMWG hydrogels based on amino acids and peptides have been used for controlled release, for example hydrogels based on FmocF and FmocY¹⁷. Other examples include hydrogels based on FmocFF^{12, 22, 23}. The controlled release from a hybrid hydrogel based on FmocFF and konjac glucomannan (KGM) has been studied²⁴. The hydrogel was prepared by the self-assembly of FmocFF in a solution of KGM. This study provides a new self-assembly of peptide-polysaccharide hybrid hydrogels and also provides a new sustained-release drug carrier. Docetaxel was used as a model of hydrophobic drugs and incorporated into hydrogel to study the release properties of the hydrogel. Different concentrations and molecular weights of KGM solutions were prepared for controlled release experiments. The results showed that the release rate increased with hydrogel prepared in KGM more than that without the KGM. Also the mechanical properties showed that the hybrid hydrogel (FmocFF conjugate to KGM) was higher (G') than FmocFF hydrogel. This means that KGM

increases the mechanical properties of the hydrogel. In all these cases, the controlled release of a model dye from the hydrogel to a solution placed on the top of the hydrogel was studied^{14, 25} (Fig. 5.1).

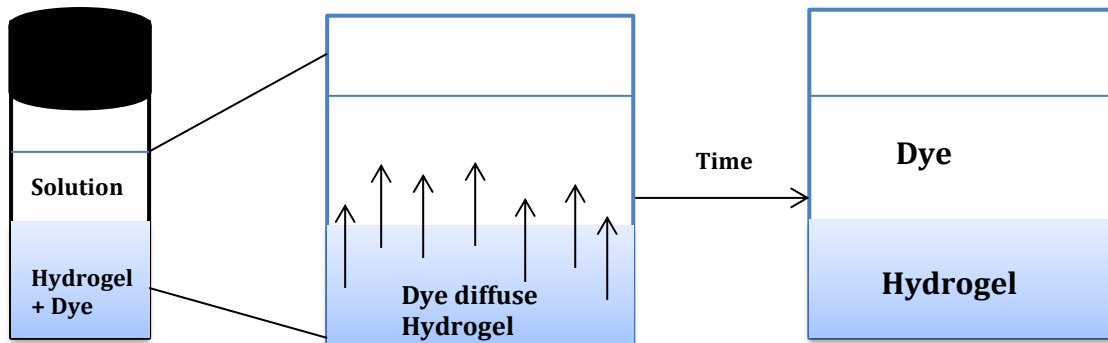


Figure 5.1: the controlled release study of the dye from hydrogel.

To measure the rates of release, the diffusion coefficient (D) of each (dye/gel) system can be calculated^{13, 26} using the non-steady-state diffusion model equation:

$$M_t/M_\infty = 4(Dt/\pi\lambda^2)^{1/2}$$

Where M_t is the total amount of molecules released during the measurement, M_∞ is the total amount of molecules that are loaded at the start, λ is the hydrogel thickness, t is the time of the measurement and D is the diffusion coefficient of the molecules²⁴. If the results show a linear relationship between M_t/M_∞ and the square root of time, this indicates that the release of dye from the hydrogel is under Fickian control²⁷.

To investigate dipeptide hydrogels for drug delivery, we have decided to study the controlled release of a model dyes from the hydrogel. To do this, we have to control factors that are important for controlled release such as the pH, the mesh size, the microstructure and the strength of the gel. We have used the solvent switch method, using DMSO and water, to control the microstructure because the hydrogel should be injectable¹⁴ (Fig. 5.2). Also, by using the solvent switch method, the hydrogel is formed in a few minutes compared to the GdL method, which takes overnight to fully form the gel.



Figure 5.2: an example of image of injectable hydrogel loaded dyes using DMSO: Water method. The gels were prepared in a syringe and then injected on to a microscope slide through a needle.

Also, we studied the release of the hydrogel at different concentrations. We thought that this would allow us to control the mesh size²⁸, which is important as the rate of the release increases with increase of the mesh size. Therefore, by studying the concentration of LMWG, we can find which the best concentration for controlling the rate of the release. Furthermore, we have studied the release of the hydrogels at different pHs. For drug delivery, we have to choose the dipeptide that can form a hydrogel at pH 7 (the pH of the body). Moreover, we have studied the rheology of the hydrogel loaded with dyes. We need to ensure that the hydrogel will remain stable as a scaffold while it delivers the drug. Therefore, to be a good gelator, a good peptide should form hydrogel at pH 7, at a concentration that forms strong gel using the solvent switch method, must be injectable and must allow us to control the rate of the release for drug delivery application.

5.2- Experimental section:

The hydrogels that were used to study controlled release were prepared using the solvent switch method described in Chapter 3, but we loaded dyes in the water. These dye solutions were added to solutions of the gelators in DMSO. The peptide that was used for controlled release was FmocFF (Fig. 5.3) and compound **42** (Fig. 5.4). We have chosen these dipeptides because the FmocFF was commonly used as a good hydrogelator and in controlled release. It has been used previously for controlled release by using different dyes and method of the release study¹⁷, therefore we used this gelator as a control. We have used other dyes here to probe the effect of dye solubility

and size. The other gelator, compound **42**, was chosen because it is the only peptide prepared in this Thesis that forms hydrogel at pH 7.

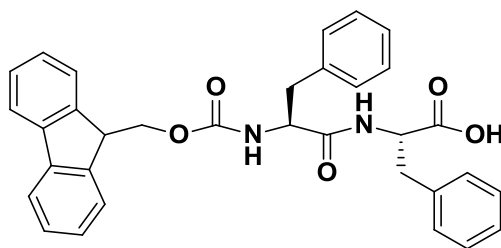


Figure 5.3: The chemical structure of FmocFF.

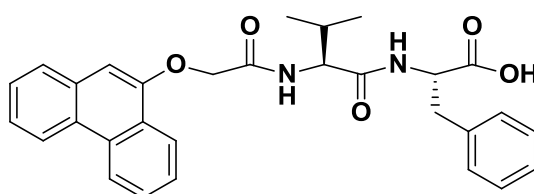
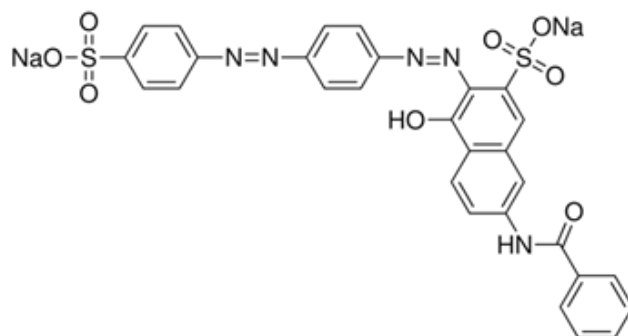
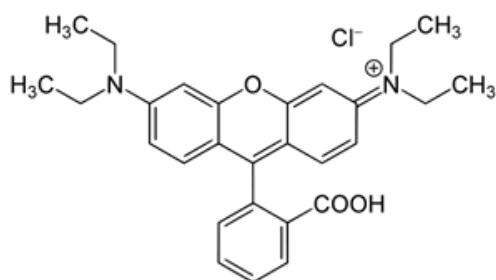


Figure 5.4: The chemical structure of compound **42**.

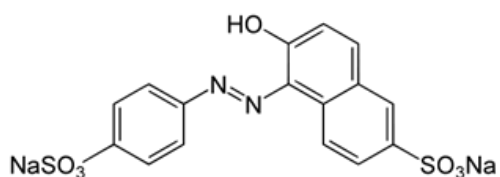
Dyes used in this study were Direct Red 81 (**DR**), Rhodamine B (**RB**) and Sunset Yellow (**SN**). Figure 5.5 shows the chemical structures of the dyes. We have chosen these dyes because they have different structure, different molecular weight and different hydrophobicity, therefore we can study the release rate of each dye and compare the results between them and also to correlate between the release rate and the molecular weight, the structure and the hydrophobicity of the dye. All of these dyes were used at a concentration of 0.078 mg/mL. The concentration was chosen according to the calibration curves; where is the UV-vis data at this concentration showed a good peak and absorption of the dyes.



Direct Red 81 (DR)



Rhodamine B (RB)



Sunset Yellow (SN)

Figure 5.5: The chemical structure of Direct Red, Rhodamine B, and Sunset Yellow.

We have prepared the hydrogels at different concentrations of peptides (10 mg/mL, 7 mg/mL, 5 mg/mL and 2.5 mg/mL) and at different pH (pH 4, pH 5, pH 6 and pH 7) to compare the rate of the release under these different conditions.

5.2.1- Hydrogel loaded dyes preparation:

5.2.1.1- Release from FmocFF gels:

FmocFF was dissolved in 100 μ L DMSO and then an acetate buffer solution at pH of 4, 5, or 6 loaded with dye of Direct Red (DR), Rhodamine B (RB) or Sunset Yellow (SN) at concentration of 0.078 mg/mL (1.9 mL) was added. The final FmocFF concentrations were 10, 7, 5 and 2.5 mg/mL). The samples were left to stand overnight before being tested.

5.2.1.2- Release from gels formed from 42:

Compound **42** was dissolved in 100 μ L DMSO and then an acetate buffer solution at pH of 4, 5, or 6 loaded with dye of Direct Red (DR), Rhodamine B (RB) or Sunset Yellow (SN) at concentration of 0.078 mg/mL (1.9 mL) was added. The final FmocFF

concentrations were 10, 7, 5 and 2.5 mg/mL). The samples were left to stand overnight before being tested.

5.2.2- Release study:

5.2.2.1- FmocFF and compound 42:

After the formation of the hydrogel, we added a buffer solution to the top of the hydrogel. At specific times, the total buffer solution on top of the gel was carefully removed by pipette and the amount of dye measured using UV-Vis spectroscopy at different wavelengths depending on the dye (523 nm for DR, 556 nm for RB, and 481 nm for SN). Then, we returned the buffer solution carefully to the top of the gel. This was repeated at regular times to follow the release. The release of dyes was studied at room temperature and the errors of the release study were calculated from the average of measuring three samples of the same hydrogel and the errors were +/- 0.005 for DR, 0.0015 for RB, and 0.003 for SN.

5.3- Result and discussion:

5.3.1- Calibration curves:

Figures 5.6, 5.7, and 5.8 show the calibration curves for the DR, RB, and SN dyes. From the Figures, we can see a linear relationship between the concentration and the intensity providing an equation that we can use to calculate M_t/M_∞ in order to calculate the diffusion coefficient of the release of dye from the hydrogel.

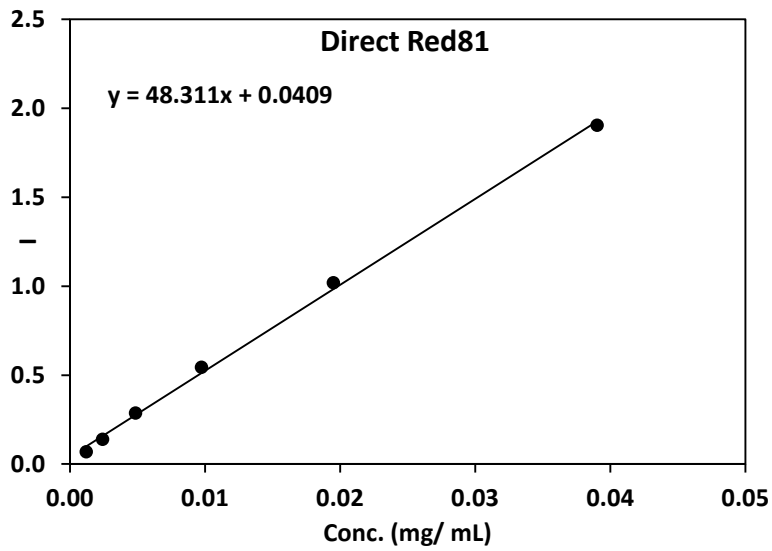


Figure 5.6: the calibration curve for DR.

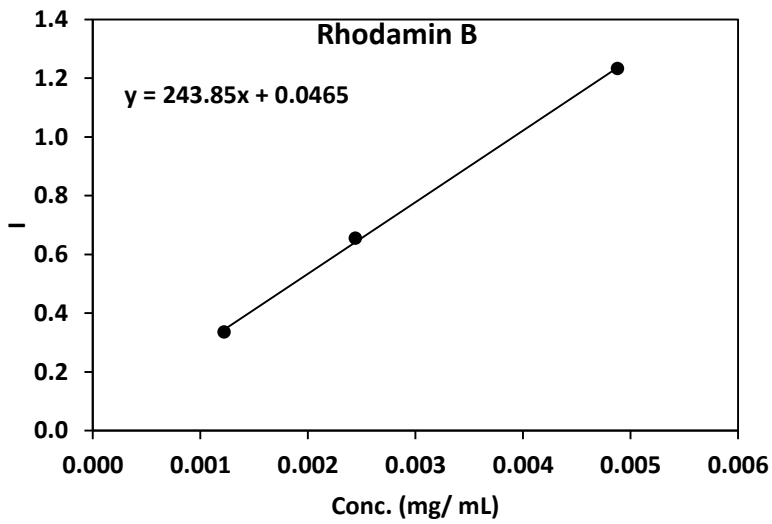


Figure 5.7: The calibration curve for RB.

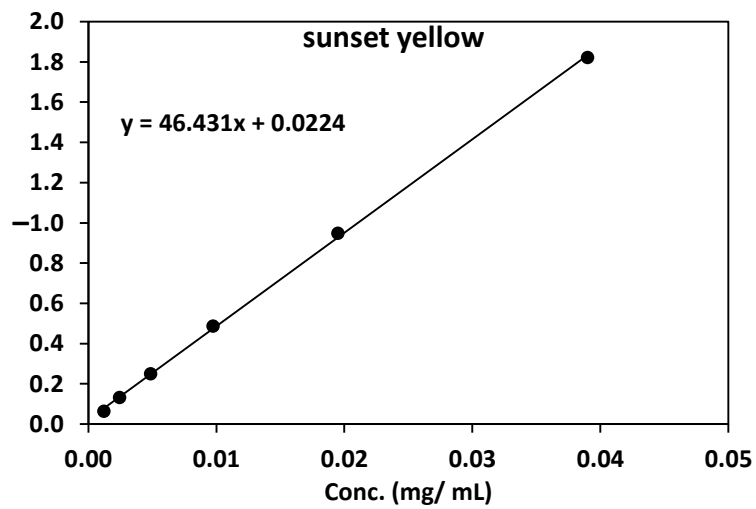


Figure 5.8: The calibration curve for SN.

We have also studied the confocal microscopy images of hydrogels loaded with dyes at concentration of the peptide at 5 mg/mL. Figure 5.9 shows the confocal microscopy images of a FmocFF hydrogel loaded with RB (left) and a hydrogel loaded with SN (right). This data demonstrates the effect of the structure of the dye and the mesh size on the rate of the release. From the Figures, we can see that there is a differences of the confocal image of hydrogel loaded SN and RB. The confocal image of RB shows the fibres and dark areas which might indicate the presence of RB dye. Here, the dye might stick to the fibres and this may affect the rate of release, and so perhaps decrease the release of the dye from the hydrogel. This is probably because the RB is a hydrophobic dye (this is similar to dansyl that we studied its fluorescence and shows effect of its hydrophobicity on the fluorescence properties; where it sticks with the fibres (see Chapter 4). Also the charge on the RB dye may affect the interaction between the RB and the fibres. The RB contains positive charge which might interact strongly with the fibre networks, hence affect its release from the hydrogel²⁹. In contrast, the confocal image of SN does not show clear fibres and this might be because it formed weak fibres and also has a negative charge, therefore the SN will not stick with the fibres and lead to release quicker. Furthermore, the release of the dye might be affected by other factors, such as the size of the dye, where large dye may diffuse less well through the network. Moreover, the mesh size can also affect the rate of the release, where changing the concentration of the peptide to form hydrogel can lead to change in the mesh size. Here, the confocal images show the hydrogels formed at concentration of 5 mg/mL, but if we decrease the concentration of the peptide from 5 mg/mL to 2.5 mg/mL, this may result in a decrease in the fibre structure and an increase in the mesh size, leading to increase the rate of the release.

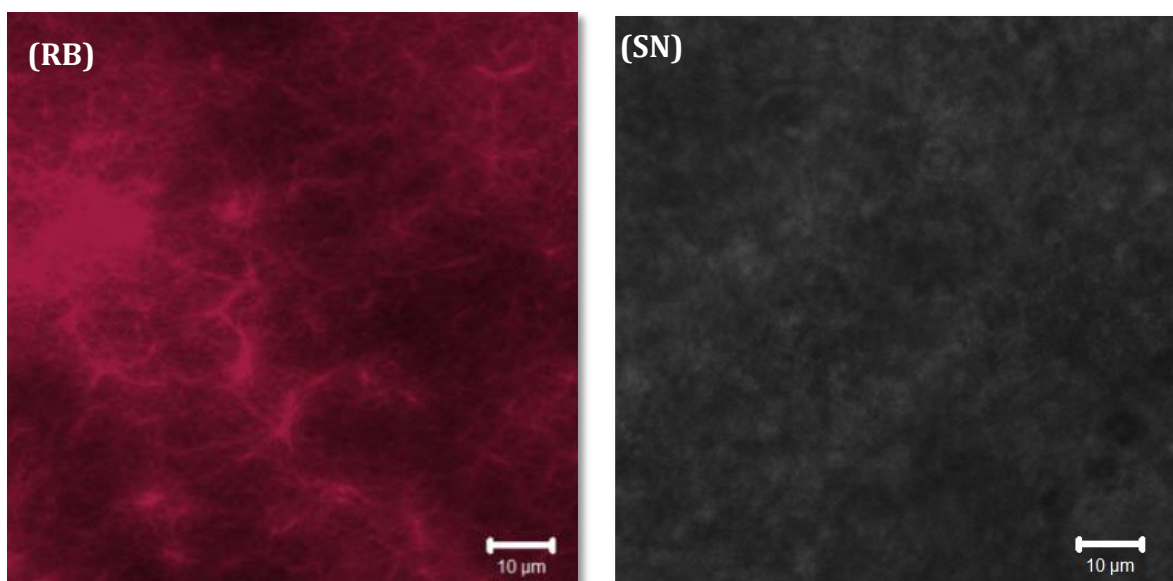


Figure 5.9: an example of confocal microscopy image of hydrogel loaded dyes (Rhodamine B (RB) (left) and Sunset yellow (SN) (right)) showing the effect of the mesh size at concentration of peptide of 5mg/ mL.

5.3.2- *FmocFF loaded dye hydrogel and release study:*

We have prepared hydrogels using FmocFF, loaded with the different dyes (DR, RB, and SN) at different concentrations of peptide and at different pHs. We have used the solvent switch method to prepare the hydrogels. The hydrogels formed after few minutes. Figure 5.10 shows the process of preparing hydrogels loaded with dyes for the controlled release study. Figure 5.10 (A) shows the solution of the FmocFF dipeptides immediately after adding the water, but before the gel has forming (the red sample is a solution of dipeptide with DR, the pink sample with RB and the yellow with SN). Figure 5.10(B) shows the hydrogels that formed after few minutes of adding the buffer solution. We can see the change of the sample appearance before and after the gelation, especially for the hydrogel loaded with SN, as we can see the transparent hydrogel that formed after few minutes. Figure 5.10(C) shows the addition of the buffer to the top of the hydrogel in order to study the release of the dyes from the hydrogel to this added buffer.

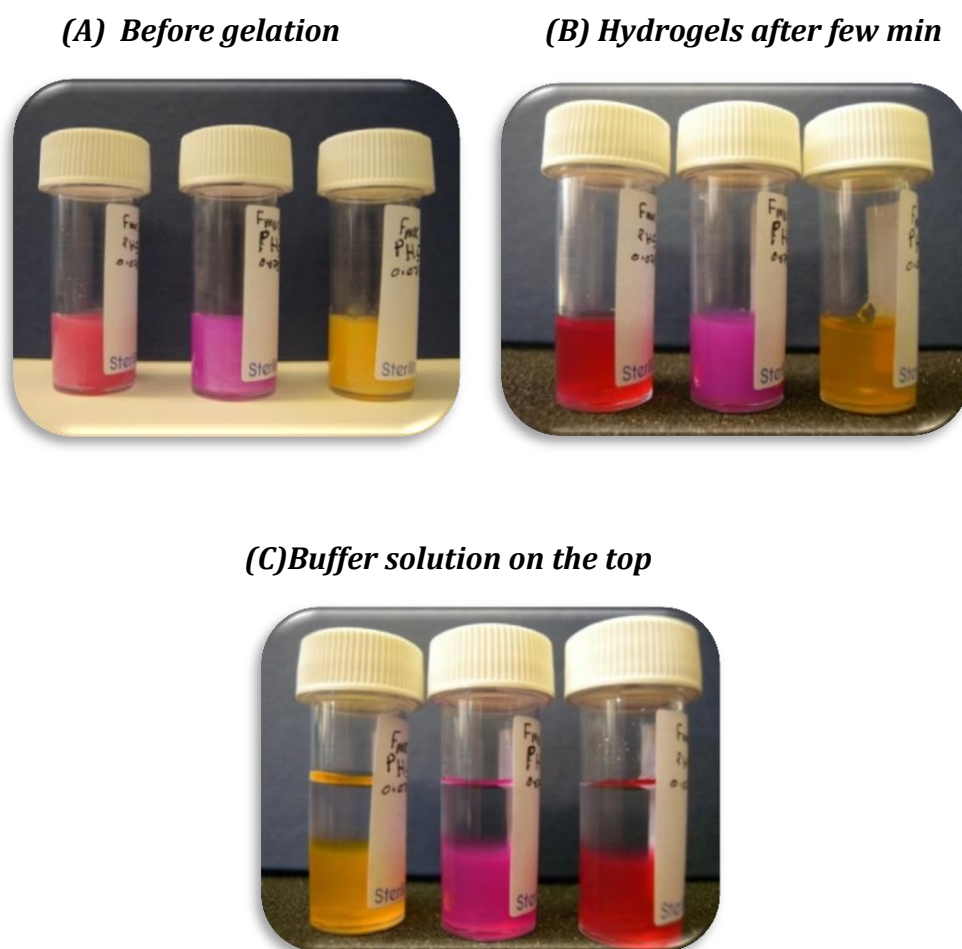


Figure 5.10: The process of preparing samples for controlled release study.

5.3.2.1- Release study at different pHs and dyes at the same concentration of the peptide (5 mg/mL):

Here, we have changed the pH and the dyes while using the same concentration of FmocFF (5 mg/mL). The data is shown in Figures 5.11, 5.12 and 5.13. We found that the release increased at higher pH for DR and RB. At pH 5 and 6, we noted that the concentration of DR did not increase in the first day (Fig. 5.11). After about 23 hours, the concentration of the dye started to increase with time, indicating the release of the dye with the time. On the other hand at pH 4, the concentration of DR did not increase with the time over the three days, showing a strong pH effect on the release. At pH 5, the release of DR was quicker than that at pH 4 but it still takes a long time to release from the hydrogel. For RB, the release rates at different pH have similar results (Fig. 5.12). The rate of release was higher at pH 6 than at pH 4. However, we noted that SN release

results were very similar at all of the pH studied. Fig. 5.13 shows that there is an increase in the concentration after 30 minutes of adding the buffer on the top of the hydrogel, indicating that the SN is released quickly from the hydrogel. Therefore, we note that changing the pH can affect the rate of the release and also the structure of the dye can affect the rate of the release.

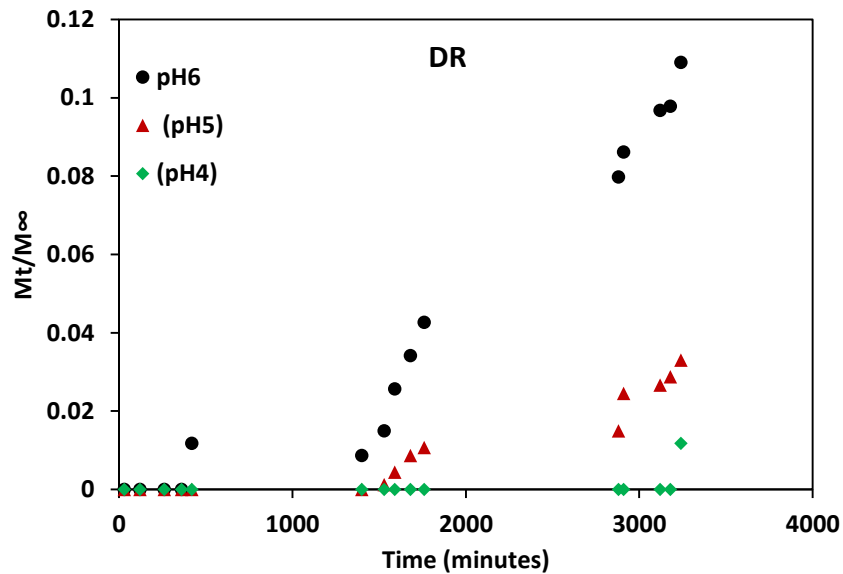


Figure 5.11: The release results of DR at different pH (pH 4, 5, and 6).

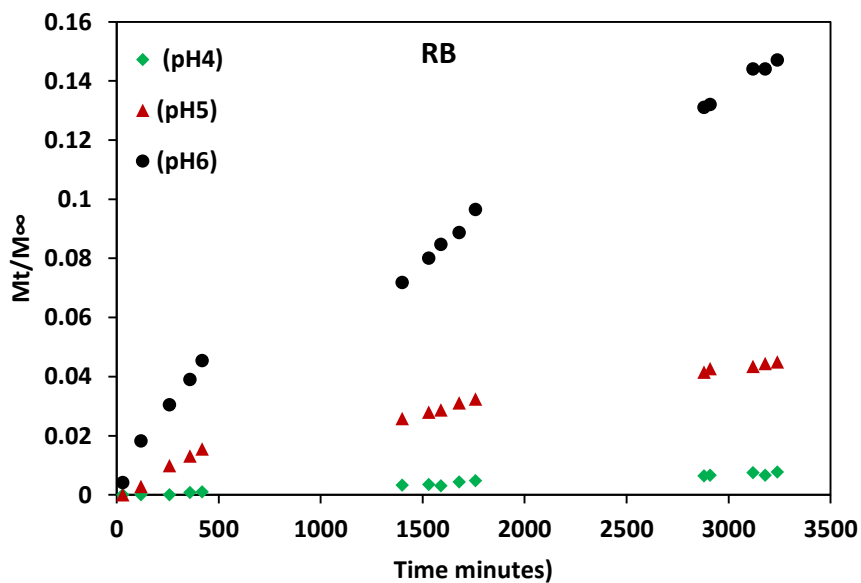


Figure 5.12: The release results of RB at different pH (pH 4, 5, and 6).

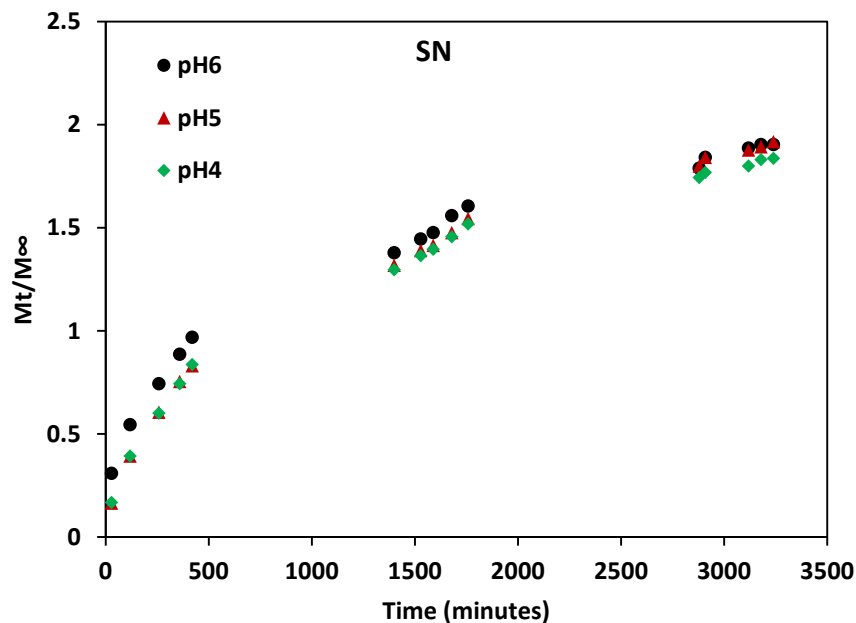


Figure 5.13: The release results of SN at different pH (pH 4, 5, and 6).

Also, we have studied the rheology of the hydrogel loaded with dyes at different pHs (Fig. 5.14). From the Figure, we noted that at all pHs a strong hydrogel was formed. Also, it can be seen that the hydrogel at pH 5 has the highest G' , indicating that at this pH the peptide formed a strong hydrogel. This agrees with previous work on the pH dependence of FmocFF hydrogels³⁰. For this reason, we have studied further the release of the dyes at this pH at the concentration of 5 mg/mL (data shown in more details in Section 5.3.2.3).

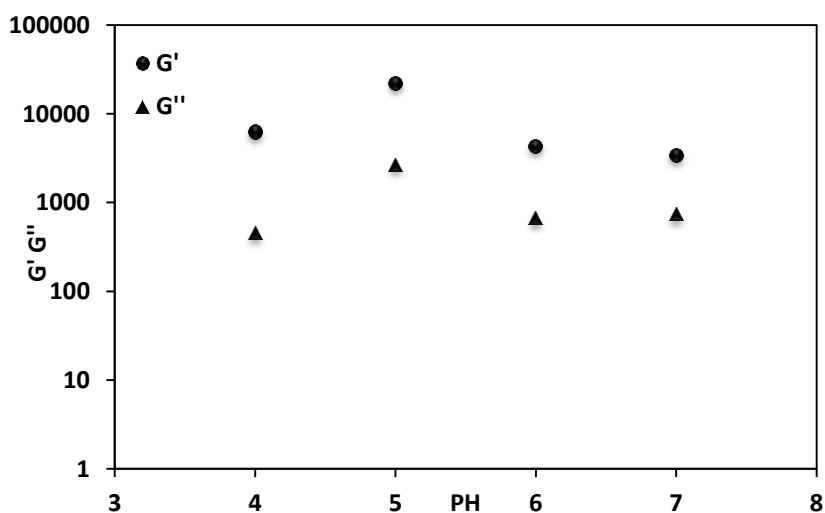


Figure 5.14: The rheology results of hydrogel at different pHs (pH 4, 5, and 6).

5.3.2.2- Release study at different concentration of the peptide and dyes at the same pH:

Here, we have changed the concentration of peptide and dyes at the same pH (pH 5). We have prepared hydrogels of FmocFF at different concentration (2.5 mg/mL, 5 mg/mL, 7.5 mg/mL, and 10 mg/mL) to study the effect of changing the concentration on the rate of the release, because the mesh size can affect the rate of the release of the dyes from the hydrogel. It is expected that increasing the concentration will lead to a decrease in the mesh size and this may lead to decrease the rate of the release. This expectation agreed with our results except at a concentration of 10 mg/mL. Figures 5.15, 5.16, and 5.17 shows the release of DR, RB, and SN respectively at pH 5 from gels formed at different concentrations (2.5 mg/mL, 5 mg/mL, 7.5 mg/mL, and 10 mg/mL). From the Figures, for DR and RB, we can see that the release increases with decreasing FmocFF concentration except at concentration of 10 mg/mL. It is clearly seen that dyes release more quickly at concentrations of 2.5 mg/mL, then 5 mg/mL and the lowest release rate was at concentration of 7.5 mg/mL. This result agrees with the idea of decreasing the mesh size with increasing the dipeptide concentration. However, at a concentration of FmocFF of 10 mg/mL, the release was the highest. This is because at this concentration the hydrogel was unstable and shrunk after adding the buffer on the top, so the dyes can release quickly from the weak hydrogel; where the weak hydrogel has less fibre, hence this allows the dye to release quickly. For the release of SN, the rate is very similar from gels at all concentrations of FmocFF.

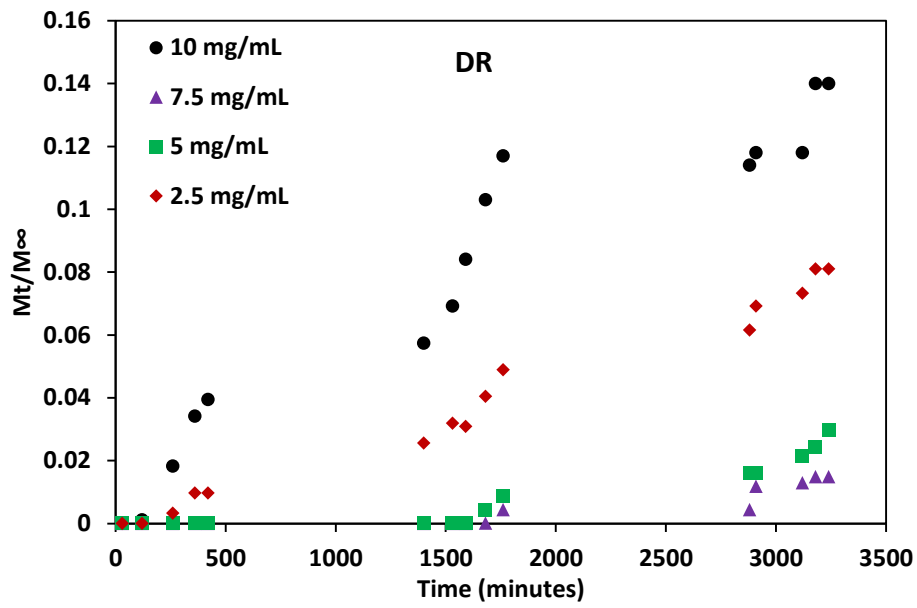


Figure 5.15: The release results of DR at different concentrations (10, 7.5, 5, and 2.5 mg/mL) at the same pH (pH 5).

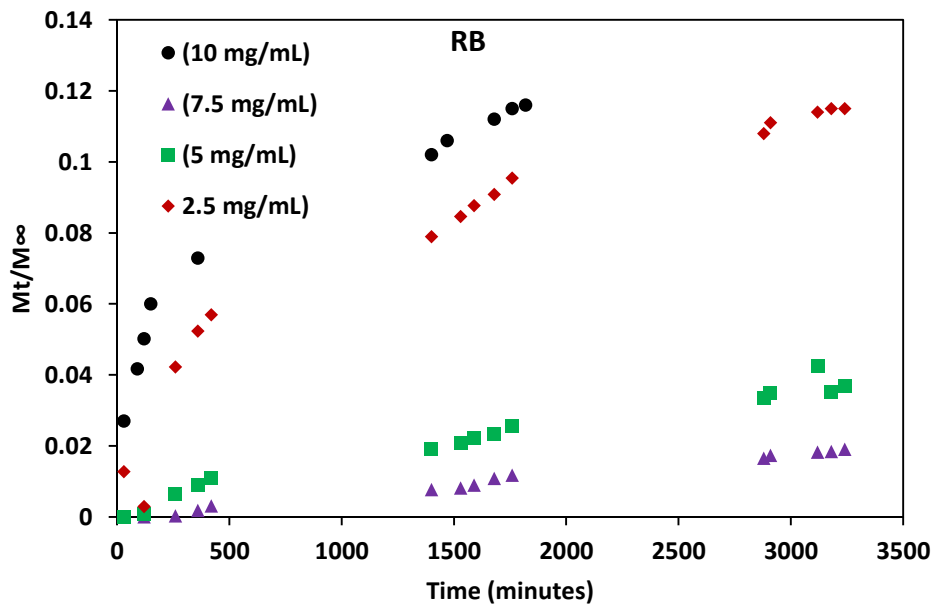


Figure 5.16: The release results of RB at different concentrations (10, 7.5, 5, and 2.5 mg/mL) at the same pH (pH 5).

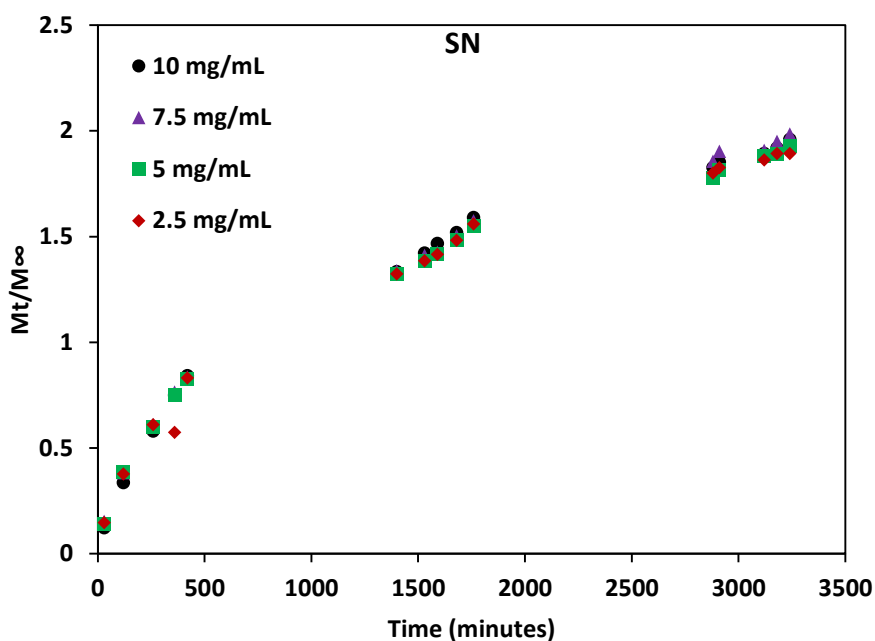


Figure 5.17: The release results of SN at different concentrations (10, 7.5, 5, and 2.5 mg/mL) at the same pH (pH 5).

Again, we studied the rheology of the hydrogel-loaded dyes at different concentrations (Fig. 5.18). From Figure 5.18, we noted that the strength of the gel increased with increase of the concentration over the time except at concentration of 10 mg/mL where the hydrogel was unstable, although there is not a significant difference between the G' at all concentrations. In all cases, G' is greater than G'' by an order of magnitude. This shows that it is difficult to always understand all the properties of a hydrogel from a simple rheological measurement. We can see from the Figure 5.16 we did not study the release at concentration of 10 mg/mL on the third day because the hydrogel has shrunk and it mixed with the buffer due to its instability; where RB shows an increase in the concentration with the time in the first two days and then the hydrogel has shrunk, so the release did not study after this time. As a result, it is expected that the mesh size of the hydrogel will affect the rate of the release for the hydrogel-loaded dye.

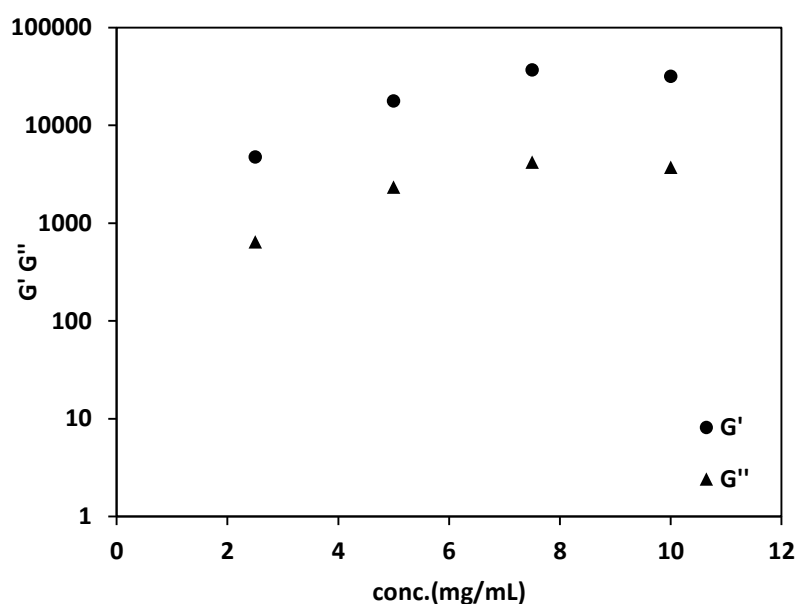


Figure 5.18: The rheology results of the hydrogels at different concentrations (10, 7.5, 5, and 2.5 mg/mL).

5.3.2.3- Compare the release study of different dyes at the same pH (pH5) and the same concentration (5 mg/mL):

From the above results of different concentrations and pH, we have compared the release results of the three dyes at pH 5 and at the concentration of 5 mg/mL. Figure 5.19 shows the release results of the dyes at pH 5 for three days. From the Figure, we noted that the concentration of (DR) and (RB) increased very slowly over the three days, indicating to that they released very slowly, while the concentration of Sunset Yellow (SN) increased with the time quickly. These differences between the dyes are might be due to the differences of the structure and the hydrophobicity. DR has the largest structure and molecular weight, so it is difficult to release from the hydrogel resulting in low concentration of the dye diffused from the hydrogel; and hence the slow release. Therefore, we noted that the size and the molecular weight of the dyes and the hydrophobicity may affect the rate of the release. This results agreed with other works³¹, where it is been reported that the release properties of the dye from the hydrogel can be affected by the molecular weight of the dye^{32, 33}.

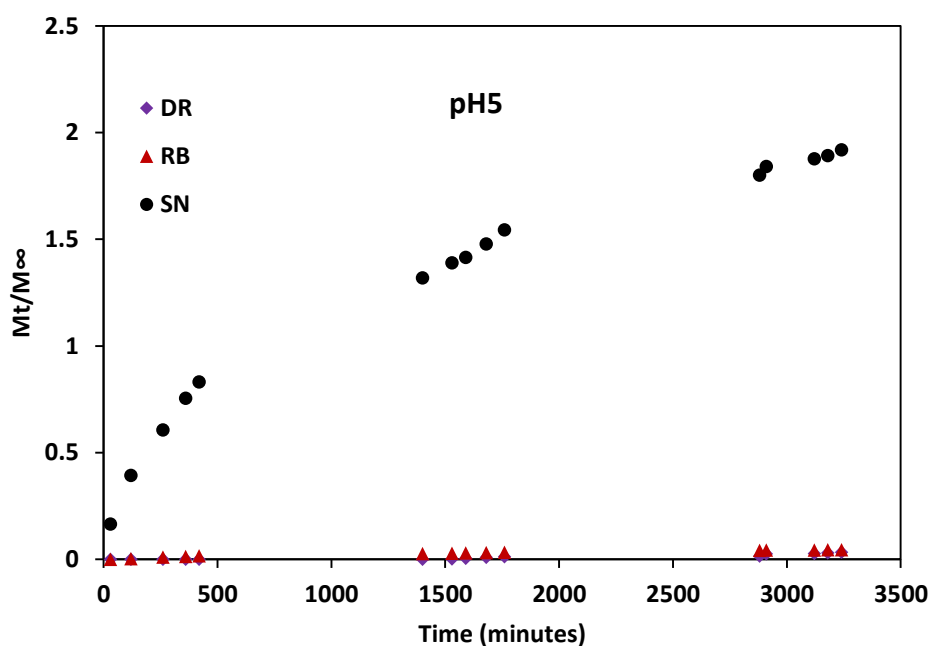


Figure 5.19: The comparison between the release results of different dyes (DR, RB, and SN) at the same concentration (5 mg/mL) and pH (pH 5).

The size of the three dyes was estimated by Dan Holden (University of Liverpool) using Materials Studio 5.5. The three dimensions of the size of DR result are 25.39 Å, 8.43 Å and 6.30 Å (Fig. 5.20). These first were measured from the Na atom, across the dye, to the extreme oxygen atom. The second was from the Na atom to the hydroxyl hydrogen, and the third from the nitrogen to the extreme hydrogen atom. Atom van der Waals radii have not been taken into account here; this is from atom centre to atom centre. The three dimensions of the size of RB are 14.75 Å, 11.93 Å and 10.84 Å, and the two dimensions of the size of SN are 11.19 Å and 14.9 Å. These were measured from the Na atoms, across the dye, to the extreme hydrogen atom (Fig. 5.20). From the proximate calculations, we noted that the dyes showed different sizes; where DR has the largest size and the SN has the smallest size, therefore this result provided that the size of the molecules may affect their release from the hydrogel. However, all of these dyes are smaller than the expected mesh size³⁴.

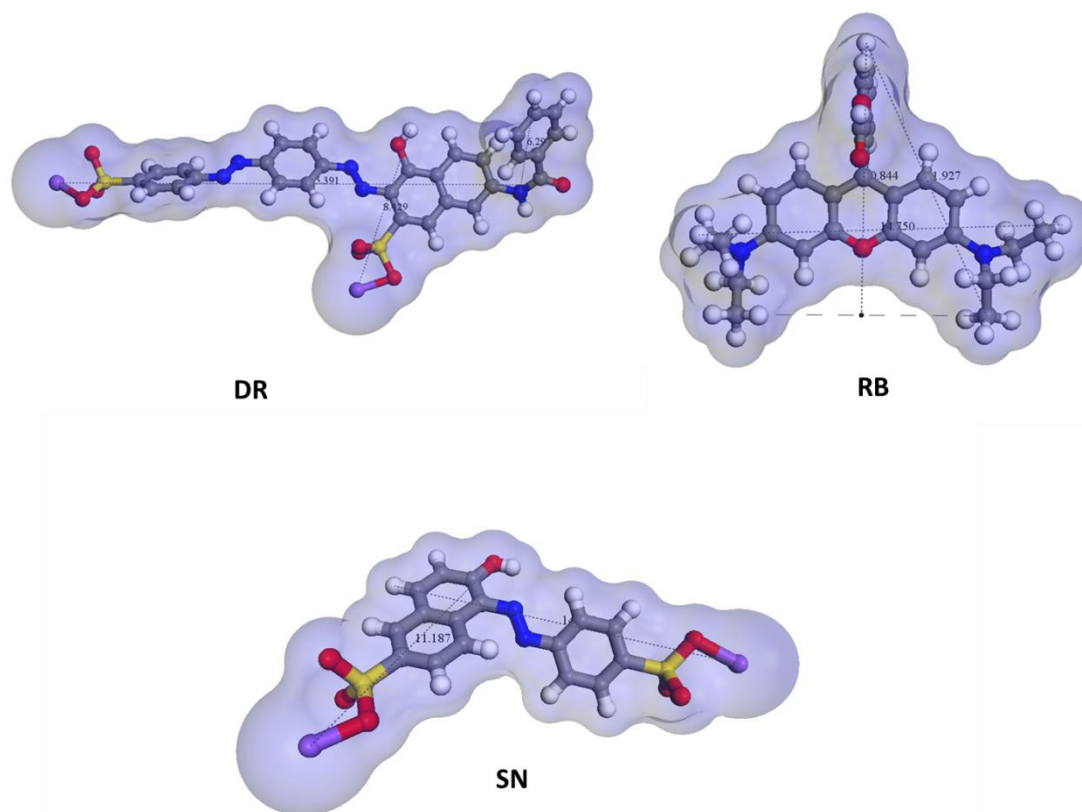


Figure 5.20: The molecular structure of the three dyes (DR, RB, and SN) with the calculation of their sizes.

Also, we have estimated the hydrophobicity of the three dyes using logP that was calculated for the dyes³⁵. From the calculations, we found that logP of DR, RB, and SN are 2.75, 2.74, and 0.27 respectively. From these results, we noted that DR and RB have similar hydrophobicity while the SN has a significantly lower hydrophobicity. Hence, SN is significantly more water-soluble and hence is released much more quickly from the gels. From the same calculation programme, we estimated the molecular volume of the three dyes (molecular volume is expected to determine the transport characteristics of molecules. Volume is therefore often used to model molecular properties and biological activity). From these calculations, we found the molecular volume of DR, RB, and SN is 493.3, 424.7, and 299.9 Å³ respectively. Hence, DR has the large molecular volume and the SN has the smallest molecular volume which indicates that the molecular volume of the dye can also affect their rate of the release. From these data, SN has the smallest volume and the lowest logP. As expected therefore, this dye is released the most quickly from the gels.

5.3.2.4- Diffusion coefficient:

The diffusion coefficient (D) of each model dye in the hydrogel was calculated using non-steady state diffusion model equation:

$$M_t/M_\infty = 4(Dt/\pi\lambda^2)^{1/2}$$

where M_t is the total amount of molecules released during the measurement, M_∞ is the total amount of molecules that are kept in the matrix, λ is the hydrogel thickness, t is the time of the measurement and D is the diffusion coefficient of the molecules²⁴.

The diffusion coefficient was calculated from the equation for the three dyes from the gels prepared at FmocFF concentration of 5 mg/mL and at pH 5. The diffusion coefficients over the time were between 3.77×10^{-10} and 7.72×10^{-11} m²/s for DR, between 4.87×10^{-9} and 7.14×10^{-11} m²/s for RB, and between 1.05×10^{-7} and 3.98×10^{-10} m²/s for SN (Table 5.1, 5.2, and 5.3). The diffusion coefficient of the three dyes for the three days was different due to differences in the structure and the molecular weight of the dyes. The highest diffusion coefficient was for SN dye (3.98×10^{-10} m²/s). Also, from Table 1, we note that we were unable to calculate the diffusion coefficient of the release of DR dye in the first day, because its rate of the release was very slow at that time and after about 26 hours started to increase with the time. Moreover, when we plotted the square root of time against M_t/M_∞ , a good linear relationship was found, demonstrating that the release of dyes from the hydrogel is following Fickian diffusion control²⁷ (Fig. 5.21, 5.22, and 5.23). As a result, we noted that there is a great influence of the dye size and their molecular weight on the rate of the release, hence on the diffusion coefficient as reported on other work³¹⁻³³.

Direct Red

Conc.	Time	M_t/M_∞	$D(m^2/s)$
0	50	0	0
0	80	0	0
0	110	0	0
0	300	0	0
0	360	0	0
0.000167	1440	0.0085	3.77×10^{-10}
0.000354	1560	0.019	5.21×10^{-10}
0.000416	1740	0.0213	4.94×10^{-10}
0.000436	3180	0.0223	2.77×10^{-10}
0.000478	3240	0.0245	2.84×10^{-10}
0.000602	7200	0.0309	1.42×10^{-10}
0.000623	7320	0.032	1.44×10^{-10}
0.00136	20160	0.07	7.72×10^{-11}

Table 5.1: The results of the release of DR that calculated from the diffusion coefficient equation.

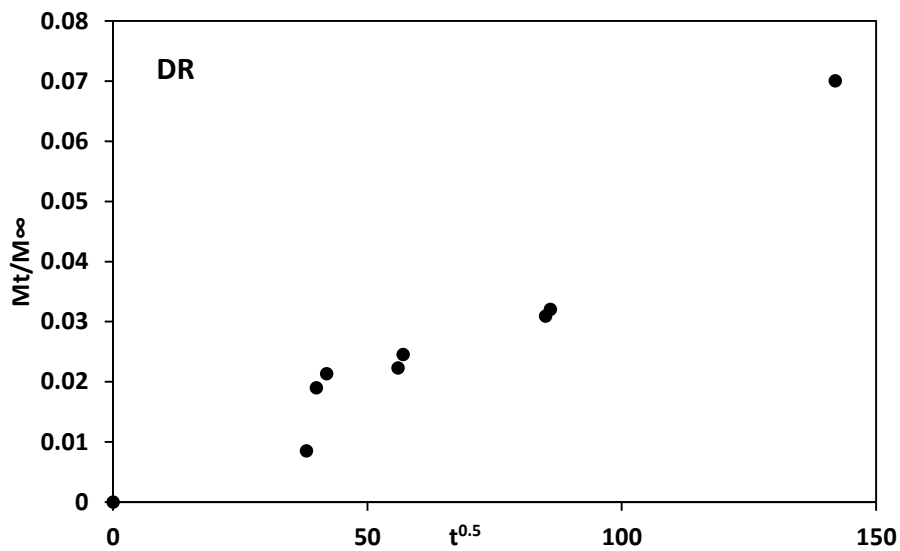


Figure 5.21: Plot of released DR dye against the square root of time that calculated from the calibration curve of the dye.

Rhodamin B

Conc.	Time	M_t/M_∞	$D(m^2/s)$
0.0000164	35	0.00084	4.87×10^{-9}
0.000154	85	0.0078	6.11×10^{-9}
0.000244	210	0.0125	3.13×10^{-9}
0.000527	1410	0.027	6.86×10^{-10}
0.000531	1440	0.027	6.71×10^{-10}
0.00099	5760	0.05	2.28×10^{-10}
0.00096	5880	0.05	2.24×10^{-10}
0.00108	7200	0.06	2.01×10^{-10}
0.0012	20160	0.06	7.14×10^{-11}

Table 5.2: The results of the release of RB that calculated from the diffusion coefficient equation.

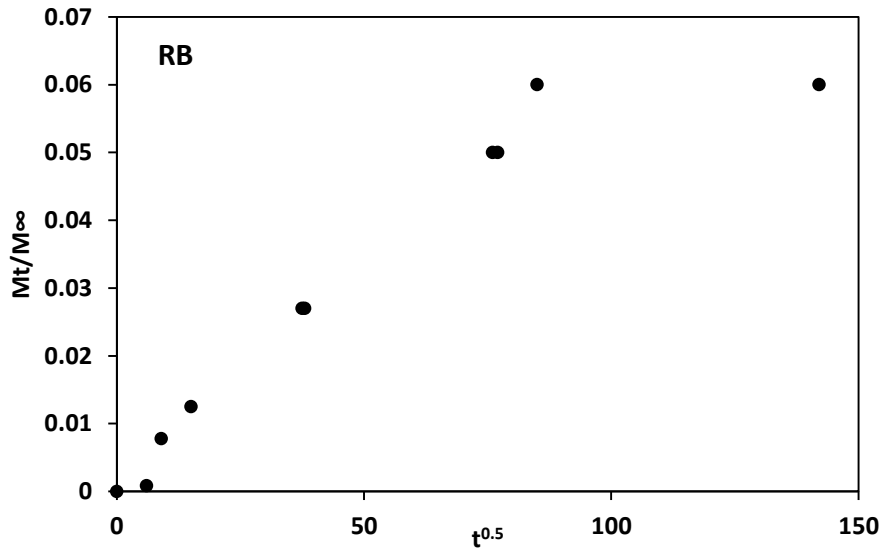


Figure 5.22: Plot of released RB dye against the square root of time showing a linear relationship between them.

Sunset Yellow:

Conc.	Time	M_t/M_∞	$D(m^2/s)$
0.0025	20	0.128	1.05×10^{-7}
0.0057	90	0.292	3.53×10^{-8}
0.0095	300	0.486	1.37×10^{-8}
0.0188	1440	0.965	4.01×10^{-9}
0.0196	1500	1.007	3.93×10^{-9}
0.0316	5760	1.62	1.30×10^{-9}
0.0322	5900	1.65	1.28×10^{-9}
0.0337	7200	1.73	1.07×10^{-9}
0.0363	20160	1.86	3.98×10^{-10}

Table 5.3: The results of the release of SN that calculated from the diffusion coefficient equation.

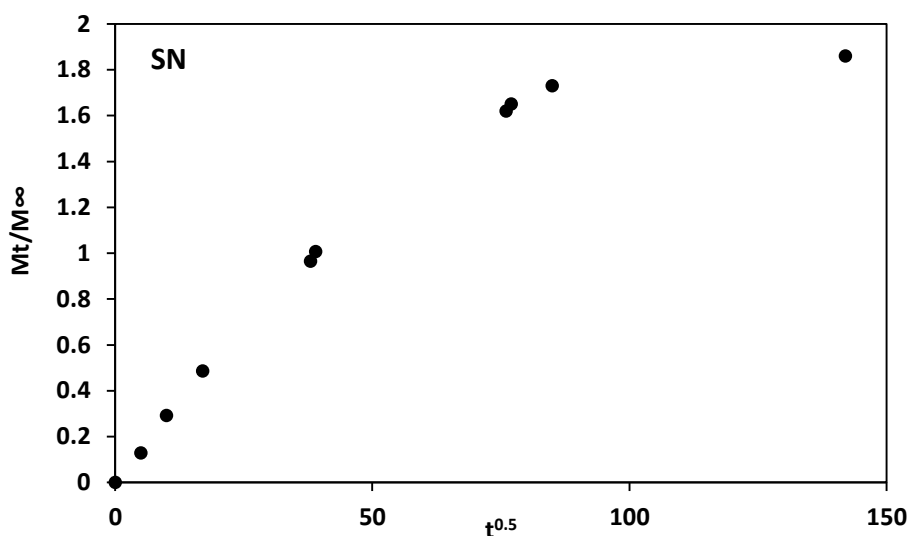


Figure 5.23: Plot of released SN dye against the square root of time showing the linear relationship between them.

5.3.3- Compound 42 release study:

Here hydrogels have been prepared from compound **42** at pH 5 and a concentration of 5 mg/mL using different dyes (DR, RB, and SN) at concentrations of 0.078 mg/mL. After hydrogel had formed, we placed on each sample buffer of pH 5. Then we studied the release of the dye over time using the UV-vis spectroscopy at different wavelength for each dye (523 nm for DR, 556 nm for RB, and 481 nm for SN). Figure 5.24 shows the release results of the dyes at pH 5 for three days. From the Figure, we can see that RB is released slowly, while the SN is released quickly. From the Figure, it can be clearly seen that the DR was also released slowly. This result is similar to the release results of DR from the FmocFF hydrogel described above. This shows that DR release has similar behaviour despite the change of the hydrogelator. Similarly the SN released very quickly with only small differences of the release result compared to that from the FmocFF hydrogel. On the other hand, RB release from gel formed from **42** has a different behaviour compared to that from the FmocFF hydrogel. RB released very slowly. Also, we noted that after that time, the intensity of the UV data started to decrease. This is might be because the RB affected by the light and decomposed lead to an apparent decrease of its release³⁶. These differences between the results are might be due to the differences of the structure and the hydrophobicity as described above. Therefore, we noted that the structure and the molecular weight of the dyes and the hydrophobicity

can affect the rate of the release. This results agreed with the above results and other research, where it is been reported that the release properties of the dye from the hydrogel can be affected by the molecular weight of the dye¹⁷. Hence, by studying these factors of control release we can choose the appropriate hydrogel that can be used for drug delivery applications.

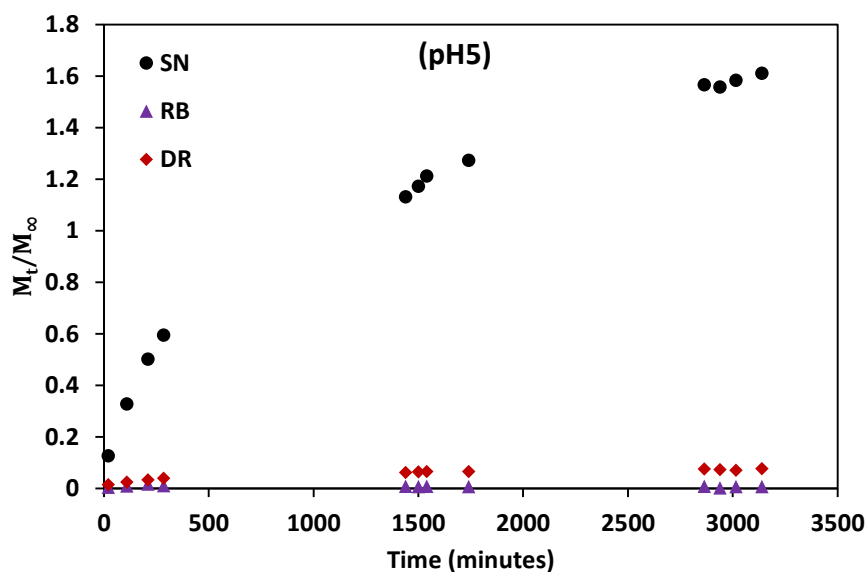


Figure 5.24: The release results of different dyes (DR, RB, and SN) at pH 5 and concentration of peptide of 5 mg/mL.

We have also studied the release of the dyes (DR, RB, and SN) from gels formed using **42** at pH 7.4, because the eventual aim of this study is to study the release of dyes at pH 7 (the pH of the body) in order to use it for drug delivery application. This peptide formed hydrogels at pH 7 using the PBS buffer solution. Figure 5.25 shows the release study of these dyes from the hydrogel at pH 7 over three days. From the Figure and comparing to previous data, we can see that the DR was released more quickly at pH 7 than that at pH 5. In contrast, RB still has a low rate release at pH 7, which is the same as at pH 5.

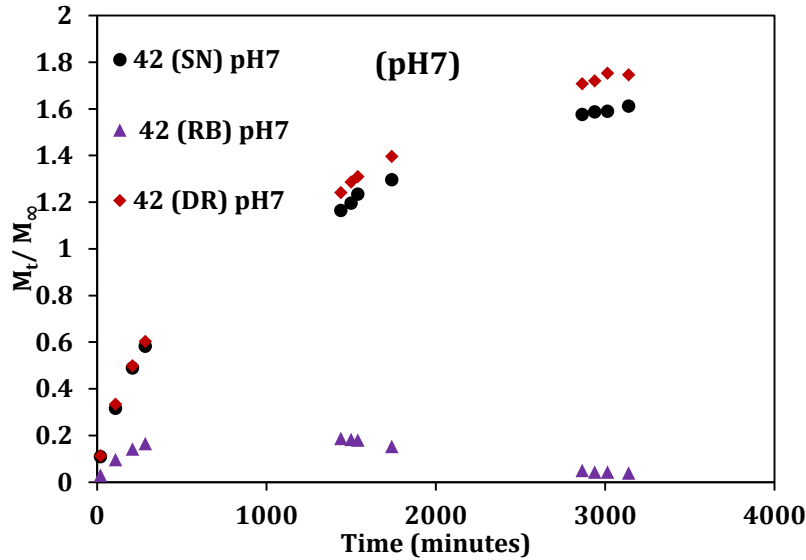


Figure 5.25: the release results of different dyes (DR, RB, and SN) at pH7 and concentration of peptide of 5 mg/mL.

Diffusion coefficient:

We have calculated the diffusion coefficients of the dyes from gels form from **42** at pH 7. The diffusion coefficients over the three days were between 8.07×10^{-08} and 2.52×10^{-09} m^2/s for DR, 5.45×10^{-09} and 5.38×10^{-11} m^2/s for RB, and 9.07×10^{-08} and 2.56×10^{-09} m^2/s for SN (Table 5.4, 5.5, and 5.6). We noted that the diffusion coefficients of the three dyes over the three days were different due to differences in the structure and the molecular weight of the dyes. From the results, we found that after three days of the release of dyes from the hydrogel, the diffusion coefficient for SN dye and DR dye was very similar. However, the diffusion coefficient of RB is significantly lower, agreeing with its release rate, which was low in the first day and increased slowly in the second day, and then it started decreasing in the third day. This might be because the RB affected by the light and decomposed lead to an apparent decrease of its release³⁶. Furthermore, when we plotted the square root of time against the M_t/M_∞ , a good linear relationship was found, indicating that the release of dyes from the hydrogel is following Fickian diffusion control²⁷ (Fig. 5.26 and 5.28), except the RB which its release start to decrease in the third day due to its light effect (Fig. 5.27). Again, we note that there is a great effect of the dye size and their molecular weight on the rate of the release, therefore the significant change in the diffusion coefficient with change the dye.

Direct Red:

Conc.	Time	M_t/M_∞	D(m²/s)
0.00147	20	0.0754	8.07 x10 ⁻⁰⁸
0.00607	110	0.31	2.89 x10 ⁻⁰⁸
0.00946	210	0.485	5.61 x10 ⁻⁰⁸
0.0116	285	0.595	4.13 x10 ⁻⁰⁸
0.0248	1440	1.272	4.61 x10 ⁻⁰⁹
0.0258	1500	1.323	4.51 x10 ⁻⁰⁹
0.0262	1540	1.344	4.42 x10 ⁻⁰⁹
0.0281	1740	1.441	4.06 x10 ⁻⁰⁹
0.0345	2865	1.769	2.73 x10 ⁻⁰⁹
0.0348	2940	1.785	2.67 x10 ⁻⁰⁹
0.0354	3015	1.815	2.63 x10 ⁻⁰⁹
0.0353	3140	1.81	2.52 x10 ⁻⁰⁹

Table 5.4: The results of the release of DR dye that calculated from the diffusion coefficient equation.

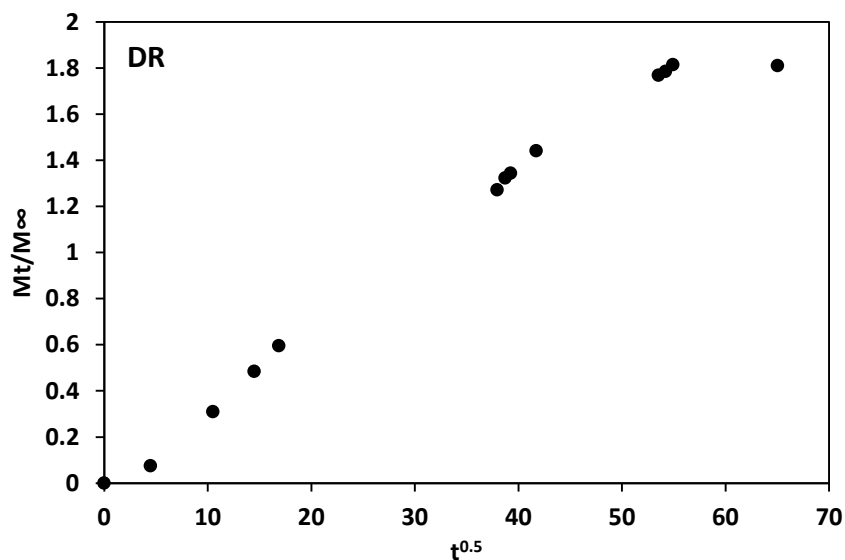


Figure 5.26: Plot of released DR dye against the square root of time, showing a linear relationship between them.

Rhodamine B:

Conc.	Time	M_t/M_∞	$D(m^2/s)$
0	20	0	0
0.000203	110	0.0104	5.45×10^{-09}
0.000388	210	0.0198	3.94×10^{-09}
0.000486	285	0.0249	3.25×10^{-08}
0.000576	1440	0.0295	7.02×10^{-10}
0.000561	1500	0.0287	6.64×10^{-10}
0.000547	1540	0.0281	6.41×10^{-10}
0.000437	1740	0.0224	5.06×10^{-10}
0.0000144	2865	0.00073	5.38×10^{-11}

Table 5.5: The results of the release of RB that calculated from the diffusion coefficient equation.

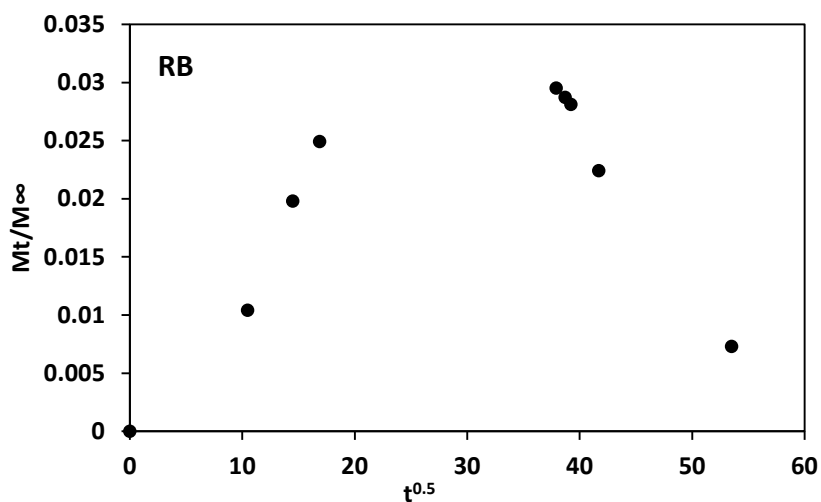


Figure 5.27: Plot of released RB dye against the square root of time.

Sunset Yellow:

Conc.	Time	M_t/M_∞	$D(m^2/s)$
0.00184	20	0.0944	9.07×10^{-08}
0.00632	110	0.324	3.05×10^{-08}
0.01	210	0.513	2.01×10^{-08}
0.0121	285	0.62	1.63×10^{-08}
0.0251	1440	1.287	4.63×10^{-09}
0.0253	1500	1.297	4.46×10^{-09}
0.0261	1540	1.338	4.41×10^{-09}
0.0274	1740	1.405	4.01×10^{-09}
0.0334	2865	1.713	2.68×10^{-09}
0.0337	2940	1.728	2.63×10^{-09}
0.0338	3015	1.733	2.56×10^{-09}
0.0342	3140	1.754	2.48×10^{-09}

Table 5.6: the results of the release of SN that calculated from the diffusion coefficient equation at pH 7.

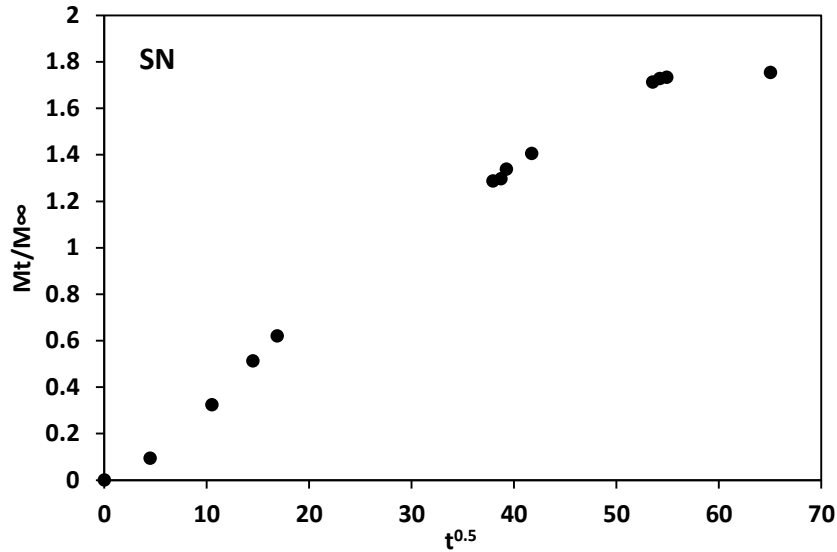


Figure 5.28: Plot of released SN dye against the square root of time, showing the linear relationship between them.

5.4- Conclusion:

Controlled release drug delivery systems can be used to deliver drug to the body over long periods of time. Here, hydrogels loaded dyes were formed by the self-assembly of peptides for controlled release. The release of the dye from the hydrogel can be controlled by many factors, including the pH, peptide concentration, the microstructure and the mesh size. Moreover, choosing the right method to prepare hydrogel allows us to control the microstructure for hydrogel to be injectable. We have also examined the effect of concentration on both the strength of the gel (by studying the rheology) and the mesh size, by studying the release of the dye using gels formed at different concentrations of the dipeptide. There is a correlation between the release results and the rheological data. Also, we found that changing the concentration, dyes size and molecular weight can affect the rate of the release, where the rate of the release decreases with increase of the concentration and decreasing the mesh size. Similarity, the large dye with high molecular weight was restricted in the rate of the release. Therefore, these results showed that the rate of the release can be affected by these factors and these gels may be useful for applications in drug delivery.

5.5- References:

1. Y. Wang, Z. Zhang, L. Xu, X. Li and H. Chen, *Colloids and Surfaces B: Biointerfaces*, 2013, **104**, 163-168.
2. H. Wang, C. Ren, Z. Song, L. Wang, X. Chen and Z. Yang, *Nanotechnology*, 2010, **21**, 1-5.
3. J. Raeburn, G. Pont, L. Chen, Y. Cesbron, R. Levy and D. J. Adams, *Soft Matter*, 2012, **8**, 1168-1174.
4. L. Chen, K. Morris, A. Laybourn, D. Elias, M. R. Hicks, A. Rodger, L. Serpell and D. J. Adams, *Langmuir*, 2009, **26**, 5232-5242.
5. L. Chen, S. Revel, K. Morris, L. C. Serpell and D. J. Adams, *Langmuir*, 2010, **26**, 13466-13471.
6. D. J. Adams, L. M. Mullen, M. Berta, L. Chen and W. J. Frith, *Soft Matter*, 2010, **6**, 1971-1980.
7. J. Raeburn, T. O. McDonald and D. J. Adams, *Chemical Communications*, 2012, **48**, 9355-9357.
8. D. J. Adams and P. D. Topham, *Soft Matter*, 2010, **6**, 3707-3721.
9. D. J. Adams, *Macromolecular Bioscience*, 2011, **11**, 160-173.
10. Z. Yang, G. Liang and B. Xu, *Chemical Communications*, 2006, **7**, 738-740.
11. C. Tang, R. Ulijn and A. Saiani, *The European Physical Journal* 2013, **36**, 1-11.
12. A. M. Smith, R. J. Williams, C. Tang, P. Coppo, R. F. Collins, M. L. Turner, A. Saiani and R. V. Ulijn, *Advanced Materials*, 2008, **20**, 37-41.
13. J. J. Panda, A. Mishra, A. Basu and V. S. Chauhan, *Biomacromolecules*, 2008, **9**, 2244-2250.
14. A. Mahler, M. Reches, M. Rechter, S. Cohen and E. Gazit, *Advanced Materials*, 2006, **18**, 1365-1370.
15. S. R. Thomas Liebmann, Victor Akpe and Hjalmar Brismar, *BMC Biotechnol.*, 2007, **7**, 1-11.
16. V. Jayawarna, M. Ali, T. A. Jowitt, A. F. Miller, A. Saiani, J. E. Gough and R. V. Ulijn, *Advanced Materials*, 2006, **18**, 611-614.
17. S. Sutton, N. L. Campbell, A. I. Cooper, M. Kirkland, W. J. Frith and D. J. Adams, *Langmuir*, 2009, **25**, 10285-10291.
18. C. K. He, Sung Wan; Lee, Doo Sung, *J. Controlled Release*, 2008, **127**, 189-207.
19. T. R. K. Hoare, Daniel S., *Polymer*, 2008, **49**, 1993-2007.
20. F. Bierbrauer, *Hydrogel Drug Delivery: Diffusion Models*, 2012.
21. S. Koutsopoulos and S. Zhang, *Journal of Controlled Release*, 2012, **160**, 451-458.
22. M. A. V. Jayawarna, T. A. Jowitt, A. E. Miller, A. Saiani, J. E. Gough and R. V. Ulijn *Adv. Mater*, 2006, **18**, 611-614.
23. D. J. Adams, M. F. Butler, W. J. Frith, M. Kirkland, L. Mullen and P. Sanderson, *Soft Matter*, 2009, **5**, 1856-1862.
24. R. Huang, W. Qi, L. Feng, R. Su and Z. He, *Soft Matter*, 2011, **7**, 6222-6230.
25. G. Liang, Z. Yang, R. Zhang, L. Li, Y. Fan, Y. Kuang, Y. Gao, T. Wang, W. W. Lu and B. Xu, *Langmuir*, 2009, **25**, 8419-8422.
26. Y. U. Nagai, Larry D.; Koutsopoulos, Sotirios; Zhang, Shuguang, *J. Controlled Release*, 2006, **115**, 18-25.
27. P. L. P. Ritger, Nikolaos A., *Journal of Controlled Release*, 1987, **5**, 23-36.
28. M. Wallace, D. J. Adams and J. A. Iggo, *Soft Matter*, 2013, **9**, 5483-5491.
29. R. Zhang, M. Hummelgård, G. Lv and H. Olin, *Carbon*, 2011, **49**, 1126-1132.
30. G. Pont, L. Chen, D. G. Spiller and D. J. Adams, *Soft Matter*, 2012, **8**, 7797-7802.
31. C. J. C. Dunlap, Peter W., *J. Chromatogr. A*, 1996, **746**, 199-210.
32. M. B. S. Mellott, K.; Pishko, M. V., *Biomaterials*, 2001, **22**, 929-941.
33. G. M. S. Cruise, David S.; Hubbell, Jeffrey A., *Biomaterials*, 1998, **19**, 1287-1294.
34. N. Amdursky, R. Orbach, E. Gazit and D. Huppert, *The Journal of Physical Chemistry C*, 2009, **113**, 19500-19505.
35. <http://www.molinspiration.com>.

36. L. Pan, J.-J. Zou, X.-Y. Liu, X.-J. Liu, S. Wang, X. Zhang and L. Wang, *Industrial & Engineering Chemistry Research*, 2012, **51**, 12782-12786.

CHAPTER 6

Conclusion

5.1- Conclusion:

Dipeptides hydrogels are LMWG that have great potential. Previously, hydrogels based on functionalised dipeptides such as naphthalene dipeptides and Fmoc-dipeptides have been used in different applications, energy transfer, cell culture and controlled release. In this thesis, we have synthesised a large number of functionalised dipeptides to study their ability to form hydrogels and study some of their applications.

In the second Chapter, we have synthesised a large number of functionalised dipeptide derivatives with different aromatic protecting groups such as naphthalene, anthracene, pyrene, phenanthrol, anthraquinone and carbazole in order to study their ability to form gel because it is still unclear why some peptides form gel and others not when a small change in the molecular structure is applied. We have synthesised 35 dipeptides conjugated to different aromatic groups.

In the next chapter, hydrogels were formed from these dipeptides functionalised with naphthalene, phenanthrol, anthraquinone, pyrene and carbazole using one of two different methods, the solvent method (DMSO: Water) or the GdL method. We have also studied the mechanical properties of the hydrogels, as well as comparing pK_a and pH measurements. From the results, it can be seen that there is a correlation between the pK_a and the hydrophobicity of the peptides. We established that the hydrophobicity increases with the increase of the pK_a . As with other similar LMWG, for our dipeptides, the properties of the hydrogel can be modified by changing the structure, amino acid order or by the method of preparing hydrogel, it is still not fully understood why some peptides formed gel and others not.

In Chapter 4, we have studied the fluorescence and energy transfer between different aromatic groups. The fluorescence of naphthalene, pyrene, anthracene, phenanthrol and carbazole dipeptides was studied. The results showed that all dipeptides conjugated to different aromatic groups can emit light at the same excitation with different fluorescence properties. We also noted that energy transfer occurred between two dipeptides (pyrene and anthracene dipeptides), and between dipeptide and dansyl derivative (phenanthrol and dansyl, or carbazole and dansyl). These results showed that energy transfers can occur between two dipeptides hydrogel or between dipeptide

and dansyl derivative. In other cases, no evidence for energy transfer was found. This might indicate that the packing of the fibres is important for energy transfer and this should be the focus of future work.

In Chapter 5, we demonstrate the controlled release between components in such gels using different dyes. We also studied controlled release of FmocFF hydrogel and another functionalised dipeptide hydrogel (chosen as it can be used to form a gel at pH 7) at different concentrations and different pHs. The data shows that the release of the dye from the hydrogel can be controlled by different factors, including the pH, peptide concentration, the microstructure and the mesh size. Furthermore, choosing the right method to prepare hydrogel allows us to control the microstructure for hydrogel to be injectable. Therefore, by controlling these entire factors we can use these kinds of hydrogels for drug delivery applications.

Further work will need to consider the following areas:

- Focus on studying the self-sorting system because it is still unclear whether the mixing of two peptides can be self-sorted or forms random fibres, where the efficiency of the energy transfer might be affected by the system of how the hydrogel formed, self-sorting or a random system formed. This may give expand to this project to be studied in more details.
- In this thesis, we have found one gelator that form hydrogel at pH 7.4 for studying the controlled release. Further work might be concentrated on finding the gelators that can form hydrogel at pH 7.4 in order to expand the work and study the similar effect on the controlled release and drug delivery application.
- Further work might be concentrated on examining the SEM of other conjugated dipeptide hydrogels.